U.PORTO

DOUTORAMENTO

CIÊNCIAS BIOMÉDICAS

Unravelling the Role of Keratins in Bacterial Infections

Rui Filipe Cruz

D

2018

U.PORTO

Rui Filipe Cruz. Unravelling the Role of Keratins in Bacterial Infections

D.ICBAS 2018

Unravelling the Role of Keratins in Bacterial Infections

Rui Filipe Cruz

INSTITUTO DE CIÊNCIAS BIOMÉDICAS ABEL SALAZAR

RUI FILIPE DA SILVA E CRUZ

UNRAVELLING THE ROLE OF KERATINS IN BACTERIAL INFECTIONS

Tese de Candidatura ao grau de Doutor em Ciências Biomédicas, submetida ao Instituto de Ciências Biomédicas Abel Salazar da Universidade do Porto.

Instituição de acolhimento - Instituto de Biologia Molecular e Celular - Instituto de Investigação e Inovação em Saúde

Orientador – Doutora Sandra Manuela Rodrigues Sousa Cabanes
Categoria – Investigador auxiliar
Afiliação – Instituto de Biologia Molecular e Celular - Instituto de Investigação e Inovação em Saúde

Coorientador – Professor Doutor Rui Appelberg Gaio Lima
Categoria – Professor catedrático
Afiliação – Instituto de Ciências Biomédicas Abel Salazar da Universidade do Porto

Many people helped me through this long journey. Inside and outside the lab, I could always count with their support, kindness, patience, wisdom and laughter. To all of my travel companions, my most humble and sincere thank you.

Rui Cruz

De acordo com o disposto no ponto n.º 2 do Art.º 31º do Decreto-Lei n.º 74/2006, de 24 de Março, aditado pelo Decreto-Lei n.º 230/2009, de 14 de Setembro, o autor esclarece que na elaboração desta tese foram incluídos dados das publicações abaixo indicadas, e declara ter participado ativamente na conceção e execução das experiências que estiveram na origem dos mesmos, assim como na sua interpretação, discussão e redação.

According to the relevant national legislation, the author clarifies that this thesis includes data from the publications listed below, and declares that he participated actively in the conception and execution of the experiments that produced such data, as well as in their interpretation, discussion and writing.

PUBLICAÇÕES / PUBLICATIONS

Cruz, R., Castro, I.P., Almeida, M.T., Moreira, A., Cabanes, D., and Sousa, S. (2018) Epithelial keratins modulate cMet expression and signalling and promote InlB-mediated *Listeria monocytogenes* infection of HeLa cells. *Front Cell Infect Microbiol.* doi: 10.3389/fcimb.2018.00146. (Publication accepted and manuscript production ongoing)

FUNDING

This work received funding from Norte-01-0145-FEDER-000012 - Structured program on bioengineered therapies for infectious diseases and tissue regeneration, supported by Norte Portugal Regional Operational Programe (NORTE 2020), under the PORTUGAL 2020 Partnership Agreement, through the European Regional Development Fund (FEDER). Publication fees were supported by ICBAS, University of Porto. The author was supported by an FCT Doctoral Fellowship grant (SFRH/BD/90607/2012) through FCT/MEC co-funded by QREN (Quadro de Referência Estratégico Nacional) and POPH (Programa Operacional Potencial Humano). The supervisor (SS) was supported by FCT Investigator program (COMPETE, POPH, and FCT).

TABLE OF CONTENTS

ABSTRACT

To promote infection, pathogens interfere with crucial intracellular pathways of the host. Different pathogens often hijack the same signaling pathways, allowing the microbes to invade, proliferate and disseminate to the whole organism. In particular, host cytoskeleton components are preferential targets of infecting bacteria. The study of the cell biology of infection provided insights in the way bacteria manipulate the host cytoskeleton and revealed novel functions of cellular proteins, leading to deeper understanding of basic cellular processes. *Listeria monocytogenes* is a facultative intracellular Gram-positive pathogen adapted to thrive in diverse environments. In humans, *L. monocytogenes* is able to cause listeriosis, a pernicious foodborne disease that can lead to septicemia, encephalitis, meningitis and abortions in pregnant women. Successful *L. monocytogenes* infection depends on its ability to infect phagocytic and non-phagocytic cells. For this, *L. monocytogenes* takes the control of host actin polymerization machinery to favor its own internalization, intracellular motility and intercellular spread. The involvement of actin cytoskeleton in *L. monocytogenes pathogenesis* is thoroughly characterized.

Keratins are cytoskeletal proteins that are the major components of intermediate filaments in epithelial cells. Although keratins were reported to be targeted by several microbes, the molecular and functional details behind keratin involvement in bacterial pathogenesis remain largely elusive.

In this work, we examined the role of keratin 8 and 18 (K8 and K18), the major keratins in simple epithelia, during *L. monocytogenes* cellular infection. Using RNAi techniques to knockdown K8 and K18 expression, we found that both keratins are necessary for successful InlB/cMet-dependent *L. monocytogenes* entry, but are dispensable for InlA/E-cadherin-mediated invasion. In addition, K8 and K18 are enriched at the InlB-mediated internalization sites following actin recruitment, and modulate actin dynamics at those sites. Our data also reveals the importance of K8 and K18 in HGF-induced signalling which occurs downstream the activation of cMet. Strikingly, we show that K18, and to a less extent K8, controls the expression of cMet and other transmembrane receptors such as TfR and integrin β1, by promoting the stability of their corresponding transcripts. Finally, we identified potential K18 binding partners that can assist in mRNA processing.

Altogether, these results reveal novel functions for K8 and K18 in the modulation of actin dynamics at the bacterial entry sites and in the control of surface receptors mRNA stability and expression.

RESUMO

Para promover infeção, patógenos interferem com importantes vias de sinalização do hospedeiro. Diferentes patógenos frequentemente sequestram as mesmas vias de sinalização, permitindo que os patógenos invadam, proliferem e disseminem no organismo. Os componentes do citoesqueleto do hospedeiro são alvos preferenciais de bactérias infeciosas. O estudo da biologia celular de infeção tem revelado como as bactérias manipulam o citoesqueleto do hospedeiro e ajudou na descoberta de novas funções de proteínas celulares, promovendo assim uma melhor compreensão de processos celulares básicos. *Listeria monocytogenes* é um patógeno Gram-positivo, facultativo intracelular, que está adaptado para prosperar vários ambientes. Em humanos, *L. monocytogenes* pode causar listeriose, uma doença infeciosa de origem alimentar que pode provocar septicemia, encefalite, meningite e aborto em mulheres grávidas. Para infetar o hospedeiro, *L. monocytogenes* depende da sua capacidade para invadir células fagociticas e não-fagociticas. Para tal, *L. monocytogenes* controla a maquinaria de polimerização de actina para favorecer a sua internalização, mobilidade intracelular e disseminação intercelular. O envolvimento do citoesqueleto de actina na patogénese de *L. monocytogenes* encontra-se bem caracterizado.

Queratinas são proteínas do citoesqueleto que constituem a subfamília predominante de filamentos intermédios em epitélios. Apesar das queratinas terem sido reportadas como alvo de vários micróbios, os detalhes moleculares e funcionais por detrás do envolvimento das queratinas em patogénese bacteriana permanecem pouco claros.

Neste estudo examinamos o papel das queratinas 8 e 18 (K8 e K18), as principais queratinas em epitélio simples, na infeção de *L. monocytogenes*. Para tal, silenciamos K8 e K18 utilizando técnicas de RNAi e observamos que ambas as queratinas são necessárias para uma internalização *via* InlB/cMet da bactéria. Pelo contrario, estas queratinas são dispensáveis na entrada mediada pela interação InlA/E-cadherin. Demonstramos que K8 e K18 são recrutadas para os locais de internalização mediada por InlB depois de actina, e que regulam a dinâmica de actina nesses locais. Revelamos ainda a importância de K8 e K18 na sinalização induzida por HGF, que ocorre após ativação de cMet. Surpreendentemente, observamos que K18, e menos proeminentemente K8, controla a expressão de cMet e outros recetores transmembranares como TfR e integrin β1, pela promoção da estabilidade dos correspondentes transcritos. Finalmente, identificamos potenciais proteínas que ligam a K18 e que podem participar no processamento de mRNA.

Em suma, estes resultados revelam novas funções de K8 e K18 na modulação da dinâmica de actina nos locais de entrada de bactéria, bem como no controlo da estabilidade do mRNA e respetiva expressão de recetores de superfície.

LIST OF ABBREVIATIONS

ActA - Actin assembly-inducing protein
Akt - Protein kinase B (serine/threonine-specific protein kinase)
AE1/2 - Anion Exchange Protein 1
AP - clathrin–adaptor protein complex
Arp2/3 – Actin-related proteins 2 and 3
BHI - Brain heart infusion
Cdc25 – Cell division cycle 25
CFU - Colony-forming unit
CFTR - Cystic fibrosis transmembrane conductance regulator
CK II - Casein kinase II
ClfB - Clumping factor B
cMet - Hepatocyte growth factor receptor
CNS - Central Nervous System
DMEM - Dulbecco's modified Eagle medium
DMSO - Dimethyl sulfoxide
DRA - Down-Regulated In Adenoma Protein
EBS - Epidermolysis bullosa simplex
ECM - Extracellular matrix
EHEC - Enterohemorrhagic *Escherichia coli*
EMEM - Eagle's Minimal Essential Medium
ENaC - Sodium Channel Epithelial 1
EPEC - Enteropathogenic *Escherichia coli*
ERK - Extracellular-signal-regulated kinases
Fas receptor - First apoptosis signal receptor
FBS - Fetal bovine serum
GAPDH - Glyceraldehyde 3-phosphate dehydrogenase
gC1qR – Receptor for complement component C1q
GFAP - Glial fibrillary acidic protein
GTPase - Guanosine triphosphate hydrolase
HGF - Hepatocyte growth factor
HIV - Human Immunodeficiency Virus
hnRNP K - Heterogeneous Nuclear Ribonucleoprotein K
hnRNP K - Heterogeneous Nuclear Ribonucleoprotein R
HPV - Human papilloma virus

Hsc70 - Heat-shock cognate protein 70
HSP - Heat shock protein
HSV-2 - Herpes simplex virus type 2
IFs - Intermediate filaments
IgG - Immunoglobulin G
InlA - Internalin A
InlB - Internalin B
InlC - Internalin C
IR - inter-repeat spacer region
JNK - c-Jun N-terminal kinase
K – Keratin
K18 - Keratin 18
K8 - Keratin 8
kDa – kiloDalton
LAMP-1 - Lysosomal-associated membrane protein 1
LAMP-2 - Lysosomal-associated membrane protein 2
LB - Lysogeny broth media
LIMK - LIM kinase
LINC - Linker of nucleoskeleton and cytoskeleton
LLO - Listeriolysin O
LMB - Leptomycin B
LRRs - Leucine rich repeats
MAPK - Mitogen-activated protein kinase
MMP9 - Matrix Metallopeptidase 9
MOI - Multiplicity of infection
mRNA - messenger RNA
MTOC - Microtubule organizing centers
mTOR - Mammalian target of rapamycin
NES - Nuclear export signal
NF – Neurofilament
NF-L - Neurofilament light
NF-M – Neurofilament medium
NF-H – Neurofilament heavy
NF-κB - Nuclear factor-kB
NLS - Nuclear localization signal
NMHC-IIA - Non-muscle myosin heavy chain isoform IIA
N-WASP - neuronal Wiskott-Aldrich syndrome protein

OCRL - Oculocerebrorenal syndrome of Lowe (Inositol polyphosphate 5-phosphatase)
PAGE - Polyacrylamide gel electrophoresis
PBS - Phosphate-buffered saline
PC - Phosphatidylcholine
PC-PLC/PLC-B - Phosphatidylcholine-specific phospholipase C
PI3K - Phosphatidylinositol 3-kinase
PI4K - Phosphatidylinositol 4-kinase
PI5K - Phosphatidylinositol 5-kinase
PI - Phosphoinositol
PIP - Phosphatidylinositol 1-phosphate
PIP2 - Phosphatidylinositol biphosphate
PIP3 - Phosphatidylinositol triphosphate
PIP4 - Phosphatidylinositol 4-phosphate
PI-PLC/PLC-A - Phosphatidylinositol-specific phospholipase C
PKA - Protein kinase A
PKC - Protein kinase C
PMF - Peptide mass fingerprinting
PrfA - Positive regulatory factor A
PSF - PTB-associated splicing factor
PTM - Posttranslational modification
qRT-PCR - Quantitative Real-time Polymerase Chain Reaction
RBP – RNA binding protein
RBPDB - RNA-Binding Protein Database
RIP – RNA immunoprecipitation
SCVs - *Salmonella* containing vacuoles
SDS - Sodium dodecylsulfate
SGLT1 - Sodium-glucose co-transporter 1
Src - c-Src tyrosine kinase
T3SS – Type 3 secretion system
Tir - Translocated intimin receptor
TfR – Transferrin receptor
TNFR2 - Tumor necrosis factor receptor 2
TRADD - TNF receptor-associated death domain-containing protein
UTR – Untranslated region
WAVE - WASP family verprolin homologous protein
YTHDC1 - YTH Domain Containing 1 protein

ZO-1 - Zona Occludens 1

CHAPTER I – INTRODUCTION

A. *Listeria monocytogenes*

A.1. Overview

The earliest descriptions of what is believed to be *Listeria* infection occurred in France and Germany and date back to the end of the nineteen century (1891 and 1893, respectively). Gram-positive rods were found in tissue sections of deceased patients that, in retrospect, most likely succumbed to listeriosis (Gray and Killinger, 1966). *Listeria* infection also appeared to be the cause of a minor epidemic of meningitis that was reported in Australia in 1917 (Atkinson, 1917). The first isolation of the pathogen occurred in 1911 by Hülphers, which named the microbe *Bacillus hepatis* (Hülphers, 1911). *Listeria* was later on isolated from a soldier who died from meningitis (Dumont and Cotoni, 1921). Despite these and other reports (Gray and Killinger, 1966), it was not until 1926 that the pathogen was described by Murray, Webb and Swann, who reported an in house laboratory outbreak that killed six rabbits in Cambridge, England. They reported that infection led to increase of blood monocytes – hence the species name *monocytogenes* (Murray *et al.*, 1926). The organism had multiple names (Lamont *et al.*, 2011) until the establishment of the current nomenclature - *Listeria monocytogenes* - in 1940 (Pirie, 1940).

Despite the occurrence of circumstantial human cases (Nyfeldt and others, 1929; Hof, 2003), *L. monocytogenes* infection was generally considered a zoonosis until the first human outbreak in Canada in 1981, in which ingestion of contaminated food resulted in 41 cases and 18 deaths, most of them pregnant women and neonates (Schlech *et al.*, 1983). That and posterior outbreaks established *L. monocytogenes* as a foodborne pathogen that poses serious economic (Ivanek *et al.*, 2004) and public health problems. In the United States, *Listeria* infection was responsible for 20%–65% of deaths resulting from food-borne infections (Bortolussi, 2008).

Up until 1961 *L. monocytogenes* was the only described species in the *Listeria* genus (Roccourt, 1982). The genus currently comprises eighteen species, ten of which were described since 2009 (Orsi and Wiedmann, 2016). The *Listeria* genus currently includes: *L. innocua* (Seeliger, 1981), *L. welshimeri*, *L. seeligeri* (Rocourt and Grimont, 1983)*, L. ivanovii* (formerly *L. bulgarica*) (Seeliger *et al.*, 1984), *L. grayi* (Larsen *et al.*, 1966)*, L. rocourtiae* (Leclercq *et al.*, 2010)*, L. riparia, L. floridensis, L. aquatica, L. cornellensis, L. grandensis* (den Bakker *et al.*, 2014)*, L. fleischmannii* (Bertsch *et al.*, 2013)*, L. marthii* (Graves *et al.*, 2010)*, L. weihenstephanensis* (Lang Halter *et al.*, 2013)*, L. booriae* and *L. newyorkensis* (Weller *et al.*, 2015). The most recent addition to the *Listeria* genus is *Listeria costaricensis* (Núñez-Montero *et al.*, 2018).

The majority of these species live as non-pathogenic saprophytes in nature (McLauchlin *et al.*, 2014). Only two of them are considered pathogenic: *L. monocytogenes* infects humans and animals (Ramaswamy *et al.*, 2007), whereas *L. ivanovi* mainly targets ruminants (Vázquez-Boland *et al.*, 2001). Infection of humans by non-pathogenic species are extremely rare, but have been reported (Rapose *et al.*, 2008; Guillet *et al.*, 2010). Still, *L. monocytogenes* remains the most important *Listeria* species concerning public health and economic impact (Orsi and Wiedmann, 2016).

A.2. General characteristics

L. monocytogenes is a gram-positive, rod shaped (measuring 0.4 by 1-1.5 µm), facultative anaerobic pathogen that does not have capsule and does not form spores (McLauchlin *et al.*, 2014). This bacterium is ubiquitous in nature. For that the pathogen relies on its ability to survive and proliferate in a wide range of environmental conditions. Indeed, and unlike most foodborne pathogens (de Noordhout *et al.*, 2014), *L. monocytogenes* is able to survive in harsh pH and salt conditions (pH 4.3 -9.5, 10% NaCl) (McClure *et al.*, 1991; Cheroutre-Vialette *et al.*, 1998), and temperatures ranging from -0.4 to 45ºC (Farber and Peterkin, 1991). Optimal growth conditions are 30-37ºC (Low and Donachie, 1997), neutral pH and 0.5%NaCl (McClure *et al.*, 1991; Cheroutre-Vialette *et al.*, 1998). *L. monocytogenes* harbors up to six flagella that confers motility to the bacteria in an environmental temperature up to 30ºC. The synthesis of the flagella is temperature regulated, as at 37ºC its expression is significantly reduced due to transcriptional repression (Gründling *et al.*, 2004). The presence of the flagella structure is crucial for the pathogen biofilm formation (Lemon *et al.*, 2007). Altogether, these features allow *L. monocytogenes* to survive and/or thrive in multiple habitats including rotting plants, soil, waste water, cattle milk, animal and human aliments and inert surfaces such as equipment in food-processing facilities (Ivanek *et al.*, 2006).

L. monocytogenes can also be found in several animals such as insects, ruminants, crustaceans, fish and humans (Ramaswamy *et al.*, 2007). *L. monocytogenes* is in fact so ubiquitous that it is estimated that up to 21% of cattle gastrointestinal tracts and 10% of human gastrointestinal tracts may be colonized by the pathogen (Ramaswamy *et al.*, 2007; Esteban *et al.*, 2009). This widespread presence in the environment, associated with the microbe resilience, makes *L. monocytogenes* especially difficult to control and contributes to the increasing number of food borne outbreaks in industrialized countries, thus making this pathogen a serious public health issue (de Noordhout *et al.*, 2014; L.Buchanan *et al.*, 2017).

A.3. Listeriosis

A.3.1. Transmission and Pathogenesis

L. monocytogenes is the etiological agent of listeriosis, a pernicious foodborne disease. Transmission of *L. monocytogenes* can occur vertically (mother to child) (Becroft *et al.*, 1971), in an hospital setting (Fullerton *et al.*, 2015) and through direct animal contact (Dhama *et al.*, 2015). However, most *L. monocytogenes* infections (up to 99%) are resultant from oral ingestion of contaminated raw and processed foods such as fruits and vegetables, charcuterie meats, raw seafood, soft cheeses, unpasteurized milk and other dairy products (Swaminathan and Gerner-Smidt, 2007; Allerberger and Wagner, 2010; Hernandez-Milian and Payeras-Cifre, 2014)

Upon ingestion, *L. monocytogenes* is able to survive the acidic conditions of the stomach and reach the intestinal lumen (Gahan and Hill, 2005). The bacterium can then cross the intestinal epithelium through enterocytes, mucus-secreting goblet cells, and M-cells in peyer's patches (Lecuit *et al.*, 2001; Pentecost *et al.*, 2006; Chiba *et al.*, 2011; Nikitas *et al.*, 2011), to then spread via the lymph or blood to colonize mesenteric lymph nodes, liver and spleen (Fig 1). Experiments in mice demonstrate that clearance of most of the circulating bacteria is executed by professional phagocytes in the spleen and liver (Vázquez-Boland *et al.*, 2001). The bacteria that survives these initial rounds of clearance can replicate and spread in the liver hepatocytes up to 5 days post-infection. If the infection is not controlled at this stage (as it happens in immunocompromised individuals), the death of bacteria-full hepatocytes results in the pathogen release into circulation. The bacteria can then reach and cross critical barriers such as the placenta and blood-brain barrier, leading to fetal infections, abortions, encephalitis and meningitis (McLauchlin *et al.*, 2004; Orsi *et al.*, 2010; Hernandez-Milian and Payeras-Cifre, 2014).

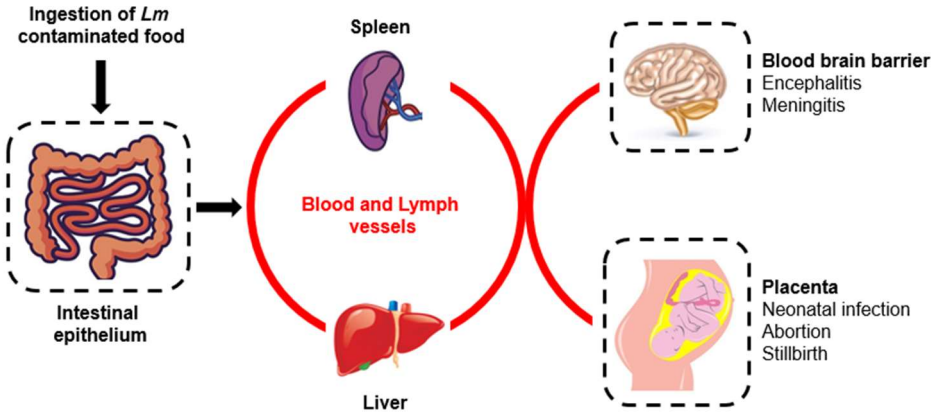

Figure 1. Overview of human listeriosis

A.3.2. Clinical manifestations and epidemiology

In healthy individuals, the pathogen can be found in the intestine causing asymptomatic infections. In high doses, *L. monocytogenes* causes non-invasive, non-life threatening form of listeriosis characterized by gastroenteritis and influenza-like symptoms (Chen *et al.*, 2003; McLauchlin *et al.*, 2004). These immunocompetent individuals rarely contract a more severe, potentially lethal, invasive form of the disease (Orsi *et al.*, 2010), that generally occurs after ingestion of highly contaminated food (up to 10^9 bacteria (Schlech *et al.*, 1983). The control and clearance of *L. monocytogenes* depends on strong innate and adaptive immune response to the pathogen (Zenewicz and Shen, 2007). Thus, individuals with weakened immune systems such as elderly, HIV patients, pregnant women and children are more susceptible to invasive listeriosis, which can result from ingestion of food contaminated with low levels of *L. monocytogenes* (Schlech, 2000; Hernandez-Milian and Payeras-Cifre, 2014; Radoshevich and Cossart, 2017). Other risk groups include patients that suffer from alcoholism, diabetes mellitus and cardiovascular disease (Swaminathan and Gerner-Smidt, 2007).

Listeriosis has been mostly reported in the elderly and perinatal populations (Allerberger and Wagner, 2010; de Noordhout *et al.*, 2014). *L. monocytogenes* infection can lead to stillbirth or miscarriage and is one of the most common causes of meningitis in the newborn. Transmission of the pathogen occurs from mother to fetus by ascending colonization from the vagina, inhalation of infected amniotic fluid or placental crossing from the blood of the mother (Lamont *et al.*, 2011). In a non-pregnancy context, infection can lead to septicemia, encephalitis and meningitis. The incidence of the later condition is particularly significant, as the bacteria has a tropism for the Central Nervous System (CNS) (Hernandez-Milian and Payeras-Cifre, 2014). Despite the frequent human contact with *L. monocytogenes*, listeriosis is an uncommon/rare disease. Although the disease can manifest as an epidemic outbreak, most of the cases result from sporadic infections (Allerberger and Wagner, 2010). Listeriosis incidence ranges between 0.1 and 11.3 cases per million people worldwide (Swaminathan and Gerner-Smidt, 2007). Despite the low incidence, *L. monocytogenes* infection has a mortality rate up to 20-30%, making it one of the deadliest foodborne pathogens. Additionally, listeriosis also results in the highest hospitalization rate among foodborne microbes (Mead *et al.*, n.d.; Lomonaco *et al.*, 2015).

A meta-analysis study from 2014 (de Noordhout *et al.*, 2014) estimated that in 2010, Listeriosis resulted in 23 150 illnesses and 5 463 deaths worldwide. Of these, 20.7% were associated with pregnancy, whereas in non-perinatal cases most of the fatalities resulted from septicemia (61.6%) and CNS infections (30.7%). Despite the efforts by food industries and regulators, the number of listeriosis cases has increased in Europe in the latest years, likely

due to increase of elderly population and consumption of ready-to-eat foods (Goulet *et al.*, 2013; Hernandez-Milian and Payeras-Cifre, 2014; European Food Safety Authority, 2016).

A.3.3. Treatment

Listeriosis is treated with antibiotics. The intracellular nature of *L. monocytogenes* hinders treatment, as the antibiotic must reach and be stable in the cellular cytoplasm (Lamont *et al.*, 2011). Most listeriosis cases are treated with ampicillin or penicillin, alone or in combination with gentamicin, although the synergistic effect has only been proven in *in vitro* studies. Other drugs used include erythromycin, amoxicillin, trimethoprim, sulfamethoxazole and vancomycin. *In vitro*, *Listeria* resistance to antibiotics has not changed significantly in the last decades, although occasional resistance to ampicillin and vancomycin has been reported in patients. No resistance to penicillin has been detected. Treatment can range from two to six weeks, depending on the clinical manifestations of the disease (Allerberger and Wagner, 2010; Lamont *et al.*, 2011). There is no immunization available for listeriosis (Calderón-González *et al.*, 2014).

A.4. Cellular infection cycle

L. monocytogenes has a remarkable ability to adapt to its environment and to quickly respond to environmental cues (Gahan and Hill, 2014). Indeed, once ingested and inside the gastrointestinal tract, the bacterium initiates a profound lifestyle transition from saprophyte to virulent intracellular, a process that is regulated by significant transcriptional changes (Toledo-Arana *et al.*, 2009; Camejo *et al.*, 2009; Gahan and Hill, 2014). Such modifications provide *L. monocytogenes* with an arsenal of virulence factors that favors the pathogen crossing of the intestinal barrier and eventual penetration into deeper tissues of the host (Gahan and Hill, 2014). These molecular tools allow *L. monocytogenes* to penetrate and cross multiple barriers, and to invade and thrive in multiple cell types, both phagocytic and non-phagocytic such as enterocytes, hepatocytes, fibroblasts, neurons and epithelial cells (Lecuit, 2007; Cossart, 2011; Pizarro-Cerdá *et al.*, 2012). Indeed, one of the hallmarks of *L. monocytogenes* infection is the pathogen ability to actively promote its own internalization into non-phagocytic cells by exploiting the host receptor-mediated endocytosis machinery (Radoshevich and Cossart, 2017). *L. monocytogenes* cellular infection cycle usually encompasses the following sequential steps: adhesion and invasion, lysis of the phagocytic vacuole, intracellular replication, intracellular motility and cell-to-cell spread (Fig 2). Each step of this cycle depends on active

usurpation of the host molecular machinery by *L. monocytogenes* virulence factors (Camejo *et al.*, 2011). Remarkably, the expression of most of the key virulence factors is regulated by a major transcriptional regulator, the transcription positive regulatory factor A (PrfA) (Scortti *et al.*, 2007). PrfA is positively regulated by temperature. At low temperatures the 5´-UTR of the *prfa* mRNA displays a hairpin structure that blocks access to ribosomes, impairing translation. At 37ºC, this secondary structure is destabilized, allowing translation of the gene and consequent expression of genes under PrfA control (Johansson *et al.*, 2002). PrfA is also positively regulated by the host cell intracellular levels of glutathione and L-glutamine (Reniere *et al.*, 2015; David and Cossart, 2017). Bellow I will describe each step of the infection cycle and address some of the most relevant bacterial virulence factors deployed by *L. monocytogenes* to successfully infect the host organism.

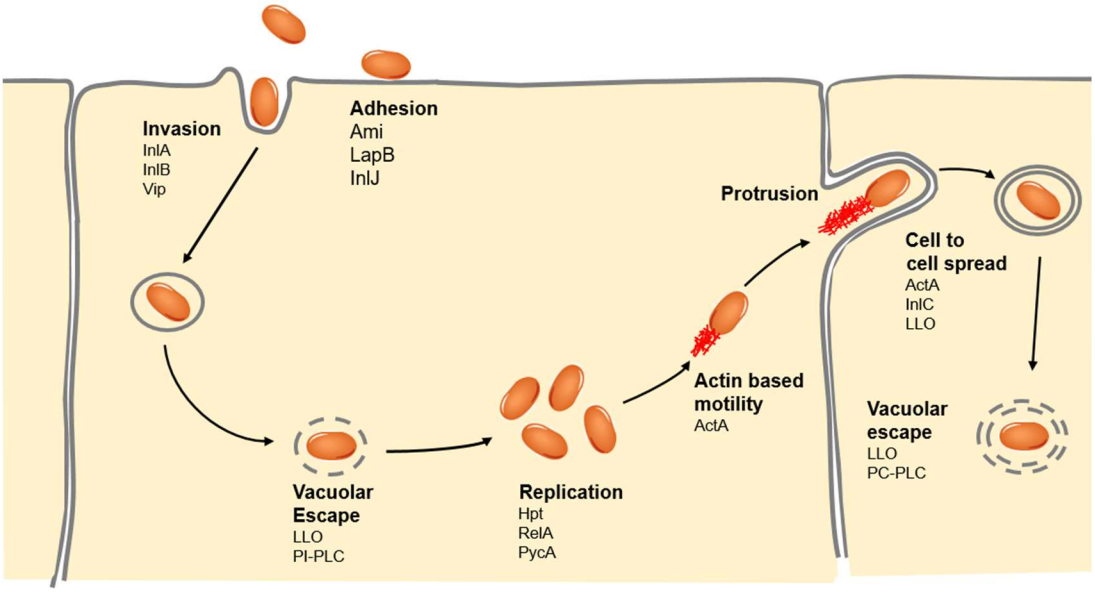

Figure 2. Cellular infection cycle of *L. monocytogenes*. The major virulence factors involved in the different steps of the cycle are indicated. Host actin is depicted in red.

A.4.1. Adhesion and entry

L. monocytogenes infection cycle starts with adhesion of the pathogen to the surface of the host cells. Multiple *L. monocytogenes* surface adhesins recognize and interact with specific host cell surface proteins (Bierne and Cossart, 2007; Camejo *et al.*, 2011), which promote intimate contact between the pathogen and the host cell target. This allows further interactions between surface *L. monocytogenes* proteins that mediate invasion with specific host cell receptors triggering the activation of signaling cascades that result in membrane

remodeling and bacterial engulfment by a zipper-like mechanism (Ham *et al.*, 2011). Entry of *L. monocytogenes* into non-phagocytic cells is extensively characterized (Radoshevich and Cossart, 2017). It is mainly mediated by two *L. monocytogenes* proteins that belong to the internalin family, namely internalin A (InlA) and internalin B (InlB), which interact with the host receptors E-cadherin and cMet, respectively (Mengaud *et al.*, 1996; Shen *et al.*, 2000). InlA and InlB were the first *Listeria* invasion proteins to be identified and are critical for the uptake of the pathogen by the host cells (Bierne *et al.*, 2007).

cMet is the receptor for hepatocyte growth factor (HGF) and is ubiquitously expressed in human cells (Organ and Tsao, 2011). E-cadherin expression is restricted to certain cell types (such as epithelial cells) where it participates in the formation of adherens junctions between epithelial cells that form barriers such as intestinal epithelia, placenta and the choroid plexus (a blood-cerebrospinal fluid barrier) (Disson and Lecuit, 2012; Doran *et al.*, 2013). The InlA/E-cadherin interaction is necessary and sufficient for *L. monocytogenes in vivo* crossing of the intestinal epithelia (Lecuit *et al.*, 2001; Nikitas *et al.*, 2011). On the other hand, crossing of the placenta requires the participation of both InlA and InlB (Lecuit *et al.*, 2004; Disson *et al.*, 2008). Interestingly, interaction of either internalins with the host receptors is species specific. Thus, while *L. monocytogenes* InlA does not recognize mouse E-cadherin, InlA/E-cadherin interplay is necessary for *L. monocytogenes* intestinal crossing in human, guinea pig, gerbil and humanized mouse models that harbor human E-cadherin (Doran *et al.*, 2013; Pan *et al.*, 2014). Similarly, cMet of human, mouse and gerbil recognizes and functions as a receptor for *L. monocytogenes* InlB, whereas rabbits and guinea pigs are not permissive to InlB /cMet mediated infection (Disson *et al.*, 2009).

A common theme in both InlA and InlB mediated internalization pathways is the usurpation of endogenous host molecular machinery by the pathogen. Accordingly, InlA interaction with E-cadherin elicits a signaling cascade similar to the one that occurs when E-cadherin molecules from adjacent cells interact with each other to form adherens junctions (Bonazzi *et al.*, 2009). Similarly, InlB functionally mimics HGF, the natural ligand of cMet (Pizarro-Cerdá *et al.*, 2012). The resultant signaling cascades triggered by both InlA and InlB elicit actin-mediated membrane remodeling that ultimately results in clathrin mediated *L. monocytogenes* internalization (Pizarro-Cerdá *et al.*, 2012), as will be described below.

A.4.1.1. InlA mediated entry

InlA is an 800 aminoacid protein that contains at its N-terminal 15 Leucine-rich repeats (LRRs) followed by an inter-repeat (IR) spacer region and a B-repeat domain. At its C-terminal,

InlA harbors a sorting peptide and an LPXTG motif that enables covalent anchoring of the protein to the bacterial cell wall (Kobe and Deisenhofer, 1994; Cabanes *et al.*, 2002; Bierne *et al.*, 2007). The LRR domain and the IR regions are required and sufficient to interact with E-cadherin and promote pathogen adhesion and internalization into epithelial cells (Lecuit *et al.*, 1997).

In the context of *L. monocytogenes* invasion, interaction of InlA with E-cadherin leads to the receptor clustering into lipid rafts, followed by tyrosine phosphorylation of the receptor by Src and posterior ubiquitination by Hakai (Fig 3) (Seveau *et al.*, 2004; Bonazzi *et al.*, 2008). Afterwards, the clathrin adaptor Dab2 is recruited to the *L. monocytogenes* entry site, favoring the recruitment of clathrin heavy and light chains, with Src-mediated phosphorylation of clathrin heavy chain being required for *L. monocytogenes* internalization (Bonazzi *et al.*, 2008; Bonazzi *et al.*, 2011). Furthermore, the actin-interacting proteins Hip 1R and Myosin VI are recruited to *L. monocytogenes* entry sites and are required for pathogen invasion (Bonazzi *et al.*, 2011). Interestingly, knockdown of Myosin VI does not prevent the recruitment of clathrin machinery proteins, nor accumulation of actin at *L. monocytogenes* entry site, indicating that the recruitment of this unconventional myosin occurs in later stages of the signaling cascade (Bonazzi *et al.*, 2011). Since myosin VI moves on actin filaments toward the minus ends, it was suggested that in the context of *L. monocytogenes* infection, myosin VI likely provides the pulling force required for bacterial internalization (Bonazzi *et al.*, 2011). Additional studies demonstrated that other components of clathrin mediated endocytosis are important for *L. monocytogenes* entry, in particular dynamin, which can recruit cortactin, an activator of the major actin nucleator Arp2/3 (Fig 3) (Veiga and Cossart, 2005).

Altogether, these observations indicate that clathrin-mediated endocytosis machinery is necessary for the promotion of an initial wave of actin polymerization at the *L. monocytogenes* internalization foci (Bonazzi *et al.*, 2011; Pizarro-Cerdá *et al.*, 2012). Following these events or concomitantly, a second wave of actin polymerization occurs during *L. monocytogenes* invasion (Pizarro-Cerdá *et al.*, 2012). Thus, E-cadherin-mediated Src activation leads to recruitment and phosphorylation of cortactin, which promotes the activation of Arp2/3 complex and actin polymerization (Fig 3) (Sousa *et al.*, 2007). Additionally, activation of Rac1 is also required for InlA dependent *L. monocytogenes* uptake, although the mechanism by which this small GTPase activates Arp2/3 remains unclear (Sousa *et al.*, 2007). Interaction between E-cadherin and actin filaments in adherens junctions is mediated by α and β catenins, among other proteins (Lecuit *et al.*, 2000). These catenins exhibit similar functions during *L. monocytogenes* infection, linking E-cadherin with actin and favoring bacterial internalization (Lecuit *et al.*, 2000). Furthermore, the transmembrane protein vezatin and its binding partner, the unconventional myosin VIIa, are found at adherens junctions and *L. monocytogenes* entry sites, together with actin, suggesting that vezatin acts as a molecular bond between myosin

VIIa and E-cadherin/catenins/actin complex (Sousa *et al.*, 2004). Accordingly, both myosin VIIa and vezatin are required for InlA/E-cadherin *L. monocytogenes* internalization (Sousa *et al.*, 2004).

A.4.1.2. InlB mediated entry

InlB (630 aa) contains 6 LRRs, an IR region and a B repeat. The InlB LRRs are necessary and sufficient to induce *L. monocytogenes* internalization into epithelial cells (Braun *et al.*, 1999). The C-terminal domain of InlB harbors three repeats of approximately 80 amino-acids each, that start with the dipeptide GW (hence GW repeats) (Braun *et al.*, 1997). These GW repeats mediate a non-covalent attachment of the protein to the lipoteichoic acids of the cell wall (Jonquières *et al.*, 1999; Percy *et al.*, 2016). Due to this fragile attachment, InlB that is attached to the cell surface can be released to the extracellular medium. Soluble and bacteria-bound InlB can stimulate cMet and elicit actin polymerization. In addition, soluble InlB can induce membrane ruffling and cell scattering (Braun *et al.*, 1999; Shen *et al.*, 2000).

InlB interacts with multiple cell surface proteins of the host that favor *L. monocytogenes* internalization, namely glycosamino-glycans (Jonquières *et al.*, 2001), the receptor of the globular head domain of the complement component C1q (gC1qR) (Braun *et al.*, 2000) and cMet (Shen *et al.*, 2000). The most relevant interaction for bacteria internalization occurs with cMet (Shen *et al.*, 2000), a tyrosine kinase receptor that is involved in several physiological processes such as migration, growth and development (Organ and Tsao, 2011).

cMet engagement by InlB promotes the receptor auto-phosphorylation in tyrosine residues followed by Cbl mediated ubiquitination (Fig 3) (Shen *et al.*, 2000; Veiga and Cossart, 2005). Similar to what was described above for InlA/E-cadherin, this initial engagement elicits an wave of actin polymerization that is dependent on recruitment and activation of clathrin machinery in the *L. monocytogenes* entry site (Veiga and Cossart, 2005; Veiga *et al.*, 2007; Bonazzi *et al.*, 2011; Pizarro-Cerdá *et al.*, 2012). Furthermore, cMet autophosphorylation also leads to recruitment and phosphorylation of adaptor proteins Shc, Gab1 and CrkII, which in turn promote the activation and recruitment of the p85 subunit of type IA phosphoinositide 3-kinase (PI3K) to the *L. monocytogenes* entry site (Ireton *et al.*, 1999; Shen *et al.*, 2000; Sun *et al.*, 2005). In turn, PI3K converts phosphoinositide-4,5-bisphosphate (PIP2) into phosphoinositide-3,4,5-trisphosphate (PIP3), which gets redistributed within lipid rafts at the plasma membrane (Seveau *et al.*, 2004; Seveau *et al.*, 2007). The accumulation of these phospholipids at the membrane leads to the recruitment and activation of the small GTPases Rac1 and/or Cdc42 (depending on cell type), which in turn activate WAVE1, WAVE2 and N-WASP, leading to Arp2/3 mediated actin polymerization that drives membrane remodeling and

bacterial internalization (Fig 3) (Bierne *et al.*, 2001; Bierne *et al.*, 2005). We have recently demonstrated that non-muscle myosin IIA (NMHC-IIA) limits *L. monocytogenes* infection (Almeida *et al.*, 2015). Additionally, we also observed that infection leads to Src-mediated tyrosine phosphorylation of NMHC-IIA at residue Y158. Abrogation of this phosphorylation site renders cells more susceptible to infection, highlighting the importance of this post-translational modification in the context of *L. monocytogenes* infection (Almeida *et al.*, 2015).

Successful *L. monocytogenes* internalization relies on a delicate equilibrium between actin polymerization and depolymerization events (Pizarro-Cerdá *et al.*, 2012). Cofilin, an actin depolymerization factor, is recruited to *L. monocytogenes* entry sites (Bierne *et al.*, 2001). Inactivation of this enzyme by phosphorylation of LIM kinase (LIMK) results in accumulation of actin filaments beneath *L. monocytogenes* in different cell lines and internalization failure, highlighting the importance of actin depolymerization in later stages of *L. monocytogenes* entry process (Bierne *et al.*, 2001; Pizarro-Cerdá *et al.*, 2012). Furthermore, the 5'-phosphatase OCRL controls actin polymerization events and bacterial entry by reducing the PIP2 and PIP3 pools at *L. monocytogenes* internalization foci (Kühbacher *et al.*, 2012). Accordingly, OCRL depletion in HeLa cells results in enhanced presence of actin, PIP2 and PIP3 at bacterial internalization site, which reflects in increased internalization levels of *L. monocytogenes* (Kühbacher *et al.*, 2012).

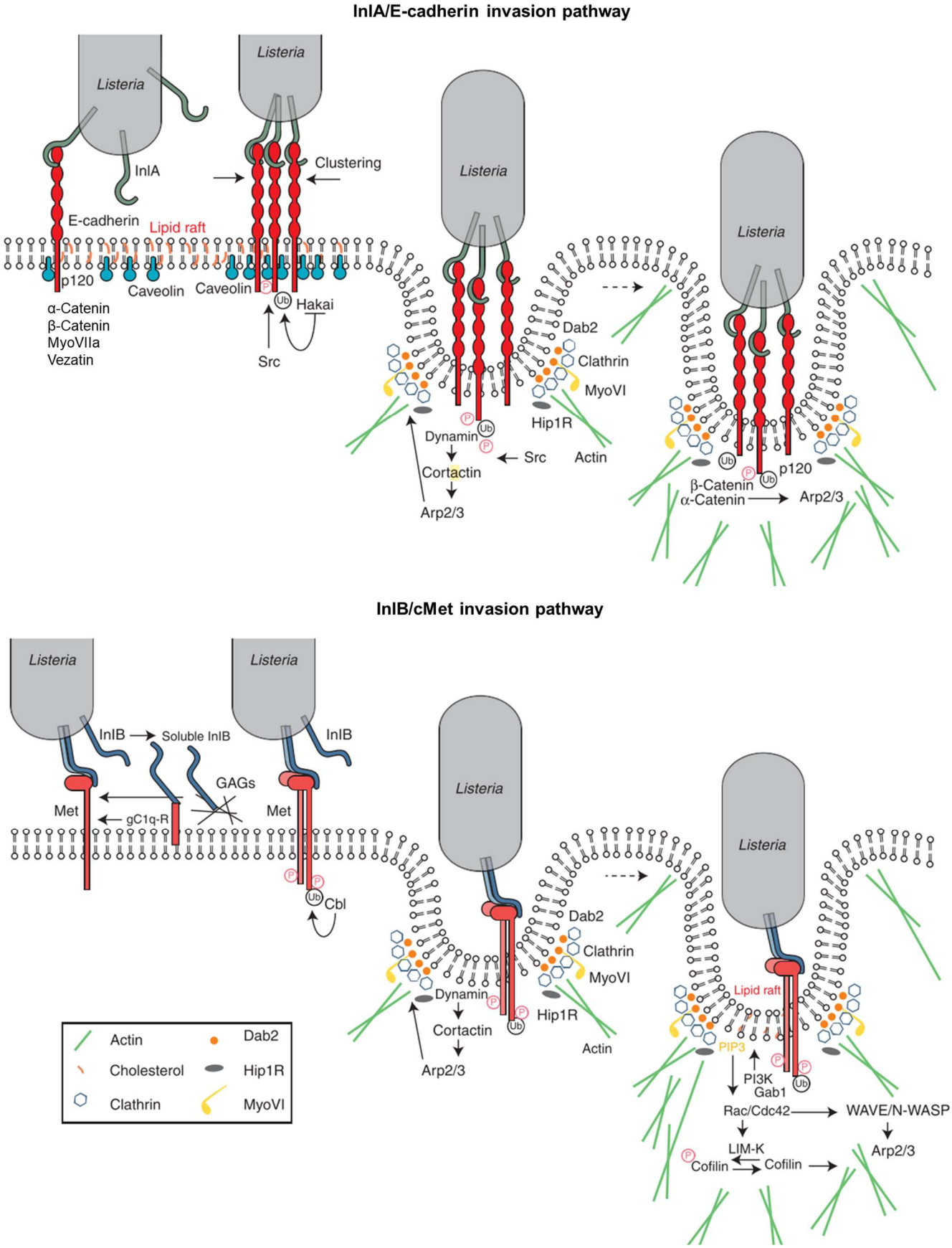

Figure 3. Schematic representation of InlA and InlB-mediated *L. monocytogenes* entry pathways in epithelial cells. Bacterial surface proteins InlA and InlB interact with the host receptors E-cadherin and cMet, respectively, triggering phosphorylation and ubiquitination of the receptors. The recruitment of clathrin

endocytosis machinery favours actin polymerization events at the pathogen entry site. Further stimulation of E-cadherin and cMet elicits Arp/3 activation, leading to actin polymerization events that drive the remodeling of the plasmatic membrane and enable *L. monocytogenes* internalization. Adapted from (Pizarro-Cerdá et al., 2012).

A.4.2. Escape from internalization vacuole

As a result of the internalization process, *L. monocytogenes* is enclosed within a single-membrane phagocytic vacuole (Tilney and Portnoy, 1989). Here, *L. monocytogenes* secretes the cytolysin listeriolysin O (LLO) and the phosphatidylinositol-specific phospholipase C (PI-PLC) to disrupt the compartment, allowing the escape of the bacterium into the host cell cytosol (Portnoy *et al.*, 1988; Camilli *et al.*, 1991; Smith, Marquis, *et al.*, 1995; Gedde *et al.*, 2000). LLO, the first *L. monocytogenes* virulence factor to be identified and characterized, is a cholesterol-dependent pore forming toxin that binds to vacuolar membranes as monomers that assemble into functional pore complexes (Peraro and Van Der Goot, 2016; Osborne and Brumell, 2017). Acidification of *L. monocytogenes* internalization vacuole enhances LLO activity, whereas the toxin is less active at neutral pH of the cytosol, thus minimizing toxin induced host cell damage (Beauregard *et al.*, 1997). In addition, LLO contains a PEST-like sequence that targets the toxin to degradation once it reaches the host-cell cytosol (Dacatur and Portnoy, 2000; Schnupf *et al.*, 2006). Escape from the phagocytic vacuole is a critical step of *L. monocytogenes* intracellular lifecycle. Indeed, bacteria that lack LLO exhibits impaired intracellular replication rates and attenuated virulence in *in vivo* models (Portnoy *et al.*, 1988; Cossart *et al.*, 1989). Together with phosphatidylcholine-specific phospholipase C (PC-PLC), LLO is also involved in the rupture of the double membrane vacuole that is resultant from the bacteria cell to cell spread (Smith, Marquis, *et al.*, 1995; Gedde *et al.*, 2000).

In addition to its role in vacuolar evasion by bacteria, other functions have been attributed to LLO (Osborne and Brumell, 2017). Thus, extracellular LLO promotes *L. monocytogenes* internalization in certain cell types (Vadia *et al.*, 2011), induce apoptosis during infection (Rogers *et al.*, 1996; Guzmán *et al.*, 1996), stimulates production of proinflammatory cytokines, promotes histone modifications and activates several signaling pathways of the host such as ERK-1, c-Jun, p38 and MEK-MAP kinases (Hamon *et al.*, 2012). Interestingly, a significant part of these effects are consequence of the calcium influx that occurs when the LLO pores are established in the cell membrane (Hamon *et al.*, 2012). Furthermore, when present in the cellular cytosol, LLO elicits mitochondrial fragmentation and damage of the endoplasmic reticulum (Gekara *et al.*, 2007; Stavru *et al.*, 2011; Mesquita, Brito, Cabanes, *et al.*, 2017; Mesquita, Brito, Mazon Moya, *et al.*, 2017), increases degradation of host proteins in a SUMO dependent manner (Ribet *et al.*, 2010) and enhances inflammasome

activation (Theisen and Sauer, 2016). Additionally, LLO-mediated plasma membrane damage is exploited by *L. monocytogenes* to promote cell-to-cell spread of the pathogen (Czuczman *et al.*, 2014), as I will discuss bellow. Finally, it was recently shown that the endoplasmic reticulum chaperone Gp96 and myosin IIA interact upon LLO exposure and coordinate plasma membrane blebbing. Accordingly, both proteins protect the plasma membrane integrity from *L. monocytogenes* infection and LLO intoxication, with Gp96 promoting survival of zebrafish infected with *L. monocytogenes* (Mesquita, Brito, Cabanes, *et al.*, 2017; Mesquita, Brito, Mazon Moya, *et al.*, 2017).

A.4.3. Intracellular life, actin-based motility and intercellular spread

Upon successful escape from the internalization vacuole, *L. monocytogenes* adjusts its transcriptional program to promote intracellular growth and cell-to-cell spread (Chatterjee *et al.*, 2006; Camejo *et al.*, 2009). For that, intracellular *L. monocytogenes* expresses multiple genes that allow the exploitation of host cell metabolic resources such as glucose (Chico-Calero *et al.*, 2002; Eylert *et al.*, 2008; Camejo *et al.*, 2009), oligopeptides (Borezee *et al.*, 2000), and iron (Olsen *et al.*, 2005). Furthermore, intracellular *L. monocytogenes* upregulates genes associated with stress response, protein synthesis, cell division and multiplication (Chatterjee *et al.*, 2006; Camejo *et al.*, 2009). Altogether, these adaptations allow the bacterium to thrive within the cell, with intracellular *L. monocytogenes* exhibiting a doubling time similar to that observed in pure culture (Portnoy *et al.*, 2002).

One of the hallmarks of *L. monocytogenes* infection is the pathogen capacity to promote its own motility within the host cellular cytosol. For that, *L. monocytogenes* exploits the host actin polymerization machinery through the activity of ActA, a major *L. monocytogenes* virulence factor that is required and sufficient for *L. monocytogenes* actin-based motility (Kocks *et al.*, 1992; Domann *et al.*, 1992; Pistor *et al.*, 1994). Expression of ActA is enhanced upon bacterial escape from the phagocytic vacuole into the host cell cytosol (Moors *et al.*, 1999). ActA is anchored to the *L. monocytogenes* surface and at earlier time points of *L. monocytogenes* cytosolic life is found homogeneously distributed around the bacteria surface, leading to the formation of an actin cloud (Fig 4) that surrounds the bacteria (Rafelski and Theriot, 2006). Later on, ActA distribution is shifted into a single pole, leading to the formation of an actin rich, comet tail like structure (Fig 4) that is the result of polarized actin polymerization and depolymerization events that drive the unidirectional propulsion of intracellular *L. monocytogenes* (Kocks *et al.*, 1992; Smith, Portnoy, *et al.*, 1995). ActA induces actin polymerization by mimicking the activity of the host WASP proteins, leading to the direct activation of the Arp2/3 complex and subsequent actin polymerization (Welch *et al.*, 1997; Welch *et al.*, 1998; Boujemaa-Paterski *et al.*, 2001). It is noteworthy that ActA can also

participate in other aspects of *L. monocytogenes* pathogenesis, namely cell invasion and autophagy evasion (Suárez *et al.*, 2001; Yoshikawa *et al.*, 2009; Vadia *et al.*, 2011; Travier *et al.*, 2013).

While it has been generally considered that this ActA-mediated actin polymerization generates force by the protrusion of the growing actin filaments, recent evidence proposes that, in alternative, *L. monocytogenes* intracellular propulsion can be driven by large scale deformation of the actin network (David and Cossart, 2017). Indeed, cryo-electron tomography studies of *L. monocytogenes* comet tails show the presence of F-actin bundles that are perpendicular to the direction of motion (Jasnin *et al.*, 2013). Additionally, the bacteria surface exhibits tangentially orientated F-actin filaments. Altogether, these observations indicate that *L. monocytogenes* elicits deformation of the actin network, propelling the pathogen through the cytoplasm (David and Cossart, 2017).

L. monocytogenes-induced actin-based motility also enables the formation of bacterial-containing host plasma membrane protrusions (Fig 4) that can penetrate adjacent cells, thus allowing the dissemination of the pathogen (Kocks *et al.*, 1995). In this context, *L. monocytogenes* secreted protein InlC facilitates cell-to-cell spread by weakening the cortical tension of the host cell (Rajabian *et al.*, 2009). It has been recently shown that *L. monocytogenes* also promotes cell spreading by exploiting the efferocytosis process, in which macrophages engulf dead or dying cells. For that, secreted LLO damages the protrusion membrane, which leads to surface exposition of the lipid phosphatidylserine present in the inner leaflet of the plasma membrane. These phosphatidylserine-presenting protrusions will then be recognized and uptaken by neighboring macrophages, where significant replication of *L. monocytogenes* occurs (Czuczman *et al.*, 2014).

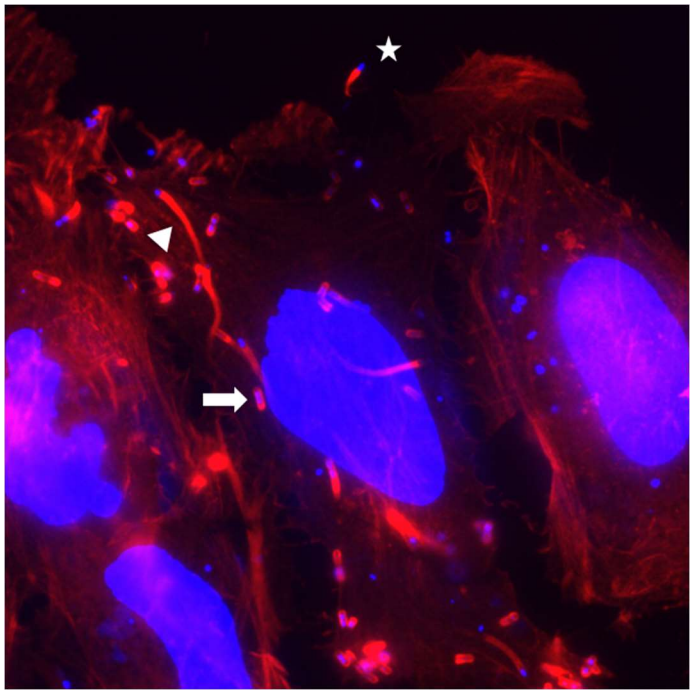

Figure 4. *L. monocytogenes*-infected HeLa cells exhibiting actin comet tails (arrowhead), actin clouds (arrow) and protrusions (star). Image from Molecular Microbiology Group. Red: Actin. Blue: DNA.

A.4.4. Cytoskeleton manipulation by *Listeria* infection

The cytoskeleton of the host cell is a common target of pathogens such as *L. monocytogenes* (Bhavsar et al., 2007). As described above, *L. monocytogenes* exploits the actin network to invade and disseminate in the host cells. It is important to note that *L. monocytogenes* does not interact directly with actin but rather interfere with effectors that control actin polymerization (Bhavsar *et al.*, 2007). This is also true for other pathogens that exploit actin cytoskeleton for their benefit. The involvement of actin in *L. monocytogenes* infection is extensively studied. While less characterized than actin, participation of other cytoskeletal components in *L. monocytogenes* pathogenesis has been reported (Bhavsar *et al.*, 2007). For instance, microtubules interact with dynamin-2, a GTPase involved in endocytic vesicle formation and modulation of microtubule dynamics (Radhakrishnan and Splitter, 2012). In turn, dynamin-2 co-localizes with *L. monocytogenes* actin comet tails (Henmi *et al.*, 2011) and its depletion in HeLa cells results in slower and shorter actin comets tails. This phenotype can be rescued by disruption of the microtubule network, suggesting that microtubules are involved in controlling the dynamics of *L. monocytogenes* actin comet tail (Henmi *et al.*, 2011). Microtubules also interact with stathmin, a protein that destabilizes the microtubule network (Maucuer *et al.*, 1995). In its turn, stathmin associate with LaXp180, a mammalian protein that

interacts with *L. monocytogenes* ActA, as determined by a yeast two-hybrid screen network (Maucuer *et al.*, 1995; Pfeuffer *et al.*, 2000). Whether *L. monocytogenes* mediated recruitment of stathmin has an impact on actin rearrangements at the comet tail and influence on *L. monocytogenes* movement and spread remains to be determined (Radhakrishnan and Splitter, 2012).

A growing body of evidence suggests that septins are important players in *L. monocytogenes* pathogenesis (Torraca and Mostowy, 2016). Septins are a family of GTP-binding proteins that are involved in regulation of membrane remodeling, cytokinesis and cytoskeleton dynamics (Rolhion and Cossart, 2017). Septins associate with cellular membrane to form nonpolar filaments, bundles or rings. Additionally, septins interact with microtubules and actin filaments (Mostowy and Cossart, 2012). Septins are recruited to *L. monocytogenes* entry site and are required for its internalization (Mostowy, Nam Tham, *et al.*, 2009; Mostowy, Danckaert, *et al.*, 2009). Recruitment of septins to *L. monocytogenes* entry foci is dependent on previous actin rearrangements, as treatment of cells with cytochalasin D, an actin polymerization inhibitor, inhibits septin recruitment (Huang *et al.*, 2008; Mostowy, Nam Tham, *et al.*, 2009). Adding complexity to these observations, different septins have opposite outcomes in *L. monocytogenes* internalization, with SEPT2 contributing to bacterial invasion whereas SEPT11 blocks it (Mostowy, Nam Tham, *et al.*, 2009; Mostowy, Danckaert, *et al.*, 2009). Septin rings are also found surrounding actin comet tails, although their function is unclear in this context (Mostowy *et al.*, 2010).

The participation of intermediate filaments cytoskeletal network in *L. monocytogenes* infection is poorly characterized. Vimentin was reported to influence motility parameters of intracellular *L. monocytogenes* such as speed fluctuations and turning behavior (Giardini and Theriot, 2001). A recent report indicates that vimentin is important for *L. monocytogenes* entry and colonization of the mouse brain (Ghosh *et al.*, 2018). The authors demonstrated that interaction of the *L. monocytogenes* protein InlF with vimentin that is present at the surface of cells such as fibroblasts, human cerebral microvascular endothelial cells (hCMEC), and bEnd.3 mouse brain endothelial cells, is required for successful *L. monocytogenes* infection. Additionally, vimentin knockout mice display reduced bacterial burden in the brain and spleen (Ghosh *et al.*, 2018). Despite these observations, the study of the relevance of IFs in *L. monocytogenes* pathogenesis is in its infancy.

B. Intermediate filaments

B.1. General properties

Metazoan cells are characterized by the presence of three major cytoskeletal networks that are interconnected and influence most aspects of cell life: microtubules, microfilaments and intermediate filaments (IFs) (Fletcher and Mullins, 2010). In addition, and although still understudied, septins are increasingly recognized as the fourth component of the cytoskeleton (Mostowy and Cossart, 2012).

Microfilaments and microtubules are assembled from monomers of globular (G)-actin and hetero-polymers of α/β-tubulin, respectively, and form polar networks that are used as tracks by molecular motors such as myosins and dynein (Huber *et al.*, 2015). IFs, on the other hand, are assembled from a diverse group of fibrous polymers that form non-polar filaments. This lack of polarity makes IFs unsuitable substrates for molecular motors (Herrmann *et al.*, 2009; Margiotta and Bucci, 2016). As the nomenclature indicates, IFs fibers exhibit a diameter of intermediate size of approximately 10 nm, while microfilaments and microtubules diameter are 5-8 nm and 25nm, respectively (Fig 5) (Omary *et al.*, 2006).

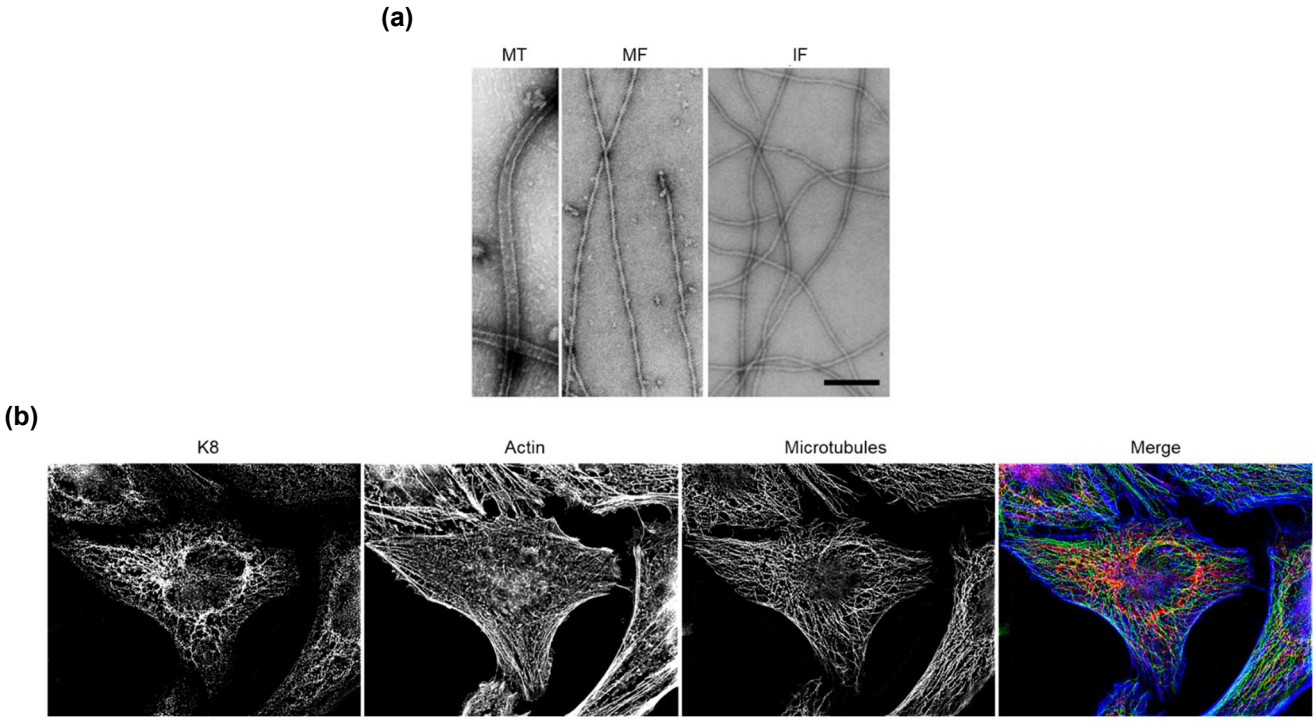

Figure 5. The cytoskeleton networks *in vitro* and in HeLa cells. (a) Transmission electron microscopy images of microtubules (MT), microfilaments (MF) and intermediate filaments (IF) reconstituted *in vitro*. The differences of the networks diameter are visible. Scale bar: 100 nm. Adapted from (Herrmann *et al.*, 2009). (b) Staining of the three networks in HeLa cells. Image from Molecular Microbiology Group. Green: microtubules. Red: K8. Blue: Actin.

The three filamentous systems are intimately connected and in constant communication. Cytolinker proteins as plectin and BPAG1 form cross-bridges linking microtubules, microfilaments and IFs (Fig 6) (Sonnenberg and Liem, 2007; Castañón *et al.*, 2013). Furthermore, the protein complex LINC (linker of nucleoskeleton and cytoskeleton) anchors the nuclear IFs (termed lamins) to microfilaments, microtubules and cytoplasmic IFs (Fridkin *et al.*, 2009). Interaction between the different filamentous systems can also be mediated by motor proteins such as dyneins, kinesins and myosins (Fig 6) (Huber *et al.*, 2015). Direct interactions between the cytoskeletal filaments has also been reported (Hisanaga and Hirokawa, 1990; Esue *et al.*, 2006; Huber *et al.*, 2015). As a result of this deep crosstalk, perturbation of one cytoskeleton network frequently reflects in the dynamics and organization of the others (Leduc and Etienne-Manneville, 2015; Huber *et al.*, 2015).

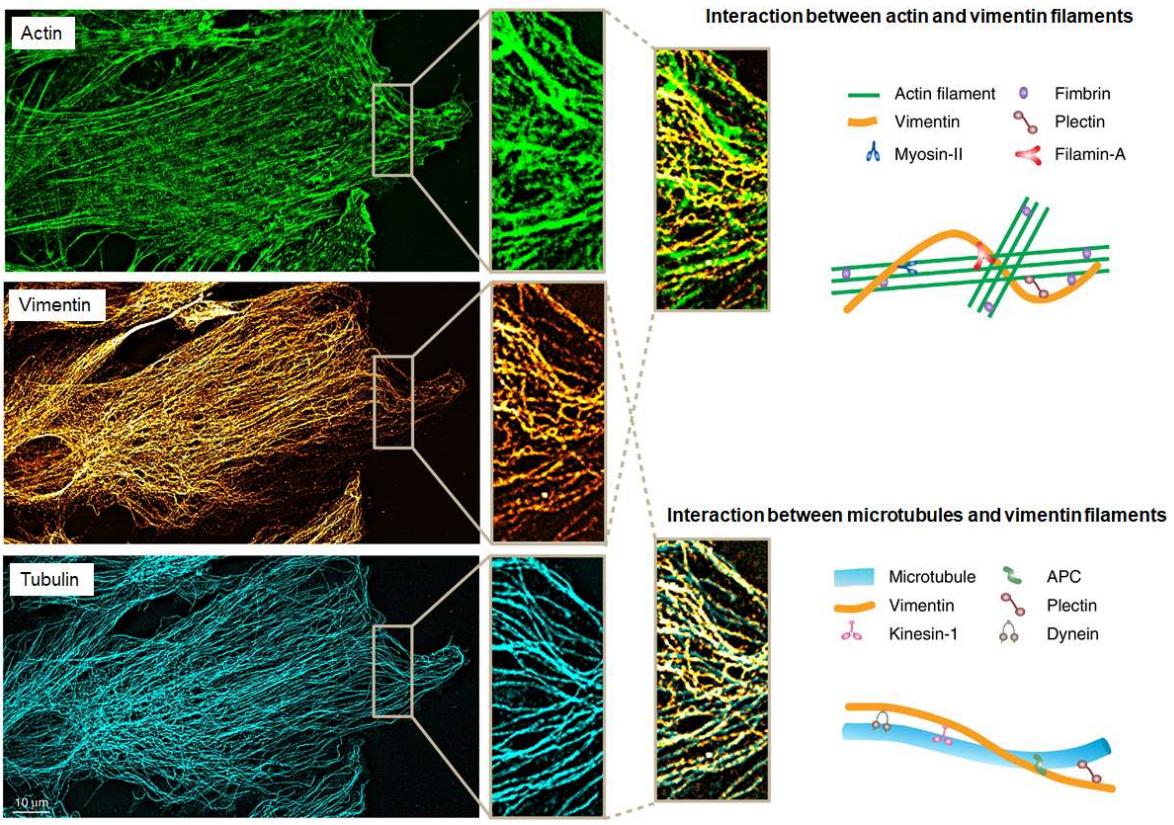

Figure 6. Interplay between cytoskeletal networks and associated proteins. Astrocyte stained for actin (green), vimentin (gold) and tubulin (blue). In the high magnification insets, regions of signal co-localization of vimentin with actin or microtubules are visible. Scale bar: 10 µm. The right panels exemplify some of the cytoskeleton interactions mediated by molecular bridges as plectins and motor proteins. Adapted from (Leduc and Etienne-Manneville, 2015).

B.2. Distribution in cells and tissues

IFs were first described in skeletal muscle cells in the late 1960s (Ishikawa *et al.*, 1968). They form an extensive and intricate network that connects the cell cortex to intracellular organelles, providing structural and organizational support for the cytoplasm and nucleus of mammalian cells (Erber *et al.*, 1998; Lee and Coulombe, 2009). With at least 70 encoding genes, IFs are one of the largest protein families in mammalians (Kim and Coulombe, 2007; Szeverenyi *et al.*, 2008). IFs are grouped into six classes, according to primary sequence similarities, and their expression is cell and tissue specific (Fig 7) (Herrmann *et al.*, 2007). Type 1 (acidic) and type 2 (basic) IFs constitute the keratin subfamily which are typically expressed in epithelia (Bragulla and Homberger, 2009). Type 3 IFs are the most heterogeneous group and include desmin, peripherin, glial fibrillary acidic protein (GFAP) and vimentin. Peripherin is found in neurons of the peripheral and central nervous system, while desmin is restricted to muscle cells (Paulin and Li, 2004; Yuan *et al.*, 2012). Vimentin is the most widely distributed IF protein and can be found in some hematopoietic, epithelial and mesenchymal cells, as well endothelia of blood vessels (Kornreich *et al.*, 2015). Type 4 IFs are constituted by nestin, syncoilin, synemin, α-internexin and neurofilament (NF) triplet proteins (NF-L, NF-M, NF-H). The NF triplet and α-internexin are found in neurons (Benson *et al.*, 1996), syncoilin in skeletal and cardiac muscle cells, synemin in muscle cells (Olivé *et al.*, 2003) and nestin is expressed in neuronal stem cells (Lendahl *et al.*, 1990). Type 1-4 IFs are cytoplasmic proteins. In contrast, type 5 IFs, lamins, are found exclusively in the nucleus of all nucleated cells, were they ensure structural integrity of the organelle (Dechat *et al.*, 2008). Finally, type 6 IF was recently added to the IF family and includes two proteins (phakinin and filensin) that are present only in differentiated lens fiber cells (FitzGerald *et al.*, 2016).

(a)

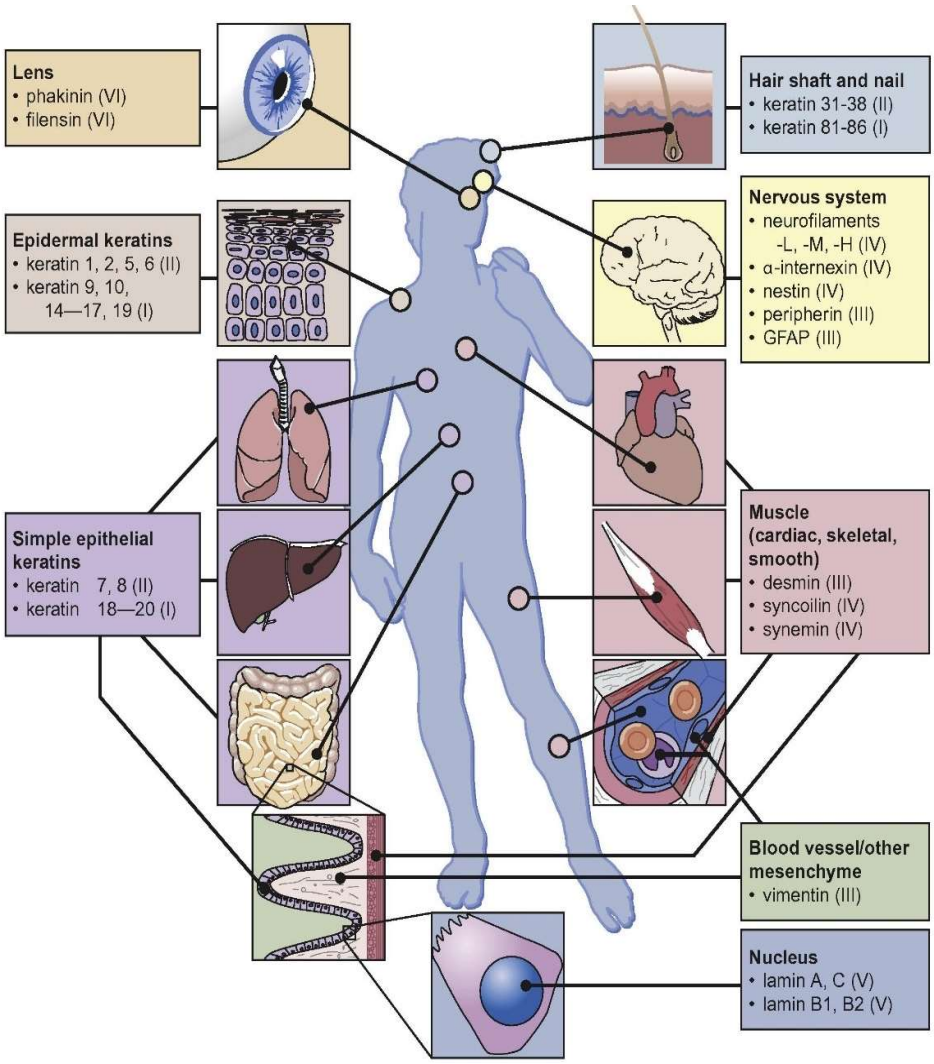

(b)

IF type	IF protein	# of genes	Tissue/ cell distribution	Associated diseases
I and II	Acidic and basic keratins	28 and 26	Simple and stratified epithelia, hair, nails	Skin disorders (e.g. EBS), hair and nail disorders, liver disease, pancreatitis
III	Vimentin GFAP Peripherin Synchoilin Desmin	1 1 1 1 1	Mesenchyma Astrocytes, glia Neurons Muscle Muscle	Cataract Alexander disease ALS None reported Myopathies
IV	Neurofilaments Nestin Synemins Alpha-internexin	3 1 1 (2 variants) 1	Neurons Neural stem cells Muscle Neurons	Pakinsons disease, Charcot-Marie-Tooth disease None reported None reported None reported
V	Lamins	3	All nucleated cells	Muscular dystrophies, lipodystrophy, cardiomopathy, axonal neuropathy
VI	Phakinin Filensin	1 1	Ocular lens Ocular lens	Cataract Cataract

Figure 7. The intermediate filaments (IF) family overview and associated pathologies. (a) Distribution of IF proteins in the human body areas. The same cell type /tissue system can harbor multiple types of IFs. Adapted from (Kornreich et al., 2015) (b) Detailed view of IF proteins distribution by type, their cellular/ tissue

presence and involvement in some human diseases. Based on (Chung et al., 2013; Snider and Omary, 2014; Leduc and Etienne-Manneville, 2015) and www.interfil.org

B.3. Structure, assembly and regulation

While IFs have distinct primary sequences, they share common domain organization (Herrmann *et al.*, 2007). IFs harbor a tripartite structural organization, consisting of an α-helical central “rod” domain that is flanked by non-helical N-terminal (“head”) and C-terminal (“tail”) domains (Herrmann *et al.*, 2009). The size and sequence of the rod domain is generally conserved across IFs, while the head and tail domains are highly variable (Parry *et al.*, 2007). Contrarily to microtubules and F-actin, the three dimensional structure of IFs is still not fully characterized (Chernyatina *et al.*, 2015). The crystal structure characterization of IFs has been challenging, due to IF characteristic propensity to associate and form filaments, high insolubility and lack of assembly inhibitors (Kim and Coulombe, 2007). Nevertheless, the existing crystallographic studies and *in silico* structural predictions indicates that the rod domain contains three α-helical segments interconnected by linkers (Fig 8). The first two segments mainly contain heptad repeats resulting in a left-handed coiled coil, while the third segment exhibits hendecad periodicity that favors the formation of a parallel coil (Chernyatina *et al.*, 2015; Kornreich *et al.*, 2015). These structural features allow the parallel association of IF monomers into dimers, the basic building blocks of filament assembly. These dimers in turn assemble in an anti-parallel fashion, forming a half-staggered tetramer. Tetramers then associate laterally to form 60 nm unit length filaments (ULF) which will quickly (within seconds in *in vitro* conditions) anneal longitudinally and be radially compacted to create the characteristic ~10 nm thick, rope-like filament that compose the IF network (Fig 8) (Herrmann *et al.*, 2002; Strelkov *et al.*, 2003; Margiotta and Bucci, 2016).

Focal adhesion sites at cell periphery appear to be hotspots for formation of vimentin and keratins precursors (Windoffer *et al.*, 2006; Kölsch *et al.*, 2009; Burgstaller *et al.*, 2010). Furthermore, actin promotes keratin network assembly by retrograde (centripetal) transport of the keratin precursors that are found in the focal adhesion sites, resulting in the formation of thicker bundles towards the cell nucleus (Fig 9) (Windoffer *et al.*, 2006; Kölsch *et al.*, 2009; Windoffer *et al.*, 2011). The polymerization and assembly of IF filaments is regulated by different signaling molecules such as 14-3-3 adaptor proteins, heat shock proteins and multiple kinases and phosphatases (Magin *et al.*, 2007; Bragulla and Homberger, 2009).

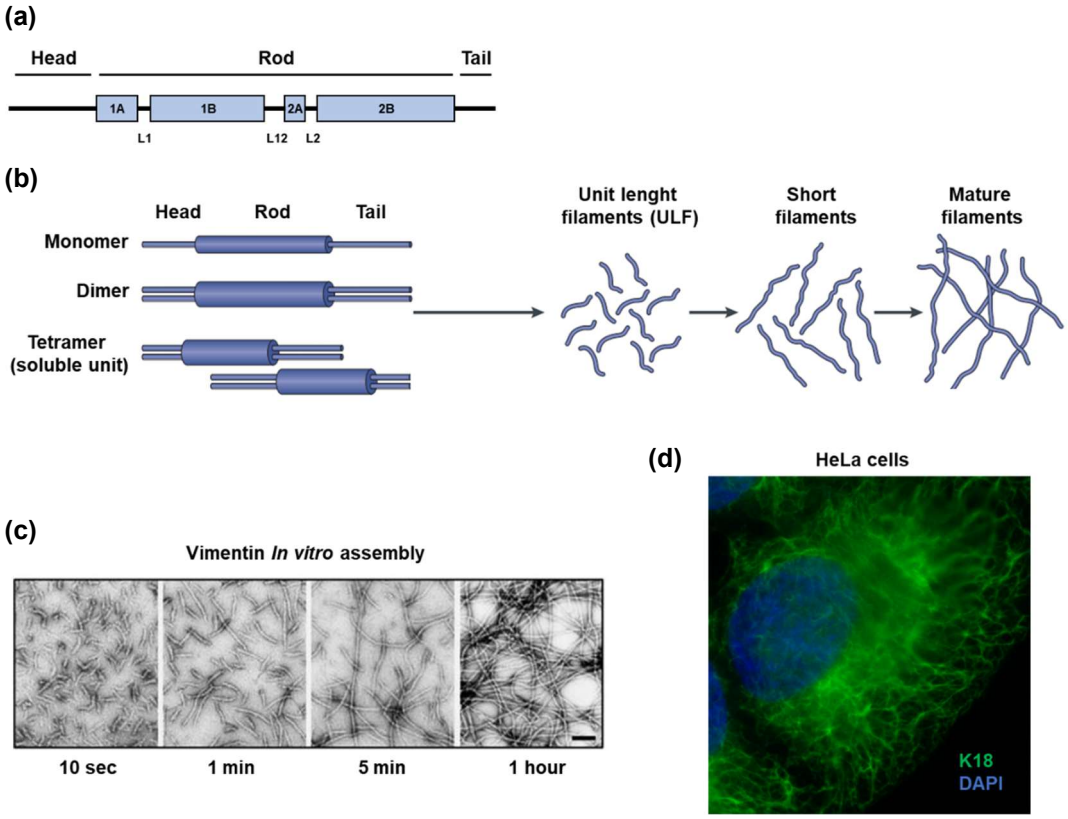

Figure 8. Assembly of cytoplasmic IFs. (a) Schematic representation of K18 domain structure. Non-helical head and tail domains flank an α-helical, central rod domain. The different segments of the rod-domain are interconnected by linkers. Based on www.interfil.org. (b) Depiction of sequential events leading to formation of IF network. IF dimers associate, forming tetramers that by further association will form the IF network. Adapted from (Snider and Omary, 2014) (c) Negative-stain electron microscope images of vimentin IF assembly throughout time, depicting the fast pace at which IFs assemble and form networks. Adapted from (Lowery *et al.*, 2015). (d) Immunofluorescence microscopy image of HeLa stained for K18. Image from Molecular Microbiology Group. K18 in green, nucleus in blue.

It is noteworthy that while the rod domain is crucial for formation of IFs dimers, the presence of the head and tail domains is critical for tetramer formation and further filament assembly and organization (Kornreich *et al.*, 2015). Dimer association is thus a requisite for IF network formation. This association can be homodimeric (e.g., vimentin). It can also be heterodimeric, as in type 3 IFs (vimentin and desmin (Quinlan and Franke, 1982)) and between type 3 and type 4 IFs (for example vimentin and neurofilaments (Monteiro and Cleveland, 1989)). Finally, keratin IFs are resultant from obligate heterodipolymerization between acidic and basic keratins in equimolar quantities (Miller *et al.*, 1993). Human cells can thus contain at least two IF networks, one nuclear and another in the cytoplasm, with a single cell being able to express multiple IFs (Herrmann *et al.*, 2009; Gruenbaum and Aebi, 2014). Due to their ubiquitous expression, IFs can constitute up to 5% of total protein content in certain cell types/tissues (Zhong *et al.*, 2004; Toivola *et al.*, 2010).

IFs constitute highly dynamic networks that can be rapidly disassembled and reassembled according to cellular needs, thus providing plasticity to the cytoskeleton (Kim *et al.*, 2015). Network remodeling occurs during physiological and pathophysiological events such as mechanical and non-mechanical stress, mitosis, apoptosis, and in response to mutations (Fig 9) (Snider and Omary, 2014). Filament reorganization is driven by interaction of IFs with other proteins and by post-translational events, namely phosphorylation (Green *et al.*, 2005; Snider and Omary, 2014). Phosphorylation of IFs, which typically occurs at Ser/Thr residues located in the head and tail domains, generally promote IF solubility, which is a requirement for maintenance of filament structural dynamics (Omary *et al.*, 2006; Snider and Omary, 2014).

In general IFs are stable proteins and their half-life ranges from 15 hours to vimentin, up to four days for Keratin 8 (K8) and Keratin 18 (K18) (Denk *et al.*, 1987; Podolin and Prystowsky, 1991). Degradation is mediated by ubiquitin-proteasome pathway (Rogel *et al.*, 2010).

Expression of cytoplasmic IF proteins is tightly regulated during embryonic development and cellular differentiation (Schweizer *et al.*, 2006; Toivola *et al.*, 2010; Margiotta and Bucci, 2016). Examples include neurofilament expression during generation of neuronal structures (Cochard and Paulin, 1984), vimentin transient expression in developing muscle tissue and neuronal regions (Sax *et al.*, 1989; Kommata and Dermon, 2017), shift of K5/K14 expression to K1/K10 in maturing keratinocytes (Coulombe *et al.*, 1989; Byrne *et al.*, 1994) and nestin transient expression in dividing cells during development or regeneration of central and peripheral nervous system (Michalczyk and Ziman, 2005). Due to this development-specific pattern of expression, keratins are widely used as diagnostic markers in tumor pathology, as epithelial malignancies usually exhibit keratin expression patterns that are similar to their respective cells of origin (Karantza, 2010).

The diversity of elements and the temporal and spatial regulation of IF expression point to functional differences between IF family members (Schweizer *et al.*, 2006). Research of IF functions has been challenging due to several reasons. There are no drugs that specifically target IFs, and model organisms such as drosophila and yeast cannot be used as they lack IFs. Furthermore, the study of a single IF can be hindered by the frequent presence of multiple IFs in a single cell, promiscuity of IFs at the dimerization stage and compensatory functions by other IF members (Oshima, 2007; Leduc and Etienne-Manneville, 2015; Salas *et al.*, 2016). Different approaches have been applied to circumvent the limitations described above and they include utilization of truncated dominant negative constructs that lead to the collapse of the IF network and knockdown/knockout of IFs in cell lines and mice, respectively. IFs decrease itself can be technically challenging, as knockout mice can be embryonically lethal or display mild phenotypes due to IF redundancy. To minimize this, researchers have

performed simultaneous depletion of all IF proteins and use cell types that harbor minimal number of IF proteins, thus preventing IF redundancy (e.g., hepatocytes, which only express K8 and K18 (Omary *et al.*, 2002; Leduc and Etienne-Manneville, 2015; Salas *et al.*, 2016).

(a)

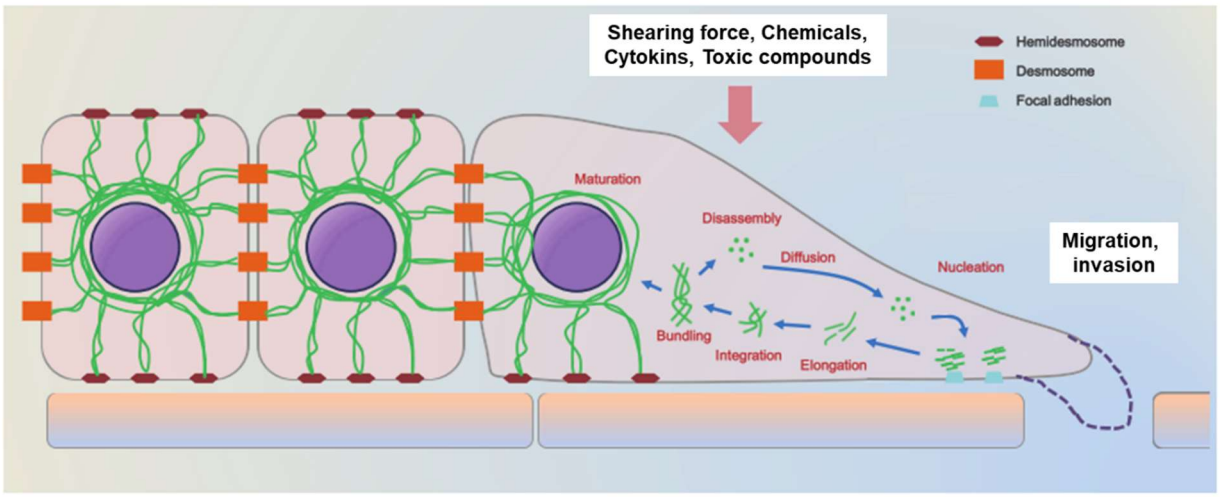

(b)

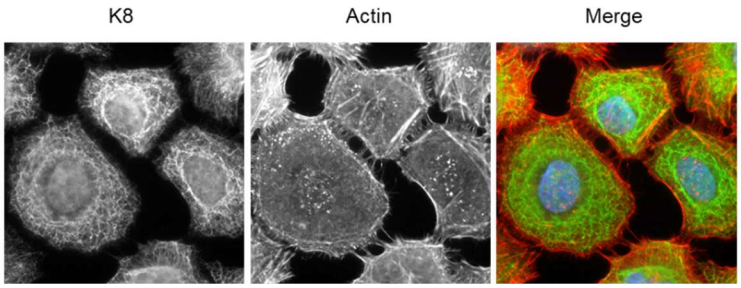

Figure 9. The keratin assembly and disassembly cycle. (a) Soluble keratin precursors nucleate in the cell periphery, at the vicinity of focal adhesion sites. These particles elongate, while moving towards the cell center in an actin-dependent manner. The particles further integrate and bundle as they are transported towards the perinuclear region. Here, they can maturate, forming a stable perinuclear cage. Network breakdown and reorganization can be triggered by multiple events such as mitosis, cell migration and different types of stress. The soluble particles can afterwards be used for another round of keratin network formation. Adapted from (Kim *et al.*, 2015) (b) Expression pattern of Keratin 8 in HeLa cells. K8 forms an intricate meshwork that spans the entire cell area. Network assembly usually results in thicker keratin bundles in the perinuclear region (as observed in the upper right side cells). Image from Molecular Microbiology Group. Green: K8. Red: Actin. Blue: DNA.

Decades of research demonstrate that IFs are crucial for the maintenance of cellular and tissue structural support and resilience to mechanical and non-mechanical stress (Herrmann *et al.*, 2009). In addition, it is also becoming evident that IFs are important players in governing signaling mechanisms that determine major aspects of cell life such as differentiation, replication, metabolism, apico-basal polarization, protein synthesis, innate immunity, motility and death (Pan *et al.*, 2012; Salas *et al.*, 2016). Importantly, IFs regulation

by post-translational modifications (e.g. phosphorylation, O-glycosylation, sumoylation and ubiquitination) (Chung *et al.*, 2013) and their interaction with multiple proteins as kinases, phosphatases and adaptor proteins (Green *et al.*, 2005; Toivola *et al.*, 2005), are primary determinants in regulating IFs functional aspects (Hyder *et al.*, 2008). I will describe next some of the major functions of IFs in general and keratins in particular.

B.4. Mechanical functions of IFs

The abundance and ubiquitous nature of IFs already suggests that these proteins are important for architectural homeostasis of the cell (Oshima, 2007). IFs anchor to sites of cell-cell and cell-extracellular matrix (ECM) contact, the desmosome and hemidesmosome, respectively (Fig 10). These interactions, together with IF association with intracellular organelles such as the nucleus, confer mechanical continuity across the cell and tissue, thus favoring structural resilience to mechanical tensions (Haines and Lane, 2012; Hol and Etienne-Manneville, 2015). The micromechanical properties of IFs also contribute to their role in ensuring cellular and tissue integrity, as IFs (in contrast to microtubules and microfilaments) are highly viscoelastic, being able to bend and recover quickly from deformation without breakage (Magin *et al.*, 2007).

IFs mutations or absence thus compromise the cell and tissue structural integrity, rendering them more susceptible to mechanical pressures. Earlier studies demonstrated that hepatocytes deficient for K8, K18 or expressing a mutant K18 exhibited higher fragility upon manipulation of the cell (Ku *et al.*, 1995; Loranger *et al.*, 1997; Ku and Omary, 2006). Furthermore, mice harboring mutations in the rod-domain of K14 display disruption of the keratin network in subsets of epidermal cells and exhibit skin blistering upon trauma (Vassar *et al.*, 1989; Vassar *et al.*, 1991). Interestingly, the phenotypes displayed by these animals are remarkably similar to the symptoms exhibited by human patients with the disease epidermolysis bullosa simplex (EBS), which was indeed associated with lack of K14 expression or presence of point mutations in K14 or its partner, K5 (Coulombe *et al.*, 1991; Lane *et al.*, 1992; Chan *et al.*, 1994). EBS was the first IF disease to be identified and characterized (Oshima, 2007).

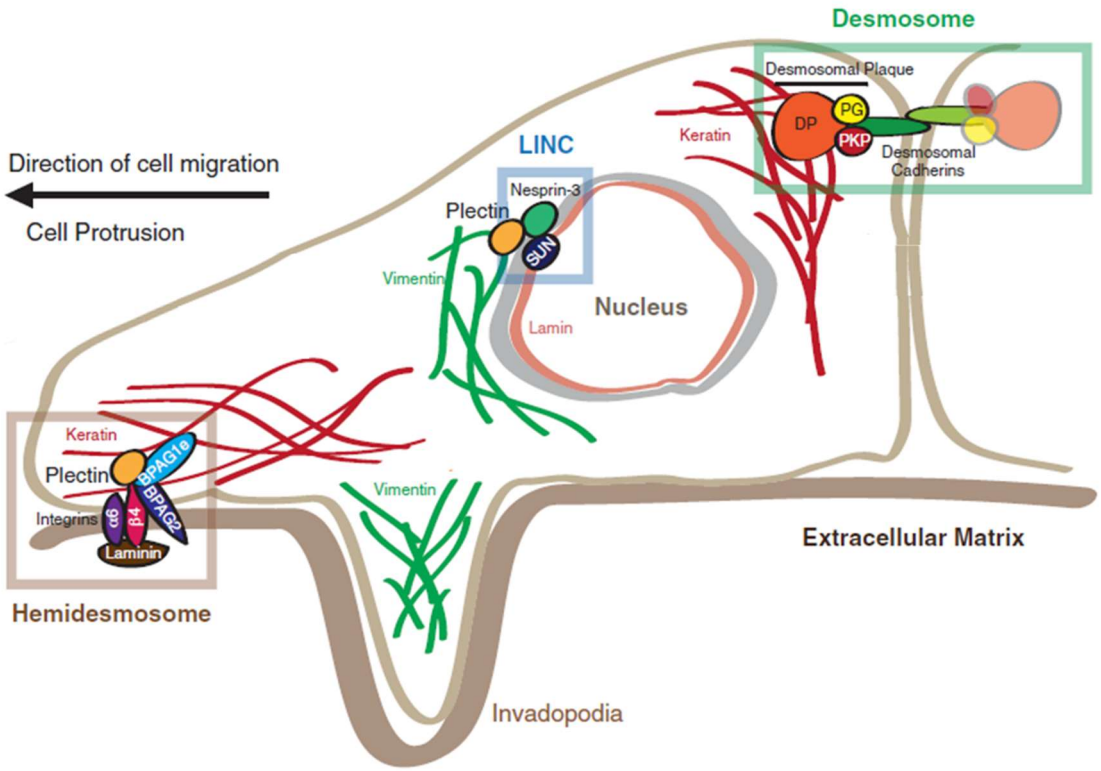

Figure 10. Schematic representation of IF anchorage to different sub-cellular regions. IFs as keratins can anchor to molecular complexes that allow cell-cell and cell-extracellular matrix contact, the desmosome and hemidesmosome, respectively. This anchorage is mediated by linker proteins such as plectin and desmoplakin (DP). Nuclear lamins attach to the linker of nucleoskeleton and cytoskeleton (LINC) complex. LINC participates in the anchoring of the nuclear lamina to cytoskeletal proteins (such as vimentin) on the cytoplasmic side of the nucleus. Adapted from (Chung *et al.*, 2013)

EBS became a paradigm of mechanical-related pathologies derived from mutant keratins (Oshima, 2007). Accordingly, muscle cells harboring mutant desmin display compromised IF network and exhibit structural and functional deficiencies, resulting in severe myopathies that can be lethal (Dalakas *et al.*, 2000; Goldfarb *et al.*, 2008). Furthermore, mutations of lamin IF results in nuclear abnormal structure, increased fragility and decreased resistance to mechanical stress, as observed in multiple laminopathic diseases (Schreiber and Kennedy, 2013; Gruenbaum and Aebi, 2014).

Interestingly, while IFs mutations may compromise mechanical stability by preventing IF assembly, there is also evidence that such mutations may alter the mechanical properties of the IF network itself, thus resulting in the formation of unstable IF networks (Russell, 2004). Additionally, IF mutations (or reduced expression) result in impaired expression of linker proteins and desmosome components, leading to higher fragility of the tissues (Haines and Lane, 2012).

Currently there are at least 119 diseases (including cataracts, cardiomyopathy, neuropathies, premature aging, muscular dystrophy) associated with mutations of most genes of all IF types (Omary *et al.*, 2004; Szeverenyi *et al.*, 2008) (up-to-date list can be found at the Human Intermediate Filament Database, http://www.interfil.org). While many of these pathologies confirm the importance of IFs for structural support of cells and tissues, some observations indicate that in some of those diseases IFs may exert other, non-mechanical functions (Kim and Coulombe, 2007). Examples include formation of intracellular IF aggregates that are toxic for the cells (Watson *et al.*, 2007; Kim and Coulombe, 2007), perturbation of gene transcription when lamin mutants are expressed (Hutchison, 2002; Omary *et al.*, 2004; Mewborn *et al.*, 2010) and activation of JNK signaling in the presence of mutated K14 (Wagner *et al.*, 2013). Non-mechanical functions of IFs have been focus of intense research in the last years, as will be highlighted next.

B.5. Non-mechanical functions of IFs

B.5.1. Vectorial processes

IFs like peripherin, desmin and vimentin interact with components of intracellular vesicular trafficking, modulating their distribution and activity (Margiotta and Bucci, 2016). In particular, the absence of vimentin in fibroblasts results in abnormal distribution of AP-3, an adaptor complex important for lysosomal sorting, leading to accumulation of these vesicles in the perinuclear region (Styers *et al.*, 2004). Lack of vimentin also results in altered levels of lysosomal proteins LAMP-1 and LAMP-2 and decrease of autophagosomes (Styers *et al.*, 2004). Interestingly, the disruption of vesicular transport significantly affects the conformation of the vimentin network, highlighting the interdependence of this partnership (Styers *et al.*, 2006). IFs also partake in other vectorial processes of the cell. Accordingly, vimentin, neurofilaments, K8, K18 and desmin influence the spatial organization and/or function of organelles such as mitochondria and the golgi apparatus (Fig 11) (Milner *et al.*, 2000; Gao and Sztul, 2001; Kumemura *et al.*, 2004; Toivola *et al.*, 2005; Tao *et al.*, 2009). Furthermore, IFs regulate the distribution of multiple surface and cytosolic proteins, ion channels and junctional proteins (Fig 11) (Salas *et al.*, 2016). For instance, primary kidney cells that lack vimentin exhibit altered localization of SGLT1, a sodium-glucose co-transporter (Runembert *et al.*, 2002). K8 null cells show mislocalization of multiple proteins such as syntaxin 3, apoptotic receptor Fas and ion transporters DRA, AE1/2, ENaC among others (Ameen *et al.*, 2001; Gilbert *et al.*, 2001; Asghar *et al.*, 2016). In addition, K18 controls the cystic fibrosis transmembrane conductance regulator (CFTR) surface location, K18 mutants elicit

mistargeting of intercellular junction factors ZO-1, beta-catenin and desmoplakin (Hanada *et al.*, 2005) and expression of mutant lamin-A causes aberrant distribution of connexin proteins at gap junction of cardiac cells (Mounkes *et al.*, 2005). IFs thus favor the maintenance of normal apico-basal epithelial polarity of polarized cells (Salas *et al.*, 2016). Importantly, the disruptive effect that IF absence has on microtubules and microtubule organizing centers (MTOC) may explain some of the protein targeting anomalies described above (Oriolo *et al.*, 2007; Kim and Coulombe, 2007).

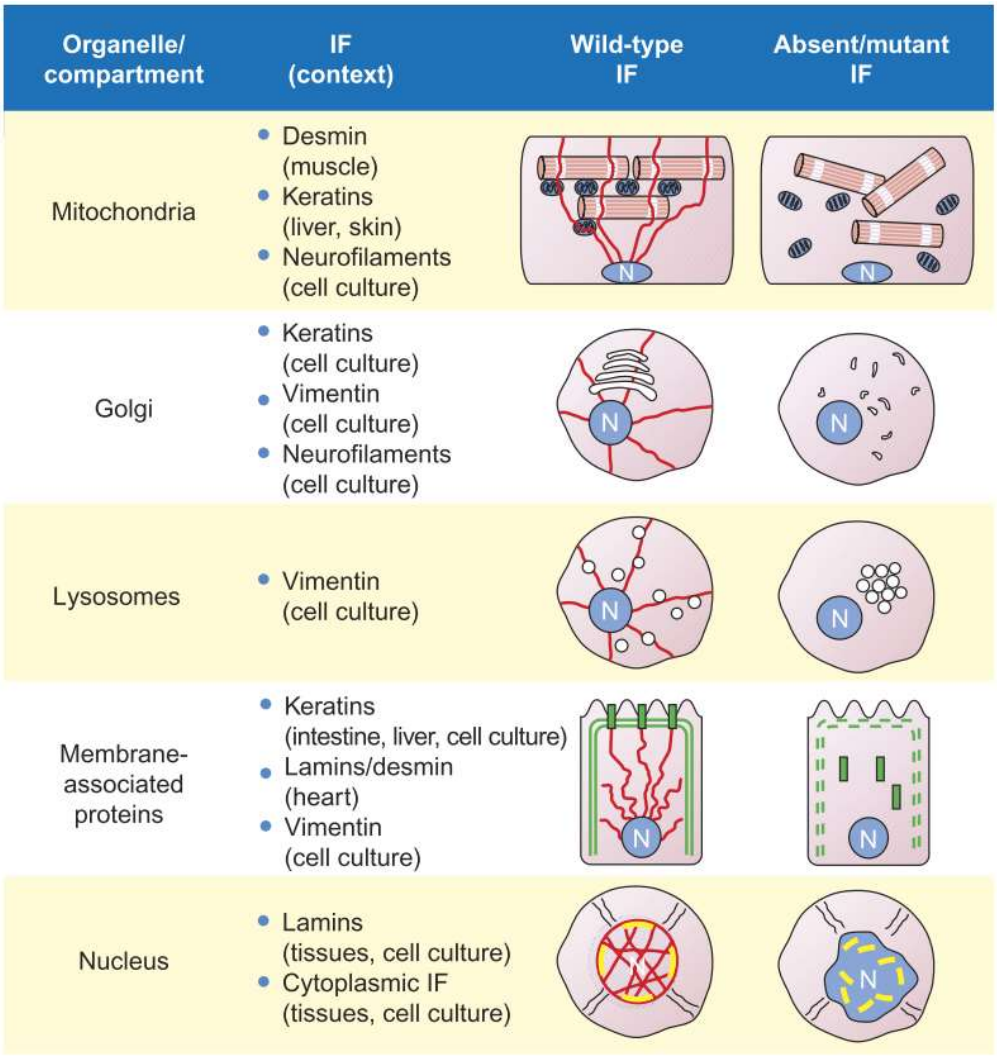

Figure 11. Intermediate filaments organize intracellular structures. Mutations or absence of specific IFs perturb the distribution and structural organization of various organelles and cellular compartments in different cells/ tissues. Color scheme: red, cytoplasmic or nuclear IFs involved with organelle or compartment changes; green, membrane-proximal proteins including F-actin; orange, myofibrils; yellow, nuclear heterochromatin. The detachment of desmin IFs (black) from the nucleus in some myocytes owing to lamin mutation is also shown. Abbreviation: N, nucleus. Adapted from (Toivola *et al.*, 2005).

B.5.2. Cellular adhesion, invasion and migration

IFs are important regulators of cellular adhesion and motility (Chung *et al.*, 2013; Leduc and Etienne-Manneville, 2015). IF modulation of these events can be mechanic, cytoarchitectural and regulatory (Chung *et al.*, 2013). As described above, IFs are anchored to desmosomes and hemidesmosomes. These adhesion complexes, which are crucial for maintenance of tissue integrity, incorporate transmembrane cadherins and α6β4 integrin hetero-dimers, armadillo proteins and linker proteins such as plectin 1a and desmoplakin, which anchor IFs to these sites (Walko *et al.*, 2011; Chung *et al.*, 2013; Leduc and Etienne-Manneville, 2015). IFs are also found at focal adhesion sites, regulating their turnover (Valencia *et al.*, 2013; Gregor *et al.*, 2014; Jones *et al.*, 2017). Desmoplakin knockout cells fail to anchor IFs in the desmosome and exhibit weaker cell-cell adhesion, suggesting that efficient desmosomal adhesion requires localized *in situ* attachment of IF (Vasioukhin *et al.*, 2001; Jones *et al.*, 2017). K1 and K10 deletion results in desmosomes of smaller size and with less desmocollin and desmoplakin (Wallace *et al.*, 2012). Additionally, through modulation of PKC-α activity, K5/K14 stabilize desmosomes and epithelial cell adhesion (Kröger *et al.*, 2013; Loschke *et al.*, 2016). Furthermore, keratin knockout cells are slower to adhere to the extracellular matrix and display altered localization of hemidesmosomes (Seltmann *et al.*, 2012). These perturbations in adhesion dynamics can reflect in cellular motility, as migration is frequently coupled to weaker adhesions (Roberts *et al.*, 2011; Chung *et al.*, 2013). Accordingly, GFAP knockdown in astrocytoma cells results in enhanced adhesion and motility impairment (Moeton *et al.*, 2014), while vimentin expression favors motility and weakened adhesion in breast carcinoma (Messica *et al.*, 2017).

IFs such as nestin and vimentin generally favor cellular migration and invasion (Leduc and Etienne-Manneville, 2015). Vimentin expression correlates with metastatic potential of epithelial cancers and its down-regulation leads to decreased invasive capacity of carcinoma cells (Leduc and Etienne-Manneville, 2015). Vimentin is also a marker of epithelial to mesenchymal transition (EMT), a process associated with acquisition of migratory capacities such as desmosome destabilization and increase of focal adhesion dynamics (Mendez *et al.*, 2010). Interestingly, EMT is also associated with down-regulation of keratins such as K5/K14 and respective destabilization of hemidesmosomes, favoring cellular motility and invasion (Seltmann *et al.*, 2012; Leduc and Etienne-Manneville, 2015). The mechanisms behind vimentin dependent promotion of motility likely include vimentin-dependent modulation of Rac1/RhoA pathway, which influence types of cell migration, and vimentin enhancement of Notch signaling which itself is associated with tumor metastasis and invasion (Havel *et al.*, 2015; Antfolk *et al.*, 2017; Messica *et al.*, 2017). Additionally, PKCε mediated vimentin

phosphorylation controls the trafficking of plasma membrane integrins and consequently cellular migration (Ivaska *et al.*, 2005). In contrast to vimentin, Keratins contribution to cellular motility is more intricate and variable, depending largely on patterns of expression of keratin pairs and cellular context (Leduc and Etienne-Manneville, 2015). For example, K8 silencing in rat hepatoma cells lead to decreased cellular migration (Bordeleau *et al.*, 2012), whereas targeted depletion of the same keratin in human breast cancer cells results in enhanced migration (Iyer *et al.*, 2013).

B.5.3. Microbial infection

IFs participation in infection is poorly characterized (Mak and Brüggemann, 2016; Geisler and Leube, 2016). Nevertheless, there is increasing evidence that IFs can affect infection outcome through their involvement in different aspects of microbial pathogenesis. Accordingly, the intermediate filament GFAP was found to restrict spread and multiplication of *Staphylococcus aureus* and *Toxoplasma encephalitis* within the CNS of mice (Stenzel *et al.*, 2004). In addition, Lamin A is required for Herpes simplex virus (HSV) replication in murine fibroblasts (Silva *et al.*, 2008). Several studies demonstrate the participation of vimentin in microbial infection (Mak and Brüggemann, 2016). Indeed, surface-exposed vimentin can favor binding and/or internalization of pathogens such as *L. monocytogenes* (Ghosh *et al.*, 2018), *Escherichia coli* (Zou *et al.*, 2006; Chi *et al.*, 2010), *Streptococcus pyogenes* (Bryant *et al.*, 2006), *Mycobacterium avium* (Babrak *et al.*, 2015) and Enterovirus 71 (Du *et al.*, 2014). Vimentin is also required for stable docking of *Shigella flexneri* on cells and for efficient translocation of T3SS effectors into cells (Russo *et al.*, 2016). Remodeling of vimentin network was reported to be induced by parvovirus (Fay and Panté, 2013), *Anaplasma phagocytophilum* (Truchan *et al.*, 2016) and *Chlamydia trachomatis* (Kumar and Valdivia, 2008), generally favoring the maintenance of the respective intracellular replication niches. Vimentin filaments rearrangements are also observed during *Salmonella enterica* infection (Murli *et al.*, 2001; Guignot and Servin, 2008). In addition, the vimentin cage that surrounds the *Samonella*-containing vacuoles (SCVs) keeps the vacuolar structures close to the juxtanuclear area (Guignot and Servin, 2008), although the significance of this finding remains to be determined (Guignot and Servin, 2008; Mak and Brüggemann, 2016).

The involvement of keratins in pathogenic infection will be discussed in the section below.

B.6. Keratins as multifunctional cytoskeleton components

B.6.1. Overview

Encoded by 54 genes, keratins are the largest IF family (Bragulla and Homberger, 2009). Besides their division as “acidic” and “basic”, keratins can be further sub-divided in two groups, “hard” and “soft” keratins. Hard keratins are found in epithelial tissues like hair, nails and oral filiform papillae, whereas most of keratins are expressed in “soft” epithelial tissues (Coulombe and Omary, 2002; Kornreich *et al.*, 2015). As described above, keratins confer mechanical resilience and flexibility to epithelial cells and tissues. The unravelling of keratins non-mechanical roles demonstrate that these IFs indeed influence most aspects of cell life. By acting as scaffolds that integrate and transduce mechanical and biological inputs, keratins (and IFs in general) are increasingly viewed as signaling platforms that govern cell fate (Pallari and Eriksson, 2006; Hyder *et al.*, 2008; Eriksson *et al.*, 2009).

In this section, I will focus in some of the most relevant non-mechanical roles of keratins, including their surprising involvement in regulation of gene expression.

B.6.2. Cell cycle

Keratins are generally viewed as positive regulators of cell cycle progression. During mitosis of *in vivo* hepatocytes, K18 is phosphorylated in Ser33, promoting re-organization of the network and association with the adaptor protein 14-3-3 (Ku *et al.*, 2002). When this phosphorylation site is blocked by site directed mutagenesis, K18 distribution is altered and 14-3-3 aberrantly accumulates in nuclear speckles, leading to partial mitotic arrest in S/G2 phase (Ku *et al.*, 2002; Snider and Omary, 2014). Furthermore, K18/14-3-3 interaction regulates binding of 14-3-3 with phosphorylated Cdc25, a checkpoint regulator of mitosis (Toivola *et al.*, 2001; Margolis *et al.*, 2006). Cdc25 association with 14-3-3, prevents Cdc25 dephosphorylation of its target cyclin dependent kinases, blocking progression of the cell cycle. However, if 14-3-3 is bound to phosphorylated K18, it is not available to associate with Cdc25, which is then free to promote mitosis progression. These observations suggest that IFs provide a “14-3-3 sink” that may prevent uncontrolled and possibly harmful 14-3-3 interactions (Toivola *et al.*, 2001; Margolis *et al.*, 2006; Galarneau *et al.*, 2007; Eriksson *et al.*, 2009). Keratins can regulate cell cycle progression through additional mechanisms. Thus, it was recently shown that K17 promotes cell cycle in human cervical epithelia by favoring nuclear export and degradation of p27, a negative regulator of G1 to S transition (Escobar-Hoyos *et al.*, 2015). Additionally, K14 knockdown in human immortalized keratinocytes leads to delayed S-phase

progression and late entry in M phase, likely due to reduced Akt activation in these cells (Alam *et al.*, 2011).

B.6.3. Protein synthesis and cell growth

Observations of interaction of keratins with components of translation machinery such as eIF3 and eEF1B-γ suggested that keratins could modulate protein synthesis and cell growth (Lin *et al.*, 2001; Bousquet *et al.*, 2001). More recently it was demonstrated that mice lacking type II keratins display mislocalization of glucose transporters, downregulation of protein synthesis machinery and severe growth retardation (Kellner and Coulombe, 2009; Vijayaraj *et al.*, 2009). Furthermore, K8-knockout hepatocytes exhibit reduced levels of bulk protein synthesis and smaller cellular size (Galarneau *et al.*, 2007). Similar observations were made for K17-knockout keratinocytes (Kim *et al.*, 2006). K17 regulates protein synthesis and cell growth by interacting with 14-3-3σ, a positive regulator of the Akt/mammalian target of rapamycin (Akt/mTOR) signaling pathway, a major protein synthesis pathway. In cells lacking K17, 14-3-3σ shifts to a nuclear location, resulting in impaired mTOR stimulation and compromised cell growth (Kim *et al.*, 2006). Interestingly, the role of keratins in Akt signaling appear to be keratin and context dependent. Indeed, recent studies have shown K8-knockout hepatocytes display enhanced insulin-mediated Akt activation that is associated with increased glucose metabolism (Mathew *et al.*, 2013; Roux *et al.*, 2017). On the other hand, K18 depletion in nasopharyngeal carcinoma cell lines negatively regulates Akt activation and cellular proliferation (Deng *et al.*, 2012). Similarly, K10 impact on Akt activity is context specific (Pan *et al.*, 2012). Thus, K10 interacts with Akt and impairs its activity in basal cells of the epidermis, resulting in impaired proliferation of these cells in mice (Paramio *et al.*, 2001; Santos *et al.*, 2002). In contrast, K10-knockout has no effect on Akt activation in suprabasal layers of the epidermis (Reichelt *et al.*, 2004; Paramio *et al.*, 2007). These observations highlight the increasing relevance of keratins as regulatory determinants of signaling pathways.

B.6.4. Apoptosis modulation

Keratins can also regulate cell and tissue growth by modulating cell death (Pan *et al.*, 2012). They generally protect cells from apoptosis and appear to achieve this protective effect through different mechanisms (Toivola *et al.*, 2010). Thus, keratin defects can exacerbate cell death through increased surface expression of cell death receptors such as Fas receptor, and

decreased levels of anti-apoptotic protein c-Flip (Gilbert *et al.*, 2001; Gilbert *et al.*, 2004; Gilbert *et al.*, 2012). In addition, various keratins interact with and "sequester" pro-apoptotic molecules such as TNF receptor-associated death domain-containing protein (TRADD) and tumor necrosis factor receptor 2 (TNFR2), resulting in attenuated apoptotic signaling (Caulin *et al.*, 2000; Inada *et al.*, 2001; Yoneda *et al.*, 2004; Tong and Coulombe, 2006). Finally, keratins can also limit apoptosis by "absorbing" excessive stress and pro-apoptotic signals, as will be discussed below (Pan *et al.*, 2012). In this context, phosphorylation of K8 in residue S74 is crucial for hepatic protection, as mutations in the K8 S74 site renders mice particularly susceptible to Fas-mediated apoptosis (Ku and Omary, 2006).

Interestingly, despite keratin anti-apoptotic roles, once apoptosis is initiated keratins (and other IFs) are required for efficient progression to cell death (Kim and Coulombe, 2007; Marceau *et al.*, 2007). One hallmark of apoptosis is caspase-mediated cleavage of multiple keratins at conserved sites. Failure to do so (by expression of mutant keratin, for example) shunts cells towards necrosis (Kim and Coulombe, 2007; Weerasinghe *et al.*, 2014). It is noteworthy that in a clinical setting, detection of caspase cleaved keratins (resultant from apoptosis of epithelial cells) in the serum is increasingly used as a prognostic marker. In this context, detection of keratin fragments in the serum generally correlates with worse prognosis (Karantza, 2010).

While less characterized, observations with nestin, vimentin and desmin also support the concept of IFs as anti-apoptotic proteins (Sahlgren *et al.*, 2006; Schietke *et al.*, 2006; Capetanaki *et al.*, 2007).

B.6.5. Stress protection

The observations above point to a broader role of keratins in protecting cells and tissues from non-mechanical stress and injury, suggesting that keratins can serve as stress response proteins (Toivola *et al.*, 2010). Interestingly, keratins share features with classical stress proteins such as heat shock proteins (HSPs). Indeed, keratins are abundant proteins whose RNA and/or protein levels are increased several fold in response to multiple stressors (Fig 12) (Toivola *et al.*, 2010). A proteomics meta-study found that keratins are the protein family whose expression is most frequently altered in different disease settings in human, mouse and rat (Petrak *et al.*, 2008). Also similar to other stress proteins, mutated or absent keratins are associated with injury and disease, reflecting keratins protective role in different scenarios (Toivola *et al.*, 2010), as will be discussed below. Furthermore, chronic stress may result in the formation of HSPs and keratins aggregates (also known as inclusions), which, while useful pathology markers, have unclear contributions to malignancy (Fig 12) (Toivola *et al.*, 2010).

Keratins commonly undergo post-translational modifications such as phosphorylation and O-linked glycosylation upon chemical, oxidative and metabolic stresses (Omary *et al.*, 2006; Toivola *et al.*, 2010). These modifications frequently translate into re-organization of the keratin filaments (Fig 12). The importance of those post-translational events is evident when their inhibition generally renders cells more susceptible to stress. For instance, compared to wild type, mice that overexpress human K18 S30/31/49A substitution mutants (which fail to undergo O-glycosylation) exhibit higher incidence of kidney, liver and spleen injury and failure upon treatment with streptozotocin or PUGNAc. Accordingly, these animals show higher mortality rates (Ku *et al.*, 2010). Additionally, the authors observed impaired activity of cell survival kinases Akt and PKC in these mice, suggesting that K18 protects cells and tissues by favoring pro-survival pathways (Ku *et al.*, 2010).

Stress conditions also elicit K8 and K18 phosphorylation events that are important for stress resilience (Omary *et al.*, 2006; Snider and Omary, 2014). Mutation of K18 major phosphorylation site serine 52 to alanine (S52A), which blocks the Ser52 phosphorylation, results in increased susceptibility of transgenic mice to hepatoxins-induced damage as compared with wild type K18-expressing animals (Ku *et al.*, 1998). Similarly, transgenic mice expressing K8 mutated in the phosphorylation site S74 are predisposed to Fas-mediated liver injury and cell death (Ku and Omary, 2006). In addition, the authors made identical observations in mice expressing a human K8 variant (G62C) that predisposes to cirrhosis and fibrosis progression. Remarkably, K8 G62C mutation inhibited stress-induced phosphorylation at K8 Ser74 by p38, p42 and JNK kinases. In this circumstances, these kinases are thus available to activate other pro-apoptotic substrates, further promoting pro-apoptosis signaling (Ku and Omary, 2006).

Collectively, these observations suggest that K8 and K18 may work as phosphate “sponges” that protect cells and tissues by absorbing excessive stress-induced kinase activity (Ku and Omary, 2006; Snider and Omary, 2014). The observation that other keratins as K4, K5 and K6 are phosphorylated in response to stress in amino acid motifs similar to K8 S74 suggests that various keratins can serve as phosphate buffers in stress scenarios (Snider and Omary, 2014).

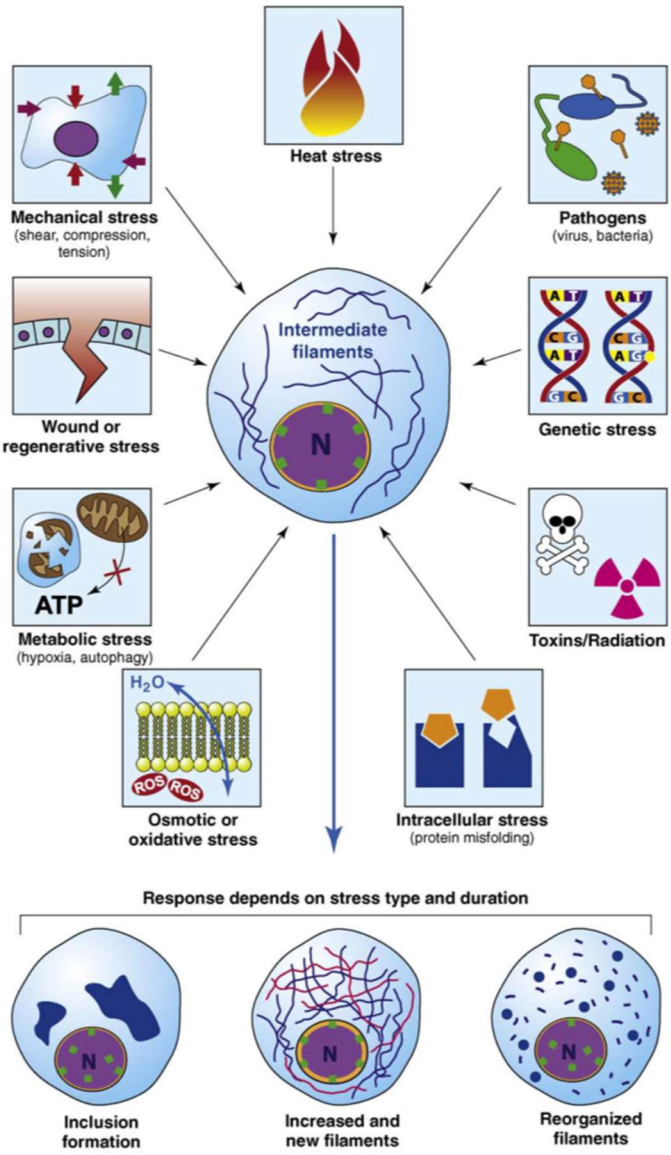

Figure 12. Stress modulates keratins. Cells are exposed to different types and durations of stress, with different consequences for the keratin network. Stress can thus result in *de novo* formation of filaments or reorganization of the network. Chronic stress can lead to the generation of keratin containing protein inclusions. Adapted from (Toivola *et al.*, 2010).

B.6.6. Gene expression

A growing body of evidence suggests that keratins regulate gene expression and translation (Asghar *et al.*, 2016). Indeed, studies in mice that lack type I or type II keratins demonstrate that these animals display significant transcriptomic perturbations (Kumar *et al.*, 2015; Kumar *et al.*, 2016) and impaired protein expression (Vijayaraj *et al.*, 2009). Knockout of K8 results in perturbed messenger RNA (mRNA) levels of multiple genes, including DRA, Hey1 and Hey2, transglutaminase 3, survivin and TLR9 (Habtezion *et al.*, 2011; Asghar *et al.*,

2016; Lähdeniemi *et al.*, 2017). Mutated K18 results in expression changes of oxidative stress genes (Zhou *et al.*, 2005). Mutation or loss of expression of keratins K1, K5, K10, K16 and K17 results in altered transcriptional expression profile of inflammatory modulators as CXC, CXCL9-11, IL-18, TNF α and IL-1β, some of which are associated with inflammatory skin diseases as psoriasis and atopic eczema (Fu and Wang, 2012; Roth *et al.*, 2012; Lessard *et al.*, 2013; Chung *et al.*, 2015; Salas *et al.*, 2016). Furthermore, K17 absence in cervical tissue dysregulates transcriptional expression of key effectors of important signaling pathways such as Wnt, Notch and mTOR (R P Hobbs *et al.*, 2016). The expression of Notch signaling components is also altered in breast cancer cells silenced for K19 (Saha *et al.*, 2017).

The study of the molecular mechanisms behind the role of keratins in governing gene expression is in its infancy. Nevertheless, the existing evidences suggest that keratins (and IFs in general), may relay extracellular and intracellular cues to the nucleus by regulating multiple signaling cascades and interacting with key regulators such as Raf-1 and 14-3-3 proteins (Ku *et al.*, 2004; Zhou *et al.*, 2005; Toivola *et al.*, 2005; Salas *et al.*, 2016). Interestingly, recent findings suggest that keratins may have a more direct role in gene transcription, derived from their unexpected presence in the nucleus (Kumeta *et al.*, 2013; Hobbs *et al.*, 2015; Ryan P. Hobbs *et al.*, 2016). Nuclear localization of keratins K7, K8, K17 and K18 was detected by treating cells with Leptomycin B (LMB), an inhibitor of CRM1, a nuclear protein that mediates nucleocytoplasmic export of proteins containing a nuclear export signal (NES). Thus, LMB treated cells display keratin accumulation in the nucleus. Accordingly, keratin variants that lack the NES-like sequence also accumulate in the nucleus (Kumeta *et al.*, 2013; Hobbs *et al.*, 2015; Escobar-Hoyos *et al.*, 2015). In some settings however, LMB treatment is not required to detect nuclear K17, as it is the case of BT-20-cultured cells and biopsy samples of human BCC skin tumors (Hobbs *et al.*, 2015; Ryan P. Hobbs *et al.*, 2016).

While the functional relevance of these intriguing observations remains largely uncharacterized, recent studies provide some insight on K17 putative roles in the nucleus, which includes modulation of gene expression (Chung *et al.*, 2015; Hobbs *et al.*, 2015; Escobar-Hoyos *et al.*, 2015). K17 contains a nuclear localization signal (NLS) that is recognized by importin-α/β, allowing translocation of K17 into the nucleus (Escobar-Hoyos *et al.*, 2015). Inside the nucleus, K17 does not exhibit a filamentous form, being rather present in discrete punctae and/or diffuse patterns (Ryan P. Hobbs *et al.*, 2016). In skin tumor keratinocytes, nuclear K17 interacts with the p65 subunit of NFκB and with the transcriptional regulator Aire, affecting its nuclear distribution. Additionally, K17 affects the expression and associates with the promoter region of the cytokine genes MMP9, CXCL10, CXCL11 and CXCL19, implicating K17 in chromatin binding and transcriptional regulation events (Hobbs *et al.*, 2015; Ryan P. Hobbs *et al.*, 2016). It is noteworthy that keratins such as K17 and K19 interact with multiple proteins that shuttle in and out of the nucleus, including 14-3-3, hnRNP

K, p27 and β-catenin (Kim *et al.*, 2006; Chung *et al.*, 2015; Escobar-Hoyos *et al.*, 2015; Saha *et al.*, 2017).

B.7. Keratins in infection

Keratins are targeted by multiple microbes, however the molecular and functional details behind keratin involvement in bacterial pathogenesis remain largely elusive (Geisler and Leube, 2016). Keratins have been reported to facilitate pathogen adhesion to host cells. For instance, K18 interacts with Tir, an EPEC effector that is injected through the T3SS, forming a complex with 14-3-3. K18 is required for the formation of actin pedestals at the base of EPEC adhesion sites, thus participating in the pathogen adhesion to the host cell (Batchelor *et al.*, 2004). Interestingly, some of the host-pathogen interactions are mediated through keratins that are themselves found at the surface of certain cell types. Indeed, while classically viewed as cytoplasmic proteins, there is evidence that keratins may be present at cellular surface and mediate host-pathogen interactions. Such is the case of K10, which enhances adhesion of *Staphylococcus aureus* by interacting with the bacterial protein clumping factor B (ClfB) (O'Brien *et al.*, 2002). Furthermore, K4 mediates adhesion of *Streptococcus agalactiae* through interaction with bacterial Srr-1 for effective colonization (Samen *et al.*, 2007). Similarly, surface K13 can function as a receptor for *Burkholderia cepacia* (Sajjan *et al.*, 2000). It is unclear how keratins are processed and exposed at the cell surface. Furthermore, whether the pathogens themselves can promote the presence of keratins at cellular surface remains an open question (Geisler and Leube, 2016).

A role for keratins in the internalization process of pathogens was described for K18, with expression of the dominant negative K18 mutant K18-R89C resulting in impaired internalization of *Salmonella typhimurium* (Carlson *et al.*, 2002). Several pathogens have been shown to interfere with keratin networks, usually inducing its disruption either by triggering phosphorylation events that are associated with keratin network disassembly or by direct proteolysis of the network (Geisler and Leube, 2016). The human papilloma virus (HPV) type 16 protein E1^E4 protein interacts with K18, leading to disruption of the keratin network (McIntosh *et al.*, 2010). Interestingly, these effects are accompanied by hyperphosphorylation at K8/18 residues which, in turn, are associated with keratin network reorganization induced by apoptosis, mitosis and cell stress (Wang *et al.*, 2003; McIntosh *et al.*, 2010). Following HPV-mediated network disruption, keratins are ubiquitinated and degraded (McIntosh *et al.*, 2010). Together, these effects may compromise the integrity of the epithelium, facilitating the release of viral particles (McIntosh *et al.*, 2010). Similar observations were made for herpes simples virus type 2 (HSV-2), with the viral kinase US3 promoting phosphorylation and network

collapse of K17 (Murata *et al.*, 2002). Likewise, rotavirus infection induces K8 hyperphosphorylation and network re-arrangements (Liao *et al.*, 1995).

When internalized, *Chlamydia trachomatis* is found within an inclusion vacuole that is surrounded and supported by F-actin and keratins (Dong *et al.*, 2004). There, *Chlamydia* secretes a protease (CFAP) that cleaves K8 and K18, allowing a dynamic re-organization of the keratin scaffold as the intracellular *Chlamydia* replicates and the respective vacuole expands (Kumar and Valdivia, 2008). Other examples of pathogen-mediated proteolytic breakdown of keratins include K18 disruption by the action of the adenovirus effector L3-23 kDa proteinase (Chen *et al.*, 1993), and K8 cleavage by rhinovirus infection (Seipelt *et al.*, 2000). Pathogens can also affect keratin network dynamics by regulating interactions between keratins and modulators of keratin solubility. That is the case of EPEC infection, which leads to a fast keratin network fragmentation by enhancing K18 interaction with 14-3-3, a known K18 solubility factor (Viswanathan *et al.*, 2004).

K8 depletion restricts hepatitis B virus replication in hepatic cells (Zhong *et al.*, 2014). Similarly, K18 knockdown was shown to compromise *Trypanosoma cruzi* ability to replicate inside HeLa cells (Claser *et al.*, 2008). Additionally, the peptide TS9 derived from the parasite glycoprotein gp85 was recently shown to interact with keratins and vimentin, and to block pathogen adhesion and invasion into cells (Teixeira *et al.*, 2015). Nava-Acosta and Navarro-Garcia demonstrated that K8 not only interacts with the *Enterobacteriaceae* Pet toxin, but is also required for its clathrin mediated internalization and cytotoxic effects (Nava-Acosta and Navarro-Garcia, 2013). Further evidence of keratin interaction with pathogenic effectors include K18 association with translocon pore from *Shigella* and K8 interaction with multiple proteins from gram-negative cocci and group B streptococci strains (Tamura and Nittayajarn, 2000; Russo *et al.*, 2016). In general, the significance of those interactions remains to be determined.

Finally, it was recently described that K6a can exhibit antimicrobial activities in cornea epithelial cells (Tam *et al.*, 2012; Chan *et al.*, 2018). Indeed, bacterial ligands trigger K6a phosphorylation and consequent disassembly of the network. The soluble K6a is then ubiquitinated and processed by the proteasome. The resulting fragments exhibit significant anti-bacterial activity against *Pseudomonas aeruginosa* and the ocular pathogens *Staphylococcus aureus* and *Streptococcus pyogenes* (Tam *et al.*, 2012; Chan *et al.*, 2018).

CHAPTER II – PROJECT PRESENTATION

The relationship between microbes and host organisms is ancient, complex and fragile. Evolutionary pressure favored pathogens harboring molecular tools that allow efficient host infection. Given the relevance of microbial infection in a public health context, the interplay between pathogen and host has been the subject of intense research in the last decades. As a result, different aspects of the biology of infection have been illuminated. Such findings are particularly important in the design of antimicrobial therapeutics. The exploitation of host cellular machinery to promote and establish infection emerged as a common theme in the infectious process of different microbes. Importantly, discoveries on host usurpation by invasive bacteria were also pivotal to unravel key cellular processes of the host. For that reason, diverse pathogens have been actively used as powerful model organisms to study molecular pathways of the host organism. In this context, *L. monocytogenes* is one of the most documented pathogens, and the study of its infection process has been instrumental in the discovery of unknown cellular components and in the unravelling of basic cell biology mechanisms such as actin polymerization, formation of adherens junctions and clathrin-mediated internalization.

L. monocytogenes, as other human pathogens, targets the host cytoskeleton to promote infection. In particular, the involvement of actin in *L. monocytogenes* pathogenesis is extensively studied, with the microbe exploiting the actin network to favor internalization, intracellular motility and cell-to-cell spread. *L. monocytogenes* does not interact directly with actin filaments, but rather subverts the activity of host effectors that control actin polymerization, such as the Arp2/3 complex. In contrast to actin, the involvement of other major cytoskeletal networks such as microtubules and intermediate filaments in *L. monocytogenes* infection is poorly characterized.

Our research group is interested in understanding the intimate molecular crosstalk that occurs between *L. monocytogenes* and the host during pathogenic infection. For that, we explore the *L. monocytogenes* virulence mechanisms employed to invade and thrive within the host. In particular, we aim to unravel the role of host cytoskeleton components in the establishment of cellular infection. In this context, we have recently shown that the actin-binding protein myosin IIA controls *L. monocytogenes* infection (Almeida *et al.*, 2015) and, together with the endoplasmic reticulum chaperone Gp96, regulates cytoskeleton response to *L. monocytogenes* pore-forming toxin LLO (Mesquita, Brito, Mazon Moya, *et al.*, 2017).

Considering the underappreciated role of intermediate filaments in *L. monocytogenes* infection, our aim with this PhD project was to clarify the relevance of these cytoskeletal proteins in *L. monocytogenes* pathogenesis. Our study focused on the highly abundant keratin pair K8 and K18, the most common keratin pair in simple epithelial cells. The importance of K8 and K18 in different stages of *L. monocytogenes* cellular infection was addressed.

CHAPTER III – RESULTS

The results obtained in this work are presented in two parts.

Part I – Epithelial keratins modulate cMet expression and signaling and promote InlB-mediated *Listeria monocytogenes* infection of HeLa cells

The results presented here correspond to the work developed as the main research line of this PhD project. We describe the role of major epithelial keratins in *L. monocytogenes* internalization and actin dynamics at entry site. We also address how keratins modulate gene expression and downstream signaling of the receptor cMet. These findings were accepted for publication in **Frontiers in Cellular and Infection Microbiology on** 20 April 2018. The accepted version of the manuscript is appended in Chapter VI- ANNEX.

Part II – K18 interaction with putative RBPs

In this part we include unpublished results from ongoing work, in which we further explore Keratin 18 involvement in the regulation of the gene expression of multiple receptors.

Part I – Epithelial keratins modulate cMet expression and signaling and promote InlB-mediated *Listeria monocytogenes* infection of HeLa cells

Epithelial keratins modulate cMet expression and signaling and promote InlB-mediated *Listeria monocytogenes* infection of HeLa cells

Rui Cruz[1,2,3], Isabel Pereira-Castro[1,4], Maria Teresa Almeida[1,2], Alexandra Moreira[1,3,4], Didier Cabanes[1,2], Sandra Sousa[1,2,*]

[1] i3S - Instituto de Investigação e Inovação em Saúde, Universidade do Porto, Porto, Portugal

[2] Group of Molecular Microbiology, IBMC – Institute for Molecular and Cell Biology, Porto, Portugal

[3] ICBAS - Instituto de Ciências Biomédicas Abel Salazar, Universidade do Porto, Porto, Portugal

[4] Gene Regulation Group, IBMC – Institute for Molecular and Cell Biology, Porto, Portugal

*correspondence: srsousa@ibmc.up.pt

Running title: Keratins control gene expression.

Keywords: Intermediate filaments, keratins, cMet signaling, *Listeria monocytogenes*, cellular infection, mRNA stability, gene expression

I.1. Abstract

The host cytoskeleton is a major target for bacterial pathogens during infection. In particular, pathogens usurp the actin cytoskeleton function to strongly adhere to the host cell surface, to induce plasma membrane remodelling allowing invasion and to spread from cell to cell and disseminate to the whole organism. Keratins are cytoskeletal proteins that are the major components of intermediate filaments in epithelial cells however, their role in bacterial infection has been disregarded. Here we investigate the role of the major epithelial keratins, keratins 8 and 18 (K8 and K18), in the cellular infection by *Listeria monocytogenes*. We found that K8 and K18 are required for successful InlB/cMet-dependent L. monocytogenes infection, but are dispensable for InlA/E-cadherin-mediated invasion. Both K8 and K18 accumulate at InlB-mediated internalization sites following actin recruitment and modulate actin dynamics at those sites. We also reveal the key role of K8 and K18 in HGF-induced signaling which occurs downstream the activation of cMet. Strikingly, we show here that K18, and at a less extent K8, controls the expression of cMet and other surface receptors such TfR and integrin b1, by promoting the stability of their corresponding transcripts. Together, our results reveal novel functions for major epithelial keratins in the modulation of actin dynamics at the bacterial entry sites and in the control of surface receptors mRNA stability and expression.

I.2. Introduction

Intracellular pathogens exploit the host machinery to promote and establish infection. The host cytoskeleton is one of the preferential targets of pathogens and plays essential roles in cellular infection (Haglund and Welch, 2011; Carabeo, 2011; de Souza Santos and Orth, 2015). The role of host actin cytoskeleton in bacterial pathogenesis is by far the most documented (Colonne *et al.*, 2016). Actin filaments and their polymerization machinery are hijacked by several human pathogens at different stages of the infection process. In particular subversion of actin is critical for: 1) stable adhesion of pathogenic *Escherichia coli* (EPEC and EHEC) to the host cell surface, through the formation of actin-rich pedestals (Goosney *et al.*, 2000; Gruenheid *et al.*, 2001; Stradal and Costa, 2017); 2) invasion of epithelial cells by a variety of intracellular bacteria such as *Salmonella typhimurium*, *Shigella flexneri* and *Listeria monocytogenes* which induce actin cytoskeleton rearrangements and host membrane remodelling (Bierne *et al.*, 2005; Sousa *et al.*, 2007; de Souza Santos and Orth, 2015; Valencia-Gallardo *et al.*, 2015; Rolhion and Cossart, 2017); and 3) intracellular movement of cytosolic pathogens such as *S. flexneri*, *Rickettsia conorii* and *L. monocytogenes* which are able to elicit the formation of actin comet tails to promote cell-to-cell spread (Bernardini *et al.*, 1989; Mounier *et al.*, 1990; Welch *et al.*, 1997; Heinzen *et al.*, 1999; Egile *et al.*, 1999; Czuczman *et al.*, 2014; Kuehl *et al.*, 2015).

In contrast to actin, the role of intermediate filaments (IFs), in particular keratins, during bacterial infection is poorly characterized. IFs are also part of the host cytoskeleton and include a large group of proteins that share structural features and form apolar 10 nM wide fibrous filaments (Goldman *et al.*, 2012). Keratins are the largest subfamily of IFs, mainly expressed in the cytoplasm of epithelial cells and their expression profile is regulated in a tissue and differentiation dependent manner (Loschke *et al.*, 2015). Type I and type II keratins form heterodimers and organize into filaments that ensure structural integrity of epithelia and confers mechanical resilience to stress (Haines and Lane, 2012). In epithelial cells, Keratin 8 (K8) and Keratin 18 (K18) are the most common keratin pair (Moll *et al.*, 2008). Besides their biomechanical functions, several studies point keratins as important players in regulatory mechanisms defining health and disease (Pan *et al.*, 2012). K8 and K18 participate in cell cycle regulation by associating with and modulating the distribution of 14-3-3 adaptor proteins (Eriksson *et al.*, 2009). K17 was also reported to interact with 14-3-3 proteins modulating protein synthesis by interfering with mTOR signaling (Kim *et al.*, 2006). Additionally, mice lacking type II keratins display mislocalization of glucose transporters and downregulation of the protein synthesis machinery (Kellner and Coulombe, 2009; Vijayaraj *et al.*, 2009). Keratin defects exacerbate cell death through increased surface expression of cell death receptors

and enhanced activation of apoptotic signaling cascades (Caulin *et al.*, 2000; He *et al.*, 2002; Gilbert *et al.*, 2012). Keratins are also increasingly regarded as stress proteins protecting cells and tissues from stress and injury (Toivola *et al.*, 2010).

In the context of infection, keratins are targeted for degradation during adenovirus and *Chlamydia* infection (Chen *et al.*, 1993; Savijoki *et al.*, 2008), facilitate adhesion of EPEC to HeLa cells (Batchelor *et al.*, 2004), and promote internalization of *Salmonella* (Carlson *et al.*, 2002) and intracellular replication of *Trypanosoma cruzi* (Claser *et al.*, 2008). Interestingly, a recent study showed that in corneal epithelial cells keratin 6a is processed into antimicrobial fragments by the ubiquitin-proteasome system to protect the host against infection (Chan *et al.*, 2018). Despite these observations, the molecular and functional details behind keratin involvement in bacterial pathogenesis remain elusive (Geisler and Leube, 2016) and the possible role of keratins in *L. monocytogenes* infection was never addressed.

L. monocytogenes is a facultative intracellular gram-positive pathogen adapted to thrive in diverse environments (Freitag *et al.*, 2009). In humans, it causes listeriosis, a pernicious foodborne disease (Swaminathan and Gerner-Smidt, 2007) that relies on *L. monocytogenes* capacity to enter and survive into epithelial non-phagocytic cells, through the expression of an arsenal of virulence factors (Camejo *et al.*, 2011). *L. monocytogenes* internalization into non-phagocytic cells is mainly driven by the interaction of the bacterial surface proteins InlA and InlB, with their specific host receptors, respectively E-cadherin and cMet (Mengaud *et al.*, 1996; Shen *et al.*, 2000; Pizarro-Cerdá *et al.*, 2012). The engagement of these host receptors by the bacterial ligands triggers the activation of intracellular signaling pathways that lead to actin polymerization, myosin recruitment and further membrane remodelling, ultimately resulting in the internalization of the bacteria (Ireton *et al.*, 1996; Ireton *et al.*, 1999; Bierne *et al.*, 2001; Sousa *et al.*, 2004; Sousa *et al.*, 2007; Pizarro-Cerdá *et al.*, 2012; Almeida *et al.*, 2015).

In this study, we assessed the role of epithelial keratins K8 and K18, during *L. monocytogenes* infection. We found that both K8 and K18 are required for successful InlB/cMet-mediated internalization of *L. monocytogenes* and HGF-induced signaling. We also observed that K8 and K18 modulate actin dynamics during InlB-driven internalization. Interestingly, we also showed here that K18, and to a lesser extent K8, control the expression of cMet and other surface receptors such as Transferrin Receptor (TfR) and Integrin b1. Indeed, K18 confers transcript stability, thus regulating post-transcriptionally the expression of such membrane proteins.

I.3. Results

I.3.1. K8 and K18 favor InlB/cMet-mediated *L. monocytogenes* cellular invasion

We assessed the relevance of keratins during *L. monocytogenes* cellular infection of epithelial cell lines, which mainly express K8 and K18 (Moll *et al.*, 2008). HeLa and Caco-2 cells were depleted for K8 and/or K18 through an siRNA approach and intracellular *L. monocytogenes* numbers were evaluated by gentamicin protection assays (Almeida *et al.*, 2015). Numbers of intracellular bacteria were significantly decreased in K8, K18 and K8/K18-depleted HeLa cells, as compared to control cells (Fig 13a). In turn, in Caco-2 cells, the depletion of K8 and/or K18 had no effect on the number of intracellular bacteria (Supp Fig 1). Furthermore, K8 and/or K18 depletion in HeLa had no impact on the ability of bacteria to adhere to the cells (Fig 13b). The efficiency of K8 and/or K18 depletion in the different cell lines was confirmed by western blot analysis, using GAPDH as loading control (Supp Fig 2). Altogether these data indicate that K8 and K18 are required for internalization of *L. monocytogenes* in HeLa cells, but not in Caco-2 cells.

L. monocytogenes invasion of epithelial cells is mainly driven by the interaction of the bacterial surface proteins InlA and InlB with their host receptors E-cadherin and cMet, respectively (Mengaud et al., 1996; Shen et al., 2000). In HeLa cells Listeria internalization largely occurs through the InlB/cMet axis, while in Caco-2 cells invasion relies essentially on the InlA/E-cadherin interplay (Shen *et al.*, 2000; Sousa *et al.*, 2007). The observation that keratins are specifically required for L. monocytogenes infection of HeLa, but not Caco-2 cells suggested that K8 and K18 are particularly important for the InlB/cMet-mediated internalization pathway. To confirm this, we evaluated in K8- and/or K18-depleted HeLa cells the internalization of *Listeria innocua* expressing InlB (*L. innocua*-InlB), which invades non-phagocytic cells exclusively through the InlB pathway (Braun *et al.*, 1999). Similarly to what we observed for L. monocytogenes, internalization of *L. innocua*-InlB was compromised in K8- and/or K18-depleted cells (Fig 13c and d), thus confirming that K8 and K18 are required for efficient InlB/cMet-mediated entry of L. monocytogenes into human epithelial cells. Finally, we found that K8 and K18 are not involved in intracellular replication of *L. monocytogenes* in HeLa cells (Supp Fig 3). Taken together, these results demonstrate that K8 and K18 play a key role in InlB/cMet-mediated internalization of *L. monocytogenes*.

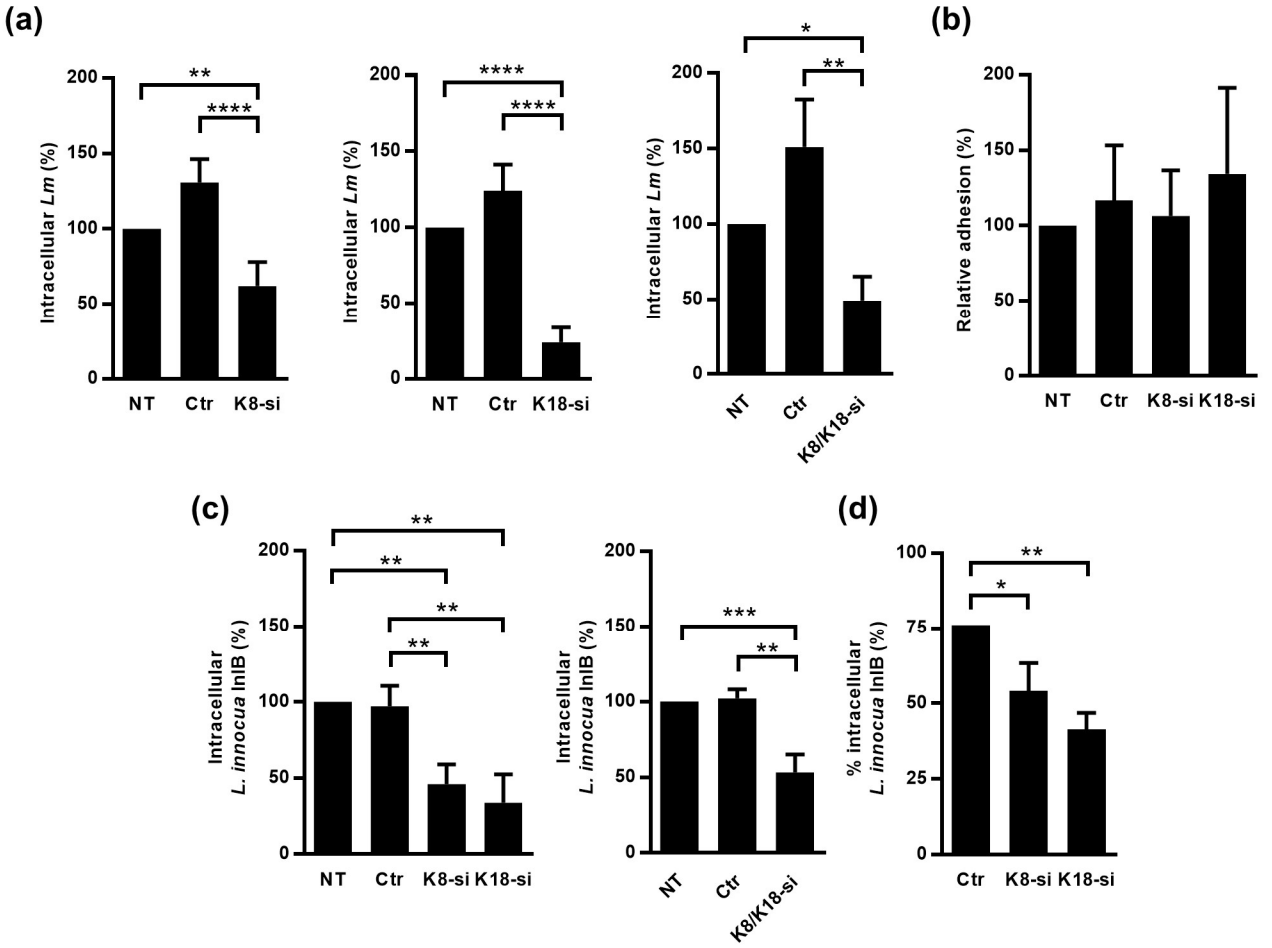

Figure 13. K8 and K18 promote Listeria infection of HeLa cells. (a) Intracellular levels of L. monocytogenes were determined by gentamicin protection assay and CFU counting in HeLa cells left untransfected (NT) or transfected with either control (Ctr) or siRNA specifically targeting K8 (K8-si, left panel), K18 (K18-si, middle panel) and both (K8/K18-si, right panel).)b) Adhesion *of L. monocytogenes* was assessed in HeLa cells left unstransfected (NT) or transfected with Ctr, K8 or K18 siRNA. (c and d) Intracellular levels of *L. innocua* expressing InlB (*L. innocua* InlB) were determined (c) by gentamicin protection assays and CFU counting in HeLa cells left unstransfected (NT) or transfected with Ctr or specific siRNA targeting K8 (K8-si left panel), K18 (K18-si, left panel) and both (K8/K18-si, right panel) or by (d) immunofluorescence scoring of extracellular and total bacteria. Values of intracellular or adherent bacteria in NT cells were normalized to 100% and the levels of infection in the remaining conditions are expressed as relative values. Values represent the mean ±S.E. of at least three independent experiments, each done in triplicate. Statistically significant differences are indicated: *, p<0.05; **, p<0.01, ***, p<0.001 and ****, p<0.0001

I.3.2. K8 and K18 accumulate at InlB-mediated internalization sites

To further characterize the role of K8 and K18 in InlB-driven invasion of *Listeria*, we investigated their cellular distribution in infected cells. HeLa cells were infected with *L. innocua*-InlB, fixed and processed for immunofluorescence. K8, K18 and cMet were immunolabelled using specific antibodies, DNA was stained using DAPI and actin was detected by phalloidin

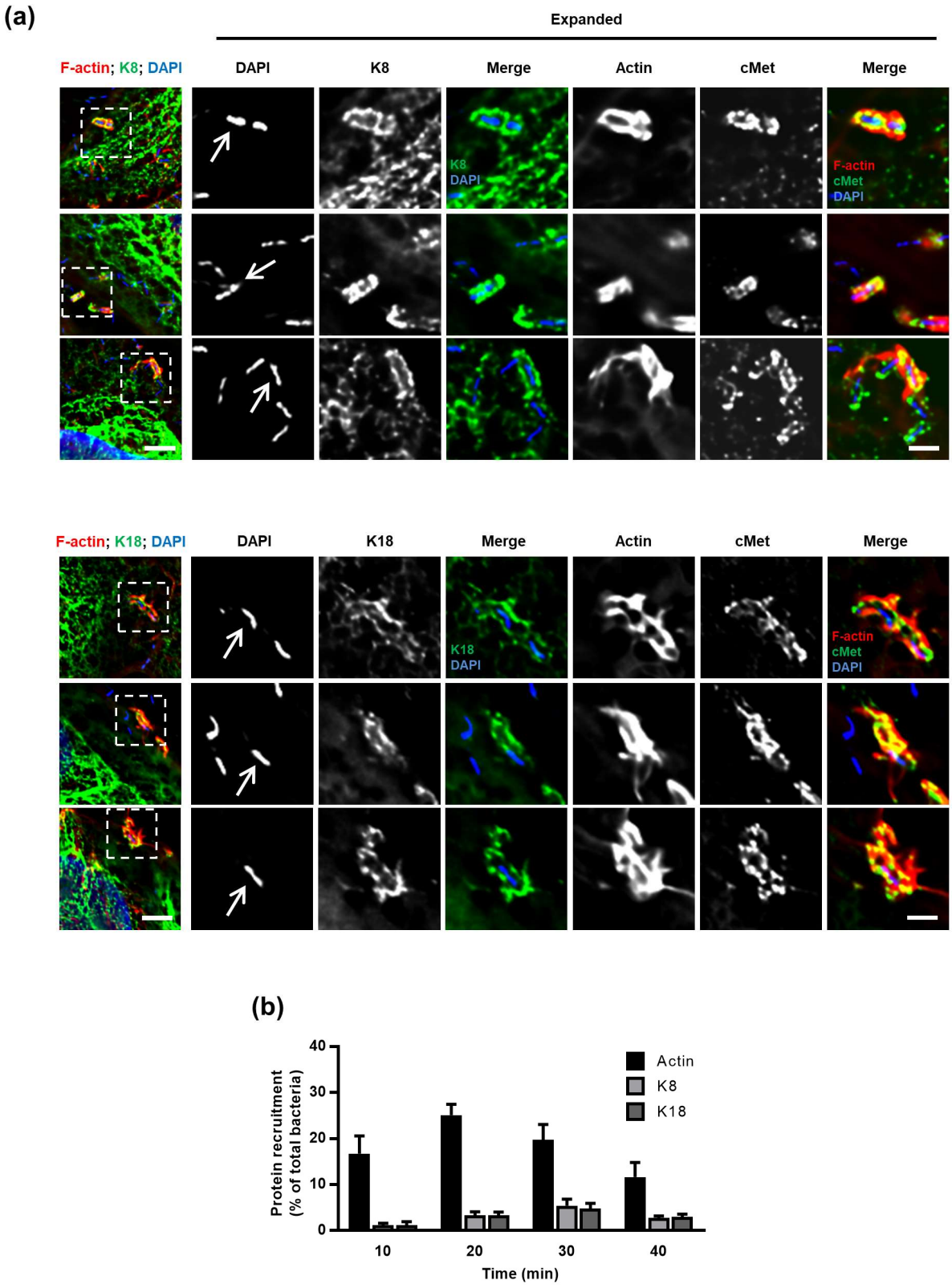

Figure 14. K8 and K18 are recruited at the bacterial entry site during InlB-mediated cellular invasion. (a) Representative widefield microscopy stack projections of HeLa cells incubated with *L. innocua* InlB for 5 minutes, fixed and immunostained for cMet (green) and for K8 (upper panels, green) or K18 (lower panels, green). F-actin was stained with phalloidin (red), DNA with DAPI (blue). Scale bar, 5 µm. Arrows indicate bacteria that display accumulation of K8, K18, cMet and F-actin at their vicinity. Insets show high-magnification images. Scale bar, 2 µm. (b) Quantification of K8, K18 and actin recruitments to the entry site

of *L. innocua* InlB. Results are expressed as the percentage of total number of bacteria associated to cells. Values are the mean ±S.E. of at least three independent experiments.

staining, K8 or K18 accumulated at the vicinity of the bacteria within minutes after infection (Fig 14a), together with F-actin and cMet, two proteins already described to accumulate at sites of entering bacteria (Bierne *et al.*, 2001). Quantifications of actin, K8 and K18 recruitments to the bacterial entry site were performed at different time points and are shown in Fig 14b. Although K8 and K18 recruitments were less frequent than actin recruitments, these observations further support the involvement of K8 and K18 in early steps of *Listeria* cellular invasion.

I.3.3. K8 and K18 modulate actin dynamics at InlB-mediated entry sites

The entry process of *L. monocytogenes* into epithelial cells is a dynamic process that engages actin rearrangements and membrane remodelling (Pizarro-Cerdá *et al.*, 2012). To gain better understanding of the dynamics of keratin recruitment to the sites of internalization and to further dissect the role of keratins in such process, we used InlB-coated beads whose entry mimics the InlB/cMet-mediated *L. monocytogenes* internalization (Braun *et al.*, 1999; Pizarro-Cerdá *et al.*, 2002). HeLa cells were incubated with InlB-coated beads for different periods of time and processed for immunofluorescence analysis. As we reported for *L. innocua*-InlB (Fig 14), K8 and K18 accumulated around entering InlB-coated beads (Fig 15a). We quantified the percentage of InlB-coated beads associated with actin, and K8 and K18 recruitments at different incubation time points (Fig 15b). As previously reported (Bierne *et al.*, 2001), actin filaments rapidly accumulate at the vicinity of InlB-coated beads. Actin recruitment peaked at 15 minutes, with 60% of the beads associated to actin filaments, and promptly decreased afterwards. In turn, K8 and K18 recruitments to the vicinity of InlB-coated beads appeared later, being maximum at 30 minutes and sustained for longer incubation periods (Fig 15b). These data indicate that actin and keratin recruitments are sequential events during the internalization process of beads. To assess the potential role of K8/K18 on actin dynamics, HeLa cells depleted for K8 or K18 were incubated with InlB-coated beads for different periods of time, processed for immunofluorescence and actin recruitments around beads were quantified. In accordance to our results in Fig 15b, in control cells actin rings surrounding InlB-coated beads peaked at 15 minutes after incubation to then rapidly decrease at later time points (Fig 15c). In K8- and K18-depleted cells, while the percentage of InlB-coated beads

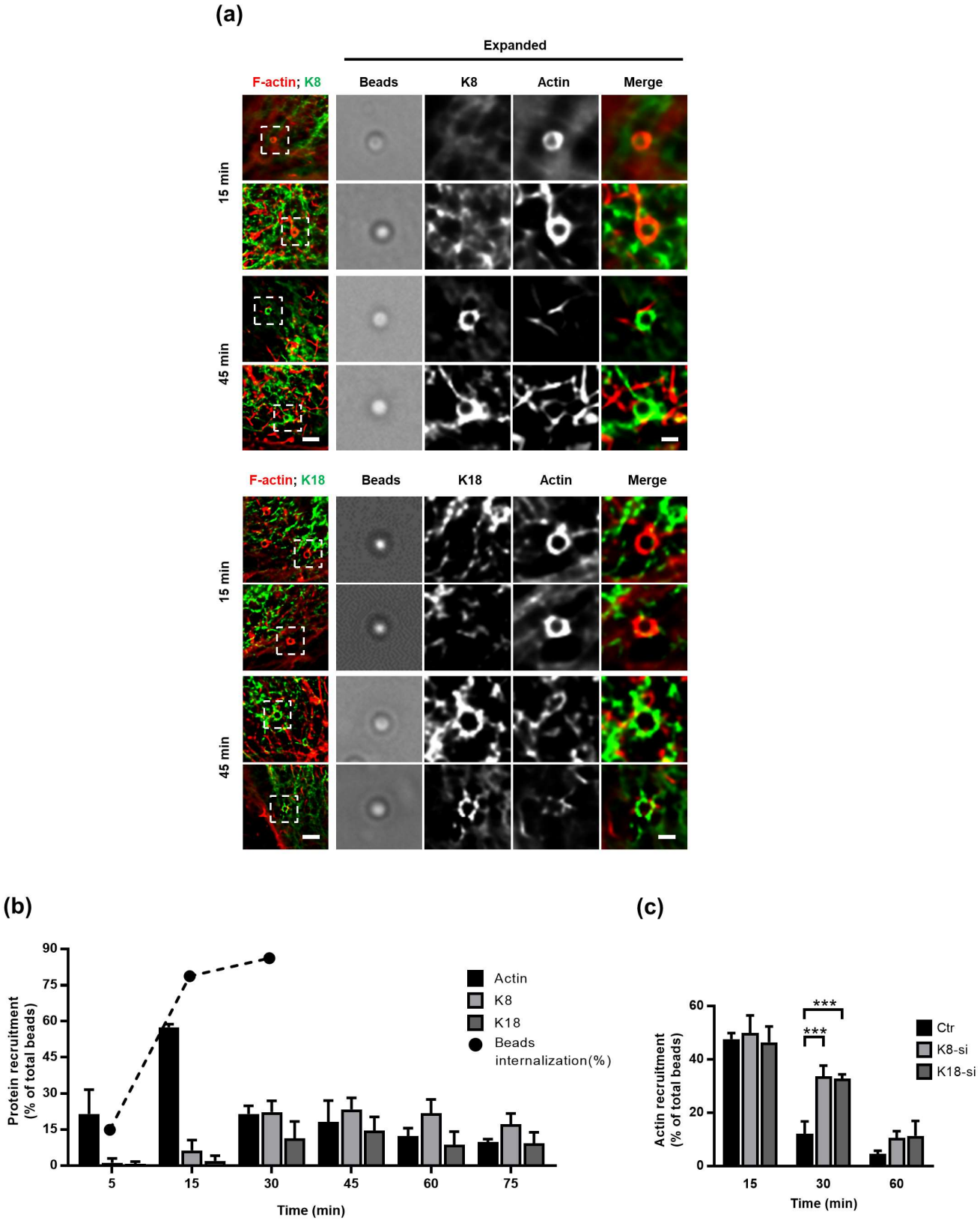

Figure 15. K8 and K18 assist actin depolymerization during later stages of internalization. (a and b) Kinetic analysis of actin, K8 and K18 recruitments during internalization of InlB-coated latex beads. (a) Stack projections of widefield microscopy images of HeLa cells incubated with InlB-coated latex beads for different periods of time, fixed, immunostained for K8 or K18 (green) and labelled for F-actin with TRITC-phalloidin (red). Scale bar, 3 µm. Insets show high-magnification images. Scale bar, 1 µm. (b) Quantification of beads positive for K8, K18 or actin recruitment. Results are expressed as the percentage of particles associated

with either protein in relation to the total number of particles associated to cells. The total number of beads was determined in brightfield. Values are the mean ±S.E. of at least three independent experiments. For determination of beads internalization, extracellular beads were stained with anti-InlB before cell permeabilization and total beads number quantified in brightfield. Values are shown in percentage and are representative of two independent experiments. (c) Quantification of InlB-coated latex beads associated to polymerized actin in HeLa cells transfected with control (Ctr) or specific siRNA targeting K8 (K8-si) or K18 (K18-si). Cells were incubated with InlB-coated latex beads for 15, 30 and 60 minutes, fixed and stained for F-actin. Beads displaying actin recruitment were considered recruitment-positive. The total number of beads associated to cells was determined in brightfield. Values represent the mean ±S.E. of at least three independent experiments. Statistically significant differences are indicated: ***, $p<0.001$.

associated to actin rings were equivalent to those of control cells at 15 minutes, they remain significantly higher at 30 minutes (Fig 15c). In cells partially depleted for K8 or K18 the levels of InlB-beads associated to actin rings are intermediate between those of control and more robustly depleted cells (Supp Fig 4). Thus, the persistence of polymerized actin around entering InlB-beads depends on the expression levels of K8 and K18. Low K8 and K18 expression increases the time during which polymerized actin associates with InlB-entering beads. These data strongly suggest a role for K8/K18 in the regulation of actin depolymerization necessary for the effective internalization of particles (Bierne *et al.*, 2001).

I.3.4. K8 and K18 control HGF/cMet-mediated signaling

The data obtained in the context of *Listeria* InlB/cMet-mediated internalization suggested a role for K8/K18 in cMet downstream signaling. It was previously demonstrated that InlB triggers cMet similarly to its natural ligand, the hepatocyte growth factor (HGF) (Li *et al.*, 2005). Indeed, both HGF and InlB bind and activate cMet, and share common downstream signaling cascades that trigger MAPK and PI3-kinase pathways to promote either cell migration and proliferation or bacterial internalization (Ireton *et al.*, 1996; Tang *et al.*, 1998; Shen *et al.*, 2000; Copp *et al.*, 2003). To assess the potential role of K8/K18 in the HGF/cMet signaling pathway, we analyzed and quantified the formation of HGF-induced membrane ruffles in control, K8- and K18-depleted cells. Cells were stimulated with HGF for different time periods, fixed and processed for immunofluorescence. Membrane ruffles were detected through actin staining, which locally accumulate at the cortex of the cells undergoing ruffling (Fig 16a). Cells with at least one actin-rich membrane ruffle were scored as positive. While in control cells, HGF stimulation quickly induced the formation of actin rich ruffles that peaked at 5 minutes, in K8-and K18-depleted cells ruffle formation was compromised even at longer time points (Fig 16b). These data indicate that K8 and K18 also play a role in HGF-induced cMet

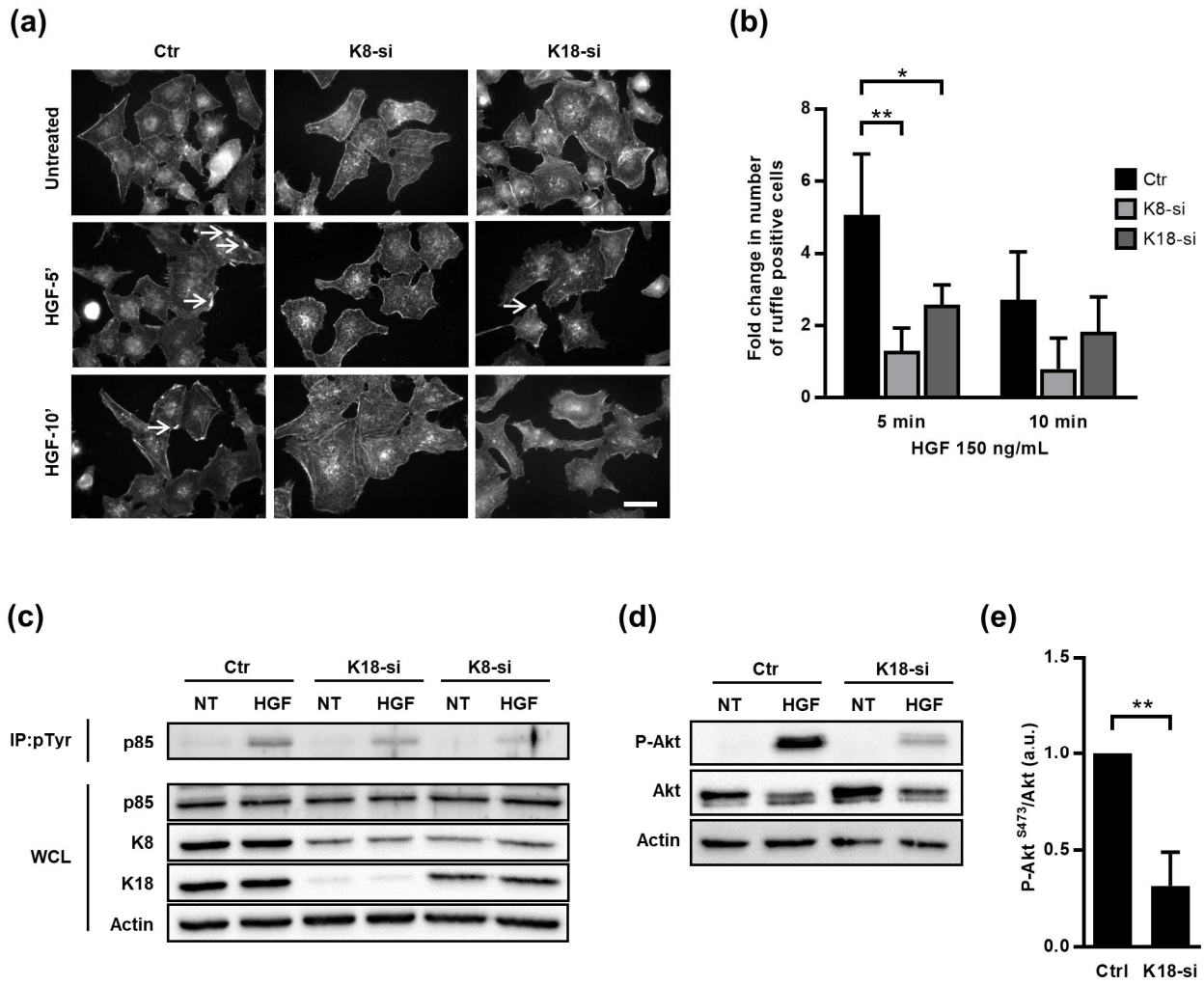

Figure 16. K8 and K18 mediate cMet downstream signaling. (a) Immunofluorescence microscopy images of control (Ctr), K8 (K8-si) or K18 (K18-si) depleted HeLa cells left untreated or incubated with HGF (150 ng/ml) for 5 and 10 min (HGF-5' and HGF-10'). Cells were fixed and stained for actin with TRITC-phalloidin. Images show the actin-rich membrane ruffles (arrows) induced by the HGF stimulation of cMet. Scale bar, 20 µm. (b) Quantification of actin-rich membrane ruffles in Ctr, K8- and K18-depleted cells. Cells without ruffles were considered ruffle-negative, whereas cells with at least one actin-rich membrane ruffle were scored as ruffle-positive. Values result from four independent experiments and are expressed as fold change with respect to untreated control cells. (c) Ctr, K8 and K18-depleted HeLa cells were incubated with 150 ng/ml HGF for 5 minutes, washed and lysed. Tyrosine phosphorylated proteins were immunoprecipitated (IP: pTyr) from whole cell lysates (WCL) and p85 was detected by immunoblot (p85) in IP fractions and WCL. Detection of actin was used as loading control. (d) Immunoblot to detect P-Akt (S473), total Akt and actin on total extracts of Ctr and K18-depleted HeLa cells left untreated (NT) or incubated with 150 ng/ml HGF for 5 minutes. (e) Densitometry analysis of the ratio of P-Akt (S473) over total Akt, in conditions of HGF stimulation. For control cells the value was arbitrarily fixed to 1. Values represent the mean ±S.E. of three independent experiments. Statistically significant differences are indicated: *, $p<0.05$ and **, $p<0.01$.

signaling. To further dissect the role of K8/K18 in cMet downstream signaling, we assessed HGF-dependent activation of PI3-kinase (PI3K) in control, K8 and K18-depleted cells. Serum-starved cells were incubated with HGF for 5 minutes, washed and lysed. Cell lysates were subjected to anti-phosphotyrosine immunoprecipitation and revealed for the PI3K p85 subunit.

Western blots of phosphotyrosine enriched protein fractions showed decreased levels of the PI3K p85 subunit in K8/K18-depleted cells (Fig 16c), indicating an impaired association of PI3K with tyrosine phosphorylated proteins in absence of keratins and suggesting a defect in PI3K activation. In addition, K18-depleted cell lysates were directly subjected to immunoblot analysis to detect phosphorylation of Akt on serine 473 (P-Akt, S473), a direct downstream target of PI3K activity (Basar *et al.*, 2005; Vanhaesebroeck *et al.*, 2012; Gessain *et al.*, 2015). As expected, in control cells HGF stimulation induced robust phosphorylation of Akt, which is extensively compromised in K18-depleted cells (Fig 16d, e). Together, these results demonstrate that K18, and to a lesser extent K8, are important players in the cMet-mediated signaling cascade and suggest that K8/K18 are involved upstream the activation of PI3K.

I.3.5. cMet expression is dependent on K8 and K18

To identify the precise role of K8/K18 in cMet-mediated signaling upstream PI3K activation, we assessed the expression and activation levels of cMet. Indeed, both InlB-mediated *L. monocytogenes* internalization and the formation of HGF-triggered membrane ruffles rely on the surface expression and auto-phosphorylation of cMet on tyrosine residues (Shen *et al.*, 2000). Interestingly, K8 and K18 were reported as modulators of the expression and/or localization of surface proteins such as the apoptotic receptor Fas, the chloride transporter DRA and the cystic fibrosis transmembrane conductance regulator (CFTR) (Gilbert *et al.*, 2001; Duan *et al.*, 2012; Asghar *et al.*, 2016). Thus, this raises the possibility that keratins may also modulate cMet expression and/or activity. We evaluated the levels of total cMet expression and activation upon HGF stimulation in whole cell lysates of control, K8- and K18-depleted cells. Surprisingly, we observed that cells depleted for K8 or K18 displayed reduced levels of total cMet (Fig 17a-c). Nevertheless, upon HGF stimulation cMet activation, as measured by phosphotyrosine immunoprecipitation assays, was detected at variable extents in those cells (Fig 17a). To determine if the low levels of total cMet expression observed in K8- and K18- depleted cells also result in a reduction of cell surface associated cMet, we specifically analyzed and quantified cell surface expression of cMet by performing biotinylation assays. Surface proteins of control, K8- and K18-depleted cells were labelled using a membrane-impermeable biotinylation reagent, recovered with neutravidin-coupled beads and analyzed by immunoblot. In agreement with the observed reduced levels of total cMet expression, K8 or K18 depletion resulted in decreased levels of cMet at the cell surface (Fig 17b, c). Altogether, these data clearly indicate that K8 and K18 control the global and surface

expression of cMet, thus impacting cMet-mediated signaling events elicited by ligands such as HGF and *L. monocytogenes* InlB.

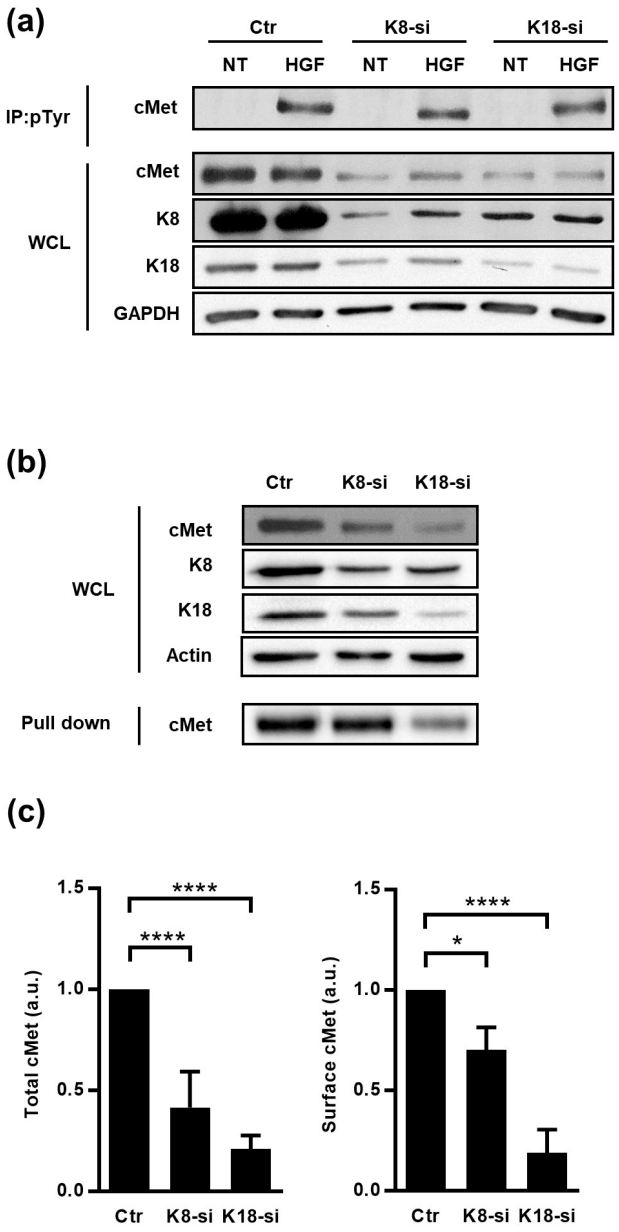

Figure 17. Total expression, surface localization and activation of cMet are perturbed in cells expressing low levels of K8 and K18. (a) HeLa cells transfected with Ctr, K8 and K18-targeting siRNAs were left untreated (NT) or incubated with 150 ng/ml HGF for 5 minutes, washed and lysed. Tyrosine phosphorylated proteins were immunoprecipitated (IP: pTyr) from whole cell lysates (WCL) and cMet was analyzed by immunoblot (cMet) in IP fractions and WCL. GAPDH detection was used as loading control. (b) Surface exposed proteins of control (Ctr), K8- (K8-si) and K18-depleted (K18-si) HeLa cells were biotinylated and recovered from total cell extracts following neutravidin pull down assays. Biotinylated samples, corresponding to surface exposed proteins, and whole cell lysates (WCL) were immunoblotted to detect cMet, K8, K18 and actin. (c) Quantifications of cMet in WCL (left panel) and in biotinylated samples (right panel) from at least three independent experiments. Statistically significant differences are indicated: *, $p<0.05$, ***, $p<0.001$ and ****, $p<0.0001$. (a.u., arbitrary units).

I.3.6. K18 controls the expression of other transmembrane receptors

Given that K8 and K18 were already reported as modulators of expression of surface proteins (Duan *et al.*, 2012; Asghar *et al.*, 2016) and taking into account our data, we hypothesized that K8 and K18 may have a broad role in controlling the expression of surface receptors. To investigate this hypothesis, we assessed the impact of K8 and K18 on the expression and surface localization of transferrin receptor (TfR) and integrin β1 in HeLa cells. Immunoblot analysis of whole cell lysates and surface biotinylated fractions revealed that K18 depletion resulted in a striking decrease of total and cell surface associated levels of both TfR and integrin β1 (Fig 18a-c). K8 depletion lead to a mild reduction of total and surface localized TfR and had no significant effect on the expression of integrin β1 (Fig 18a-c). Additionally, we performed similar experiments in Caco-2 cells and observed that K18 depletion also lead to a reduction of total and surface levels of cMet, TfR and integrin β1 (Supp Fig 5), suggesting that the mechanism through which K18 regulates the expression of these proteins is conserved in different cellular systems. Interestingly, the expression of E-cadherin is not dependent on keratins (Supp Fig 5).

To functionally assess the impact of integrin β1 downregulation induced by K18 depletion, we measured levels of internalization of *E.coli* K12 expressing the *Yersinia* invasin (K12-*inv*), which is strictly dependent on the interaction of the bacterial invasin with the host integrin β1 (Isberg and Leong, 1990). As expected, K18-depleted cells showed reduced levels of intracellular K12-*inv* (Fig 18d). Taken together, these results demonstrate that K18, and to a lesser extend K8, control the expression of some cell surface receptors, in turn modulating signaling events taking place downstream the engagement of these receptors.

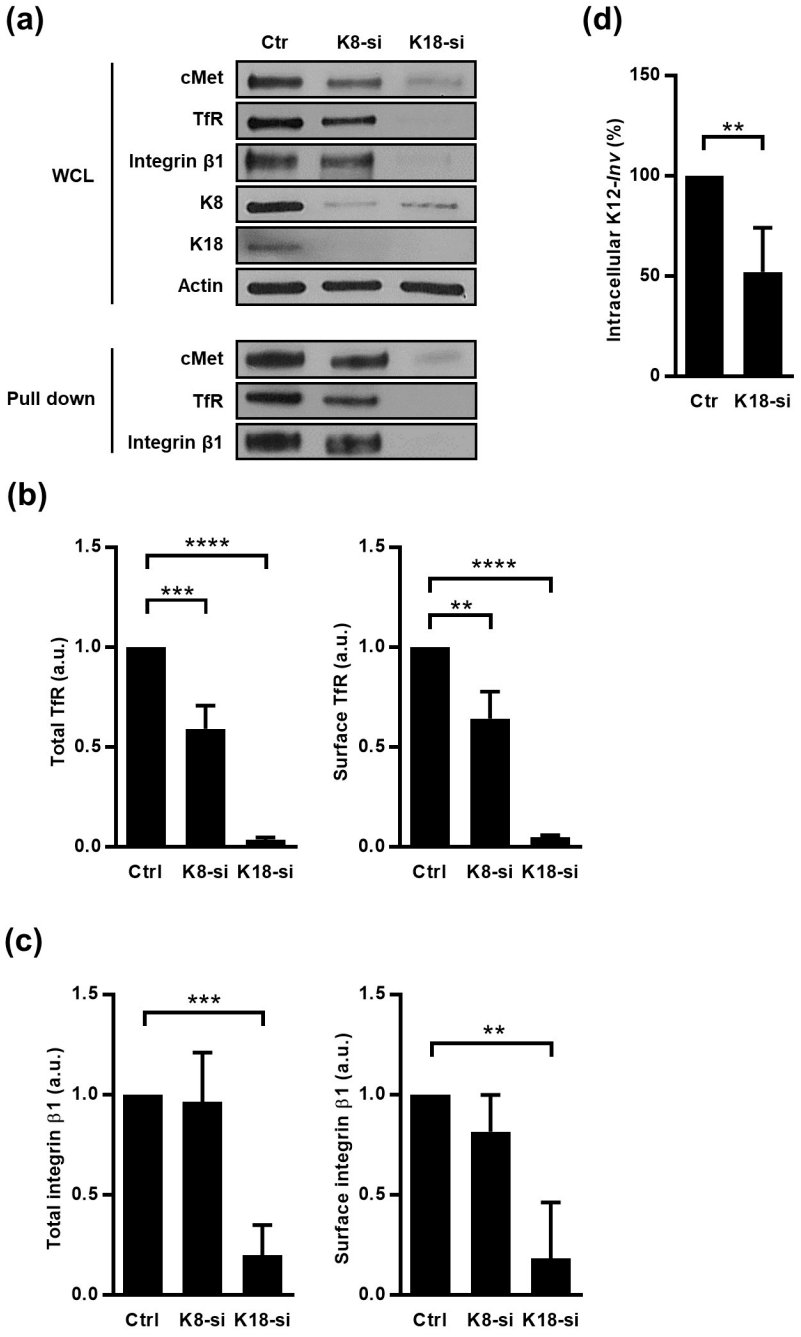

Figure 18. K8 and K18 depletion perturbs expression and surface localization of transmembrane receptors. (a) Surface proteins of control (Ctr), K8- (K8-si) and K18-depleted (K18-si) HeLa cells were biotinylated, recovered from total cell extracts and pulled down using neutravidin beads. Biotinylated samples, which corresponds to surface exposed proteins, and whole cell lysates (WCL) were immunoblotted to detect cMet, TfR and integrin β1, together with Actin, K8 and K18. (b) Quantifications of TfR in WCL (left panel) and in biotinylated samples (right panel) from at least three independent experiments. (c) Quantifications of integrin β1 in WCL (left panel) and in biotinylated samples (right panel) from at least three independent experiments. Statistically significant differences are indicated: *, p<0.05, ***, p<0.001 and ****, p<0.0001. (a.u., arbitrary units). (d) Functional impact of K18 in the expression of integrin β1 was assessed by gentamicin survival assay and CFU counting in K18-depleted HeLa cells (K18-si) incubated with invasive E. coli K12 expressing the *Y. pseudotuberculosis* invasin (K12-inv). Values of intracellular bacteria in Ctr cells were normalized to 100% and the entry levels in K18-si cells are expressed as relative values. Values are the

mean ±S.E. of three independent experiments, each done in triplicate. Statistically significant differences are indicated: **, p<0.01, ***, p<0.001 and ****, p<0.0001.

I.3.7. Protein synthesis and stability do not depend on K18 expression

The decrease of total levels of cMet, TfR and integrin β1 observed in K18-depleted cells lead us to put forward the possibility that protein synthesis would be impaired in these cells. Indeed, K8/18 depletion was reported to lead to reduced protein synthesis in human H4 neuroglioma cells (Galarneau *et al.*, 2007). In addition, mTOR signaling and, consequently, protein synthesis were shown to be impaired in keratinocytes lacking Keratin 17 (Kim *et al.*, 2006). We thus assessed if mTOR signaling and global protein synthesis were compromised in K18-depleted HeLa cells, which would account for the reduced levels of cMet, TfR and integrin β1. The ribosomal protein S6 is the target of p70S6K, a major mTOR effector (Magnuson *et al.*, 2012), and S6 phosphorylation is thus used as a readout for mTOR activity (Biever *et al.*, 2015; González *et al.*, 2015). To evaluate the involvement of K18 in mTOR signaling activity, we thus analyzed the level of phosphorylated S6 in control and K18-depleted HeLa cells. S6 phosphorylation was detected in both control and K18-depleted cells (Fig 19a), indicating that mTOR activity is not compromised and suggesting that mTOR-dependent protein synthesis is not impaired in absence of K18. To assess the rate of bulk protein synthesis, control or K18-depleted cells were incubated with radiolabeled methionine to be incorporated into newly synthesized proteins. Total protein extracts were resolved by SDS-PAGE and labelled proteins detected by autoradiography. No major defect was detected in K18-depleted as compared to control cells (Fig 19b), indicating that the global initiation rate of translation is not compromised in cells lacking K18. The same samples were used in immunoblot to confirm the down-regulation of cMet, integrin β1 and TfR expression in K18-depleted cells (Fig 19c). These observations demonstrate that K18 does not impact significantly protein translation and *de novo* synthesis and suggest that other mechanisms should govern the K18-dependent expression of cMet, TfR and integrin β1.

Interestingly, K18 was previously reported to enhance the stability of the surface protein CFTR (Duan *et al.*, 2012). We thus hypothesized that K18 could promote the stability of cMet, integrin β1 and TfR by minimizing their degradation. To investigate this hypothesis, control and K18-depleted HeLa cells were treated with the lysosomal inhibitor concanamycin A alone or together with the proteosomal inhibitor MG132 for different time periods. Cell extracts were immunoblotted for cMet and TfR. In both conditions tested, control and K18-depleted cells behaved similarly and no significant accumulation of cMet, integrin β1 and TfR was detected upon blockage of protein degradation (Fig 19d).

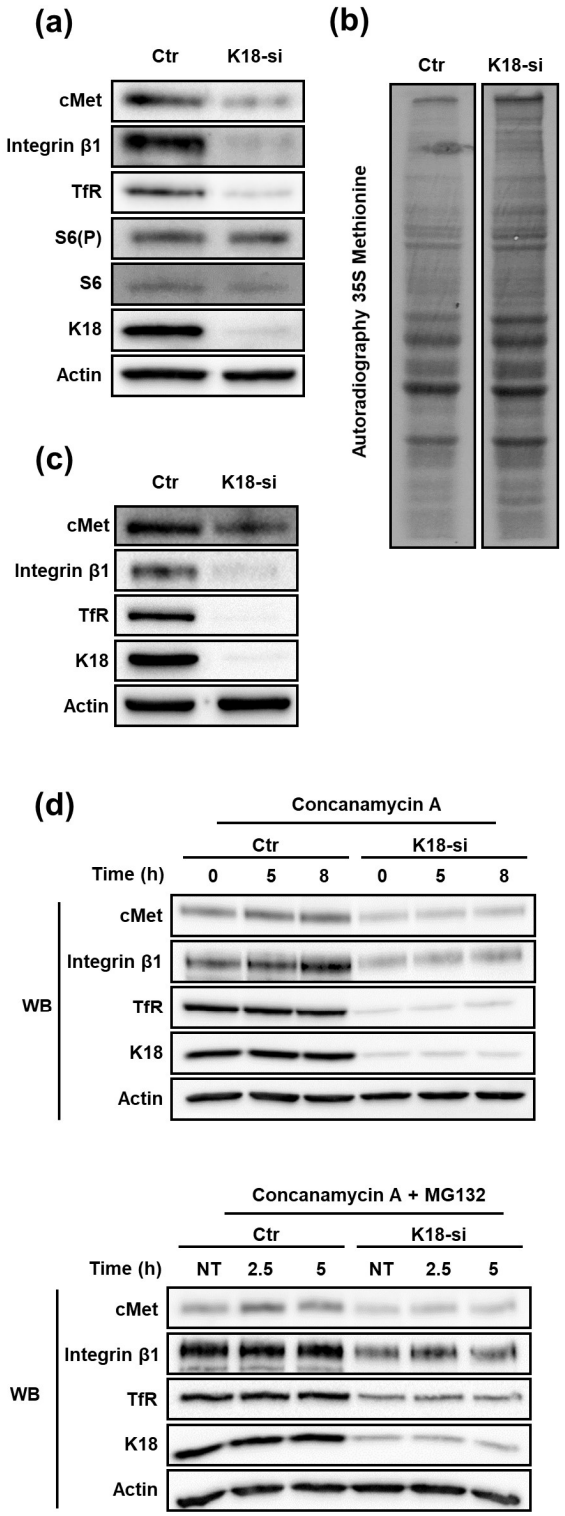

Figure 19. K18 depletion does not dampen mTOR/S6K signaling, global protein translation and receptor degradation. (a) Activation of mTOR/S6K signaling pathway in K18 (K18-si) depleted HeLa cells was assessed by immunoblotting whole cell extracts against phosphorylated S6 (S6(P)), total S6, cMet, K18 and Actin as loading control. Immunoblot representative of three different experiments. (b) Rate of total protein synthesis was assessed by 35S-methionine incorporation of HeLa cells transfected with control (Ctr) or K18 targeting (K18-si) siRNA. Autoradiography representative of two independent experiments. (c) Depletion efficiency of the samples that were used for the 35S-methionine incorporation assay. (d) After transfection with control (Ctr) or siRNA targeting K18 (K18-si), HeLa cells were incubated with 100 nM of the lysosomal inhibitor Concanamycin A alone (upper panel) or together with the proteasomal inhibitor 10 μM MG132 (lower

panel) for different periods of time. Lysates were collected and immunoblotted for cMet, TfR, integrin β1, K18 and Actin as a loading control. Immunoblots are representative of at least two independent experiments.

Altogether, these results indicate that the downregulation in the expression of cMet, TfR and integrin β1 detected in K18-depleted cells is not due to a defect on protein synthesis or stability.

I.3.8. K18 promotes transcripts stability

Besides translation and protein stability, regulation at the transcriptional level represents another mechanism to control protein expression. We therefore assessed if K18 depletion had an impact on transcript levels of the different receptors by qRT-PCR on mRNAs extracted from control and K18-depleted HeLa cells. cMet, TfR and integrin β1 mRNA levels were strongly decreased in K18-depleted cells (Fig 20a), with reductions ranging from 54% for cMet to up to 94% for TfR. Such reduced mRNA levels should therefore be responsible for the reduced cMet, TfR and integrin β1 protein levels detected in K18-depleted cells.

Decreased steady state mRNA levels may result from a reduction in transcription or from higher instability of the mRNA (Wu and Brewer, 2012). To assess the involvement of K18 in the stability of cMet, TfR and integrin β1 transcripts, we measured mRNA decay in cells treated with the transcription inhibitor Actinomycin D. Control and K18-depleted HeLa cells were left untreated (0 h) or incubated with Actinomycin D for 1 and 2 h, total RNAs were extracted and analyzed by qRT-PCR. We observed that cMet, TfR and integrin β1 mRNAs consistently displayed a higher rate of decay in K18-depleted cells (Fig 20b), thus, indicating higher instability of these transcripts in cells lacking K18.

Taken together, these results demonstrate that K18 confers stability to specific transmembrane receptor mRNAs thus ensuring steady state protein levels.

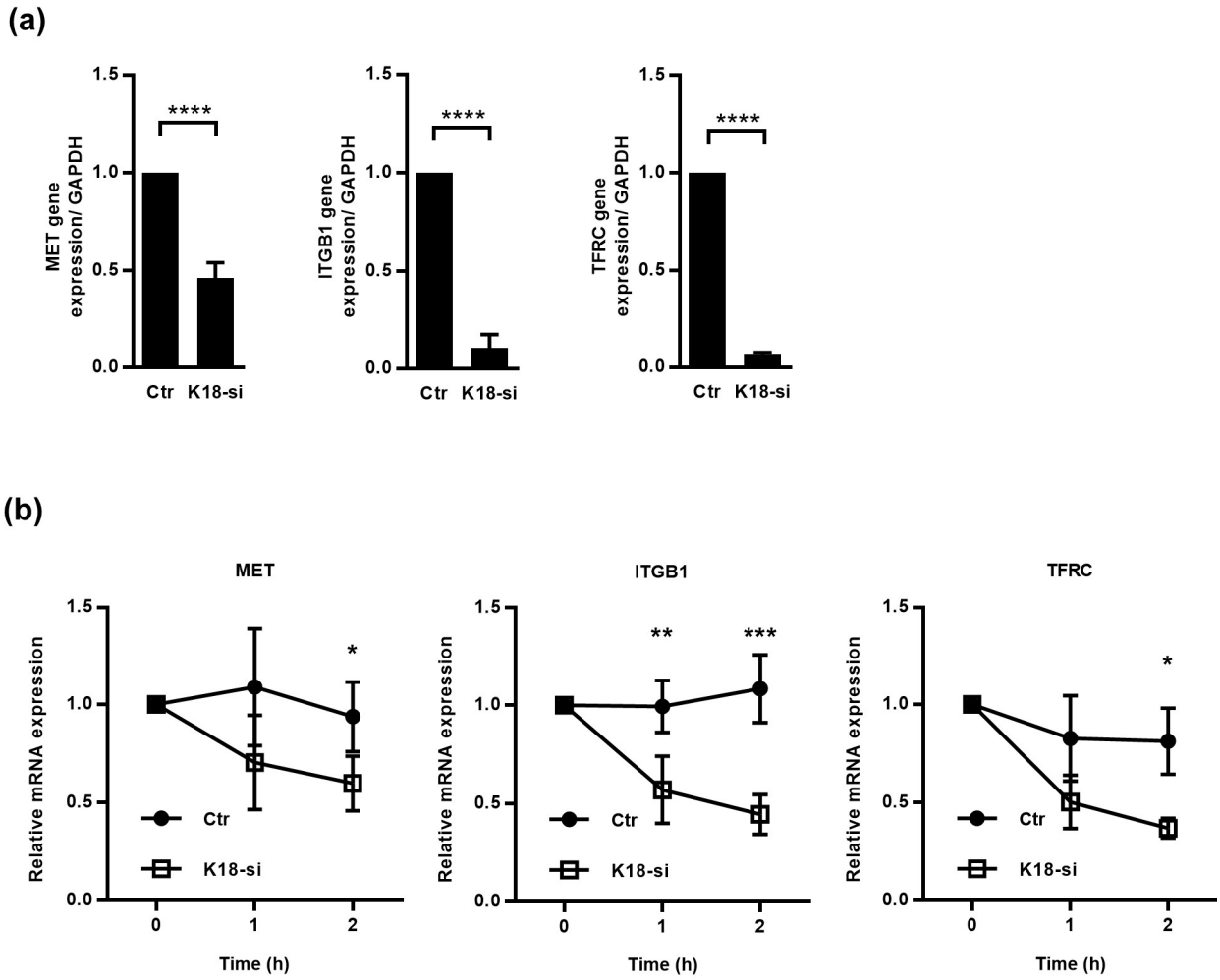

Figure 20. K18 favors expression of cMet, TfR and integrin β1, by promoting transcript stability. (a) mRNAs were extracted from control (Ctr) and K18-depleted (K18-si) HeLa cells and qRT-PCR was performed using GAPDH as a housekeeping gene. Data are represented as mean ±S.E. from at least three independent experiments (b) Control and K18 depleted cells were left untreated or were treated with 5 µg/ml of the transcriptional inhibitor Actinomycin D for different periods of time. Transcript levels for cMet (MET), TfR (TFRC) and integrin β1 (ITGB1) were determined by qRT-PCR. Fold changes are relative to GAPDH and were normalized to untreated control. Results are from at least three independent experiments. Statistically significant differences are indicated: *, $p<0.05$; **, $p<0.01$, ***, $p<0.001$ and ****, $p<0.0001$.

I.4. Discussion

Manipulation of the host cell cytoskeleton is a hallmark of the cellular infection by several human bacterial pathogens. Intermediate filaments were reported to participate in the infection process of different pathogens (Geisler and Leube, 2016), however the molecular details remain sparse. Here we demonstrate for the first time that epithelial K8 and K18 play a dual role during *L. monocytogenes* cellular infection. We found that K8 and K18 are specifically required for the successful InlB/cMet-mediated *L. monocytogenes* cell invasion by modulating the actin dynamics at the entry site and by controlling the expression of *cMet* itself. Interestingly, K18 also appeared to control the expression of other cell surface receptors, such as TfR and integrin β1, by promoting mRNA stability, thus suggesting a broader role for keratins in the regulation of gene expression.

During infection, K8 and/or K18 were previously shown to assist toxin internalization (Nava-Acosta and Navarro-Garcia, 2013), to favor intracellular pathogen replication (Claser *et al.*, 2008) and to allow stable pathogen docking to the host cell surface (Carlson *et al.*, 2002; Batchelor *et al.*, 2004; Russo *et al.*, 2016). Moreover, K8 and K18 were shown to be targeted for degradation during viral and bacterial infections (Chen *et al.*, 1993; Seipelt *et al.*, 2000; Savijoki *et al.*, 2008), however the functional details of these roles remain elusive.

Keratins, as other IFs, are dynamic filament networks that interact with a multitude of proteins serving as scaffolds to organize signaling platforms and regulate different processes (Pallari and Eriksson, 2006). How K8 and K18 modulate the actin dynamics during InlB-mediated cellular invasion is still unknown. Indeed, despite several reports pointing to an interplay between actin and keratin cytoskeletons, the molecular details of such a crosstalk remain largely unidentified (Jiu *et al.*, 2015). The link between keratins and actin is thought to be mediated by their association with linker proteins such as plectin and dystrophin (Stone *et al.*, 2005; Karashima *et al.*, 2012). However, other IFs such as vimentin interact directly with actin or indirectly through motors protein like myosin IIB (Esue *et al.*, 2006; Menko *et al.*, 2014). Actin filaments were suggested to promote the assemble of keratin network (Windoffer *et al.*, 2006; Kölsch *et al.*, 2009) by favoring the retrograde transports of keratin subunits. Interestingly, the formation of EGF-induced actin-rich lamellipodia was shown to be followed by the extension of the keratin network and *de novo* nucleation at the lamellipodia itself (Felkl *et al.*, 2012). K8 and 18 were reported to interact with Grb2 and Cbl (Robertson *et al.*, 1997; Blagoev *et al.*, 2003; Duan *et al.*, 2012), proteins involved in cMet signaling and InlB-dependent entry of *L. monocytogenes* (Ireton *et al.*, 1999). In addition, keratins were found to regulate the size and organization of lipid rafts (Gilbert *et al.*, 2012; Gilbert *et al.*, 2016), which serve as surface membrane platforms promoting clustering of signaling molecules (Pizarro-Cerdá and

Cossart, 2009), and whose integrity is required for successful InlB-mediated *L. monocytogenes* infection (Seveau *et al.*, 2004). It is thus possible that, through interaction with adaptor proteins downstream the activation of cMet at specific places at the host plasma membrane, K8 and K18 may modulate actin dynamics at InlB entry sites. The identification of host proteins interacting with K8 and K18 specifically upon *L. monocytogenes* infection or canonical HGF-induced cMet activation should uncover the molecular details of keratin-mediated actin dynamics modulation.

Strikingly, our data highlight the role of K18 in the control of the expression of several cell surface receptors such as cMet, TfR and integrin β1. These findings are in agreement with a growing body of evidence that suggests that keratins regulate gene expression and translation (Asghar *et al.*, 2016). Indeed, mice that lack type I or type II keratins display perturbed transcription (Kumar *et al.*, 2015; Kumar *et al.*, 2016) and impaired protein expression (Vijayaraj *et al.*, 2009). Keratin 17 was recently reported to be present in the nucleus where it interacts with the promoter regions of cytokine genes and the transcriptional regulator AIRE (Hobbs *et al.*, 2015) thus regulating inflammatory response. Additionally, K17 regulates the shuttling between the nucleus and the cytoplasm of proteins such as hnRNP K (Chung *et al.*, 2015), 14-3-3σ (Kim *et al.*, 2006) and $p27^{KIP1}$ (Escobar-Hoyos *et al.*, 2015). Nuclear accumulation of non-filamentous K18 was detected when exportin1-mediated nuclear export is inhibited (Kumeta *et al.*, 2013), suggesting that K18, among others, may assist the nucleocytoplasmic shutting of proteins.

These observations, together with our data showing that K18 ensures the stability of certain mRNAs and thus promotes the expression of proper protein levels, tempt us to speculate that K18 may affect the shuttling of RNA-binding proteins (RBPs) from the nucleus to the cytoplasmic compartment, or the binding of specific RBPs involved in mRNA stabilization, and thus impact mRNA stability. In support to this hypothesis, K18 was shown to interact with hnRNP R (Havugimana *et al.*, 2012), an RBP that binds and stabilizes the mRNA of MHC class I genes, thus enhancing their translation (Reches *et al.*, 2016). In addition, while searching for K18 interactors (our unpublished data), we identified by mass spectrometry the heat-shock cognate protein 70 (Hsc70), a chaperone that is able to bind and stabilize the mRNA of the proapoptotic protein Bim (Matsui *et al.*, 2007). We also identified the PTB-associated splicing factor (PSF), an RNA and DNA binding protein that regulates transcription, alternative splicing and mRNA stability (Yarosh *et al.*, 2015). Finally, K18 was reported to interact with the mRNA degradation machinery protein Pan2 (Bett *et al.*, 2013), involved in the initial trimming of polyadenylated tails of mRNA, a process that favors further mRNA deadenylation and subsequent degradation (Wu and Brewer, 2012). Together with K18, knockout of K8 results in perturbed mRNA levels of multiple genes (Habtezion *et al.*, 2011; Asghar *et al.*, 2016; Lähdeniemi *et al.*, 2017).

Grounded in these previous studies and our data, we propose here that K18 might modulate the stability of particular transcripts probably by interacting with specific RBPs in the cytoplasm, thus modulating the fate of the associated transcripts and ultimately controlling gene expression. The molecular understanding of the role of K18 in mRNA stability and protein expression requires further studies to identify putative RBPs interacting with K18.

I.5. Materials and Methods

I.5.1. Reagents and antibodies

Primary antibodies used are listed in Table 1. Goat anti-mouse HRP or anti-rabbit HRP (P.A.R.I.S.) secondary antibodies were used at 1:2000 for immunoblotting. For immunofluorescence, secondary antibodies goat anti-rabbit or anti-mouse Alexa Fluor 488 (Invitrogen) and goat anti-mouse or anti-rabbit Cy3 (Jackson Immunoresearch) were used at 1:300. Actin was labeled with Alexa Fluor 647 phalloidin (Invitrogen) or Phalloidin-Tetramethylrhodamine B isothiocyanate (TRITC, Sigma Aldrich). DNA was labeled with 2-(4-Amidinophenyl)-6-indolecarbamidine dihydrochloride (DAPI, Sigma Aldrich). Concanamycin A, MG132 and Actinomycin D were obtained from Sigma Aldrich. HGF was purchased from Peprotech.

I.5.2. Bacterial Strains and Cell Lines

L. monocytogenes EGDe strain was grown at 37ºC with shaking in brain heart infusion (BHI; BD-Difco). *L. innocua* InlB was grown in BHI supplemented with 5 µg/ml erythromycin. *E. coli* K12-*inv* was grown at 37ºC with shaking in lysogeny broth (LB) supplemented with 100 µg/ml ampicillin. HeLa cells (ATCC CCL-2) were cultured in DMEM supplemented with glucose (4.5 g/l), L-glutamine and 10% fetal bovine serum (FBS, Biowest). Caco-2 cells (ATCC HTB-37) were maintained in EMEM supplemented with 20% FBS, L-glutamine, sodium pyruvate and nonessential amino acids. Cells were maintained at 37°C in a 5% CO_2 atmosphere. Cell culture media and supplements were from Lonza.

I.5.3. Bacterial infections

Cell infections were performed as described (Reis *et al.*, 2010). For adhesion experiments, bacteria in exponential phase of growth were washed and inoculated at a multiplicity of infection (MOI) of 50. After 30 min, cells were washed 5 times with phosphate buffered saline (PBS), lysed in 0.2% Triton-X-100 and serial dilutions were plated for quantification of viable bacteria (colony forming units-CFU). For invasion assays, inoculum was prepared as above and cells were infected for 60 min, washed and incubated with medium

supplemented with 20 µg/ml gentamicin for 90 min. Cells were washed, lysed with 0.2% Triton-X-100 and serial dilutions plated for CFU counting. For immunofluorescence scoring of adhered and intracellular *L. innocua*-InlB, HeLa cells were inoculated at a MOI of 50 for 30 min, washed and fixed. Before permeabilization, extracellular bacteria were labeled with a rabbit polyclonal antibody raised against *L. innocua* (R6, kindly provided by Prof Pascale Cossart, Institut Pasteur) and an appropriate secondary antibody. Cells were then permeabilized with 0.1% Triton X-100 and total bacteria were labelled with R6 and a secondary antibody coupled to a different fluorochrome. Total and extracellular bacteria were counted under the microscope. For intracellular replication assays, cells were infected with a MOI of 1 for 60 min, washed and incubated with medium complemented with 20 mg/ml gentamicin for 90 min, washed and lysed 2.5, 5, 7, 9 and 12 h after infection. Adhesion and invasion assays were performed in triplicate and repeated at least 3 times. Replication assays were performed twice in duplicate. For immunofluorescence experiments, cells were infected with *L. innocua* InlB (MOI of 50), washed in PBS and fixed in 3% paraformaldehyde.

I.5.4. Transfection of siRNA Duplexes

HeLa cells were seeded in 24 or 6 well plates and transfected with 46 nM control siRNA-D (sc-44232, Santa Cruz Biotechnology) or with specific siRNAs for K8 or K18 depletion (oligo sequences on Table 2). For partial depletion, we used 13.8 nM of siRNA duplexes. Transfection was performed with HiPerFect (Qiagen) immediately after cell seeding, according to the manufacturer's instructions. Assays were performed 72 h pot-transfection. Transfection of Caco-2 cells was performed with Amaxa Cell line Nucleofector Kit T (Lonza) using program B-024 and following manufacturer's instructions.

I.5.5. Immunoblotting

Protein samples were diluted in Laemmli buffer containing 5% β-mercaptoethanol, resolved on SDS-PAGE gels and transferred to nitrocellulose membranes (Bio-Rad Laboratories). Membranes were blocked in 4% bovine serum albumin (BSA; Sigma Aldrich) or 5% skimmed milk dissolved in TBS-Triton (150 mM NaCl, 20 mM Tris-HCl, pH 7.4, and 0.1% Triton X-100) for 1 h. Primary antibodies were diluted in 2.5% skimmed milk or 4% BSA and incubated overnight at 4ºC, incubation with HRP-conjugated secondary antibodies was performed at room temperature for 1h. ECL (Thermo Scientific) or SuperSignal West Dura

Extended Duration Substrate (Pierce) were used for detection of signal on X-ray films (Thermo Scientific) or digitally acquired in a ChemiDoc XRS+ system (Bio-Rad Laboratories).

I.5.6. Immunoprecipitation assays

Per condition, 2 x 10^6 cells were washed twice with phosphate-buffered saline (PBS) and serum-starved for 8 h at 37°C and 5% CO_2. Then, cells were either left untreated or incubated with 150ng/ml HGF for 5 min. Cells were then washed twice with ice-cold PBS and lysed in 300 µl of lysis buffer (1% NP-40, 50 mM Tris pH 7.5, 150 mM NaCl, 2 mM EDTA, 1 mM AEBSF, PhosSTOP (Roche Pharmaceuticals) and Complete Protease Inhibitor Cocktail (Roche Pharmaceuticals)). Lysates were centrifuged at 15 000 g for 10 min at 4°C and immunoprecipitated with 0.7 µg of anti-phosphotyrosine antibody (4G10) overnight at 4°C. Immune complexes were captured with 50 µl of PureProteome Protein A magnetic beads (Millipore) at 4°C and washed three times with wash buffer (0.2% NP-40, 50 mM Tris pH 7.5, 150 mM NaCl, 2 mM EDTA, 1 mM AEBSF, PhosSTOP, Complete Protease Inhibitor Cocktail). Immunoprecipitated proteins were eluted and boiled in Laemmli buffer.

I.5.7. Cell surface biotinylation assay

Cell surface protein biotinlyation was performed using the EZ-Link Sulfo-NHS-Biotinylation kit (Thermo Scientific) as described in (Martins *et al.*, 2012) and accordingly to manufacturer's protocol. In brief, 2 x 10^6 cells were washed with ice cold PBS (pH 8), incubated with 2 mM Sulfo-NHS-biotin (2 h at 4ºC), washed with cold 100mM glycine in PBS (pH 7.2), harvested, and lysed in RIPA (sc-364162, Santa Cruz Biotechnology). Cell extracts (90 µg) were incubated with 50 µl of neutravidin agarose resin (Thermo Scientific) overnight at 4ºC, with rotation. Resin was washed and captured biotinylated proteins were eluted with Laemmli buffer.

I.5.8. Immunofluorescence microscopy

Cells were fixed in 3% paraformaldehyde (10 min), quenched with 20 mM NH_4Cl (1 h), permeabilized with 0.2% Triton X-100 (6 min), washed and blocked with 1% BSA in PBS. Antibodies were diluted in the blocking buffer. Coverslips were incubated with primary

antibodies (1 h), washed in PBS, incubated with secondary antibodies, phalloidin TRITC or Alexa 647 and DAPI for 45 min, and mounted onto microscope slides with Aqua-Poly/Mount. Images were analyzed and collected with an epifluorescent Zeiss Axio Imager Z1 microscope or an Olympus BX63 microscope. When necessary, Z-stacks were deconvoluted with Huygens Professional Software (SVI, Netherlands) and projected with ImageJ software (NIH).

I.5.9. Ruffle formation assays

Cells were serum starved for 7 h, stimulated with 150ng/ml HGF for 5 and 10 min, fixed in 3% paraformaldehyde (PFA) and processed for immunofluorescence. Cells with at least one actin rich membrane ruffle were scored as ruffle-positive, cells with no ruffles were considered ruffle-negative. Data were obtained from four independent experiments, for which at least 180 cells/condition were analyzed.

I.5.10. Rates of total protein synthesis

Cells ($2x10^6$) were labelled with ^{35}S-methionine (22.5 uCi/ml, PerkinElmer) in methionine free DMEM (2 h at 37ºC), washed twice with PBS and lysed in RIPA buffer. Protein samples diluted in Laemmli buffer were loaded into a 10% polyacrylamide gel and resolved by SDS-PAGE, followed by autoradiography.

I.5.11. Quantitative real-time PCR

Total RNAs were isolated using TripleXtractor (GRiSP), following manufacturer's protocol. Purified RNAs (1 µg) were reverse transcribed with iScript cDNA Synthesis Kit (Bio-Rad Laboratories). Quantitative real-time PCR (qRT-PCR) was performed in 10 µl reactions containing 5 µl iTaq Universal SYBR Green Supermix (Bio-Rad Laboratories), 1 µl of cDNA and 0.1 µl of 10 µM forward and reverse primers (Table 3), using the following protocol: 3 min (95ºC), followed by 40 cycles of 10 s (95ºC), 20 s (55.6ºC) and 20 s (72ºC). Each target gene was analyzed in triplicate and blank control was included for each primer pair. The comparative threshold method (ΔΔCt) was used to analyze the amplification data after normalization of the test and control sample expression values to a housekeeping reference gene (GAPDH).

I.5.12. mRNA stability assays

Cells were incubated with Actinomycin D (5 µg/ml) for 1 and 2 h to inhibit *de novo* RNA synthesis. Cells were harvested and RNAs isolated, reverse transcribed and analyzed by qRT-PCR. GAPDH was used as reference gene and fold changes were normalized to the untreated control. At least three independent experiments were performed for each gene of interest.

I.5.13. InlB-coated beads assays

Purified InlB (350 µg) was covalently coupled to 200 µl of a 4% aqueous suspension of 1.0 µm carboxylated modified latex beads (Thermo Scientific), following manufacturer's instructions. To synchronize the uptake, HeLa cells were incubated with InlB-coated beads at 4ºC, centrifuged (5 min at 320g) and incubated at 37ºC. Cells were washed in ice cold PBS and processed for immunofluorescence. At least 20 cells and more than 150 beads were analyzed per condition, in at least three independent experiments. To assess internalization, extracellular beads were stained with anti-InlB B4-6 antibody (Braun *et al.*, 1999) before cell permeabilization. Samples were then analyzed in a high-throughput widefield fluorescence microscope (IN Cell Analyzer 2000, GE Healthcare). Total beads number was quantified in brightfield. Per condition, at least 500 cells and 5000 beads were analyzed.

I.5.14. Statistical Analyses

Statistical analyses were performed with Prism 7 software (GraphPad) using: two-tailed unpaired Student's *t* test for comparison of means between two samples, one-tailed *t* test for comparisons with samples arbitrarily fixed to 100 and one-way ANOVA with Dunnett's *post hoc* analysis to compare different means in relation to a control sample. Differences were not considered statistically significant for p value≥0.05

I.6. Acknowledgments

This work received funding from Norte-01-0145-FEDER-000012 - Structured program on bioengineered therapies for infectious diseases and tissue regeneration, supported by Norte Portugal Regional Operational Programme (NORTE 2020), under the PORTUGAL 2020 Partnership Agreement, through the European Regional Development Fund (FEDER). Publication fees were supported by ICBAS, University of Porto. RC received an FCT Doctoral Fellowship (SFRH/BD/90607/2012) and IP-C a FCT Post-Doctoral Fellowship (SFRH/BPD/107901/2015) through FCT/MEC co-funded by QREN and POPH (Programa Operacional Potencial Humano). SS was supported by FCT Investigator program (COMPETE, POPH, and FCT). We thank IBMC facilities for technical assistance.

I.7. Tables

Table 1: List of antibodies used in this study. WB: Western blot, IF: immunofluorescence.

Antigen	Species	Applications	Reference	Source
Phosphotyrosine	Mouse	IP (1:360)	4G10, 05-321	Millipore
Actin	Mouse	WB (1:5000)	A5441	Sigma Aldrich
GAPDH	Mouse	WB (1:15000)	sc-32233	Santa Cruz Biotechnologies
K8	Mouse	WB (1:450), IF (1:200)	sc-8020	Santa Cruz Biotechnologies
K8	Rabbit	WB (1:10000), IF (1:400)	ab53280	Abcam
K18	Mouse	WB (1:2000), IF (1:200)	sc-6259	Santa Cruz Biotechnologies
K18	Rabbit	WB (1:10000), IF (1:400)	ab52948	Abcam
cMet	Rabbit	WB (1:175), IF (1:150)	Sc-10	Santa Cruz Biotechnologies
TfR	Mouse	WB (1:1500)	13-6800	Thermo
Integrin-β1	Rabbit	WB (1:1000)	ab52971	Abcam
PI3Kp85	Rabbit	WB (1:1500)	06-195	Millipore
E-cadherin	Rabbit	WB (1:300)	sc-7870	Santa Cruz Biotechnologies
S6	Mouse	WB (1:1600)	2317	Cell Signaling
Phospho-S6	Rabbit	WB (1:1000)	4856	Cell Signaling
Akt	Rabbit	WB (1:1000)	4685	Cell Signaling
P-Akt (S473)	Rabbit	WB (1:1500)	4060	Cell Signaling

Table 2: Sequences of siRNA duplexes used in this study.

siRNA duplexes		
Name	Oligo Sequence (5'-3')	Source
K8	Sense: CUGGGAAGGAGGCCGCUAU Antisense: AUAGCGGCCUCCUUCCCAG	SIGMA (Sasi_Hs01_00166576)
K18	Sense: GAGAGGAGCUAGACAAGUA Antisense: UACUUGUCUAGCUCCUCUCUC	SIGMA (SASI_Hs01_00145009)

Table 3: Sequences of primers used in this study.

Primer sequences (5'-3')	
cMet	Fw: CCCTATCAAATATGTCAACG Rev: TCAGAAGTGTCCTATTAAAGC
TFRC	Fw: GGAATATGGAAGGAGACT Rev: ATAGTGATCTGGTTCTACA
ITGB1	Fw: GCCATTATTATGATTATCCTTCT Rev: GTTCCTACTGCTGACTTAG
GAPDH	Fw: CCTCAAGATCATCAGCAATG Rev: CACGATACCAAAGTTGTCAT

I.8. Supplementary Figures

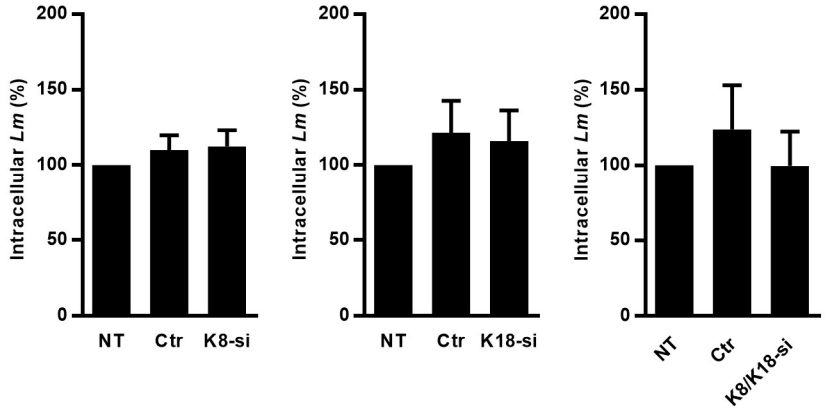

Supplemental Figure 1. Keratin 8 (K8) and Keratin 18 (K18) are dispensable for *Listeria* infection of Caco-2 cells. Intracellular levels of *L. monocytogenes* were assessed by gentamicin protection assay and CFU counting in intestinal epithelial cell line Caco-2 cells that were left untransfected (NT) or transfected with control siRNA (Ctr) or with siRNAs specifically targeting K8 (K8-si, left panel), K18 (K18-si, middle panel) or both (K8/K18-si, right panel). The number of intracellular *L. monocytogenes* in NT cells was normalized to 100%, and those in siRNA-transfected cells were expressed as relative values to NT cells. Values are the mean ±S.E. of at least three independent experiments, each done in triplicate.

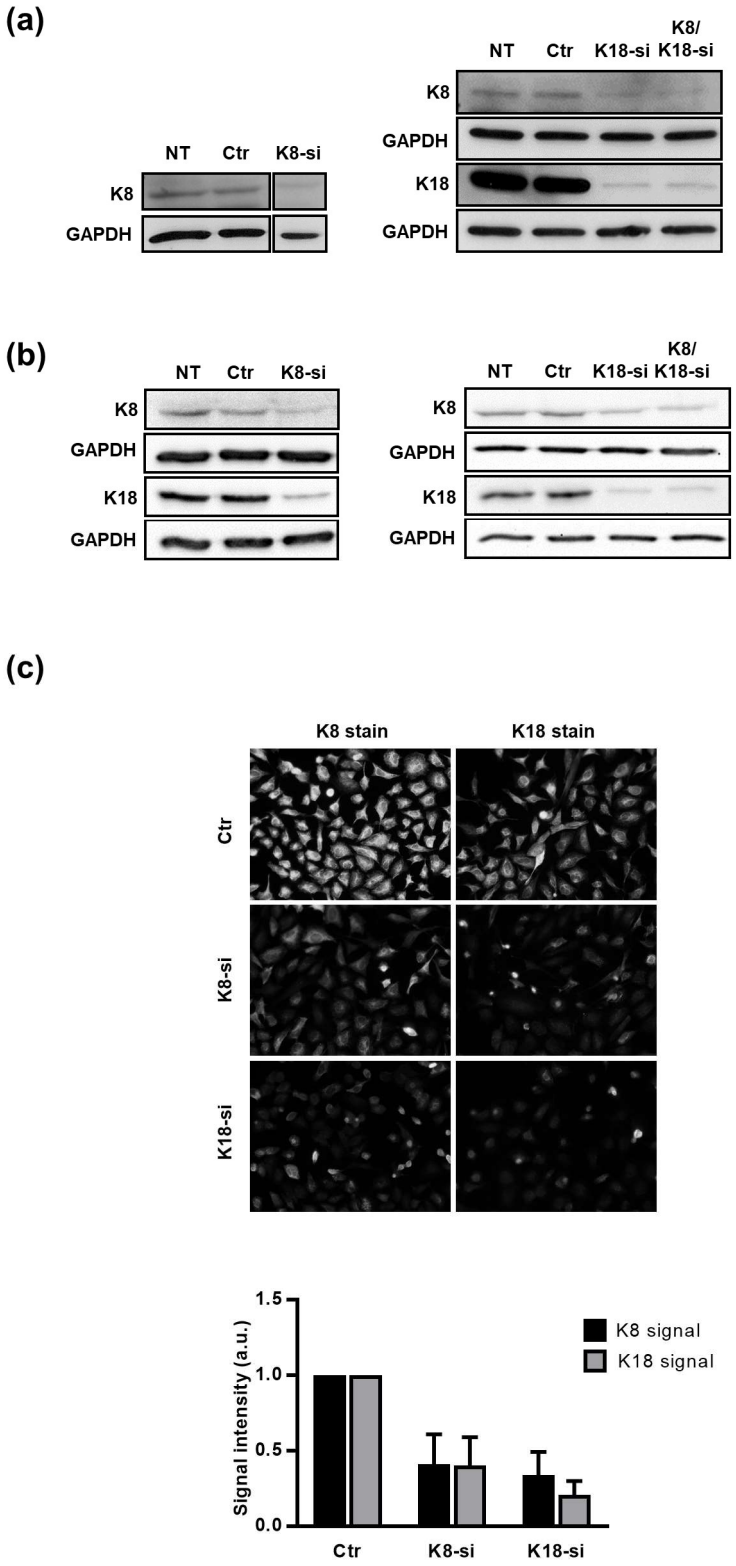

Supplemental Figure 2. K8 and K18 depletion efficiency in HeLa and Caco-2 cells. Efficiency of protein knockdown in (a) HeLa and (b) Caco-2 cells was assessed by western immunoblot using GAPDH as loading control. (c) Immunofluorescence images of Ctr and K8- (K8-si) or K18- (K18-si) depleted HeLa cells labelled for K8 and K18. Signal intensity was quantified. The values in Ctr cells were normalized to 1, and those in K8- and K18-depleted cells were expressed as relative values. Values are the mean ±S.E. of three independent experiments.

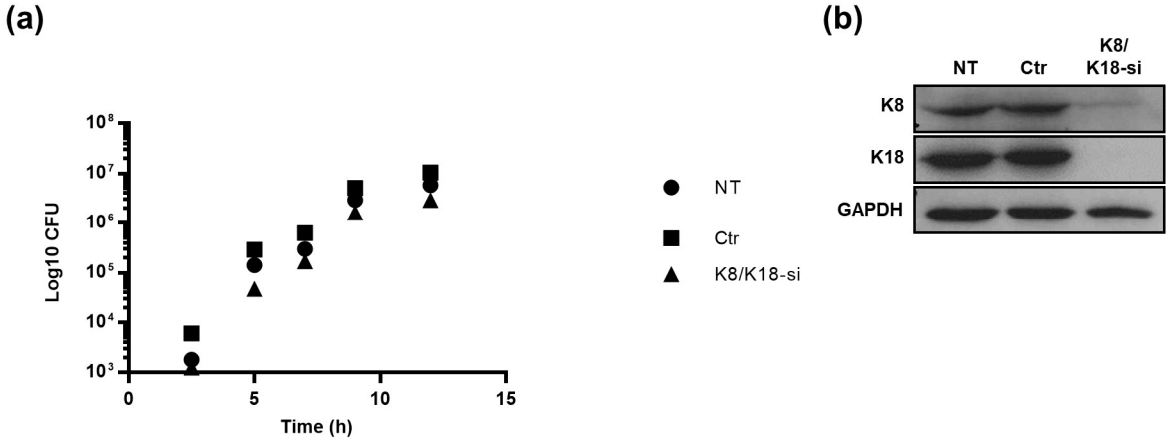

Supplemental Figure 3. K8 and K18 are not important for *Listeria* intracellular replication in HeLa cells. (a) Intracellular replication of *L. monocytogenes* in HeLa cells left untransfected (NT) or transfected with control (Ctr) or both K8 and K18 siRNA (K8/K18-si). Values represent the mean of duplicate samples from one representative experiment out of two independent experiments. (b) Efficiency of protein knockdown was assessed by western blot using GAPDH as loading control.

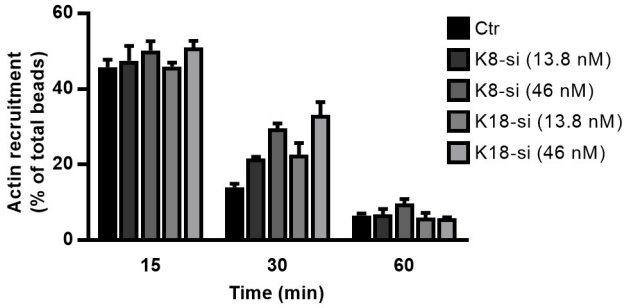

Supplemental Figure 4. K8 and K18 assist actin depolymerization during InlB-mediated internalization. Quantification of InlB-coated latex beads associated to polymerized actin in HeLa cells transfected with control (Ctr) or different concentrations of specific siRNA targeting K8 (K8-si) or K18 (K18-si). The use of 46 nM siRNA allows the maximum keratin depletion while 13.8 nM allows partial depletion. Cells were incubated with InlB-coated latex beads for 15, 30 and 60 minutes, fixed and stained for F-actin. Beads displaying actin recruitment were considered recruitment-positive. The total number of beads associated to cells was determined in brightfield. Values represent the mean ±S.E. of two independent experiments.

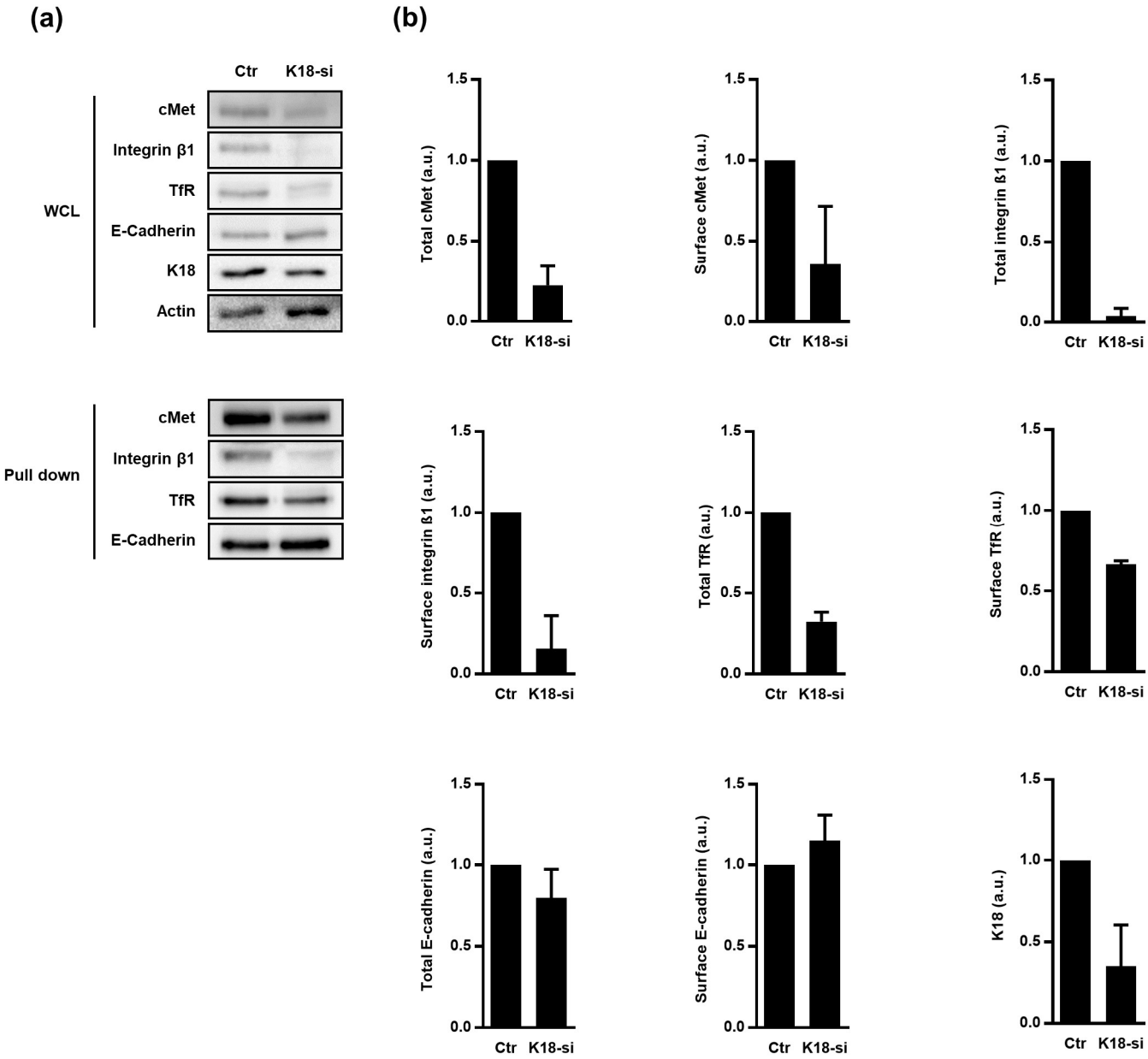

Supplemental Figure 5. K18 depletion perturbs expression and surface localization of transmembrane receptors in Caco-2 cells. Biotinylated surface proteins of control (Ctr) and K18-depleted (K18-si) Caco-2 cells were recovered from total cell extracts and pulled down using neutravidin beads. Biotinylated samples and whole cell lysates (WCL) were immunoblotted to detect cMet, TfR and integrin β1. (a) Immunoblot representative of two independent experiments. (b) Quantifications of E-cadherin, cMet, TfR and integrin β1 in WCL and in biotinylated samples from two independent experiments.

Part II – K18 interaction with putative RBPs

II.1. Introduction

In the previous chapter we showed that K18 regulates the decay rates of several transcripts, namely cMet, TfR and integrin β1, suggesting that K18 may be involved in the modulation of mRNA stability. Modulation of mRNA stability is among many processes that regulate mRNA upon transcription and consequently regulate gene expression (Schoenberg and Maquat, 2012). Indeed, mRNA is highly controlled from biogenesis to translation, and post-transcription regulation of mRNA is increasingly viewed as essential to guarantee accurate and responsive control of gene expression in response to multiple cues (Hinman and Lou, 2008; Schwerk and Savan, 2015). Accordingly, following transcription mRNA is regulated and modified by several processes such as splicing, polyadenylation, editing, nuclear export, localization, stability and translation that ultimately define gene expression (Hinman and Lou, 2008).

mRNAs do not exist as naked transcripts. Rather, in the eukaryotic cell each mRNA is coated with multiple elements that regulate the transcript fate, including microRNAs, long noncoding RNAs, and RNA-binding proteins (RBPs) (Schwerk and Savan, 2015). The fine tuning of RNA biology is mainly controlled by the mRNA-RBP interplay, as RBPs modulate nearly every step of the mRNA life cycle (Glisovic *et al.*, 2008; Imig *et al.*, 2012; Wu and Brewer, 2012; Rissland, 2017). RBPs bind mRNAs in their *cis-acting* elements, which are usually located in the 3'- untranslated regions (UTRs) (Hasan *et al.*, 2014; Rissland, 2017). mRNA-RBP complexes are diverse, dynamic and frequently transient, thus difficult to study. A single transcript can be associated with multiple RBPs, thus forming different ribonucleoprotein (RNP) complexes. In these complexes, the RBPs content and activity not only changes throughout the mRNA life cycle (Glisovic *et al.*, 2008; Rissland, 2017), but it also responds to biological and environmental cues, thus modulating gene expression according to the cellular requirements (Castello *et al.*, 2012).

The human genome encodes more than a thousand RBPs, with at least 300 of them containing one or more classical RNA-binding domain (Hinman and Lou, 2008). RBPs can be broadly divided into two subgroups, according to the specificity of their binding to mRNAs. Core RBPs such as those directly involved in mRNA degradation or protein translation can bind most transcripts through common RNA elements. Reversely, regulatory RBPs recognize and bind specific mRNAs, usually at their UTRs, altering the binding of the core factors, thus modulating gene expression (Rissland, 2017). RBPs therefore affect the regulation of specific transcripts, while controlling the transcriptome as a whole (Rissland, 2017). Reflecting their importance in the regulation of gene expression, various diseases such as cancer, muscular

atrophies and metabolic disorders are associated with anomalies of RBP expression and function (Lukong *et al.*, 2008; Cooper *et al.*, 2009; Darnell, 2010; Castello *et al.*, 2012).

Interestingly, RBPs can also associate and coordinate the localization, degradation and/or translation of subsets of mRNAs that encode functionally related proteins. These mRNA subsets are considered post-transcriptional operons or RNA regulons (Keene, 2007; Wu and Brewer, 2012; Hasan *et al.*, 2014). Coordinated expression of a specific RNA regulon is thus enabled by the presence of common sequences at the UTRs of the target mRNAs (Keene and Tenenbaum, 2002; Keene, 2007).

Within and eukaryotic cell, different mRNAs are present in different quantities, according to the gene function and cellular context. In general, the abundance of a certain mRNA is the result of an equilibrium between mRNA synthesis and decay (Pérez-Ortín, 2007; Wu and Brewer, 2012; Hasan *et al.*, 2014). Interestingly, large scale analysis suggests that the process of mRNA decay in particular can be responsible for half of all changes in the amounts of mRNA in some cellular responses, highlighting the importance of this regulatory mechanism (Garneau *et al.*, 2007). mRNA half-lives is transcript specific and can vary 100 fold in eukaryotic cells. For instance, in mammalian cells, mRNA half-life can range from 20 minutes to several days (Pérez-Ortín *et al.*, 2013; Hasan *et al.*, 2014). Degradation rates of mRNA change in response to different stimulus in order to meet the cellular needs for individual proteins (Wu and Brewer, 2012). Newly synthesized eukaryotic mRNAs are protected from exonuclease degradation by the presence of 5′ methylated guanosyl cap and the 3′ poly(A) tail. During deadenylation dependent mRNA decay, which is the major pathway in mammalian cells, degradation starts with removal of these protective structures, followed by digestion mediated by 5’ or 3’ exonucleases (Wu and Brewer, 2012; Pérez-Ortín *et al.*, 2013). The degradative machinery is composed of a small number of proteins that are conserved from yeast to humans (Garneau *et al.*, 2007). The process of mRNA decay has different stages (deadenylation, decaping and exonuclease degradation) whose rates are transcript specific (Hasan *et al.*, 2014).

RBPs are key regulators of mRNA stability, as the attachment of RBPs to mRNA determine the degradation rates of the later through the recruitment or exclusion of the mRNA degradation machinery to the transcript (Fig 21) (Wu and Brewer, 2012; Hasan *et al.*, 2014). Many of the mRNA sequences recognized by RBPs influencing transcript stability are now characterized. AU-rich elements (AREs) is a well-studied and common family of sequence elements located in the 3’-UTR of approximately 5-8% of the transcriptome (Halees *et al.*, 2008). AREs are recognized by multiple RBPs that can either promote mRNA degradation or mRNA stability (and consequently translation). For instance, HuR is a family of RBPs that in general promote stabilization of their target mRNAs, promoting their translation (Hinman and Lou, 2008). While the mechanisms behind this effect are still unclear, it appears to be mediated at least partially through protection from miRNA-mediated degradation (Simone and Keene,

2013). Other RBPs such as AUF1, KSRP, TTP and BRF1 promote mRNA decay, mainly by promoting the assembly of the core RNA degradative machinery to their target mRNAs (Wu and Brewer, 2012).

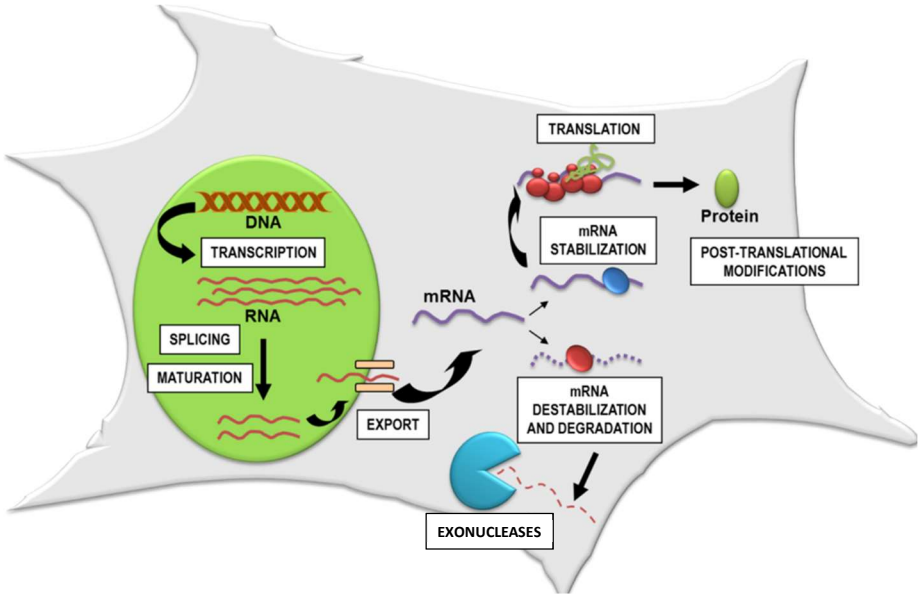

Figure 21. Regulation of mRNA stability by RNA-binding proteins (RBPs). RBPs are key regulator of post-transcriptional regulation of target mRNAs. RBPs commonly regulate gene expression by modulating the stability of the transcript. Thus, RBPs can target the transcript and promote its stability by excluding the recruitment of the degradation machinery. The stabilized mRNA can then be translated to protein. Alternatively, RBPs can specifically target the mRNA for degradation, resulting in decreased protein expression. Multiple RBPs can target a single mRNA in a cooperative, competitive or independent manner. Adapted from (Abdelmohsen, 2012)

Several RBPs can target a single transcript in a cooperative, competitive or independent manner (Wu and Brewer, 2012). For example, HuR can compete with destabilizing RBPs, promoting mRNA stabilization (Zou *et al.*, 2010). Adding complexity to these regulatory mechanisms, RBPs can exhibit opposite functions depending on the transcript and cellular context (Schwerk and Savan, 2015). Thus, HuR can block translation of the p27 mRNA by binding to a 5′UTR sequence of this mRNA (Hinman and Lou, 2008). Furthermore, AUF1, which usually promotes mRNA decay, can also stabilize mRNA and enhance translation (Schwerk and Savan, 2015). Altogether, these observations demonstrate that the abundance and translation of mRNA is fine-tuned by a complex interplay between numerous RBPs and specific RNA motifs, which allow the maintenance of protein levels according to cellular requirements (Wu and Brewer, 2012).

Keratins interplay with RBPs and general significance in mRNA processing is poorly understood. K18 was shown to interact with hnRNP R (Havugimana *et al.*, 2012), an RBP that binds and stabilizes the mRNA of MHC class I genes, thus enhancing their translation (Reches *et al.*, 2016). The protein YTHDC1, which is involved in RNA splicing and transport was also found to interact with K18 (Jian Wang *et al.*, 2011). Additionally, K18 interacts with the mRNA degradation machinery protein Pan2 (Bett *et al.*, 2013), which participates in the initial trimming of polyadenylated tails of mRNA, a process that favors further mRNA deadenylation and subsequent degradation (Wu and Brewer, 2012). K17 was recently reported to interact with the RBP hnRNP K (Chung *et al.*, 2015), regulating its shuttling between the nucleus and the cytoplasm, with direct impact on the expression of several cytokine genes (Chung *et al.*, 2015). However, it remains unclear how K17 and hnRNP K control gene expression (Chung *et al.*, 2015).

This poor characterization of keratins involvement in mRNA regulation, together with our observations that K18 can modulate mRNA stability, led us to explore possible interactions between K18, mRNA, and proteins that participate in mRNA processing.

II.2. Results

II.2.1. K18 does not interact directly with transcripts of cMet, TfR and integrin β1

During maturation, the mRNA associates with several proteins that determine the rates of transcript degradation and translation (Rissland, 2017). Furthermore, K18 was shown to bind the 3'-UTR mRNA of the transcription factor C/EBPβ mRNA, both *in vitro* and in cultured cells (Liu and Sun, 2005; Ying Wang *et al.*, 2011). Together with our data presented in Chapter II-Part I, these observations prompted us to assess if K18 can interact with cMet, integrin β1 and TfR transcripts. For that, we performed RNA immunoprecipitation (RIP) experiments in which K18 was immunoprecipitated in RNase free conditions and assessed for bound mRNAs. K18 RIP was performed in HeLa cells. Incubation of cell lysates with IgG antibody was used as a negative control. The resulting K18 and control IgG immunoprecipitates were assessed for cMet, integrin β1 and TfR transcripts by qRT-PCR. No significant enrichment of cMet or integrin β1 transcripts was detected in K18 immunoprecipitates (Fig 22), as compared to the IgG control immunoprecipitation. TfR transcript levels were too low in either K18 or IgG immunoprecipitates to allow any interpretation. These observations suggest that K18 does not interact directly and specifically with cMet and integrin β1 transcripts. Nevertheless, these results do not exclude the possibility that K18 may interact with mRNAs in an indirect manner, namely through K18 association with RBPs that bind mRNA. The mRNA-RBP complex association is highly dynamic and frequently transient (Rissland, 2017). Whether the RIP approach is adequate and/or sensible enough to detect an indirect interaction between K18 and mRNAs is thus questionable.

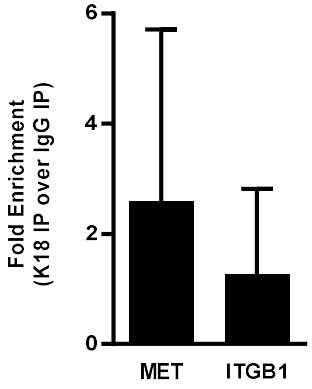

Figure 22. cMet and integrin β1 transcripts do not associate with K18 protein. RNA IP using anti-K18 or IgG control antibodies was performed in HeLa cells. cMet and integrin β1 mRNA in the immunoprecipitates was analyzed by qRT-PCR using specific primers. For each primer pair, fold enrichment was normalized to the IgG control reaction. Values are the mean ±S.E. of three independent experiments.

II.2.2. Identification of K18-interacting RBPs by mass spectrometry

Considering that keratins can associate with different RBPs (Jian Wang *et al.*, 2011; Havugimana *et al.*, 2012; Chung *et al.*, 2015) and that the results above do not exclude an RBP-mediated interaction of K18 with mRNAs, we searched for K18-interacting RBPs following an immunoprecipitation approach coupled to mass spectrometry identification. Thus, we immunoprecipitated K18 from Caco-2 cell lysates and resolved the eluted fractions by SDS-PAGE, followed by silver staining. Bands of different sizes that displayed strong intensity were excised and processed for mass spectrometry identification. Proteins were identified by a peptide mass fingerprinting (PMF) approach, in which proteins of interest are first digested by trypsin.

Hsc70 (gi|5729877) 71 kDa	
Peptide mass (Da)	**Sequence**
773.4152	DNNLLGK
989.5261	LSKEDIER
1081.5676	LLQDFFNGK
1125.5609	MVQEAEKYK
1166.5801	YKAEDEKQR
1187.6492	DISENKRAVR
1199.6742	DAGTIAGLNVLR
1228.6281	VEIIANDQGNR
1235.6241	MVNHFIAEFK
1252.6605	MKEIAEAYLGK
1253.6161	FEELNADLFR
1303.5988	NSLESYAFNMK
1391.7252	MVNHFIAEFKR
1410.6682	RFDDAVVQSDMK
1480.7543	ARFEELNADLFR
1481.8071	SQIHDIVLVGGSTR
1487.7013	TTPSYVAFTDTER
1616.7876	SFYPEEVSSMVLTK
1649.7952	NQVAMNPTNTVFDAK
1653.8318	HWPFMVVNDAGRPK
1691.7256	STAGDTHLGGEDFDNR
1787.9901	IINEPTAAAIAYGLDKK
1805.8962	NQVAMNPTNTVFDAKR

EWSR1 (gi|119580187) 47.1 kDa	
Peptide mass (Da)	**Sequence**
938.5166	GGLPPREGR
976.4702	KPPMNSMR
1165.5643	GGFRGGRGMDR
1207.5636	GGPGGPGGPGGPMGR
1684.7965	AAVEWFDGKDFQGSK
1697.8938	KKPPMNSMRGGLPPR
1955.969	GMPPPLRGGPGGPGGPGGPMGR
2056.0896	TGQPMIHIYLDKETGKPK
2234.9243	AGDWQCPNPGCGNQNFAWR
2480.053	QDHPSSMGVYGQESGGFSGPGENR

PSF (gi|4826998) 76.2 kDa	
Peptide mass (Da)	**Sequence**
786.4832	ANLSLLR
830.4478	QEELRR
869.3644	MGYMDPR
882.4203	ISDSEGFK
986.549	RQEELRR
1036.5533	QGPGPGGPKGGK
1054.4912	QREESYSR
1065.5146	NPMYQKER
1109.5078	REEEMMIR
1120.5204	GMGPGTPAGYGR
1143.627	FATHAAALSVR
1165.5558	WKSLDEMEK
1236.546	QREMEEQMR
1245.6949	GIVEFASKPAAR

Figure 23. Identification by mass spectrometry of RNA binding proteins that interact with K18. Selected bands from K18 immunoprecipitation eluates where trypsin digested and the resulting peptides analysed by peptide mass fingerprinting (PMF). Tables show the size and amino-acid sequence of the digested peptides. The accession number of the identified proteins and respective size (in kDa) are also indicated.

The resulting peptides are then analyzed by mass spectrometry where peptides absolute masses are accurately measured. This data is then compared with protein databases such as UniProtKB/Swiss-Prot and NCBI*nr.* Following this methodology, we identified Hsc70, PSF and EWSR1 as K18-interacting proteins that were previously reported as RNA binding proteins (Fig 23). All identified proteins scored a C.I. of at least 99%, indicating a near-perfect match

between experimentally and theoretically calculated peptide masses. These interactions require further validation by biochemical techniques such as K18 immunoprecipitation followed by immunoblotting against Hsc70, PSF and EWSR1.

II.2.3. *In silico* predictions of RBPs that interact with cMet, TfR and integrin β1 transcripts

We demonstrated in Chapter II-Part I that K18 depletion destabilizes cMet, TfR and integrin β1 transcripts, leading to decreased levels of the corresponding proteins. This observation raised the possibility that the lack of K18 may affect the post-transcriptional regulation of these transcripts in a similar manner. We were thus interested in the identification of RBPs that could target all the transcripts of interest (cMet, TfR and integrin β1). Aiming to shed some light on how these transcripts are being regulated, we followed a bioinformatic approach using the RNA-Binding Protein Database (RBPDB) (http://rbpdb.ccbr.utoronto.ca/) to predict the RBPs that may interact with cMet, TfR and integrin β1 transcripts. RBPDB comprises a collection of experimental observations of RNA binding sites, both in vitro and in vivo, manually curated from primary literature (Cook *et al.*, 2011). Since binding of regulatory RBPs often occurs in the transcript UTRs (Rissland, 2017), we focused our search in the 3' and 5'-UTR of cMet, TfR and integrin β1 transcripts. Each query was performed independently. For 3'-UTR queries we used a threshold of 90%. We used a reduced threshold of 80% for the 5'-UTR scan (See Methods).

The results of our analysis are present in Fig 24, grouped by 3' and 5'-UTR RBP hits. We found multiple RBPs that are predicted to interact with each mRNA. Higher number of hits were obtained for 3'-UTR regions in all transcripts (Fig 24), which is probably related with longer sequences in 3' -UTR. In general, RBPs bind more frequently to the 3'-UTR regions than to the 5'-UTR of the target mRNAs (Schoenberg and Maquat, 2012; Schwerk and Savan, 2015; Rissland, 2017). Regarding the RBPs that are predicted to associate with the transcripts at their 3' -UTR, we found 21 hits for cMet, 18 for integrin β1 and 20 for TfR. A list of 13 RBPs putatively associate with all the transcripts. The different RBPs of this list were previously shown to be involved in different steps of mRNA processing, with some RBPs exhibiting various roles during transcript maturation. Most of the identified RBPs are described as participants in mRNA splicing, translation regulation and stability modulation (Fig 24).

3'-UTR

cMet mRNA		Integrin β1 mRNA		TfR mRNA	
RBP Name	Score	RBP Name	Score	RBP Name	Score
ELAVL2	14.058233	ELAVL2	14.058233	ZRANB2	10.3039431
SNRPA	12.07871781	ZFP36	13.6606161	SNRPA	10.1470304
A2BP1	11.070935	NONO	8.9484945	HNRNPA1	9.8958058
ZRANB2	10.3039431	PABPC1	8.7178165	NONO	8.9484945
HNRNPA1	9.60877168	A2bp1	8.6471013	PABPC1	8.7178165
EIF4B	9.43167555	FUS	7.3693752	a2bp1	8.6471013
ybx2-a	9.4281438	ACO1	7.35090902	RBMY1A1	8.6272192
sap-49	8.7846348	Pum2	7.2294196	FUS	7.3693752
PABPC1	8.7178165	MBNL1	6.6279899	Pum2	7.2294196
RBMY1A1	8.6696024	EIF4B	6.4668404	ACO1	6.93292615
FUS	7.3693752	KHSRP	6.33985	SFRS9	6.63255189
Pum2	7.2294196	YTHDC1	6.23570757	EIF4B	6.4668404
SFRS9	7.08652094	RBMX	5.2682554	KHSRP	6.33985
MBNL1	6.6279899	SFRS13A	5.11052177	MBNL1	6.17832025
KHSRP	6.33985	RBM4	4.84132568	YTHDC1	5.98045052
YTHDC1	5.98045052	KHDRBS3	4.652088863	RBMX	5.2682554
RBMX	5.2682554	SFRS1	4.62028767	SFRS13A	4.6654368
SFRS13A	5.11052177	ELAVL1	4.40359056	ELAVL1	4.40359056
KHDRBS3	4.652088863			KHDRBS3	4.200710743
SFRS1	4.62028767			SFRS1	4.1881759
ELAVL1	4.40359056				

RBPs predicted for cMet, TfR, Integrin β1 mRNA	Function in mRNA processing
a2bp1	Splicing
EIF4B	Translation
ELAVL1	Stability, translation
FUS	Splicing
KHDRBS3	Splicing
KHSRP	Transcription, splicing, localization
MBNL1	Splicing
PABPC1	Stability, translation
Pum2	Stability, translation
RBMX	Transcription , splicing
SFRS1	Splicing
SFRS13A	Splicing
YTHDC1	Splicing, transport

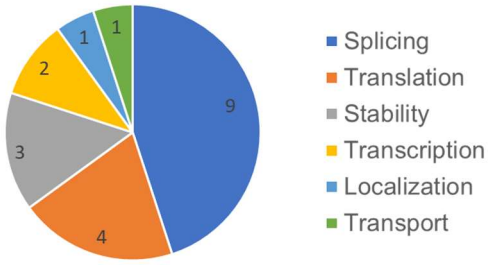

5'-UTR

cMet mRNA		Integrin β1 mRNA		TfR mRNA	
RBP Name	Score	RBP Name	Score	RBP Name	Score
sap-49	7.5622424	EIF4B	5.256645851	FUS	7.3693752
FUS	7.3693752	RBM4	4.84132568	SFRS9	7.08652094
SFRS9	6.63255189	RBMX	4.40271173	KHDRBS3	4.277494655
MBNL1	6.6279899			MBNL1	6.17832025
KHSRP	6.33985			YTHDC1	5.36340303
RBMX	5.2682554			RBMX	5.2682554
RBM4	4.84132568			EIF4B	5.256645851
SFRS1	4.62028767			RBM4	4.84132568
SFRS13A	4.2060792957			SFRS1	4.62028767

RBPs predicted for cMet, TfR, Integrin β1 mRNA	Function in mRNA processing
EIF4B	Translation
RBM4	Splicing, translation
RBMX	Transcription , splicing

Figure 24. *In silico* prediction of RNA binding proteins (RBPs) targeting cMet, integrin β1 and TfR transcripts. To identify putative RBPs that could bind and potentially modulate the cMet, integrin β1 and TfR mRNAs, we followed a bioinformatic approach using the RNA-Binding Protein Database (RBPDB) tool. (a) The 3'-UTR of each transcript was analyzed individually in RBPDB. The predicted RBPs that can bind the different transcripts are listed and sorted by PWM score (upper panel). RBPs common to the cMet, integrin β1 and Tfr transcripts are listed in the lower panel, along with their respective role in mRNA processing. Chart (right panel) illustrates the distribution of the identified RBPs in the functional categories. (b) Similar analysis was performed to the 5'-UTR of the cMet, integrin β1 and TfR transcripts.

By performing similar analysis to the 5'-UTR portions of the transcripts, we identified 3 RBPs that potentially interact with cMet, integrin β1 and TfR mRNAs (Fig 24). Altogether, these results provide us with a group of RNA interacting proteins that may share regulatory effects on the transcripts that we are studying. Interestingly, one of the identified RBPs, YTHDC1, was reported to interact with K18, as determined by yeast two-hybrid screen (Jian Wang *et al.*, 2011).

II.3. Discussion

The adjustment of protein content in response to biological and environmental cues relies in large part on the regulation of gene expression programs by the cell (Schwerk and Savan, 2015). mRNA abundance and consequent gene expression is the result of a delicate balance between mRNA synthesis and decay (Hasan *et al.*, 2014). The rate of protein synthesis is in large part determined by post-transcriptional processes that target the mRNA, such as splicing, polyadenylation, editing, nuclear export, localization, degradation and translation (Glisovic *et al.*, 2008). Pivotal in such regulatory mechanisms is the attachment of RBPs that coat the transcript in specific regions, targeting it for degradation or translation (Lunde *et al.*, 2007).

The molecular significance of keratins in the context of mRNA regulation remains essentially uncharacterized, despite multiple observations pointing to a role for keratins in mRNA levels (Chung *et al.*, 2015; Asghar *et al.*, 2016) and reporting keratins interaction with RBPs such as hnRNP R, YTHDC1 and hnRNP K (Jian Wang *et al.*, 2011; Havugimana *et al.*, 2012; Chung *et al.*, 2015)**.** This lack of knowledge on keratins involvement in transcript regulation, together with our observations that K18 regulates the expression of various mRNAs by affecting their decay rates, lead us to further explore possible interactions between K18 and proteins that participate in mRNA processing. We first show here that K18 exhibits no direct interaction with the transcripts of cMet, Tfr and integrin β1. We also identified novel K18-interacting proteins (Hsc70, PSF and EWSR1), which were previously reported to bind RNA. Through a *in silico* approach we identified several RBPs that can bind to the cMet, TfR and integrin β1 mRNA, raising the possibility that these transcripts can be target of similar regulatory mechanisms mediated by common RBPs. Importantly, at least one of these RBPs, YTHDC1, was reported to interact with K18 (Jian Wang *et al.*, 2011).

The direct interaction of keratins with nucleic acids has been reported, although it remains poorly characterized. K18 was shown to bind 3'-UTR of a transcription factor (C/EBPβ) *in vitro* (Liu and Sun, 2005) and in cells overexpressing the 3'-UTR of C/EBPβ (Ying Wang *et al.*, 2011). Remarkably, the association of this mRNA fragment with K18 promotes keratin solubility (Ying Wang *et al.*, 2011), suggesting that RNAs can regulate keratins network stability and function. Keratins can also interact with DNA, as demonstrated recently through the interaction of K17 with the promoter regions of cytokine genes (Hobbs et al., 2015). An alternative approach that can be used to explore possible K18-mRNA interactions is RNA-affinity chromatography, in which cytosolic extracts are exposed to columns coupled with the mRNAs of interest, and bound fractions analyzed for the interacting proteins (for instance K18) (Matsui *et al.*, 2007).

While our observations do not favor a direct K18-mRNA interaction, they do not exclude the possibility that RBPs may mediate such interaction. Indeed, keratins can associate with several RBPs such as hnRNP R, YTHDC1 and hnRNP K (Jian Wang *et al.*, 2011; Havugimana *et al.*, 2012; Chung *et al.*, 2015).

Heat-shock cognate protein 70 (Hsc70) is a heat shock protein that is constitutively expressed and has multiple functions in the cell (Liu *et al.*, 2012). It functions as a chaperone, promoting correct protein folding and protein homeostasis in general (Zuiderweg *et al.*, 2017). It is also involved in the disassembly of clathrin-coated vesicles during vesicle internalization (Eisenberg and Greene, 2007). Additionally, Hsc70 is a major actor in autophagy, participating in the selection of proteins to be degraded in the lysosome (Stricher *et al.*, 2013). In the context of RNA processing, earlier studies demonstrated that Hsc70 binds to 3'-UTR sequences of various lymphokine and proto-oncogene mRNAs (Henics *et al.*, 1999). Later, Hsc70 was found to bind and stabilize the mRNA of the proapoptotic protein Bim, a process triggered by cytokine signaling (Matsui *et al.*, 2007). Hsc70 is mainly cytoplasmic and can shuttle between the cytoplasm and the nucleus, where it tends to accumulate in stress conditions (Liu *et al.*, 2012).

PTB-associated splicing factor (PSF) is an essential protein that plays multiple roles in nucleic acid biology (Yarosh *et al.*, 2015). PSF is prevalent in the nucleus, although it can translocate into the cytoplasm (Cantile *et al.*, 2013). PSF is involved in DNA repair mechanisms, through the detection of double strand breaks (DSBs) and promotion repair (Salton *et al.*, 2010; Jaafar *et al.*, 2017). PSF can be a negative or positive transcriptional regulator (Yarosh *et al.*, 2015). In this context, PSF was shown to be important for transcription termination, as lack of PSF can lead to accumulation of 3' cleaved RNA (Kaneko *et al.*, 2007). Furthermore, PSF partakes in pre-mRNA splicing, although the exact mechanisms by which it regulates this activity remains unknown (Yarosh *et al.*, 2015). PSF has particular affinity towards certain RNAs, resulting in the retention of those transcripts in the nucleus and consequently decreased export to the cytoplasm (Zhang and Carmichael, 2001; Chen and Carmichael, 2009). PSF can also regulate the 3′ polyadenylation of mRNAs by ensuring that polyadenylation at non-canonical or suboptimal polyadenylation signals can take place, thus contributing to mRNA stability (Liang and Lutz, 2006; Hall-Pogar *et al.*, 2007; Yarosh *et al.*, 2015). It also favors mRNA stability of several histones in thymocytes (Heyd and Lynch, 2011).

Ewing sarcoma protein 1 (EWSR1) is a protein involved in several cellular processes including RNA processing and transport (Paronetto, 2013). EWSR1 is a nuclear protein that is able to shuttle between the nucleus and cytoplasm (Zakaryan and Gehring, 2006). It can negatively regulate the expression of cofilin 1 by inducing the nuclear retention of the respective mRNA, a process mediated by EWSR1 binding to the 3'-UTR of cofilin 1 (Huang *et al.*, 2014). EWSR1 has been implicated in transcription, as it interacts not only with RNA Polymerase II and associated subunits, but it also associates with transcriptional activators

and repressors (Paronetto, 2013). In addition, EWS also interacts with multiple splicing factors (Zhang *et al.*, 1998; Knoop and Baker, 2000) and modulates the splicing of several genes in cancer cells (Dutertre *et al.*, 2010; Paronetto *et al.*, 2011). However, the molecular mechanisms by which EWS regulates splicing remains unclear (Paronetto, 2013).

In summary, Hsc70, PSF and EWSR1 are RBPs that regulate various steps of RNA processing. Keratins are abundant proteins that are increasingly recognized as molecular and signaling scaffolds that can associate with a wide range of protein families (Pallari and Eriksson, 2006). Thus, one can speculate that by interacting with RBPs such as the ones identified here, K18 may affect their localization and/or activity, which in turn can reflect on gene expression. The interaction of these RBPs with K18 needs to be further verified and the significance of such interaction in the context of mRNA regulation studied.

Our observations suggest that cMet, TfR and integrin β1 mRNAs may be similarly impacted by K18 depletion. Interestingly, accumulating evidence suggests that RBPs may coordinate post-transcriptional processing of mRNAs that are functionally related (Keene, 2007). These mRNA subgroups, termed posttranscriptional operons (or regulons), share specific UTR sequences that in turn are recognized by the same RBPs (Hogan *et al.*, 2008). This process should therefore permit fine-tuning of functionally related proteins that are collectively needed for specific biological processes (Wu and Brewer, 2012). Our *in silico* analysis revealed an overlap of at least 60% RBPs that are shared by cMet, TfR and integrin β1 mRNAs, suggesting that these genes may be target of common regulatory post-transcriptional processes. Most of the identified RBPs were found to be related to mRNA splicing, translation and stability. Altogether, these observations raise the possibility that, as genes that code for transmembrane proteins, cMet, TfR and integrin β1 mRNAs may indeed constitute an RNA regulon (Keene, 2007; Blackinton and Keene, 2014), whose processing can be coordinated by the RBPs identified above. The significance and biological contexts associated to this putative regulation mechanism remains to be determined. Likewise, the relevance of K18 in this context needs to be addressed. This work provides new avenues by which keratins may control gene expression and protein function.

II.4. Methods

II.4.1. RNA immunoprecipitation assays

RNA immunoprecipitation (RIP) experiments were performed using the MagnaRIP RNA-Binding Protein Immunoprecipitation Kit (Merck Millipore), following the manufacturer's guidelines. Briefly, HeLa cells grown until confluence were washed and lysed with RIP lysis buffer. K18 antibody (Abcam) and control IgG was used for the immunoprecipitation. The antibodies were first incubated with the protein A/G magnetic beads. Then, the RIP lysates were added to the antibody/beads mix and incubated overnight at 4ºC, with rotation. Afterwards, the protein content was digested with Proteinase K. The bound RNA was then purified and reverse transcribed with iScript cDNA Synthesis Kit (Bio-Rad Laboratories). The samples were analyzed by quantitative real-time PCR (qRT-PCR) using primers for cMet, TfR and integrin β1 (primer sequences can be found in Table 3 of Chapter II-Part I).

II.4.2. Immunoprecipitation assays

Per condition, 2 x 10^6 cells were washed twice with phosphate-buffered saline (PBS) and lysed in 300 µl of lysis buffer (1% NP-40, 50 mM Tris pH 7.5, 150 mM NaCl, 2 mM EDTA, 1 mM AEBSF and Complete Protease Inhibitor Cocktail (Roche Pharmaceuticals)). Lysates were centrifuged at 15 000 g for 10 min at 4°C, the supernatant recovered and 700 µg of protein lysate was incubated with 3.5 µg of anti-K18 antibody (Abcam) overnight at 4°C. Immune complexes were captured with 50 µl of PureProteome Protein A magnetic beads (Millipore) at 4°C and washed three times with wash buffer (0.2% NP-40, 50 mM Tris pH 7.5, 150 mM NaCl, 2 mM EDTA, 1 mM AEBSF, Complete Protease Inhibitor Cocktail). Immunoprecipitated proteins were eluted and boiled in Laemmli buffer. Samples were then resolved in SDS-PAGE gel, which was afterwards silver-stained with using the ProteoSilverTM Plus Silver Staining Kit (Sigma-Aldrich).

II.4.3. Protein identification by mass spectrometry (MS).

Protein identification was performed by MALDI TOF/TOF mass spectrometry as reported (Osório and Reis, 2013). After excision from SDS-PAGE gel, protein bands were reduced with dithiothreitol, alkylated with iodacetamide and digested with trypsin. Peptides were then extracted, desalted and concentrated using ZipTips (Millipore). The samples were crystallized onto a MALDI sample plate and analyzed using a 4700 Proteomics Analyzer

MALDITOF/TOF (Applied Biosystems). Peptidic mass spectra were acquired in reflector positive mode at a 700-4000 m/z mass window and proteins identified by Peptide Mass Fingerprint (PMF) using the Mascot software (Matrix Science, UK). This data was searched against the SwissProt/UniProt and NCBI*nr Homo sapiens* protein sequence databases.

II.4.4. In silico prediction of RNA binding proteins

RNA-Binding Protein Database (RBPDB) (http://rbpdb.ccbr.utoronto.ca/), which curates all experimentally verified RNA binding sites in hundreds of RBPs, was used to identify RBPs that can recognize specific sequences of the cMet, integrin β1 and TfR transcripts. To determine the 3' and 5'-UTR sequences for the cMet, integrin β1 and TfR mRNAs, we used the UCSC Genome Browser tool (http://genome.ucsc.edu/index.html). Then, in the RBPDB website we queried each sequence (3' or 5'-UTR, for each mRNA) independently. For 3'-UTR analysis, the minimum threshold score for any matches between identified motifs in the queried sequences and RNA-binding sequence in the database was set to 90%. For 5'-UTR searches we decreased the threshold to 80% (the default value), to increase the number of positive hits. Functional significance of the identified RBP hits, in the context of mRNA processing, was retrieved from Entrez Gene and/or UniProtKB/Swiss-Prot.

CHAPTER IV – GENERAL DISCUSSION

Manipulation of the host cell cytoskeleton is a hallmark of the infectious process of multiple bacterial pathogens. Intermediate filaments have been described as participating in the infection process of different microbes (Geisler and Leube, 2016), however the molecular details remain sparse. In this study, we demonstrate for the first time that epithelial K8 and K18 are important players in *L. monocytogenes* infection. Our results suggest that Keratins may have a dual role in *L. monocytogenes* cellular invasion. We found that both K8 and K18 regulate the protein content and distribution of cMet, a major receptor for *L. monocytogenes* invasion of non-phagocytic cells. Accordingly, K8 and K18 are necessary for InlB/cMet-mediated *L. monocytogenes* cell invasion. Both keratins also mediate cellular signaling elicited by HGF, the natural ligand of cMet. Besides regulating cMet levels and signaling, we also provide evidence suggesting that K8 and K18 may regulate *L. monocytogenes* entry by modulating the actin dynamics at the entry site. Finally, our results demonstrate that K18 controls the expression of additional transmembrane proteins such as integrin β1 and transferrin receptor (TfR) by promoting the stability of their mRNAs, suggesting a broader role for keratins in the regulation of gene expression.

Keratins participate in different aspects of pathogenic infection (Geisler and Leube, 2016). Together with K18, K8 is targeted for degradation by adenovirus and rhinovirus (Chen *et al.*, 1993; Seipelt *et al.*, 2000). *Chlamydia*-induced remodeling of K8 and K18 allows the expansion of the inclusion vacuole in which the pathogen replicates (Dong *et al.*, 2004; Kumar and Valdivia, 2008). Both keratins also promote *Trypanosoma intracellular* replication (Claser *et al.*, 2008). Furthermore, K18 is exploited by pathogens such as EPEC and *Salmonella* to favor pathogen docking and internalization, respectively (Carlson *et al.*, 2002; Batchelor *et al.*, 2004). K18 associates with the translocon pore from *Shigella* (Russo *et al.*, 2016), and K8 controls hepatitis B virus replication in hepatic cells (Zhong *et al.*, 2014). Despite these observations, the functional details of keratins involvement in infection context remains elusive.

We showed that K8 and K18 depletion resulted in a significant reduction of InlB/cMet mediated *Listeria* internalization. InlB interaction with cMet elicits molecular cascades similar to those triggered by HGF, including activation of PI3-kinase signaling that promotes bacterial internalization (Ireton *et al.*, 1996; Tang *et al.*, 1998; Shen *et al.*, 2000; Copp *et al.*, 2003). We assessed the importance of K8 and K18 in cMet signaling events triggered by HGF. We demonstrated that these keratins are required for HGF-induced formation of actin ruffles, tyrosine phosphorylation of proteins associated with PI3K p85 subunit, and phosphorylation of Akt, a downstream target of PI3K. Importantly, these observations correlated with decreased levels of total cMet in K8 and K18 depleted cells, suggesting that by controlling cMet levels, keratins govern downstream events such as HGF-mediated signaling and InlB-mediated *Listeria* invasion.

Keratins may regulate *L. monocytogenes* infection through additional mechanisms. Indeed, accumulating evidence suggests that keratins may themselves function as receptors that mediate host-pathogen interactions, favoring infection. Accordingly, surface located K4, K10 and K13 interact and promote infection of pathogens such as *Burkholderia cepacia*, *Streptococcus agalactiae, and Staphylococcus aureus* (Sajjan *et al.*, 2000; O'Brien *et al.*, 2002; Samen *et al.*, 2007). In addition, *Enterobacteriaceae* exploits surface K8 to assist internalization of the Pet toxin (Nava-Acosta and Navarro-Garcia, 2013). Furthermore, the intermediate filament vimentin was recently shown to mediate *Listeria* infection through interplay of *L. monocytogenes* virulence factor InlF with vimentin located at the surface of brain endothelial cells (Ghosh *et al.*, 2018). It would be therefore interesting to determine if K8 and K18 are available at the surface of the cells used in our work and assess its putative functional importance by, for instance, performing infection assays in cells pretreated with K8/K18 antibodies.

Our immunofluorescence studies of cells infected with *Listeria* demonstrated that K8, K18, cMet and actin are enriched at *Listeria* entry sites within minutes of infection. A more detailed analysis of protein recruitment dynamics using InlB coated beads, which mimics InlB mediated internalization of *Listeria* (Braun *et al.*, 1999; Pizarro-Cerdá *et al.*, 2002), revealed that enrichment of K8 and K18 at bead vicinity occurred after actin, indicating that these events occur sequentially during particle internalization. Furthermore, the actin rings observed at InlB beads internalization sites persisted for longer periods in K8 and K18 depleted cells, suggesting a perturbation of actin dynamics in these cells, and raising the possibility that this altered actin behavior may influence InlB-dependent internalization efficiency.

How K8 and K18 modulate the actin dynamics during InlB-mediated cellular invasion is still unknown. Indeed, despite several reports point to an interplay between actin and keratin cytoskeletons, the molecular details of such crosstalk remain largely understudied (Huber *et al.*, 2015; Jiu *et al.*, 2015). Keratins interaction with actin is commonly mediated by association with cytolinker proteins such as plectin and dystrophin (Stone *et al.*, 2005; Karashima *et al.*, 2012). Other intermediate filaments like vimentin can interact directly with actin or indirectly through linker proteins (e.g. plectins) and motors protein such as myosin IIB (Esue *et al.*, 2006; Favre *et al.*, 2011; Menko *et al.*, 2014; Jiu *et al.*, 2015). While this protein-mediated interplay between intermediate filaments and actin may affect actin dynamics (Jiu *et al.*, 2015), there is also evidence that IFs can modulate actin dynamics and organization through regulation of signaling mechanisms (Huber *et al.*, 2015). Indeed, K8 and K18 were shown to control stiffness of simple epithelial cells through modulation of RhoA-ROCK dependent actin organization and dynamics (Bordeleau *et al.*, 2012). Regarding actin-dependent regulation of keratins, actin filaments were proposed to promote keratin network assembly by retrograde transport of keratin subunits that nucleate at focal adhesion sites (Windoffer *et al.*, 2006; Kölsch *et al.*,

2009). In this context, EGF stimulation leads to the formation of actin rich lamellas, which is followed by the extension of the keratin network and *de novo* nucleation at focal adhesion sites of the lamellipodia itself (Felkl *et al.*, 2012).

Keratins, as other IFs, are dynamic filament networks that interact with a multitude of proteins, serving as scaffolds to organize signaling platforms and regulate different processes (Pallari and Eriksson, 2006; Sanghvi-Shah and Weber, 2017). Reflecting this role as signaling integrators, we propose that keratins may influence actin dynamics during InlB mediated entry by associating with molecular effectors downstream the activation of cMet, thus regulating their location and activity. In support of this hypothesis, K8 and K18 were reported to interact with Cbl and Grb2 proteins (Robertson *et al.*, 1997; Blagoev *et al.*, 2003), which are involved in cMet signaling and InlB-dependent entry of *L. monocytogenes* (Ireton *et al.*, 1999). In addition, keratins have been found to regulate the size and organization of lipid rafts (Gilbert *et al.*, 2012; Gilbert *et al.*, 2016; Roux *et al.*, 2017). These structures serve as surface membrane platforms were clustering of signaling molecules occur (Pizarro-Cerdá and Cossart, 2009), and their integrity is required for successful *Listeria* infection (Seveau *et al.*, 2004). Finally, through yet-uncharacterized interactions with the actin depolymerization machinery, keratins may affect actin depolymerization rates during InlB entry. Actin depolymerization is essential for successful *Listeria* infection and is controlled by the actin depolymerizing factor (ADF)/ cofilin protein, whose activity is regulated by LIM kinase (LIMK) phosphorylation (Bierne *et al.*, 2001).

The identification of host proteins interacting with K8 and K18 specifically upon *L. monocytogenes* infection or canonical HGF-induced cMet activation should uncover the molecular details of keratin-mediated actin dynamics modulation. Additionally, complementation of cMet expression by overexpression of cMet in K8/K18 depleted cells could be a useful approach to better understand the role of keratins strictly on the dynamics of actin during InlB-dependent internalization.

One of the most interesting findings reported in this thesis is that K18 controls the expression of various transmembrane receptors such as cMet, TfR and integrin β1 at an mRNA level. These observations are in accordance with a significant body of evidence that links keratins to gene expression and translation (Asghar *et al.*, 2016). Indeed, studies in mice that lack type I or type II keratins demonstrate that these animal display significant transcriptomic perturbations (Kumar *et al.*, 2015; Kumar *et al.*, 2016) and deficient protein expression (Vijayaraj *et al.*, 2009). Furthermore, K8 knockout leads to perturbed mRNA levels of several genes (Habtezion *et al.*, 2011; Asghar *et al.*, 2016; Lähdeniemi *et al.*, 2017), while K18 mutation alters the expression of oxidative stress genes (Zhou *et al.*, 2005). Additional keratins that have been implicated in altered transcriptional patterns include K1, K5, K10, K16, K17 and K19 (Fu and Wang, 2012; Roth *et al.*, 2012; Lessard *et al.*, 2013; Chung *et al.*, 2015; Salas *et al.*, 2016; R P Hobbs *et al.*, 2016; Saha *et al.*, 2017).

The molecular details of how keratins regulate gene transcriptional status remain poorly understood. By acting as molecular scaffolds that relay and integrate multiple signaling pathways, keratins may contribute for gene expression regulation (Ku *et al.*, 2004; Zhou *et al.*, 2005; Toivola *et al.*, 2005; Salas *et al.*, 2016; Lähdeniemi *et al.*, 2017). Interestingly, recent evidence points to a more direct role of keratins in gene expression (Ryan P. Hobbs *et al.*, 2016). Accordingly, K18 was reported to directly interact with the mRNA of the transcription factor C/EBPβ (Liu and Sun, 2005; Ying Wang *et al.*, 2011). Later, K17 was found present within the nucleus, where it interacts directly with the promoter regions of cytokine genes and the transcriptional regulator AIRE, thus regulating inflammatory response (Hobbs *et al.*, 2015). In the nucleus, K17 also regulates the nuclear export of the cell cycle regulator $p27^{KIP1}$ (Escobar-Hoyos *et al.*, 2015). Furthermore, K17 regulates the shuttling between the nucleus and the cytoplasm of proteins such as hnRNP K (Chung *et al.*, 2015) and 14-3-3σ (Kim *et al.*, 2006). Altogether, these surprising observations raise two key ideas: first, keratins can directly associate with nucleic acids, either DNA or RNA and second, keratins, which for decades have been viewed as cytoplasmic proteins, can also be present in the nucleus, where they can be of functional relevance (Ryan P. Hobbs *et al.*, 2016).

Besides K17, K8 and K18 were are also found in the nucleus of cells upon inhibition of exportin1-mediated nuclear export by the drug Leptomycin B (LMB) (Kumeta *et al.*, 2013), suggesting that K18 may participate in the nucleocytoplasmic shuttling of proteins, including proteins that are involved in mRNA processing. LMB treatment, followed by immunofluorescence and sub-cellular fractioning studies should clarify if K18 can be found in the nucleus of the cellular systems used in our work. K18 mutants that lack a nuclear export signal (NES) sequence were found to accumulate in the nucleus (Kumeta *et al.*, 2013). Transfection of cells with this K18 variant could elucidate if K18 shuttling from the nucleus to cytoplasm is important in the maintenance of normal expression of genes such as cMet, TfR and integrin β1.

In this work we show that K18 modulates the decay rates of cMet, TfR and integrin β1 mRNA, thus promoting proper protein levels of these genes. The half-lives of mRNA are transcript specific and can be modulated by association of the transcript with RNA binding proteins (RBPs) that regulate positively or negatively the interaction of the mRNAs with the RNA degradation machinery (Hasan *et al.*, 2014). By associating with the mRNAs, RBPs can modulate several aspects of RNA biogenesis such as transcription, splicing, localization, stability, and translation (Glisovic *et al.*, 2008). Multiple RBPs can interact with the same mRNA independently or in a competitive or cooperative manner, thus allowing a fine tuning of RNA metabolism (Wu and Brewer, 2012). Furthermore, various RBPs are able to shuttle between the nucleus and the cytoplasm according to the cell needs and in response to cellular stress

(Keene, 1999; Gallouzi *et al.*, 2000; van der Houven van Oordt *et al.*, 2000; Sarkar *et al.*, 2003; Suzuki *et al.*, 2005; Lewis *et al.*, 2017).

Interestingly, K18 have been shown to interact with proteins that associate with RNAs and influence their fate. K18 interacts with hnRNP R (Havugimana *et al.*, 2012), an RBP that binds and stabilizes the mRNA of MHC class I genes, thus enhancing their translation (Reches *et al.*, 2016). In addition, K18 was also reported to interact with the mRNA degradation machinery protein Pan2 (Bett *et al.*, 2013). Furthermore, while searching for K18 interactors, we identified by mass spectrometry various novel K18-interacting proteins that were previously identified as RNA binding proteins proteins. In particular, we identified the heat-shock cognate protein 70 (Hsc70), a chaperone that is able to bind and stabilize the mRNA of the pro-apoptotic protein Bim (Matsui *et al.*, 2007). Another identified K18-interacting protein is the PTB-associated splicing factor (PSF), an RNA and DNA binding protein that regulates multiple aspects of nucleic acids such as transcription, alternative splicing, location and mRNA stability (Hall-Pogar *et al.*, 2007; Heyd and Lynch, 2011; Yarosh *et al.*, 2015). Finally, we also found in our search that K18 interacts with Ewing sarcoma protein 1 (EWSR1), a protein that has been implicated in transcriptional regulation, splicing and RNA localization (Paronetto, 2013; Campos-Melo *et al.*, 2014). In addition to these findings, our *in silico* studies identified YTH Domain Containing 1 protein (YTHDC1) as an RBP that could putatively associate with the transcripts of cMet, TfR and integrin β1. YTHDC1 participates in RNA splicing and transport (Xiao *et al.*, 2016; Roundtree *et al.*, 2017), and was reported to interact with K18 (Jian Wang *et al.*, 2011). Altogether, these observations tempt us to speculate that by interacting with multiple RNA-binding proteins, K18 may affect different stages of mRNA processing such as stability and location, thus affecting protein expression.

Different strategies could be employed to better understand the molecular mechanisms behind K18 influence in mRNA regulatory processes. For instance, it would be interesting to analyze the impact of K18 depletion in the subcellular distribution of the RBPs above-mentioned. Such study could provide insight into K18 role in RBPs location, nucleocytoplasmic shuttling dynamics and potential effects on gene expression. Furthermore, it would be pertinent to assess the mRNA levels of cMet, TfR and integrin β1 in cells depleted for RBPs that putatively interact with K18. Similar analysis in cells expressing RBPs mutants that fail to shuttle between the nucleus and the cytoplasm could highlight the importance of RBP location for proper mRNA expression. Finally, RNA immunoprecipitation experiments could be performed to determine if cMet, TfR and integrin β1 transcripts do interact with the RBPs that are predicted to associate with K18, and assess whether K18 is required for such interaction.

It is worth noting that the present study is, to our knowledge, the first to demonstrate that keratins control cMet and TfR expression. This opens new questions regarding K8 and K18 implication not only in cell migration, growth and development, but also in iron metabolism.

Additional studies are therefore needed to elucidate K8/K18 relevance in molecular mechanisms associated with the cMet and TfR receptors.

In conclusion, our findings reveal K8 and K18 as novel players in *Listeria* infection. Due to their multifunctional nature, K8/K18 likely have different roles in *Listeria* pathogenesis. The dissection of actin interaction with K8/18 at bacteria entry site may clarify actin-keratin interplay dynamics and is worthy of consideration in future studies. Our work provides new insights on how K18 can regulate gene expression and identify multiple potential K18-interacting molecules that are involved in RNA processing. Additional investigation should elucidate the molecular mechanisms underlying K18-mediated gene expression. Importantly, such studies may reveal new layers of transcriptional regulation by cytoplasmic proteins such as keratins.

Future efforts should be made to understand how broad K18-mediated gene regulation is, to determine if its impact is restricted to surface proteins, and to address the consequent implications for cell homeostasis. Though our study of keratin involvement in *Listeria* pathogenesis we uncovered new details of keratin involvement in different regulatory processes that may be of relevance in physiological conditions, demonstrating once again that the study of bacterial pathogenesis can contribute to a better understanding of basic cell biology mechanisms.

CHAPTER V – REFERENCES

Abdelmohsen, K. (2012) Modulation of gene expression by RNA binding proteins: mRNA stability and translation. In *Binding Protein*. InTech, .

Alam, H., Sehgal, L., Kundu, S.T., Dalal, S.N., and Vaidya, M.M. (2011) Novel function of keratins 5 and 14 in proliferation and differentiation of stratified epithelial cells. *Mol Biol Cell* **22**: 4068–4078.

Allerberger, F., and Wagner, M. (2010) Listeriosis: A resurgent foodborne infection. *Clin Microbiol Infect* **16**: 16–23.

Almeida, M.T., Mesquita, F.S., Cruz, R., Osório, H., Custódio, R., Brito, C., *et al.* (2015) Src-dependent tyrosine phosphorylation of non-muscle myosin heavy chain-IIA restricts Listeria monocytogenes cellular infection. *J Biol Chem* **290**: 8383–95.

Ameen, N. a, Figueroa, Y., and Salas, P.J. (2001) Anomalous apical plasma membrane phenotype in CK8-deficient mice indicates a novel role for intermediate filaments in the polarization of simple epithelia. *J Cell Sci* **114**: 563–75.

Antfolk, D., Sjöqvist, M., Cheng, F., Isoniemi, K., Duran, C.L., Rivero-Muller, A., *et al.* (2017) Selective regulation of Notch ligands during angiogenesis is mediated by vimentin. *Proc Natl Acad Sci* **114**: E4574–E4581.

Asghar, M.N., Priyamvada, S., Nyström, J.H., Anbazhagan, A.N., Dudeja, P.K., and Toivola, D.M. (2016) Keratin 8 knockdown leads to loss of the chloride transporter DRA in the colon. *Am J Physiol - Gastrointest Liver Physiol* **310**: G1147–G1154.

Atkinson, E. (1917) Meningitis associated with gram-positive bacilli of diphtheroid type. *Med J Aust* **1**: 115–118.

Babrak, L., Danelishvili, L., Rose, S.J., Kornberg, T., and Bermudez, L.E. (2015) The Environment of “Mycobacterium avium subsp. hominissuis” microaggregates induces synthesis of small proteins associated with efficient infection of respiratory epithelial cells. *Infect Immun* **83**: 625–636.

Bakker, H.C. den, Warchocki, S., Wright, E.M., Allred, A.F., Ahlstrom, C., Manuel, C.S., *et al.* (2014) Listeria floridensis sp. nov., Listeria aquatica sp. nov., Listeria cornellensis sp. nov., Listeria riparia sp. nov. and Listeria grandensis sp. nov., from agricultural and natural environments. *Int J Syst Evol Microbiol* **64**: 1882–9.

Basar, T., Shen, Y., and Ireton, K. (2005) Redundant roles for Met docking site tyrosines and the Gab1 pleckstrin homology domain in InlB-mediated entry of Listeria monocytogenes. *Infect Immun* **73**: 2061–74.

Batchelor, M., Guignot, J., Patel, A., Cummings, N., Cleary, J., Knutton, S., *et al.* (2004) Involvement of the intermediate filament protein cytokeratin-18 in actin pedestal formation during EPEC infection. *EMBO Rep* **5**: 104–10.

Beauregard, K.E., Lee, K.D., Collier, R.J., and Swanson, J.A. (1997) pH-dependent perforation of macrophage phagosomes by listeriolysin O from Listeria monocytogenes. *J Exp Med* **186**: 1159–63.

Becroft, D.M., Farmer, K., Seddon, R.J., Sowden, R., Stewart, J.H., Vines, A., and Wattie, D.A. (1971) Epidemic listeriosis in the newborn. *Br Med J* **3**: 747–51.

Benson, D.L., Mandell, J.W., Shaw, G., and Banker, G. (1996) Compartmentation of alpha-internexin and neurofilament triplet proteins in cultured hippocampal neurons. *J Neurocytol* **25**: 181–96.

Bernardini, M.L., Mounier, J., D'Hauteville, H., Coquis-Rondon, M., and Sansonetti, P.J. (1989) Identification of icsA, a plasmid locus of Shigella flexneri that governs bacterial intra- and intercellular spread through interaction with F-actin. *Proc Natl Acad Sci U S A* **86**: 3867–71.

Bertsch, D., Rau, J., Eugster, M.R., Haug, M.C., Lawson, P.A., Lacroix, C., and Meile, L. (2013) Listeria fleischmannii sp. nov., isolated from cheese. *Int J Syst Evol Microbiol* **63**: 526–32.

Bett, J.S., Ibrahim, A.F.M., Garg, A.K., Kelly, V., Pedrioli, P., Rocha, S., and Hay, R.T. (2013) The P-body component USP52/PAN2 is a novel regulator of HIF1A mRNA stability. *Biochem J* **451**: 185–94.

Bhavsar, A.P., Guttman, J.A., and Finlay, B.B. (2007) Manipulation of host-cell pathways by bacterial pathogens. *Nature* **449**: 827–34.

Bierne, H., and Cossart, P. (2007) Listeria monocytogenes Surface Proteins: from Genome Predictions to Function. *Microbiol Mol Biol Rev* **71**: 377–397.

Bierne, H., Gouin, E., Roux, P., Caroni, P., Yin, H.L., and Cossart, P. (2001) A role for cofilin and LIM kinase in Listeria-induced phagocytosis. *J Cell Biol* **155**: 101–12.

Bierne, H., Miki, H., Innocenti, M., Scita, G., Gertler, F.B., Takenawa, T., and Cossart, P. (2005) WASP-related proteins, Abi1 and Ena/VASP are required for Listeria invasion induced by the Met receptor. *J Cell Sci* **118**: 1537–47.

Bierne, H., Sabet, C., Personnic, N., and Cossart, P. (2007) Internalins: a complex family of leucine-rich repeat-containing proteins in Listeria monocytogenes. *Microbes Infect* **9**: 1156–66.

Biever, A., Valjent, E., and Puighermanal, E. (2015) Ribosomal Protein S6 Phosphorylation in

the Nervous System: From Regulation to Function. *Front Mol Neurosci* **8**: 75.

Blackinton, J.G., and Keene, J.D. (2014) Post-transcriptional RNA regulons affecting cell cycle and proliferation. *Semin Cell Dev Biol* **34**: 44–54.

Blagoev, B., Kratchmarova, I., Ong, S.-E., Nielsen, M., Foster, L.J., and Mann, M. (2003) A proteomics strategy to elucidate functional protein-protein interactions applied to EGF signaling. *Nat Biotechnol* **21**: 315–8.

Bonazzi, M., Lecuit, M., and Cossart, P. (2009) Listeria monocytogenes internalin and E-cadherin: from bench to bedside. *Cold Spring Harb Perspect Biol* **1**: a003087.

Bonazzi, M., Vasudevan, L., Mallet, A., Sachse, M., Sartori, A., Prevost, M.-C., *et al.* (2011) Clathrin phosphorylation is required for actin recruitment at sites of bacterial adhesion and internalization. *J Cell Biol* **195**: 525–36.

Bonazzi, M., Veiga, E., Pizarro-Cerdá, J., and Cossart, P. (2008) Successive post-translational modifications of E-cadherin are required for InlA-mediated internalization of Listeria monocytogenes. *Cell Microbiol* **10**: 2208–22.

Bordeleau, F., Myrand Lapierre, M.-E., Sheng, Y., and Marceau, N. (2012) Keratin 8/18 Regulation of Cell Stiffness-Extracellular Matrix Interplay through Modulation of Rho-Mediated Actin Cytoskeleton Dynamics. *PLoS One* **7**: e38780.

Borezee, E., Pellegrini, E., and Berche, P. (2000) OppA of Listeria monocytogenes, an oligopeptide-binding protein required for bacterial growth at low temperature and involved in intracellular survival. *Infect Immun* **68**: 7069–77.

Bortolussi, R. (2008) Listeriosis: a primer. *CMAJ* **179**: 795–7.

Boujemaa-Paterski, R., Gouin, E., Hansen, G., Samarin, S., Clainche, C. Le, Didry, D., *et al.* (2001) Listeria protein ActA mimics WASp family proteins: it activates filament barbed end branching by Arp2/3 complex. *Biochemistry* **40**: 11390–404.

Bousquet, O., Ma, L., Yamada, S., Gu, C., Idei, T., Takahashi, K., *et al.* (2001) The nonhelical tail domain of keratin 14 promotes filament bundling and enhances the mechanical properties of keratin intermediate filaments in vitro. *J Cell Biol* **155**: 747–54.

Bragulla, H.H., and Homberger, D.G. (2009) 11helia. *J Anat* **214**: 516–59.

Braun, L., Dramsi, S., Dehoux, P., Bierne, H., Lindahl, G., and Cossart, P. (1997) InlB: an invasion protein of Listeria monocytogenes with a novel type of surface association. *Mol Microbiol* **25**: 285–94.

Braun, L., Ghebrehiwet, B., and Cossart, P. (2000) gC1q-R/p32, a C1q-binding protein, is a receptor for the InlB invasion protein of Listeria monocytogenes. *EMBO J* **19**: 1458–66.

Braun, L., Nato, F., Payrastre, B., Mazié, J.C., and Cossart, P. (1999) The 213-amino-acid leucine-rich repeat region of the listeria monocytogenes InlB protein is sufficient for entry into mammalian cells, stimulation of PI 3-kinase and membrane ruffling. *Mol Microbiol* **34**: 10–23.

Bryant, A.E., Bayer, C.R., Huntington, J.D., and Stevens, D.L. (2006) Group A streptococcal myonecrosis: increased vimentin expression after skeletal-muscle injury mediates the binding of <i>Streptococcus pyogenes<i>. *J Infect Dis* **193**: 1685–92.

Burgstaller, G., Gregor, M., Winter, L., and Wiche, G. (2010) Keeping the Vimentin Network under Control: Cell–Matrix Adhesion–associated Plectin 1f Affects Cell Shape and Polarity of Fibroblasts. *Mol Biol Cell* **21**: 3362–3375.

Byrne, C., Tainsky, M., and Fuchs, E. (1994) Programming gene expression in developing epidermis. *Development* **120**: 2369–83.

Cabanes, D., Dehoux, P., Dussurget, O., Frangeul, L., and Cossart, P. (2002) Surface proteins and the pathogenic potential of Listeria monocytogenes. *Trends Microbiol* **10**: 238–245.

Calderón-González, R., Frande-Cabanes, E., Bronchalo-Vicente, L., Lecea-Cuello, M.J., Pareja, E., Bosch-Martínez, A., *et al.* (2014) Cellular vaccines in listeriosis: role of the Listeria antigen GAPDH. *Front Cell Infect Microbiol* **4**.

Camejo, A., Buchrieser, C., Couvé, E., Carvalho, F., Reis, O., Ferreira, P., *et al.* (2009) In vivo transcriptional profiling of Listeria monocytogenes and mutagenesis identify new virulence factors involved in infection. *PLoS Pathog* **5**: e1000449.

Camejo, A., Carvalho, F., Reis, O., Leitão, E., Sousa, S., and Cabanes, D. (2011) The arsenal of virulence factors deployed by Listeria monocytogenes to promote its cell infection cycle. *Virulence* **2**: 379–94.

Camilli, A., Goldfine, H., and Portnoy, D.A. (1991) Listeria monocytogenes mutants lacking phosphatidylinositol-specific phospholipase C are avirulent. *J Exp Med* **173**: 751–4.

Campos-Melo, D., Droppelmann, C.A., Volkening, K., and Strong, M.J. (2014) RNA-binding proteins as molecular links between cancer and neurodegeneration. *Biogerontology* **15**: 587–610.

Cantile, M., Marra, L., Franco, R., Ascierto, P., Liguori, G., Chiara, A. De, and Botti, G. (2013) Molecular detection and targeting of EWSR1 fusion transcripts in soft tissue tumors. *Med Oncol* **30**.

Capetanaki, Y., Bloch, R.J., Kouloumenta, A., Mavroidis, M., and Psarras, S. (2007) Muscle intermediate filaments and their links to membranes and membranous organelles. *Exp Cell Res* **313**: 2063–2076.

Carabeo, R. (2011) Bacterial subversion of host actin dynamics at the plasma membrane. *Cell Microbiol* **13**: 1460–9.

Carlson, S. a., Omary, M.B., and Jones, B.D. (2002) Identification of cytokeratins as accessory mediators of Salmonella entry into eukaryotic cells. *Life Sci* **70**: 1415–1426.

Castañón, M.J., Walko, G., Winter, L., and Wiche, G. (2013) Plectin-intermediate filament partnership in skin, skeletal muscle, and peripheral nerve. *Histochem Cell Biol* **140**: 33–53.

Castello, A., Fischer, B., Eichelbaum, K., Horos, R., Beckmann, B.M., Strein, C., *et al.* (2012) Insights into RNA Biology from an Atlas of Mammalian mRNA-Binding Proteins. *Cell* **149**: 1393–1406.

Caulin, C., Ware, C.F., Magin, T.M., and Oshima, R.G. (2000) Keratin-dependent, epithelial resistance to tumor necrosis factor-induced apoptosis. *J Cell Biol* **149**: 17–22.

Chan, J.K.L., Yuen, D., Too, P.H.M., Sun, Y., Willard, B., Man, D., and Tam, C. (2018) Keratin 6a reorganization for ubiquitin-proteasomal processing is a direct antimicrobial response. *J Cell Biol* **217**: 731–744.

Chan, Y.M., Anton-Lamprecht, I., Yu, Q.C., Jackel, A., Zabel, B., Ernst -, J.P., and Fuchs, E. (1994) A human keratin 14 “knockout”: The absence of K14 leads to severe epidermolysis bullosa simplex and a function for an intermediate filament protein. *Genes Dev* **8**: 2574–2587.

Chatterjee, S.S., Hossain, H., Otten, S., Kuenne, C., Kuchmina, K., Machata, S., *et al.* (2006) Intracellular gene expression profile of Listeria monocytogenes. *Infect Immun* **74**: 1323–38.

Chen, L.L., and Carmichael, G.G. (2009) Altered Nuclear Retention of mRNAs Containing Inverted Repeats in Human Embryonic Stem Cells: Functional Role of a Nuclear Noncoding RNA. *Mol Cell* **35**: 467–478.

Chen, P.H., Ornelles, D.A., and Shenk, T. (1993) The adenovirus L3 23-kilodalton proteinase cleaves the amino-terminal head domain from cytokeratin 18 and disrupts the cytokeratin network of HeLa cells. *J Virol* **67**: 3507–14.

Chen, Y., Ross, W.H., Scott, V.N., and Gombas, D.E. (2003) Listeria monocytogenes: low levels equal low risk. *J Food Prot* **66**: 570–7.

Chernyatina, A.A., Guzenko, D., and Strelkov, S. V (2015) Intermediate filament structure : the bottom-up approach. *Curr Opin Cell Biol* **32**: 65–72.

Cheroutre-Vialette, M., Lebert, I., Hebraud, M., Labadie, J.C., and Lebert, A. (1998) Effects of pH or a(w) stress on growth of Listeria monocytogenes. *Int J Food Microbiol* **42**: 71–7.

Chi, F., Jong, T.D., Wang, L., Ouyang, Y., Wu, C., Li, W., and Huang, S.-H. (2010) Vimentin-mediated signalling is required for IbeA+ E. coli K1 invasion of human brain microvascular endothelial cells. *Biochem J* **427**: 79–90.

Chiba, S., Nagai, T., Hayashi, T., Baba, Y., Nagai, S., and Koyasu, S. (2011) Listerial invasion protein internalin B promotes entry into ileal Peyer's patches in vivo. *Microbiol Immunol* **55**: 123–9.

Chico-Calero, I., Suárez, M., González-Zorn, B., Scortti, M., Slaghuis, J., Goebel, W., *et al.* (2002) Hpt, a bacterial homolog of the microsomal glucose- 6-phosphate translocase, mediates rapid intracellular proliferation in Listeria. *Proc Natl Acad Sci U S A* **99**: 431–6.

Chung, B.M., Arutyunov, A., Ilagan, E., Yao, N., Wills-Karp, M., and Coulombe, P.A. (2015) Regulation of C-X-C chemokine gene expression by keratin 17 and hnRNP K in skin tumor keratinocytes. *J Cell Biol* **208**: 613–27.

Chung, B.M., Rotty, J.D., and Coulombe, P.A. (2013) Networking galore: Intermediate filaments and cell migration. *Curr Opin Cell Biol* **25**: 600–612.

Claser, C., Curcio, M., Mello, S.M. de, Silveira, E. V, Monteiro, H.P., and Rodrigues, M.M. (2008) Silencing cytokeratin 18 gene inhibits intracellular replication of Trypanosoma cruzi in HeLa cells but not binding and invasion of trypanosomes. *BMC Cell Biol* **9**: 68.

Cochard, P., and Paulin, D. (1984) Initial expression of neurofilaments and vimentin in the central and peripheral nervous system of the mouse embryo in vivo. *J Neurosci* **4**: 2080–94.

Colonne, P.M., Winchell, C.G., and Voth, D.E. (2016) Hijacking Host Cell Highways: Manipulation of the Host Actin Cytoskeleton by Obligate Intracellular Bacterial Pathogens. *Front Cell Infect Microbiol* **6**: 1–8.

Cook, K.B., Kazan, H., Zuberi, K., Morris, Q., and Hughes, T.R. (2011) RBPDB: A database of RNA-binding specificities. *Nucleic Acids Res* **39**.

Cooper, T.A., Wan, L., and Dreyfuss, G. (2009) RNA and Disease. *Cell* **136**: 777–793.

Copp, J., Marino, M., Banerjee, M., Ghosh, P., and Geer, P. van der (2003) Multiple regions of internalin B contribute to its ability to turn on the Ras-mitogen-activated protein kinase pathway. *J Biol Chem* **278**: 7783–9.

Cossart, P. (2011) Illuminating the landscape of host-pathogen interactions with the bacterium Listeria monocytogenes. *Proc Natl Acad Sci U S A* **108**: 19484–91.

Cossart, P., Vicente, M.F., Mengaud, J., Baquero, F., Perez-Diaz, J.C., and Berche, P. (1989) Listeriolysin O is essential for virulence of Listeria monocytogenes: direct evidence obtained by gene complementation. *Infect Immun* **57**: 3629–36.

Coulombe, P.A., Hutton, M.E., Letal, A., Hebert, A., Paller, A.S., and Fuchs, E. (1991) Point mutations in human keratin 14 genes of epidermolysis bullosa simplex patients: Genetic and functional analyses. *Cell* **66**: 1301–1311.

Coulombe, P.A., Kopan, R., and Fuchs, E. (1989) Expression of keratin K14 in the epidermis and hair follicle: insights into complex programs of differentiation. *J Cell Biol* **109**: 2295–312.

Coulombe, P. a, and Omary, M.B. (2002) “Hard” and “soft” principles defining the structure, function and regulation of keratin intermediate filaments. *Curr Opin Cell Biol* **14**: 110–22.

Czuczman, M. a., Fattouh, R., Rijn, J.M. van, Canadien, V., Osborne, S., Muise, A.M., *et al.* (2014) Listeria monocytogenes exploits efferocytosis to promote cell-to-cell spread. *Nature* **509**: 230–4.

Dacatur, A.L., and Portnoy, D.A. (2000) A PEST-like sequence in listeriolysin O essential for Listeria monocytogenes pathogenicity. *Science (80-)* **290**: 992–995.

Dalakas, M.C., Park, K.-Y., Semino-Mora, C., Lee, H.S., Sivakumar, K., and Goldfarb, L.G. (2000) Desmin Myopathy, a Skeletal Myopathy with Cardiomyopathy Caused by Mutations in the Desmin Gene. *N Engl J Med* **342**: 770–780.

Darnell, R.B. (2010) RNA Regulation in Neurologic Disease and Cancer. *Cancer Res Treat* **42**: 125.

David, D.J. V., and Cossart, P. (2017) Recent advances in understanding Listeria monocytogenes infection: the importance of subcellular and physiological context. *F1000Research* **6**: 1126.

Dechat, T., Pfleghaar, K., Sengupta, K., Shimi, T., Shumaker, D.K., Solimando, L., and Goldman, R.D. (2008) Nuclear lamins: major factors in the structural organization and function of the nucleus and chromatin. *Genes Dev* **22**: 832–53.

Deng, M., Zhang, W., Tang, H., Ye, Q., Liao, Q., Zhou, Y., *et al.* (2012) Lactotransferrin acts as a tumor suppressor in nasopharyngeal carcinoma by repressing AKT through multiple mechanisms. *Oncogene* **32**: 1–11.

Denk, H., Lackinger, E., Zatloukal, K., and Franke, W.W. (1987) Turnover of cytokeratin polypeptides in mouse hepatocytes. *Exp Cell Res* **173**: 137–43.

Dhama, K., Karthik, K., Tiwari, R., Shabbir, M.Z., Barbuddhe, S., Malik, S.V.S., and Singh,

R.K. (2015) Listeriosis in animals, its public health significance (food-borne zoonosis) and advances in diagnosis and control: a comprehensive review. *Vet Q* **35**: 211–35.

Disson, O., Grayo, S., Huillet, E., Nikitas, G., Langa-Vives, F., Dussurget, O., *et al.* (2008) Conjugated action of two species-specific invasion proteins for fetoplacental listeriosis. *Nature* **455**: 1114–1118.

Disson, O., and Lecuit, M. (2012) Targeting of the central nervous system by Listeria monocytogenes. *Virulence* **3**: 213–221.

Disson, O., Nikitas, G., Grayo, S., Dussurget, O., Cossart, P., and Lecuit, M. (2009) Modeling human listeriosis in natural and genetically engineered animals. *Nat Protoc* **4**: 799–810.

Domann, E., Wehland, J., Rohde, M., Pistor, S., Hartl, M., Goebel, W., *et al.* (1992) A novel bacterial virulence gene in Listeria monocytogenes required for host cell microfilament interaction with homology to the proline-rich region of vinculin. *EMBO J* **11**: 1981–90.

Dong, F., Su, H., Huang, Y., Zhong, Y., and Zhong, G. (2004) Cleavage of host keratin 8 by a Chlamydia-secreted protease. *Infect Immun* **72**: 3863–8.

Doran, K.S., Banerjee, A., Disson, O., and Lecuit, M. (2013) Concepts and mechanisms: Crossing host barriers. *Cold Spring Harb Perspect Med* **3**.

Du, N., Cong, H., Tian, H., Zhang, H., Zhang, W., Song, L., and Tien, P. (2014) Cell Surface Vimentin Is an Attachment Receptor for Enterovirus 71. *J Virol* **88**: 5816–5833.

Duan, Y., Sun, Y., Zhang, F., Zhang, W.K., Wang, D., Wang, Y., *et al.* (2012) Keratin K18 increases cystic fibrosis transmembrane conductance regulator (CFTR) surface expression by binding to its C-terminal hydrophobic patch. *J Biol Chem* **287**: 40547–59.

Dumont, J., and Cotoni, L. (1921) Bacille semblable au bacille du rouget du porc rencontré dans le liquide céphalo-rachidien d'un méningitique. *Ann Inst Pasteur* **35**: 625–33.

Dutertre, M., Sanchez, G., Cian, M.-C. De, Barbier, J., Dardenne, E., Gratadou, L., *et al.* (2010) Cotranscriptional exon skipping in the genotoxic stress response. *Nat Struct Mol Biol* **17**: 1358–1366.

Egile, C., Loisel, T.P., Laurent, V., Li, R., Pantaloni, D., Sansonetti, P.J., and Carlier, M.F. (1999) Activation of the CDC42 effector N-WASP by the Shigella flexneri IcsA protein promotes actin nucleation by Arp2/3 complex and bacterial actin-based motility. *J Cell Biol* **146**: 1319–32.

Eisenberg, E., and Greene, L.E. (2007) Multiple roles of auxilin and hsc70 in clathrin-mediated endocytosis. *Traffic* **8**: 640–6.

Erber, A., Riemer, D., Bovenschulte, M., and Weber, K. (1998) Molecular phylogeny of metazoan intermediate filament proteins. *J Mol Evol* **47**: 751–62.

Eriksson, J.E., Dechat, T., Grin, B., Helfand, B., Mendez, M., Pallari, H., and Goldman, R.D. (2009) Introducing intermediate filaments: from discovery to disease. *J Clin Invest* **119**: 1763–71.

Escobar-Hoyos, L.F., Shah, R., Roa-Pena, L., Vanner, E. a., Najafian, N., Banach, A., *et al.* (2015) Keratin-17 Promotes p27KIP1 Nuclear Export and Degradation and Offers Potential Prognostic Utility. *Cancer Res* **75**: 3650–3662.

Esteban, J.I., Oporto, B., Aduriz, G., Juste, R.A., and Hurtado, A. (2009) Faecal shedding and strain diversity of Listeria monocytogenes in healthy ruminants and swine in Northern Spain. *BMC Vet Res* **5**.

Esue, O., Carson, A.A., Tseng, Y., and Wirtz, D. (2006) A direct interaction between actin and vimentin filaments mediated by the tail domain of vimentin. *J Biol Chem* **281**: 30393–9.

European Food Safety Authority (2016) The European Union summary report on trends and sources of zoonoses, zoonotic agents and food-borne outbreaks in 2015. *EFSA J* **14**: 231.

Eylert, E., Schär, J., Mertins, S., Stoll, R., Bacher, A., Goebel, W., and Eisenreich, W. (2008) Carbon metabolism of Listeria monocytogenes growing inside macrophages. *Mol Microbiol* **69**: 1008–17.

Farber, J.M., and Peterkin, P.I. (1991) Listeria monocytogenes, a food-borne pathogen. *Microbiol Rev* **55**: 476–511.

Favre, B., Schneider, Y., Lingasamy, P., Bouameur, J.-E., Begré, N., Gontier, Y., *et al.* (2011) Plectin interacts with the rod domain of type III intermediate filament proteins desmin and vimentin. *Eur J Cell Biol* **90**: 390–400.

Fay, N., and Panté, N. (2013) The intermediate filament network protein, vimentin, is required for parvoviral infection. *Virology* **444**: 181–190.

Felkl, M., Tomas, K., Smid, M., Mattes, J., Windoffer, R., and Leube, R.E. (2012) Monitoring the cytoskeletal EGF response in live gastric carcinoma cells. *PLoS One* **7**: e45280.

FitzGerald, P., Sun, N., Shibata, B., and Hess, J.F. (2016) Expression of the type VI intermediate filament proteins CP49 and filensin in the mouse lens epithelium. *Mol Vis* **22**: 970–89.

Fletcher, D.A., and Mullins, R.D. (2010) Cell mechanics and the cytoskeleton. *Nature* **463**: 485–92.

Freitag, N., Port, G., and Miner, M. (2009) Listeria monocytogenes—from saprophyte to intracellular pathogen. *Nat Rev Microbiol* **7**: 623–8.

Fridkin, A., Penkner, A., Jantsch, V., and Gruenbaum, Y. (2009) SUN-domain and KASH-domain proteins during development, meiosis and disease. *Cell Mol Life Sci* **66**: 1518–1533.

Fu, M., and Wang, G. (2012) Keratin 17 as a therapeutic target for the treatment of psoriasis. *J Dermatol Sci* **67**: 161–165.

Fullerton, L., Norrish, G., Wedderburn, C.J., Paget, S., Basu Roy, R., and Cane, C. (2015) Nosocomial Neonatal Listeria monocytogenes Transmission by Stethoscope. *Pediatr Infect Dis J* **34**: 1042–3.

Gahan, C.G.M., and Hill, C. (2005) Gastrointestinal phase of Listeria monocytogenes infection. In *Journal of Applied Microbiology*. pp. 1345–1353.

Gahan, C.G.M., and Hill, C. (2014) Listeria monocytogenes: survival and adaptation in the gastrointestinal tract. *Front Cell Infect Microbiol* **4**: 9.

Galarneau, L., Loranger, A., Gilbert, S., and Marceau, N. (2007) Keratins modulate hepatic cell adhesion, size and G1/S transition. *Exp Cell Res* **313**: 179–94.

Gallouzi, I.E., Brennan, C.M., Stenberg, M.G., Swanson, M.S., Eversole, A., Maizels, N., and Steitz, J.A. (2000) HuR binding to cytoplasmic mRNA is perturbed by heat shock. *Proc Natl Acad Sci U S A* **97**: 3073–8.

Gao, Y.S., and Sztul, E. (2001) A novel interaction of the Golgi complex with the vimentin intermediate filament cytoskeleton. *J Cell Biol* **152**: 877–893.

Garneau, N.L., Wilusz, J., and Wilusz, C.J. (2007) The highways and byways of mRNA decay. *Nat Rev Mol Cell Biol* **8**: 113–126.

Gedde, M.M., Higgins, D.E., Tilney, L.G., and Portnoy, D. a (2000) Role of listeriolysin O in cell-to-cell spread of Listeria monocytogenes. *Infect Immun* **68**: 999–1003.

Geisler, F., and Leube, R.E. (2016) Epithelial Intermediate Filaments: Guardians against Microbial Infection? *Cells* **5**: 1–18.

Gekara, N.O., Westphal, K., Ma, B., Rohde, M., Groebe, L., and Weiss, S. (2007) The multiple mechanisms of Ca2+ signalling by listeriolysin O, the cholesterol-dependent cytolysin of Listeria monocytogenes. *Cell Microbiol* **9**: 2008–21.

Gessain, G., Tsai, Y.-H., Travier, L., Bonazzi, M., Grayo, S., Cossart, P., *et al.* (2015) PI3-kinase activation is critical for host barrier permissiveness to Listeria monocytogenes. *J Exp*

Med **212**: 165–183.

Ghosh, P., Halvorsen, E.M., Ammendolia, D.A., Mor-Vaknin, N., O'Riordan, M.X.D., Brumell, J.H., *et al.* (2018) Invasion of the brain by Listeria monocytogenes is mediated by InlF and host cell vimentin. *MBio* **9**: 1–11.

Giardini, P.A., and Theriot, J.A. (2001) Effects of intermediate filaments on actin-based motility of Listeria monocytogenes. *Biophys J* **81**: 3193–203.

Gilbert, S., Loranger, A., Daigle, N., and Marceau, N. (2001) Simple epithelium keratins 8 and 18 provide resistance to Fas-mediated apoptosis. The protection occurs through a receptor-targeting modulation. *J Cell Biol* **154**: 763–73.

Gilbert, S., Loranger, A., Lavoie, J.N., and Marceau, N. (2012) Cytoskeleton keratin regulation of FasR signaling through modulation of actin/ezrin interplay at lipid rafts in hepatocytes. *Apoptosis* **17**: 880–94.

Gilbert, S., Loranger, A., and Marceau, N. (2004) Keratins modulate c-Flip/extracellular signal-regulated kinase 1 and 2 antiapoptotic signaling in simple epithelial cells. *Mol Cell Biol* **24**: 7072–81.

Gilbert, S., Loranger, A., Omary, M.B., and Marceau, N. (2016) Keratin impact on PKCδ- and ASMase-mediated regulation of hepatocyte lipid raft size - implication for FasR-associated apoptosis. *J Cell Sci* **129**: 3262–73.

Glisovic, T., Bachorik, J.L., Yong, J., and Dreyfuss, G. (2008) RNA-binding proteins and post-transcriptional gene regulation. *FEBS Lett* **582**: 1977–86.

Goldfarb, L.G., Olivé, M., Vicart, P., and Goebel, H.H. (2008) Intermediate filament diseases: Desminopathy. *Adv Exp Med Biol* **642**: 131–164.

Goldman, R.D., Cleland, M.M., Murthy, S.N.P., Mahammad, S., and Kuczmarski, E.R. (2012) Inroads into the structure and function of intermediate filament networks. *J Struct Biol* **177**: 14–23.

González, A., Shimobayashi, M., Eisenberg, T., Merle, D.A., Pendl, T., Hall, M.N., and Moustafa, T. (2015) TORC1 promotes phosphorylation of ribosomal protein S6 via the AGC kinase Ypk3 in Saccharomyces cerevisiae. *PLoS One* **10**: e0120250.

Goosney, D.L., Gruenheid, S., and Finlay, B.B. (2000) Gut feelings: enteropathogenic E. coli (EPEC) interactions with the host. *Annu Rev Cell Dev Biol* **16**: 173–89.

Goulet, V., King, L.A., Vaillant, V., and Valk, H. de (2013) What is the incubation period for listeriosis? *BMC Infect Dis* **13**: 11.

Graves, L.M., Helsel, L.O., Steigerwalt, A.G., Morey, R.E., Daneshvar, M.I., Roof, S.E., *et al.* (2010) Listeria marthii sp. nov., isolated from the natural environment, Finger Lakes National Forest. *Int J Syst Evol Microbiol* **60**: 1280–8.

Gray, M.L., and Killinger, A.H. (1966) Listeria monocytogenes and listeric infections. *Bacteriol Rev* **30**: 309–82.

Green, K.J., Böhringer, M., Gocken, T., and Jones, J.C.R. (2005) Intermediate filament associated proteins. *Adv Protein Chem* **70**: 143–202.

Gregor, M., Osmanagic-Myers, S., Burgstaller, G., Wolfram, M., Fischer, I., Walko, G., *et al.* (2014) Mechanosensing through focal adhesion-anchored intermediate filaments. *FASEB J* **28**: 715–729.

Gruenbaum, Y., and Aebi, U. (2014) Intermediate filaments: a dynamic network that controls cell mechanics. *F1000Prime Rep* **6**: 1–7.

Gruenheid, S., DeVinney, R., Bladt, F., Goosney, D., Gelkop, S., Gish, G.D., *et al.* (2001) Enteropathogenic E. coli Tir binds Nck to initiate actin pedestal formation in host cells. *Nat Cell Biol* **3**: 856–9.

Gründling, A., Burrack, L.S., Bouwer, H.G.A., and Higgins, D.E. (2004) Listeria monocytogenes regulates flagellar motility gene expression through MogR, a transcriptional repressor required for virulence. *Proc Natl Acad Sci U S A* **101**: 12318–23.

Guignot, J., and Servin, A.L. (2008) Maintenance of the Salmonella-containing vacuole in the juxtanuclear area: a role for intermediate filaments. *Microb Pathog* **45**: 415–22.

Guillet, C., Join-Lambert, O., Monnier, A. Le, Leclercq, A., Mechaï, F., Mamzer-Bruneel, M.-F., *et al.* (2010) Human Listeriosis Caused by Listeria ivanovii. *Emerg Infect Dis* **16**: 136–138.

Guzmán, C.A., Domann, E., Rohde, M., Bruder, D., Darji, A., Weiss, S., *et al.* (1996) Apoptosis of mouse dendritic cells is triggered by listeriolysin, the major virulence determinant of Listeria monocytogenes. *Mol Microbiol* **20**: 119–26.

Habtezion, A., Toivola, D.M., Asghar, M.N., Kronmal, G.S., Brooks, J.D., Butcher, E.C., and Omary, M.B. (2011) Absence of keratin 8 confers a paradoxical microflora-dependent resistance to apoptosis in the colon. *Proc Natl Acad Sci U S A* **108**: 1445–50.

Haglund, C.M., and Welch, M.D. (2011) Pathogens and polymers: microbe-host interactions illuminate the cytoskeleton. *J Cell Biol* **195**: 7–17.

Haines, R.L., and Lane, E.B. (2012) Keratins and disease at a glance. *J Cell Sci* **125**: 3923–8.

Halees, A.S., El-badrawi, R., and Khabar, K.S.A. (2008) ARED Organism: Expansion of ARED reveals AU-rich element cluster variations between human and mouse. *Nucleic Acids Res* **36**.

Hall-Pogar, T., Liang, S., Hague, L.K., and Lutz, C.S. (2007) Specific trans-acting proteins interact with auxiliary RNA polyadenylation elements in the COX-2 3'-UTR. *RNA* **13**: 1103–15.

Ham, H., Sreelatha, A., and Orth, K. (2011) Manipulation of host membranes by bacterial effectors. *Nat Rev Microbiol* **9**: 635–46.

Hamon, M.A., Ribet, D., Stavru, F., and Cossart, P. (2012) Listeriolysin O: the Swiss army knife of Listeria. *Trends Microbiol* **20**: 360–8.

Hanada, S., Harada, M., Kumemura, H., Omary, M.B., Kawaguchi, T., Taniguchi, E., *et al.* (2005) Keratin-containing inclusions affect cell morphology and distribution of cytosolic cellular components. *Exp Cell Res* **304**: 471–82.

Hasan, A., Cotobal, C., Duncan, C.D.S., and Mata, J. (2014) Systematic analysis of the role of RNA-binding proteins in the regulation of RNA stability. *PLoS Genet* **10**: e1004684.

Havel, L.S., Kline, E.R., Salgueiro, A.M., and Marcus, A.I. (2015) Vimentin regulates lung cancer cell adhesion through a VAV2-Rac1 pathway to control focal adhesion kinase activity. *Oncogene* **34**: 1979–1990.

Havugimana, P.C., Hart, G.T., Nepusz, T., Yang, H., Turinsky, A.L., Li, Z., *et al.* (2012) A census of human soluble protein complexes. *Cell* **150**: 1068–81.

He, T., Stepulak, A., Holmström, T.H., Omary, M.B., and Eriksson, J.E. (2002) The intermediate filament protein keratin 8 is a novel cytoplasmic substrate for c-Jun N-terminal kinase. *J Biol Chem* **277**: 10767–74.

Heinzen, R.A., Grieshaber, S.S., Kirk, L.S. Van, and Devin, C.J. (1999) Dynamics of actin-based movement by Rickettsia rickettsii in vero cells. *Infect Immun* **67**: 4201–7.

Henics, T., Nagy, E., Oh, H.J., Csermely, P., Gabain, A. Von, and Subjeck, J.R. (1999) Mammalian Hsp70 and Hsp110 proteins bind to RNA motifs involved in mRNA stability. *J Biol Chem* **274**: 17318–17324.

Henmi, Y., Tanabe, K., and Takei, K. (2011) Disruption of microtubule network rescues aberrant actin comets in dynamin2-depleted cells. *PLoS One* **6**.

Hernandez-Milian, A., and Payeras-Cifre, A. (2014) What is new in listeriosis? *Biomed Res Int* **2014**: 358051.

Herrmann, H., Bär, H., Kreplak, L., Strelkov, S. V, and Aebi, U. (2007) Intermediate filaments:

from cell architecture to nanomechanics. *Nat Rev Mol Cell Biol* **8**: 562–73.

Herrmann, H., Strelkov, S. V, Burkhard, P., and Aebi, U. (2009) Intermediate filaments: primary determinants of cell architecture and plasticity. *J Clin Invest* **119**: 1772–83.

Herrmann, H., Wedig, T., Porter, R.M., Lane, E.B., and Aebi, U. (2002) Characterization of early assembly intermediates of recombinant human keratins. *J Struct Biol* **137**: 82–96.

Heyd, F., and Lynch, K.W. (2011) PSF controls expression of histone variants and cellular viability in thymocytes. *Biochem Biophys Res Commun* **414**: 743–9.

Hinman, M.N., and Lou, H. (2008) Diverse molecular functions of Hu proteins. *Cell Mol Life Sci* **65**: 3168–3181.

Hisanaga, S., and Hirokawa, N. (1990) Dephosphorylation-induced interactions of neurofilaments with microtubules. *J Biol Chem* **265**: 21852–21858.

Hobbs, R.P., Batazzi, A.S., Han, M.C., and Coulombe, P.A. (2016) Loss of Keratin 17 induces tissue-specific cytokine polarization and cellular differentiation in HPV16-driven cervical tumorigenesis in vivo. *Oncogene* **35**: 5653–5662.

Hobbs, R.P., DePianto, D.J., Jacob, J.T., Han, M.C., Chung, B.-M., Batazzi, A.S., *et al.* (2015) Keratin-dependent regulation of Aire and gene expression in skin tumor keratinocytes. *Nat Genet* **47**: 933–8.

Hobbs, R.P., Jacob, J.T., and Coulombe, P.A. (2016) Keratins Are Going Nuclear. *Dev Cell* **38**: 227–233.

Hof, H. (2003) History and epidemiology of listeriosis. *FEMS Immunol Med Microbiol* **35**: 199–202.

Hogan, D.J., Riordan, D.P., Gerber, A.P., Herschlag, D., and Brown, P.O. (2008) Diverse RNA-binding proteins interact with functionally related sets of RNAs, suggesting an extensive regulatory system. *PLoS Biol* **6**: 2297–2313.

Hol, E.M., and Etienne-Manneville, S. (2015) Cell architecture: Intermediate filaments — from molecules to patients. *Curr Opin Cell Biol* **32**: v–vi.

Houven van Oordt, W. van der, Diaz-Meco, M.T., Lozano, J., Krainer, A.R., Moscat, J., and Cáceres, J.F. (2000) The MKK(3/6)-p38-signaling cascade alters the subcellular distribution of hnRNP A1 and modulates alternative splicing regulation. *J Cell Biol* **149**: 307–16.

Huang, L., Kuwahara, I., and Matsumoto, K. (2014) EWS represses cofilin 1 expression by inducing nuclear retention of cofilin 1 mRNA. *Oncogene* **33**: 2995–3003.

Huang, Y.-W., Yan, M., Collins, R.F., Diciccio, J.E., Grinstein, S., and Trimble, W.S. (2008) Mammalian septins are required for phagosome formation. *Mol Biol Cell* **19**: 1717–26.

Huber, F., Boire, A., López, M.P., and Koenderink, G.H. (2015) Cytoskeletal crosstalk: when three different personalities team up. *Curr Opin Cell Biol* **32**: 39–47.

Hülphers, G. (1911) Lefvernekros hos kanin orsakad af en ej förut beskrifven bakterie. *Sven Vet Tidskr* **2**: 265–273.

Hutchison, C.J. (2002) Lamins: Building blocks or regulators of gene expression? *Nat Rev Mol Cell Biol* **3**: 848–858.

Hyder, C.L., Pallari, H.-M., Kochin, V., and Eriksson, J.E. (2008) Providing cellular signposts--post-translational modifications of intermediate filaments. *FEBS Lett* **582**: 2140–8.

Imig, J., Kanitz, A., and Gerber, A.P. (2012) RNA regulons and the RNA-protein interaction network. *Biomol Concepts* **3**: 403–414.

Inada, H., Izawa, I., Nishizawa, M., Fujita, E., Kiyono, T., Takahashi, T., *et al.* (2001) Keratin attenuates tumor necrosis factor-induced cytotoxicity through association with TRADD. *J Cell Biol* **155**: 415–26.

Ireton, K., Payrastre, B., Chap, H., Ogawa, W., Sakaue, H., Kasuga, M., and Cossart, P. (1996) A role for phosphoinositide 3-kinase in bacterial invasion. *Science* **274**: 780–782.

Ireton, K., Payrastre, B., and Cossart, P. (1999) The Listeria monocytogenes protein InlB is an agonist of mammalian phosphoinositide 3-kinase. *J Biol Chem* **274**: 17025–32.

Isberg, R.R., and Leong, J.M. (1990) Multiple beta 1 chain integrins are receptors for invasin, a protein that promotes bacterial penetration into mammalian cells. *Cell* **60**: 861–71.

Ishikawa, H., Bischoff, R., and Holtzer, H. (1968) Mitosis and intermediate-sized filaments in developing skeletal muscle. *J Cell Biol* **38**: 538–55.

Ivanek, R., Gröhn, Y.T., Tauer, L.W., and Wiedmann, M. (2004) The cost and benefit of Listeria monocytogenes food safety measures. *Crit Rev Food Sci Nutr* **44**: 513–23.

Ivanek, R., Gröhn, Y.T., and Wiedmann, M. (2006) Listeria monocytogenes in multiple habitats and host populations: review of available data for mathematical modeling. *Foodborne Pathog Dis* **3**: 319–36.

Ivaska, J., Vuoriluoto, K., Huovinen, T., Izawa, I., Inagaki, M., and Parker, P.J. (2005) PKCε-mediated phosphorylation of vimentin controls integrin recycling and motility. *EMBO J* **24**: 3834–3845.

Iyer, S. V., Dange, P.P., Alam, H., Sawant, S.S., Ingle, A.D., Borges, A.M., *et al.* (2013) Understanding the role of keratins 8 and 18 in neoplastic potential of breast cancer derived cell lines. *PLoS One* **8**: e53532.

Jaafar, L., Li, Z., Li, S., and Dynan, W.S. (2017) SFPQ•NONO and XLF function separately and together to promote DNA double-strand break repair via canonical nonhomologous end joining. *Nucleic Acids Res* **45**: 1848–1859.

Jasnin, M., Asano, S., Gouin, E., Hegerl, R., Plitzko, J.M., Villa, E., *et al.* (2013) Three-dimensional architecture of actin filaments in Listeria monocytogenes comet tails. *Proc Natl Acad Sci U S A* **110**: 20521–6.

Jiu, Y., Lehtimäki, J., Tojkander, S., Cheng, F., Jäälinoja, H., Liu, X., *et al.* (2015) Bidirectional Interplay between Vimentin Intermediate Filaments and Contractile Actin Stress Fibers. *Cell Rep* **11**: 1511–8.

Johansson, J., Mandin, P., Renzoni, A., Chiaruttini, C., Springer, M., and Cossart, P. (2002) An RNA thermosensor controls expression of virulence genes in Listeria monocytogenes. *Cell* **110**: 551–61.

Jones, J.C.R., Kam, C.Y., Harmon, R.M., Woychek, A. V, Hopkinson, S.B., and Green, K.J. (2017) Intermediate Filaments and the Plasma Membrane. *Cold Spring Harb Perspect Biol* **9**: a025866.

Jonquières, R., Bierne, H., Fiedler, F., Gounon, P., and Cossart, P. (1999) Interaction between the protein InlB of Listeria monocytogenes and lipoteichoic acid: a novel mechanism of protein association at the surface of gram-positive bacteria. *Mol Microbiol* **34**: 902–14.

Jonquières, R., Pizarro-Cerdá, J., and Cossart, P. (2001) Synergy between the N- and C-terminal domains of InlB for efficient invasion of non-phagocytic cells by Listeria monocytogenes. *Mol Microbiol* **42**: 955–65.

Kaneko, S., Rozenblatt-Rosen, O., Meyerson, M., and Manley, J.L. (2007) The multifunctional protein p54nrb/PSF recruits the exonuclease XRN2 to facilitate pre-mRNA 3′ processing and transcription termination. *Genes Dev* **21**: 1779–1789.

Karantza, V. (2010) Keratins in health and cancer: more than mere epithelial cell markers. *Oncogene* **30**: 127–138.

Karashima, T., Tsuruta, D., Hamada, T., Ishii, N., Ono, F., Hashikawa, K., *et al.* (2012) Interaction of plectin and intermediate filaments. *J Dermatol Sci* **66**: 44–50.

Keene, J.D. (1999) Why is Hu where? Shuttling of early-response-gene messenger RNA

subsets. *Proc Natl Acad Sci U S A* **96**: 5–7.

Keene, J.D. (2007) RNA regulons: coordination of post-transcriptional events. *Nat Rev Genet* **8**: 533–543.

Keene, J.D., and Tenenbaum, S.A. (2002) Eukaryotic mRNPs may represent posttranscriptional operons. *Mol Cell* **9**: 1161–1167.

Kellner, J.C., and Coulombe, P.A. (2009) Keratins and protein synthesis: the plot thickens. *J Cell Biol* **187**: 157–9.

Kim, H.J., Choi, W.J., and Lee, C.H. (2015) Phosphorylation and Reorganization of Keratin Networks: Implications for Carcinogenesis and Epithelial Mesenchymal Transition. *Biomol Ther (Seoul)* **23**: 301–12.

Kim, S., and Coulombe, P.A. (2007) Intermediate filament scaffolds fulfill mechanical, organizational, and signaling functions in the cytoplasm. *Genes Dev* **21**: 1581–97.

Kim, S., Wong, P., and Coulombe, P. a (2006) A keratin cytoskeletal protein regulates protein synthesis and epithelial cell growth. *Nature* **441**: 362–5.

Knoop, L.L., and Baker, S.J. (2000) The splicing factor U1C represses EWS/FLI-mediated transactivation. *J Biol Chem* **275**: 24865–24871.

Kobe, B., and Deisenhofer, J. (1994) The leucine-rich repeat: a versatile binding motif. *Trends Biochem Sci* **19**: 415–21.

Kocks, C., Gouin, E., Tabouret, M., Berche, P., Ohayon, H., and Cossart, P. (1992) L. monocytogenes-induced actin assembly requires the actA gene product, a surface protein. *Cell* **68**: 521–31.

Kocks, C., Marchand, J.B., Gouin, E., D'Hauteville, H., Sansonetti, P.J., Carlier, M.F., and Cossart, P. (1995) The unrelated surface proteins ActA of Listeria monocytogenes and IcsA of Shigella flexneri are sufficient to confer actin-based motility on Listeria innocua and Escherichia coli respectively. *Mol Microbiol* **18**: 413–23.

Kölsch, A., Windoffer, R., and Leube, R.E. (2009) Actin-dependent dynamics of keratin filament precursors. *Cell Motil Cytoskeleton* **66**: 976–85.

Kommata, V., and Dermon, C.R. (2017) Transient vimentin expression during the embryonic development of the chicken cerebellum. *Int J Dev Neurosci* **65**: 11–20.

Kornreich, M., Avinery, R., Malka-Gibor, E., Laser-Azogui, A., and Beck, R. (2015) Order and disorder in intermediate filament proteins. *FEBS Lett* .

Kröger, C., Loschke, F., Schwarz, N., Windoffer, R., Leube, R.E., and Magin, T.M. (2013) Keratins control intercellular adhesion involving PKC-α-mediated desmoplakin phosphorylation. *J Cell Biol* **201**: 681–692.

Ku, N.-O., Michie, S., Resurreccion, E.Z., Broome, R.L., and Omary, M.B. (2002) Keratin binding to 14-3-3 proteins modulates keratin filaments and hepatocyte mitotic progression. *Proc Natl Acad Sci U S A* **99**: 4373–8.

Ku, N.-O., and Omary, M.B. (2006) A disease- and phosphorylation-related nonmechanical function for keratin 8. *J Cell Biol* **174**: 115–25.

Ku, N.-O., Toivola, D.M., Strnad, P., and Omary, M.B. (2010) Cytoskeletal keratin glycosylation protects epithelial tissue from injury. *Nat Cell Biol* **12**: 876–85.

Ku, N.O., Fu, H., and Omary, M.B. (2004) Raf-1 activation disrupts its binding to keratins during cell stress. *J Cell Biol* **166**: 479–485.

Ku, N.O., Michie, S. a, Soetikno, R.M., Resurreccion, E.Z., Broome, R.L., and Omary, M.B. (1998) Mutation of a major keratin phosphorylation site predisposes to hepatotoxic injury in transgenic mice. *J Cell Biol* **143**: 2023–32.

Ku, N.O., Michie, S., Oshima, R.G., and Omary, M.B. (1995) Chronic hepatitis, hepatocyte fragility, and increased soluble phosphoglycokeratins in transgenic mice expressing a keratin 18 conserved arginine mutant. *J Cell Biol* **131**: 1303–14.

Kuehl, C.J., Dragoi, A.-M., Talman, A., and Agaisse, H. (2015) Bacterial spread from cell to cell: beyond actin-based motility. *Trends Microbiol* **23**: 558–66.

Kühbacher, A., Dambournet, D., Echard, A., Cossart, P., and Pizarro-Cerdá, J. (2012) Phosphatidylinositol 5-phosphatase oculocerebrorenal syndrome of Lowe protein (OCRL) controls actin dynamics during early steps of Listeria monocytogenes infection. *J Biol Chem* **287**: 13128–36.

Kumar, V., Behr, M., Kiritsi, D., Scheffschick, A., Grahnert, A., Homberg, M., *et al.* (2016) Keratin-dependent thymic stromal lymphopoietin expression suggests a link between skin blistering and atopic disease. *J Allergy Clin Immunol* **138**: 1461–1464.e6.

Kumar, V., Bouameur, J.-E., Bär, J., Rice, R.H., Hornig-Do, H.-T., Roop, D.R., *et al.* (2015) A keratin scaffold regulates epidermal barrier formation, mitochondrial lipid composition, and activity. *J Cell Biol* **211**: 1057–75.

Kumar, Y., and Valdivia, R.H. (2008) Actin and intermediate filaments stabilize the Chlamydia trachomatis vacuole by forming dynamic structural scaffolds. *Cell Host Microbe* **4**: 159–69.

Kumemura, H., Harada, M., Omary, M.B., Sakisaka, S., Suganuma, T., Namba, M., and Sata, M. (2004) Aggregation and loss of cytokeratin filament networks inhibit golgi organization in liver-derived epithelial cell lines. *Cell Motil Cytoskeleton* **57**: 37–52.

Kumeta, M., Hirai, Y., Yoshimura, S.H., Horigome, T., and Takeyasu, K. (2013) Antibody-based analysis reveals “filamentous vs. non-filamentous” and “cytoplasmic vs. nuclear” crosstalk of cytoskeletal proteins. *Exp Cell Res* **319**: 3226–37.

L.Buchanan, R., Gorris, L.G.M., Hayman, M.M., Jackson, T.C., and Whiting, R.C. (2017) A review of Listeria monocytogenes: An update on outbreaks, virulence, dose-response, ecology, and risk assessments. *Food Control* **75**: 1–13.

Lähdeniemi, I.A.K., Misiorek, J.O., Antila, C.J.M., Landor, S.K.-J., Stenvall, C.-G.A., Fortelius, L.E., *et al.* (2017) Keratins regulate colonic epithelial cell differentiation through the Notch1 signalling pathway. *Cell Death Differ* **24**: 984–996.

Lamont, R.F., Sobel, J., Mazaki-Tovi, S., Kusanovic, J.P., Vaisbuch, E., Kim, S.K., *et al.* (2011) Listeriosis in human pregnancy: a systematic review. *J Perinat Med* **39**: 227–36.

Lane, E.B., Rugg, E.L., Navsaria, H., Leigh, I.M., Heagerty, A.H., Ishida-Yamamoto, A., and Eady, R.A. (1992) A mutation in the conserved helix termination peptide of keratin 5 in hereditary skin blistering. *Nature* **356**: 244–246.

Lang Halter, E., Neuhaus, K., and Scherer, S. (2013) Listeria weihenstephanensis sp. nov., isolated from the water plant Lemna trisulca taken from a freshwater pond. *Int J Syst Evol Microbiol* **63**: 641–7.

Larsen, H.E., Seeliger, H.P.R., and others (1966) A mannitol fermenting Listeria: Listeria grayi sp. n. In *Proceedings of the Third International Symposium on Listeriosis*. pp. 35–39.

Leclercq, A., Clermont, D., Bizet, C., Grimont, P.A.D., Flèche-Matéos, A. Le, Roche, S.M., *et al.* (2010) Listeria rocourtiae sp. nov. *Int J Syst Evol Microbiol* **60**: 2210–4.

Lecuit, M. (2007) Human listeriosis and animal models. *Microbes Infect* **9**: 1216–25.

Lecuit, M., Hurme, R., Pizarro-Cerda, J., Ohayon, H., Geiger, B., and Cossart, P. (2000) A role for alpha - and beta -catenins in bacterial uptake. *Proc Natl Acad Sci* **97**: 10008–10013.

Lecuit, M., Nelson, D.M., Smith, S.D., Khun, H., Huerre, M., Vacher-Lavenu, M.-C., *et al.* (2004) Targeting and crossing of the human maternofetal barrier by Listeria monocytogenes: role of internalin interaction with trophoblast E-cadherin. *Proc Natl Acad Sci U S A* **101**: 6152–7.

Lecuit, M., Ohayon, H., Braun, L., Mengaud, J., and Cossart, P. (1997) Internalin of Listeria

monocytogenes with an intact leucine-rich repeat region is sufficient to promote internalization. *Infect Immun* **65**: 5309–19.

Lecuit, M., Vandormael-Pournin, S., Lefort, J., Huerre, M., Gounon, P., Dupuy, C., *et al.* (2001) A transgenic model for listeriosis: role of internalin in crossing the intestinal barrier. *Science* **292**: 1722–5.

Leduc, C., and Etienne-Manneville, S. (2015) Intermediate filaments in cell migration and invasion: the unusual suspects. *Curr Opin Cell Biol* **32**: 102–112.

Lee, C.-H., and Coulombe, P. a (2009) Self-organization of keratin intermediate filaments into cross-linked networks. *J Cell Biol* **186**: 409–21.

Lemon, K.P., Higgins, D.E., and Kolter, R. (2007) Flagellar motility is critical for Listeria monocytogenes biofilm formation. *J Bacteriol* **189**: 4418–24.

Lendahl, U., Zimmerman, L.B., and McKay, R.D. (1990) CNS stem cells express a new class of intermediate filament protein. *Cell* **60**: 585–95.

Lessard, J.C., Piña-Paz, S., Rotty, J.D., Hickerson, R.P., Kaspar, R.L., Balmain, A., and Coulombe, P.A. (2013) Keratin 16 regulates innate immunity in response to epidermal barrier breach. *Proc Natl Acad Sci U S A* **110**: 19537–42.

Lewis, C.J.T., Pan, T., and Kalsotra, A. (2017) RNA modifications and structures cooperate to guide RNA-protein interactions. *Nat Rev Mol Cell Biol* **18**: 202–210.

Li, N., Xiang, G.-S.S., Dokainish, H., Ireton, K., and Elferink, L. a. (2005) The Listeria protein internalin B mimics hepatocyte growth factor-induced receptor trafficking. *Traffic* **6**: 459–73.

Liang, S., and Lutz, C.S. (2006) p54nrb is a component of the snRNP-free U1A (SF-A) complex that promotes pre-mRNA cleavage during polyadenylation. *RNA* **12**: 111–121.

Liao, J., Lowthert, L.A., and Omary, M.B. (1995) Heat stress or rotavirus infection of human epithelial cells generates a distinct hyperphosphorylated form of keratin 8. *Exp Cell Res* **219**: 348–57.

Lin, L., Holbro, T., Alonso, G., Gerosa, D., and Burger, M.M. (2001) Molecular interaction between human tumor marker protein p150, the largest subunit of eIF3, and intermediate filament protein K7. *J Cell Biochem* **80**: 483–90.

Liu, D.G., and Sun, L. (2005) Direct isolation of specific RNA-interacting proteins using a novel affinity medium. *Nucleic Acids Res* **33**: 1–5.

Liu, T., Daniels, C.K., and Cao, S. (2012) Comprehensive review on the HSC70 functions,

interactions with related molecules and involvement in clinical diseases and therapeutic potential. *Pharmacol Ther* **136**: 354–74.

Lomonaco, S., Nucera, D., and Filipello, V. (2015) The evolution and epidemiology of Listeria monocytogenes in Europe and the United States. *Infect Genet Evol* **35**: 172–83.

Loranger, a, Duclos, S., Grenier, a, Price, J., Wilson-Heiner, M., Baribault, H., and Marceau, N. (1997) Simple epithelium keratins are required for maintenance of hepatocyte integrity. *Am J Pathol* **151**: 1673–83.

Loschke, F., Homberg, M., and Magin, T.M. (2016) Keratin isotypes control desmosome stability and dynamics through PKCα. *J Invest Dermatol* **136**: 202–213.

Loschke, F., Seltmann, K., Bouameur, J., and Magin, T.M. (2015) Regulation of keratin network organization. *Curr Opin Cell Biol* **32**: 56–64.

Low, J.C., and Donachie, W. (1997) A review of Listeria monocytogenes and listeriosis. *Vet J* **153**: 9–29.

Lowery, J., Kuczmarski, E.R., Herrmann, H., and Goldma, R.D. (2015) Intermediate filaments play a pivotal role in regulating cell architecture and function. *J Biol Chem* **290**: 17145–17153.

Lukong, K.E., Chang, K., Khandjian, E.W., and Richard, S. (2008) RNA-binding proteins in human genetic disease. *Trends Genet* **24**: 416–425.

Lunde, B.M., Moore, C., and Varani, G. (2007) RNA-binding proteins: modular design for efficient function. *Nat Rev Mol Cell Biol* **8**: 479–90.

Magin, T.M., Vijayaraj, P., and Leube, R.E. (2007) Structural and regulatory functions of keratins. *Exp Cell Res* **313**: 2021–32.

Magnuson, B., Ekim, B., and Fingar, D.C. (2012) Regulation and function of ribosomal protein S6 kinase (S6K) within mTOR signalling networks. *Biochem J* **441**: 1–21.

Mak, T., and Brüggemann, H. (2016) Vimentin in Bacterial Infections. *Cells* **5**: 18.

Marceau, N., Schutte, B., Gilbert, S., Loranger, A., Henfling, M.E.R., Broers, J.L. V, *et al.* (2007) Dual roles of intermediate filaments in apoptosis. *Exp Cell Res* **313**: 2265–81.

Margiotta, A., and Bucci, C. (2016) Role of Intermediate Filaments in Vesicular Traffic. *Cells* **5**.

Margolis, S.S., Perry, J.A., Forester, C.M., Nutt, L.K., Guo, Y., Jardim, M.J., *et al.* (2006) Role for the PP2A/B56δ Phosphatase in Regulating 14-3-3 Release from Cdc25 to Control Mitosis. *Cell* **127**: 759–773.

Martins, M., Custoḍio, R., Camejo, A., Almeida, M.T., Cabanes, D., and Sousa, S. (2012) Listeria monocytogenes triggers the cell surface expression of Gp96 protein and interacts with its N terminus to support cellular infection. *J Biol Chem* **287**: 43083–43093.

Mathew, J., Loranger, A., Gilbert, S., Faure, R., and Marceau, N. (2013) Keratin 8/18 regulation of glucose metabolism in normal versus cancerous hepatic cells through differential modulation of hexokinase status and insulin signaling. *Exp Cell Res* **319**: 474–86.

Matsui, H., Asou, H., and Inaba, T. (2007) Cytokines direct the regulation of Bim mRNA stability by heat-shock cognate protein 70. *Mol Cell* **25**: 99–112.

Maucuer, A., Camonis, J.H., and Sobel, A. (1995) Stathmin interaction with a putative kinase and coiled-coil-forming protein domains. *Proc Natl Acad Sci U S A* **92**: 3100–4.

McClure, P.J., Kelly, T.M., and Roberts, T.A. (1991) The effects of temperature, pH, sodium chloride and sodium nitrite on the growth of Listeria monocytogenes. *Int J Food Microbiol* **14**: 77–91.

McIntosh, P.B., Laskey, P., Sullivan, K., Davy, C., Wang, Q., Jackson, D.J., *et al.* (2010) E1--E4-mediated keratin phosphorylation and ubiquitylation: a mechanism for keratin depletion in HPV16-infected epithelium. *J Cell Sci* **123**: 2810–22.

McLauchlin, J., Mitchell, R.T., Smerdon, W.J., and Jewell, K. (2004) Listeria monocytogenes and listeriosis: a review of hazard characterisation for use in microbiological risk assessment of foods. *Int J Food Microbiol* **92**: 15–33.

McLauchlin, J., Rees, C.E.D., and Dodd, C.E.R. (2014) Listeria monocytogenes and the genus Listeria. In *The Prokaryotes*. Springer, pp. 241–259.

Mead, P.S., Slutsker, L., Dietz, V., McCaig, L.F., Bresee, J.S., Shapiro, C., *et al.* Food-related illness and death in the United States. *Emerg Infect Dis* **5**: 607–25.

Mendez, M.G., Kojima, S.-I., and Goldman, R.D. (2010) Vimentin induces changes in cell shape, motility, and adhesion during the epithelial to mesenchymal transition. *FASEB J* **24**: 1838–51.

Mengaud, J., Ohayon, H., Gounon, P., Mege R-M, and Cossart, P. (1996) E-cadherin is the receptor for internalin, a surface protein required for entry of L. monocytogenes into epithelial cells. *Cell* **84**: 923–32.

Menko, A.S., Bleaken, B.M., Libowitz, A.A., Zhang, L., Stepp, M.A., and Walker, J.L. (2014) A central role for vimentin in regulating repair function during healing of the lens epithelium. *Mol Biol Cell* **25**: 776–90.

Mesquita, F.S., Brito, C., Cabanes, D., and Sousa, S. (2017) Control of cytoskeletal dynamics during cellular responses to pore forming toxins. *Commun Integr Biol* **10**.

Mesquita, F.S., Brito, C., Mazon Moya, M.J., Pinheiro, J.C., Mostowy, S., Cabanes, D., and Sousa, S. (2017) Endoplasmic reticulum chaperone Gp96 controls actomyosin dynamics and protects against pore-forming toxins. *EMBO Rep* **18**: 303–318.

Messica, Y., Laser-Azogui, A., Volberg, T., Elisha, Y., Lysakovskaia, K., Eils, R., *et al.* (2017) The role of Vimentin in Regulating Cell Invasive Migration in Dense Cultures of Breast Carcinoma Cells. *Nano Lett* **17**: 6941–6948.

Mewborn, S.K., Puckelwartz, M.J., Abuisneineh, F., Fahrenbach, J.P., Zhang, Y., MacLeod, H., *et al.* (2010) Altered chromosomal positioning, Compaction, and gene expression with a lamin A/C gene mutation. *PLoS One* **5**.

Michalczyk, K., and Ziman, M. (2005) Nestin structure and predicted function in cellular cytoskeletal organisation. *Histol Histopathol* **20**: 665–71.

Miller, R.K., Khuon, S., and Goldman, R.D. (1993) Dynamics of keratin assembly: exogenous type I keratin rapidly associates with type II keratin in vivo. *J Cell Biol* **122**: 123–35.

Milner, D.J., Mavroidis, M., Weisleder, N., and Capetanaki, Y. (2000) Desmin cytoskeleton linked to muscle mitochondrial distribution and respiratory function. *J Cell Biol* **150**: 1283–1297.

Moeton, M., Kanski, R., Stassen, O.M.J.A., Sluijs, J.A., Geerts, D., Tijn, P. Van, *et al.* (2014) Silencing GFAP isoforms in astrocytoma cells disturbs laminin-dependent motility and cell adhesion. *FASEB J* **28**: 2942–2954.

Moll, R., Divo, M., and Langbein, L. (2008) The human keratins: biology and pathology. *Histochem Cell Biol* **129**: 705–33.

Monteiro, M.J., and Cleveland, D.W. (1989) Expression of NF-L and NF-M in fibroblasts reveals coassembly of neurofilament and vimentin subunits. *J Cell Biol* **108**: 579–93.

Moors, M.A., Levitt, B., Youngman, P., and Portnoy, D.A. (1999) Expression of listeriolysin O and ActA by intracellular and extracellular Listeria monocytogenes. *Infect Immun* **67**: 131–9.

Mostowy, S., Bonazzi, M., Hamon, M.A., Tham, T.N., Mallet, A., Lelek, M., *et al.* (2010) Entrapment of intracytosolic bacteria by septin cage-like structures. *Cell Host Microbe* **8**: 433–44.

Mostowy, S., and Cossart, P. (2012) Septins: the fourth component of the cytoskeleton. *Nat Rev Mol Cell Biol* **13**: 183–94.

Mostowy, S., Danckaert, A., Tham, T.N., Machu, C., Guadagnini, S., Pizarro-Cerdá, J., and Cossart, P. (2009) Septin 11 restricts InlB-mediated invasion by Listeria. *J Biol Chem* **284**: 11613–21.

Mostowy, S., Nam Tham, T., Danckaert, A., Guadagnini, S., Boisson-Dupuis, S., Pizarro-Cerdá, J., and Cossart, P. (2009) Septins regulate bacterial entry into host cells. *PLoS One* **4**: e4196.

Mounier, J., Ryter, A., Coquis-Rondon, M., and Sansonetti, P.J. (1990) Intracellular and cell-to-cell spread of Listeria monocytogenes involves interaction with F-actin in the enterocytelike cell line Caco-2. *Infect Immun* **58**: 1048–58.

Mounkes, L.C., Kozlov, S. V., Rottman, J.N., and Stewart, C.L. (2005) Expression of an LMNA-N195K variant of A-type lamins results in cardiac conduction defects and death in mice. *Hum Mol Genet* **14**: 2167–2180.

Murata, T., Goshima, F., Nishizawa, Y., Daikoku, T., Takakuwa, H., Ohtsuka, K., *et al.* (2002) Phosphorylation of cytokeratin 17 by herpes simplex virus type 2 US3 protein kinase. *Microbiol Immunol* **46**: 707–19.

Murli, S., Watson, R.O., and Galán, J.E. (2001) Role of tyrosine kinases and the tyrosine phosphatase SptP in the interaction of Salmonella with host cells. *Cell Microbiol* **3**: 795–810.

Murray, E.G.D., Webb, R.A., and Swann, M.B.R. (1926) A disease of rabbits characterised by a large mononuclear leucocytosis, caused by a hitherto undescribed bacillus Bacterium monocytogenes (n.sp.). *J Pathol Bacteriol* **29**: 407–439.

Nava-Acosta, R., and Navarro-Garcia, F. (2013) Cytokeratin 8 is an epithelial cell receptor for Pet, a cytotoxic serine protease autotransporter of Enterobacteriaceae. *MBio* **4**: e00838-13.

Nikitas, G., Deschamps, C., Disson, O., Niault, T., Cossart, P., and Lecuit, M. (2011) Transcytosis of Listeria monocytogenes across the intestinal barrier upon specific targeting of goblet cell accessible E-cadherin. *J Exp Med* .

Noordhout, C.M. de, Devleesschauwer, B., Angulo, F.J., Verbeke, G., Haagsma, J., Kirk, M., *et al.* (2014) The global burden of listeriosis: A systematic review and meta-analysis. *Lancet Infect Dis* **14**: 1073–1082.

Núñez-Montero, K., Leclercq, A., Moura, A., Vales, G., Peraza, J., Pizarro-Cerdá, J., and Lecuit, M. (2018) Listeria costaricensis sp. nov. *Int J Syst Evol Microbiol* .

Nyfeldt, A., and others (1929) Etiologie de la mononucleose infectieuse. *CR Soc Biol* **101**: 590–591.

O'Brien, L.M., Walsh, E.J., Massey, R.C., Peacock, S.J., and Foster, T.J. (2002) Staphylococcus aureus clumping factor B (ClfB) promotes adherence to human type I cytokeratin 10: implications for nasal colonization. *Cell Microbiol* **4**: 759–70.

Olivé, M., Goldfarb, L., Dagvadorj, A., Sambuughin, N., Paulin, D., Li, Z., *et al.* (2003) Expression of the intermediate filament protein synemin in myofibrillar myopathies and other muscle diseases. *Acta Neuropathol* **106**: 1–7.

Olsen, K.N., Larsen, M.H., Gahan, C.G.M., Kallipolitis, B., Wolf, X.A., Rea, R., *et al.* (2005) The Dps-like protein Fri of Listeria monocytogenes promotes stress tolerance and intracellular multiplication in macrophage-like cells. *Microbiology* **151**: 925–33.

Omary, M.B., Coulombe, P.A., and McLean, W.H.I. (2004) Intermediate filament proteins and their associated diseases. *N Engl J Med* **351**: 2087–100.

Omary, M.B., Ku, N.-O., Tao, G.-Z., Toivola, D.M., and Liao, J. (2006) "Heads and tails" of intermediate filament phosphorylation: multiple sites and functional insights. *Trends Biochem Sci* **31**: 383–94.

Omary, M.B., Ku, N.-O., and Toivola, D.M. (2002) Keratins: guardians of the liver. *Hepatology* **35**: 251–7.

Organ, S.L., and Tsao, M.-S. (2011) An overview of the c-MET signaling pathway. *Ther Adv Med Oncol* **3**: S7–S19.

Oriolo, A.S., Wald, F. a, Canessa, G., and Salas, P.J.I. (2007) GCP6 binds to intermediate filaments: a novel function of keratins in the organization of microtubules in epithelial cells. *Mol Biol Cell* **18**: 781–794.

Orsi, R.H., Bakker, H.C. Den, and Wiedmann, M. (2010) Listeria monocytogenes lineages: Genomics, evolution, ecology, and phenotypic characteristics. *Int J Med Microbiol* **301**: 79–96.

Orsi, R.H., and Wiedmann, M. (2016) Characteristics and distribution of Listeria spp., including Listeria species newly described since 2009. *Appl Microbiol Biotechnol* **100**: 5273–87.

Osborne, S.E., and Brumell, J.H. (2017) Listeriolysin O: from bazooka to Swiss army knife. *Philos Trans R Soc Lond B Biol Sci* **372**: 20160222.

Oshima, R.G. (2007) Intermediate filaments: a historical perspective. *Exp Cell Res* **313**: 1981–94.

Osório, H., and Reis, C.A. (2013) Mass spectrometry methods for studying glycosylation in cancer. *Methods Mol Biol* **1007**: 301–16.

Pallari, H.-M., and Eriksson, J.E. (2006) Intermediate filaments as signaling platforms. *Sci STKE* **2006**: pe53.

Pan, X., Hobbs, R.P., and Coulombe, P. a (2012) The expanding significance of keratin intermediate filaments in normal and diseased epithelia. *Curr Opin Cell Biol* **25**: 47–56.

Pan, X., Yang, Y., and Zhang, J.-R. (2014) Molecular basis of host specificity in human pathogenic bacteria. *Emerg Microbes Infect* **3**: e23.

Paramio, J.M., Santos, M., and Jorcano, J.L. (2007) The ends of a conundrum? *J Cell Sci* **120**: 1145-7-8.

Paramio, J.M., Segrelles, C., Ruiz, S., and Jorcano, J.L. (2001) Inhibition of protein kinase B (PKB) and PKCzeta mediates keratin K10-induced cell cycle arrest. *Mol Cell Biol* **21**: 7449–59.

Paronetto, M.P. (2013) Ewing sarcoma protein: a key player in human cancer. *Int J Cell Biol* **2013**: 642853.

Paronetto, M.P., Minana, B., and Valcarcel, J. (2011) The Ewing sarcoma protein regulates DNA damage-induced alternative splicing. *Mol Cell* **43**: 353–368.

Parry, D. a D., Strelkov, S. V, Burkhard, P., Aebi, U., and Herrmann, H. (2007) Towards a molecular description of intermediate filament structure and assembly. *Exp Cell Res* **313**: 2204–16.

Paulin, D., and Li, Z. (2004) Desmin: a major intermediate filament protein essential for the structural integrity and function of muscle. *Exp Cell Res* **301**: 1–7.

Pentecost, M., Otto, G., Theriot, J. a, and Amieva, M.R. (2006) Listeria monocytogenes invades the epithelial junctions at sites of cell extrusion. *PLoS Pathog* **2**: e3.

Peraro, M.D., and Goot, F.G. Van Der (2016) Pore-forming toxins: Ancient, but never really out of fashion. *Nat Rev Microbiol* **14**: 77–92.

Percy, M.G., Karinou, E., Webb, A.J., and Gründling, A. (2016) Identification of a lipoteichoic acid glycosyltransferase enzyme reveals that gw-domain-containing proteins can be retained in the cell wall of Listeria monocytogenes in the absence of lipoteichoic acid or its modifications. *J Bacteriol* **198**: 2029–2042.

Pérez-Ortín, J.E. (2007) Genomics of mRNA turnover. *Briefings Funct Genomics Proteomics* **6**: 282–291.

Pérez-Ortín, J.E., Alepuz, P., Chávez, S., and Choder, M. (2013) Eukaryotic mRNA decay:

methodologies, pathways, and links to other stages of gene expression. *J Mol Biol* **425**: 3750–75.

Petrak, J., Ivanek, R., Toman, O., Cmejla, R., Cmejlova, J., Vyoral, D., *et al.* (2008) Déjà vu in proteomics. A hit parade of repeatedly identified differentially expressed proteins. *Proteomics* **8**: 1744–1749.

Pfeuffer, T., Goebel, W., Laubinger, J., Bachmann, M., and Kuhn, M. (2000) LaXp180, a mammalian ActA-binding protein, identified with the yeast two-hybrid system, co-localizes with intracellular Listeria monocytogenes. *Cell Microbiol* **2**: 101–114.

Pirie, J.H. (1940) THE GENUS LISTERELLA PIRIE. *Science* **91**: 383.

Pistor, S., Chakraborty, T., Niebuhr, K., Domann, E., and Wehland, J. (1994) The ActA protein of Listeria monocytogenes acts as a nucleator inducing reorganization of the actin cytoskeleton. *EMBO J* **13**: 758–63.

Pizarro-Cerdá, J., and Cossart, P. (2009) Listeria monocytogenes membrane trafficking and lifestyle: the exception or the rule? *Annu Rev Cell Dev Biol* **25**: 649–70.

Pizarro-Cerdá, J., Jonquières, R., Gouin, E., Vandekerckhove, J., Garin, J., and Cossart, P. (2002) Distinct protein patterns associated with Listeria monocytogenes InlA- or InlB-phagosomes. *Cell Microbiol* **4**: 101–15.

Pizarro-Cerdá, J., Kühbacher, A., and Cossart, P. (2012) Entry of Listeria monocytogenes in mammalian epithelial cells: an updated view. *Cold Spring Harb Perspect Med* **2**.

Podolin, P.L., and Prystowsky, M.B. (1991) The kinetics of vimentin RNA and protein expression in interleukin 2-stimulated T lymphocytes. *J Biol Chem* **266**: 5870–5.

Portnoy, D.A., Jacks, P.S., and Hinrichs, D.J. (1988) Role of hemolysin for the intracellular growth of Listeria monocytogenes. *J Exp Med* **167**: 1459–71.

Portnoy, D. a, Auerbuch, V., and Glomski, I.J. (2002) The cell biology of Listeria monocytogenes infection: the intersection of bacterial pathogenesis and cell-mediated immunity. *J Cell Biol* **158**: 409–14.

Quinlan, R.A., and Franke, W.W. (1982) Heteropolymer filaments of vimentin and desmin in vascular smooth muscle tissue and cultured baby hamster kidney cells demonstrated by chemical crosslinking. *Proc Natl Acad Sci U S A* **79**: 3452–6.

Radhakrishnan, G.K., and Splitter, G.A. (2012) Modulation of host microtubule dynamics by pathogenic bacteria. *Biomol Concepts* **3**: 571–580.

Radoshevich, L., and Cossart, P. (2017) Listeria monocytogenes: towards a complete picture of its physiology and pathogenesis. *Nat Rev Microbiol* **16**: 32–46.

Rafelski, S.M., and Theriot, J.A. (2006) Mechanism of polarization of Listeria monocytogenes surface protein ActA. *Mol Microbiol* **59**: 1262–79.

Rajabian, T., Gavicherla, B., Heisig, M., Müller-Altrock, S., Goebel, W., Gray-Owen, S.D., and Ireton, K. (2009) The bacterial virulence factor InlC perturbs apical cell junctions and promotes cell-to-cell spread of Listeria. *Nat Cell Biol* **11**: 1212–8.

Ramaswamy, V., Cresence, V.M., Rejitha, J.S., Lekshmi, M.U., Dharsana, K.S., Prasad, S.P., and Vijila, H.M. (2007) Listeria--review of epidemiology and pathogenesis. *J Microbiol Immunol Infect* **40**: 4–13.

Rapose, A., Lick, S.D., and Ismail, N. (2008) Listeria grayi bacteremia in a heart transplant recipient. *Transpl Infect Dis* **10**: 434–6.

Reches, A., Nachmani, D., Berhani, O., Duev-Cohen, A., Shreibman, D., Ophir, Y., *et al.* (2016) HNRNPR Regulates the Expression of Classical and Nonclassical MHC Class I Proteins. *J Immunol* **196**: 4967–4976.

Reichelt, J., Furstenberger, G., and Magin, T.M. (2004) Loss of keratin 10 leads to mitogen-activated protein kinase (MAPK) activation, increased keratinocyte turnover, and decreased tumor formation in mice. *J Invest Dermatol* **123**: 973–981.

Reis, O., Sousa, S., Camejo, A., Villiers, V., Gouin, E., Cossart, P., and Cabanes, D. (2010) LapB, a novel Listeria monocytogenes LPXTG surface adhesin, required for entry into eukaryotic cells and virulence. *J Infect Dis* **202**: 551–62.

Reniere, M.L., Whiteley, A.T., Hamilton, K.L., John, S.M., Lauer, P., Brennan, R.G., and Portnoy, D.A. (2015) Glutathione activates virulence gene expression of an intracellular pathogen. *Nature* **517**: 170–173.

Ribet, D., Hamon, M., Gouin, E., Nahori, M.-A., Impens, F., Neyret-Kahn, H., *et al.* (2010) Listeria monocytogenes impairs SUMOylation for efficient infection. *Nature* **464**: 1192–1195.

Rissland, O.S. (2017) The organization and regulation of mRNA-protein complexes. *Wiley Interdiscip Rev RNA* **8**: 1–17.

Roberts, B.J., Pashaj, A., Johnson, K.R., and Wahl, J.K. (2011) Desmosome dynamics in migrating epithelial cells requires the actin cytoskeleton. *Exp Cell Res* **317**: 2814–2822.

Robertson, H., Langdon, W.Y., Thien, C.B., and Bowtell, D.D. (1997) A c-Cbl yeast two hybrid screen reveals interactions with 14-3-3 isoforms and cytoskeletal components. *Biochem*

Biophys Res Commun **240**: 46–50.

Roccourt (1982) Roccourt, J., Grimont, F., Grimont, P.A.D., Seeliger, H.P.R., 1982. DNA relatedness among serovars of Listeria monocytogenes sensu lato. Current Microbiology. 7, 383-388. .

Rocourt, J., and Grimont, P.A.D. (1983) Listeria welshimeri sp. nov. and Listeria seeligeri sp. nov. *Int J Syst Evol Microbiol* **33**: 866–869.

Rogel, M.R., Jaitovich, A., and Ridge, K.M. (2010) The role of the ubiquitin proteasome pathway in keratin intermediate filament protein degradation. *Proc Am Thorac Soc* **7**: 71–6.

Rogers, H.W., Callery, M.P., Deck, B., and Unanue, E.R. (1996) Listeria monocytogenes induces apoptosis of infected hepatocytes. *J Immunol* **156**: 679–84.

Rolhion, N., and Cossart, P. (2017) How the study of Listeria monocytogenes has led to new concepts in biology. *Future Microbiol* **12**: 621–638.

Roth, W., Kumar, V., Beer, H.-D., Richter, M., Wohlenberg, C., Reuter, U., *et al.* (2012) Keratin 1 maintains skin integrity and participates in an inflammatory network in skin through interleukin-18. *J Cell Sci* **125**: 5269–5279.

Roundtree, I.A., Luo, G.-Z., Zhang, Z., Wang, X., Zhou, T., Cui, Y., *et al.* (2017) YTHDC1 mediates nuclear export of N6-methyladenosine methylated mRNAs. *Elife* **6**.

Roux, A., Loranger, A., Lavoie, J.N., and Marceau, N. (2017) Keratin 8/18 regulation of insulin receptor signaling and trafficking in hepatocytes through a concerted phosphoinositide-dependent Akt and Rab5 modulation. *FASEB J* fj.201700036R.

Runembert, I., Queffeulou, G., Federici, P., Vrtovsnik, F., Colucci-Guyon, E., Babinet, C., *et al.* (2002) Vimentin affects localization and activity of sodium-glucose cotransporter SGLT1 in membrane rafts. *J Cell Sci* **115**: 713–724.

Russell, D. (2004) Mechanical stress induces profound remodelling of keratin filaments and cell junctions in epidermolysis bullosa simplex keratinocytes. *J Cell Sci* **117**: 5233–5243.

Russo, B.C., Stamm, L.M., Raaben, M., Kim, C.M., Kahoud, E., Robinson, L.R., *et al.* (2016) Intermediate filaments enable pathogen docking to trigger type 3 effector translocation. *Nat Microbiol* **1**: 16025.

Saha, S.K., Choi, H.Y., Kim, B.W., Dayem, A.A., Yang, G.M., Kim, K.S., *et al.* (2017) KRT19 directly interacts with β-catenin/RAC1 complex to regulate NUMB-dependent NOTCH signaling pathway and breast cancer properties. *Oncogene* **36**: 332–349.

Sahlgren, C.M., Pallari, H.M., He, T., Chou, Y.H., Goldman, R.D., and Eriksson, J.E. (2006) A nestin scaffold links Cdk5/p35 signaling to oxidant-induced cell death. *EMBO J* **25**: 4808–4819.

Sajjan, U.S., Sylvester, F.A., and Forstner, J.F. (2000) Cable-piliated Burkholderia cepacia binds to cytokeratin 13 of epithelial cells. *Infect Immun* **68**: 1787–95.

Salas, P.J., Forteza, R., and Mashukova, A. (2016) Multiple roles for keratin intermediate filaments in the regulation of epithelial barrier function and apico-basal polarity. *Tissue Barriers* **8370**: e1178368.

Salton, M., Lerenthal, Y., Wang, S.Y., Chen, D.J., and Shiloh, Y. (2010) Involvement of Matrin 3 and SFPQ/NONO in the DNA damage response. *Cell Cycle* **9**: 1568–1576.

Samen, U., Eikmanns, B.J., Reinscheid, D.J., and Borges, F. (2007) The surface protein Srr-1 of Streptococcus agalactiae binds human keratin 4 and promotes adherence to epithelial HEp-2 cells. *Infect Immun* **75**: 5405–14.

Sanghvi-Shah, R., and Weber, G.F. (2017) Intermediate Filaments at the Junction of Mechanotransduction, Migration, and Development. *Front Cell Dev Biol* **5**: 1–19.

Santos, M., Paramio, J.S.M., Bravo, A., Ramirez, A., and Jorcano, J.L. (2002) The expression of keratin K10 in the basal layer of the epidermis inhibits cell proliferation and prevents skin tumorigenesis. *J Biol Chem* **277**: 19122–19130.

Sarkar, B., Lu, J.-Y., and Schneider, R.J. (2003) Nuclear import and export functions in the different isoforms of the AUF1/heterogeneous nuclear ribonucleoprotein protein family. *J Biol Chem* **278**: 20700–7.

Savijoki, K., Alvesalo, J., Vuorela, P., Leinonen, M., and Kalkkinen, N. (2008) Proteomic analysis of Chlamydia pneumoniae-infected HL cells reveals extensive degradation of cytoskeletal proteins. *FEMS Immunol Med Microbiol* **54**: 375–84.

Sax, C.M., Farrell, F.X., and Zehner, Z.E. (1989) Down-regulation of vimentin gene expression during myogenesis is controlled by a 5'-flanking sequence. *Gene* **78**: 235–42.

Schietke, R., Bröhl, D., Wedig, T., Mücke, N., Herrmann, H., and Magin, T.M. (2006) Mutations in vimentin disrupt the cytoskeleton in fibroblasts and delay execution of apoptosis. *Eur J Cell Biol* **85**: 1–10.

Schlech, W.F. (2000) Foodborne listeriosis. *Clin Infect Dis* **31**: 770–5.

Schlech, W.F., Lavigne, P.M., Bortolussi, R.A., Allen, A.C., Haldane, E. V, Wort, A.J., *et al.* (1983) Epidemic listeriosis--evidence for transmission by food. *N Engl J Med* **308**: 203–6.

Schnupf, P., Hofmann, J., Norseen, J., Glomski, I.J., Schwartzstein, H., and Decatur, A.L. (2006) Regulated translation of listeriolysin O controls virulence of Listeria monocytogenes. *Mol Microbiol* **61**: 999–1012.

Schoenberg, D.R., and Maquat, L.E. (2012) Regulation of cytoplasmic mRNA decay. *Nat Rev Genet* **13**: 246.

Schreiber, K.H., and Kennedy, B.K. (2013) When lamins go bad: Nuclear structure and disease. *Cell* **152**: 1365–1375.

Schweizer, J., Bowden, P.E., Coulombe, P.A., Langbein, L., Lane, E.B., Magin, T.M., *et al.* (2006) New consensus nomenclature for mammalian keratins. *J Cell Biol* **174**: 169–74.

Schwerk, J., and Savan, R. (2015) Translating the Untranslated Region. *J Immunol* **195**: 2963–2971.

Scortti, M., Monzó, H.J., Lacharme-Lora, L., Lewis, D.A., and Vázquez-Boland, J.A. (2007) The PrfA virulence regulon. *Microbes Infect* **9**: 1196–207.

Seeliger, H.P. (1981) [Nonpathogenic listeriae: L. innocua sp. n. (Seeliger et Schoofs, 1977) (author's transl)]. *Zentralbl Bakteriol Mikrobiol Hyg A* **249**: 487–93.

Seeliger, H.P.R., ROCOURT, J., SCHRETTENBRUNNER, A., GRIMONT, P.A.D., and JONES, D. (1984) Listeria ivanovii sp. nov. *Int J Syst Evol Microbiol* **34**: 336–337.

Seipelt, J., Liebig, H.D., Sommergruber, W., Gerner, C., and Kuechler, E. (2000) 2A proteinase of human rhinovirus cleaves cytokeratin 8 in infected HeLa cells. *J Biol Chem* **275**: 20084–9.

Seltmann, K., Roth, W., Kröger, C., Loschke, F., Lederer, M., Hüttelmaier, S., and Magin, T.M. (2012) Keratins Mediate Localization of Hemidesmosomes and Repress Cell Motility. *J Invest Dermatol* 181–190.

Seveau, S., Bierne, H., Giroux, S., Prévost, M.-C., Cossart, P., Préost, M.C., and Cossart, P. (2004) Role of lipid rafts in E-cadherin-- and HGF-R/Met--mediated entry of Listeria monocytogenes into host cells. *J Cell Biol* **166**: 743–53.

Seveau, S., Tham, T.N., Payrastre, B., Hoppe, A.D., Swanson, J. a, and Cossart, P. (2007) A FRET analysis to unravel the role of cholesterol in Rac1 and PI 3-kinase activation in the InlB/Met signalling pathway. *Cell Microbiol* **9**: 790–803.

Shen, Y., Naujokas, M., Park, M., and Ireton, K. (2000) InlB-dependent internalization of Listeria is mediated by the Met receptor tyrosine kinase. *Cell* **103**: 501–10.

Silva, L., Cliffe, A., Chang, L., and Knipe, D.M. (2008) Role for A-type lamins in herpesviral

DNA targeting and heterochromatin modulation. *PLoS Pathog* **4**.

Simone, L.E., and Keene, J.D. (2013) Mechanisms coordinating ELAV/Hu mRNA regulons. *Curr Opin Genet Dev* **23**: 35–43.

Smith, G.A., Marquis, H., Jones, S., Johnston, N.C., Portnoy, D.A., and Goldfine, H. (1995) The two distinct phospholipases C of Listeria monocytogenes have overlapping roles in escape from a vacuole and cell-to-cell spread. *Infect Immun* **63**: 4231–7.

Smith, G.A., Portnoy, D.A., and Theriot, J.A. (1995) Asymmetric distribution of the Listeria monocytogenes ActA protein is required and sufficient to direct actin-based motility. *Mol Microbiol* **17**: 945–51.

Snider, N.T., and Omary, M.B. (2014) Post-translational modifications of intermediate filament proteins: mechanisms and functions. *Nat Rev Mol Cell Biol* **15**: 163–177.

Sonnenberg, A., and Liem, R.K.H. (2007) Plakins in development and disease. *Exp Cell Res* **313**: 2189–2203.

Sousa, S., Cabanes, D., Bougnères, L., Lecuit, M., Sansonetti, P., Tran-Van-Nhieu, G., and Cossart, P. (2007) Src, cortactin and Arp2/3 complex are required for E-cadherin-mediated internalization of Listeria into cells. *Cell Microbiol* **9**: 2629–43.

Sousa, S., Cabanes, D., El-Amraoui, A., Petit, C., Lecuit, M., and Cossart, P. (2004) Unconventional myosin VIIa and vezatin, two proteins crucial for Listeria entry into epithelial cells. *J Cell Sci* **117**: 2121–30.

Souza Santos, M. de, and Orth, K. (2015) Subversion of the cytoskeleton by intracellular bacteria: lessons from Listeria, Salmonella and Vibrio. *Cell Microbiol* **17**: 164–173.

Stavru, F., Bouillaud, F., Sartori, A., Ricquier, D., and Cossart, P. (2011) Listeria monocytogenes transiently alters mitochondrial dynamics during infection. *Proc Natl Acad Sci U S A* **108**: 3612–7.

Stenzel, W., Soltek, S., Schlüter, D., and Deckert, M. (2004) The intermediate filament GFAP is important for the control of experimental murine Staphylococcus aureus-induced brain abscess and Toxoplasma encephalitis. *J Neuropathol Exp Neurol* **63**: 631–640.

Stone, M.R., O'Neill, A., Catino, D., and Bloch, R.J. (2005) Specific interaction of the actin-binding domain of dystrophin with intermediate filaments containing keratin 19. *Mol Biol Cell* **16**: 4280–93.

Stradal, T.E.B., and Costa, S.C.P. (2017) Type III Secreted Virulence Factors Manipulating Signaling to Actin Dynamics. *Curr Top Microbiol Immunol* **399**: 175–199.

Strelkov, S. V, Herrmann, H., and Aebi, U. (2003) Molecular architecture of intermediate filaments. *Bioessays* **25**: 243–51.

Stricher, F., Macri, C., Ruff, M., and Muller, S. (2013) HSPA8/HSC70 chaperone protein: structure, function, and chemical targeting. *Autophagy* **9**: 1937–54.

Styers, M.L., Kowalczyk, A.P., and Faundez, V. (2006) Architecture of the vimentin cytoskeleton is modified by perturbation of the GTPase ARF1. *J Cell Sci* **119**: 3643–54.

Styers, M.L., Salazar, G., Love, R., Peden, A.A., Kowalczyk, A.P., and Faundez, V. (2004) The endo-lysosomal sorting machinery interacts with the intermediate filament cytoskeleton. *Mol Biol Cell* **15**: 5369–82.

Suárez, M., González-Zorn, B., Vega, Y., Chico-Calero, I., and Vázquez-Boland, J. a (2001) A role for ActA in epithelial cell invasion by Listeria monocytogenes. *Cell Microbiol* **3**: 853–64.

Sun, H., Shen, Y., Dokainish, H., Holgado-Madruga, M., Wong, A., and Ireton, K. (2005) Host adaptor proteins Gab1 and CrkII promote InlB-dependent entry of Listeria monocytogenes. *Cell Microbiol* **7**: 443–57.

Suzuki, M., Iijima, M., Nishimura, A., Tomozoe, Y., Kamei, D., and Yamada, M. (2005) Two separate regions essential for nuclear import of the hnRNP D nucleocytoplasmic shuttling sequence. *FEBS J* **272**: 3975–87.

Swaminathan, B., and Gerner-Smidt, P. (2007) The epidemiology of human listeriosis. *Microbes Infect* **9**: 1236–43.

Szeverenyi, I., Cassidy, A.J., Chung, C.W., Lee, B.T.K., Common, J.E.A., Ogg, S.C., *et al.* (2008) The Human Intermediate Filament Database: comprehensive information on a gene family involved in many human diseases. *Hum Mutat* **29**: 351–360.

Tam, C., Mun, J.J., Evans, D.J., and Fleiszig, S.M.J. (2012) Cytokeratins mediate epithelial innate defense through their antimicrobial properties. *J Clin Invest* **122**: 3665–77.

Tamura, G.S., and Nittayajarn, A. (2000) Group B streptococci and other gram-positive cocci bind to cytokeratin 8. *Infect Immun* **68**: 2129–34.

Tang, P., Sutherland, C.L., Gold, M.R., and Finlay, B.B. (1998) Listeria monocytogenes invasion of epithelial cells requires the MEK-1/ERK-2 mitogen-activated protein kinase pathway. *Infect Immun* **66**: 1106–12.

Tao, G.-Z., Looi, K.S., Toivola, D.M., Strnad, P., Zhou, Q., Liao, J., *et al.* (2009) Keratins modulate the shape and function of hepatocyte mitochondria: a mechanism for protection from apoptosis. *J Cell Sci* **122**: 3851–5.

Teixeira, A.A.R., Vasconcelos, V.D.C.S. de, Colli, W., Alves, M.J.M., and Giordano, R.J. (2015) Trypanosoma cruzi Binds to Cytokeratin through Conserved Peptide Motifs Found in the Laminin-G-Like Domain of the gp85/Trans-sialidase Proteins. *PLoS Negl Trop Dis* **9**: e0004099.

Theisen, E., and Sauer, J.-D. (2016) Listeria monocytogenes and the Inflammasome: From Cytosolic Bacteriolysis to Tumor Immunotherapy. *Curr Top Microbiol Immunol* **397**: 133–60.

Tilney, L.G., and Portnoy, D. a (1989) Actin filaments and the growth, movement, and spread of the intracellular bacterial parasite, Listeria monocytogenes. *J Cell Biol* **109**: 1597–608.

Toivola, D.M., Nieminen, M.I., Hesse, M., He, T., Baribault, H., Magin, T.M., *et al.* (2001) Disturbances in hepatic cell-cycle regulation in mice with assembly-deficient keratins 8/18. *Hepatology* **34**: 1174–1183.

Toivola, D.M., Strnad, P., Habtezion, A., and Omary, M.B. (2010) Intermediate filaments take the heat as stress proteins. *Trends Cell Biol* **20**: 79–91.

Toivola, D.M., Tao, G.-Z., Habtezion, A., Liao, J., and Omary, M.B. (2005) Cellular integrity plus: organelle-related and protein-targeting functions of intermediate filaments. *Trends Cell Biol* **15**: 608–17.

Toledo-Arana, A., Dussurget, O., Nikitas, G., Sesto, N., Guet-Revillet, H., Balestrino, D., *et al.* (2009) The Listeria transcriptional landscape from saprophytism to virulence. *Nature* **459**: 950–956.

Tong, X., and Coulombe, P.A. (2006) Keratin 17 modulates hair follicle cycling in a TNF??-dependent fashion. *Genes Dev* **20**: 1353–1364.

Torraca, V., and Mostowy, S. (2016) Septins and Bacterial Infection. *Front Cell Dev Biol* **4**.

Travier, L., Guadagnini, S., Gouin, E., Dufour, A., Chenal-Francisque, V., Cossart, P., *et al.* (2013) ActA Promotes Listeria monocytogenes Aggregation, Intestinal Colonization and Carriage. *PLoS Pathog* **9**: e1003131.

Truchan, H.K., Cockburn, C.L., May, L.J., VieBrock, L., and Carlyon, J.A. (2016) Anaplasma phagocytophilum-Occupied Vacuole Interactions with the Host Cell Cytoskeleton. *Vet Sci* **3**.

Vadia, S., Arnett, E., Haghighat, A.-C., Wilson-Kubalek, E.M., Tweten, R.K., and Seveau, S. (2011) The pore-forming toxin listeriolysin O mediates a novel entry pathway of L. monocytogenes into human hepatocytes. *PLoS Pathog* **7**: e1002356.

Valencia-Gallardo, C.M., Carayol, N., and Tran Van Nhieu, G. (2015) Cytoskeletal mechanics during Shigella invasion and dissemination in epithelial cells. *Cell Microbiol* **17**: 174–82.

Valencia, R.G., Walko, G., Janda, L., Novacek, J., Mihailovska, E., Reipert, S., *et al.* (2013) Intermediate filament-associated cytolinker plectin 1c destabilizes microtubules in keratinocytes. *Mol Biol Cell* **24**: 768–784.

Vanhaesebroeck, B., Stephens, L., and Hawkins, P. (2012) PI3K signalling: the path to discovery and understanding. *Nat Rev Mol Cell Biol* **13**: 195–203.

Vasioukhin, V., Bowers, E., Bauer, C., Degenstein, L., and Fuchs, E. (2001) Desmoplakin is essential in epidermal sheet formation. *Nat Cell Biol* **3**: 1076–1085.

Vassar, R., Coulombe, P.A., Degenstein, L., Albers, K., and Fuchs, E. (1991) Mutant keratin expression in transgenic mice causes marked abnormalities resembling a human genetic skin disease. *Cell* **64**: 365–380.

Vassar, R., Rosenberg, M., Ross, S., Tyner, a, and Fuchs, E. (1989) Tissue-specific and differentiation-specific expression of a human K14 keratin gene in transgenic mice. *Proc Natl Acad Sci U S A* **86**: 1563–7.

Vázquez-Boland, J.A., Kuhn, M., Berche, P., Chakraborty, T., Domínguez-Bernal, G., Goebel, W., *et al.* (2001) Listeria pathogenesis and molecular virulence determinants. *Clin Microbiol Rev* **14**: 584–640.

Veiga, E., and Cossart, P. (2005) Listeria hijacks the clathrin-dependent endocytic machinery to invade mammalian cells. *Nat Cell Biol* **7**: 894–900.

Veiga, E., Guttman, J. a, Bonazzi, M., Boucrot, E., Toledo-Arana, A., Lin, A.E., *et al.* (2007) Invasive and adherent bacterial pathogens co-Opt host clathrin for infection. *Cell Host Microbe* **2**: 340–51.

Vijayaraj, P., Kröger, C., Reuter, U., Windoffer, R., Leube, R.E., and Magin, T.M. (2009) Keratins regulate protein biosynthesis through localization of GLUT1 and -3 upstream of AMP kinase and Raptor. *J Cell Biol* **187**: 175–84.

Viswanathan, V.K., Lukic, S., Koutsouris, A., Miao, R., Muza, M.M., and Hecht, G. (2004) Cytokeratin 18 interacts with the enteropathogenic Escherichia coli secreted protein F (EspF) and is redistributed after infection. *Cell Microbiol* **6**: 987–97.

Wagner, M., Trost, A., Hintner, H., Bauer, J.W., and Onder, K. (2013) Imbalance of intermediate filament component keratin 14 contributes to increased stress signalling in epidermolysis bullosa simplex. *Exp Dermatol* **22**: 292–294.

Walko, G., Vukasinovic, N., Gross, K., Fischer, I., Sibitz, S., Fuchs, P., *et al.* (2011) Targeted proteolysis of plectin isoform 1a accounts for hemidesmosome dysfunction in mice mimicking

the dominant skin blistering disease EBS-ogna. *PLoS Genet* **7**.

Wallace, L., Roberts-Thompson, L., and Reichelt, J. (2012) Deletion of K1/K10 does not impair epidermal stratification but affects desmosomal structure and nuclear integrity. *J Cell Sci* **125**: 1750–8.

Wang, J., Huo, K., Ma, L., Tang, L., Li, D., Huang, X., *et al.* (2011) Toward an understanding of the protein interaction network of the human liver. *Mol Syst Biol* **7**: 536.

Wang, Q., Griffin, H., Southern, S., Jackson, D., Martin, A., McIntosh, P., *et al.* (2003) Functional Analysis of the Human Papillomavirus Type 16 E1 E4 Protein Provides a Mechanism for In Vivo and In Vitro Keratin Filament Reorganization. *J Virol* **78**: 821–833.

Wang, Y., Sun, D., and Liu, D. (2011) Tumor suppression by RNA from C/EBPβ 3'UTR through the inhibition of protein kinase Cε activity. *PLoS One* **6**: e16543.

Watson, E.D., Geary-Joo, C., Hughes, M., and Cross, J.C. (2007) The Mrj co-chaperone mediates keratin turnover and prevents the formation of toxic inclusion bodies in trophoblast cells of the placenta. *Development* **134**: 1809–1817.

Weerasinghe, S.V.W., Ku, N.-O., Altshuler, P.J., Kwan, R., and Omary, M.B. (2014) Mutation of caspase-digestion sites in keratin 18 interferes with filament reorganization, and predisposes to hepatocyte necrosis and loss of membrane integrity. *J Cell Sci* **127**: 1464–75.

Welch, M.D., Iwamatsu, A., and Mitchison, T.J. (1997) Actin polymerization is induced by Arp2/3 protein complex at the surface of Listeria monocytogenes. *Nature* **385**: 265–9.

Welch, M.D., Rosenblatt, J., Skoble, J., Portnoy, D.A., and Mitchison, T.J. (1998) Interaction of human Arp2/3 complex and the Listeria monocytogenes ActA protein in actin filament nucleation. *Science* **281**: 105–8.

Weller, D., Andrus, A., Wiedmann, M., and Bakker, H.C. den (2015) Listeria booriae sp. nov. and Listeria newyorkensis sp. nov., from food processing environments in the USA. *Int J Syst Evol Microbiol* **65**: 286–92.

Windoffer, R., Beil, M., Magin, T.M., and Leube, R.E. (2011) Cytoskeleton in motion: the dynamics of keratin intermediate filaments in epithelia. *J Cell Biol* **194**: 669–78.

Windoffer, R., Kölsch, A., Wöll, S., and Leube, R.E. (2006) Focal adhesions are hotspots for keratin filament precursor formation. *J Cell Biol* **173**: 341–8.

Wu, X., and Brewer, G. (2012) The regulation of mRNA stability in mammalian cells: 2.0. *Gene* **500**: 10–21.

Xiao, W., Adhikari, S., Dahal, U., Chen, Y.-S., Hao, Y.-J., Sun, B.-F., *et al.* (2016) Nuclear m(6)A Reader YTHDC1 Regulates mRNA Splicing. *Mol Cell* **61**: 507–519.

Yarosh, C.A., Iacona, J.R., Lutz, C.S., and Lynch, K.W. (2015) PSF: Nuclear busy-body or nuclear facilitator? *Wiley Interdiscip Rev RNA* **6**: 351–367.

Yoneda, K., Furukawa, T., Zheng, Y.J., Momoi, T., Izawa, I., Inagaki, M., *et al.* (2004) An Autocrine/Paracrine Loop Linking Keratin 14 Aggregates to Tumor Necrosis Factor α-mediated Cytotoxicity in a Keratinocyte Model of Epidermolysis Bullosa Simplex. *J Biol Chem* **279**: 7296–7303.

Yoshikawa, Y., Ogawa, M., Hain, T., Yoshida, M., Fukumatsu, M., Kim, M., *et al.* (2009) Listeria monocytogenes ActA-mediated escape from autophagic recognition. *Nat Cell Biol* **11**: 1233–40.

Yuan, A., Sasaki, T., Kumar, A., Peterhoff, C.M., Rao, M. V, Liem, R.K., *et al.* (2012) Peripherin is a subunit of peripheral nerve neurofilaments: implications for differential vulnerability of CNS and peripheral nervous system axons. *J Neurosci* **32**: 8501–8.

Zakaryan, R.P., and Gehring, H. (2006) Identification and Characterization of the Nuclear Localization/Retention Signal in the EWS Proto-oncoprotein. *J Mol Biol* **363**: 27–38.

Zenewicz, L.A., and Shen, H. (2007) Innate and adaptive immune responses to Listeria monocytogenes: a short overview. *Microbes Infect* **9**: 1208–15.

Zhang, D., Paley, A.J., and Childs, G. (1998) The transcriptional repressor, ZFM1 interacts with and modulates the ability of EWS to activate transcription. *J Biol Chem* **273**: 18086–18091.

Zhang, Z., and Carmichael, G.G. (2001) The fate of dsRNA in the Nucleus: A p54nrb-containing complex mediates the nuclear retention of promiscuously A-to-I edited RNAs. *Cell* **106**: 465–475.

Zhong, B., Zhou, Q., Toivola, D.M., Tao, G.-Z., Resurreccion, E.Z., and Omary, M.B. (2004) Organ-specific stress induces mouse pancreatic keratin overexpression in association with NF-kappaB activation. *J Cell Sci* **117**: 1709–19.

Zhong, Q., An, X., Yang, Y.X., Hu, H.D., Ren, H., and Hu, P. (2014) Keratin 8 is involved in hepatitis B virus replication. *J Med Virol* **86**: 687–694.

Zhou, Q., Ji, X., Chen, L., Greenberg, H.B., Lu, S.C., and Omary, M.B. (2005) Keratin mutation primes mouse liver to oxidative injury. *Hepatology* **41**: 517–25.

Zou, T., Rao, J.N., Liu, L., Xiao, L., Yu, T.-X., Jiang, P., *et al.* (2010) Polyamines Regulate the Stability of JunD mRNA by Modulating the Competitive Binding of Its 3' Untranslated Region

to HuR and AUF1. *Mol Cell Biol* **30**: 5021–5032.

Zou, Y., He, L., and Huang, S.H. (2006) Identification of a surface protein on human brain microvascular endothelial cells as vimentin interacting with Escherichia coli invasion protein IbeA. *Biochem Biophys Res Commun* **351**: 625–630.

Zuiderweg, E.R.P., Hightower, L.E., and Gestwicki, J.E. (2017) The remarkable multivalency of the Hsp70 chaperones. *Cell Stress Chaperones* **22**: 173–189.

CHAPTER VI – ANNEX

This chapter includes a copy of the **published version** of the following publication:

Almeida, M.T., Mesquita, F.S., **Cruz, R.**, Osório, H., Custódio, R., Brito, C., Vingadassalom, D., Martins, M., Leong, J.M., Holden, D.W., Cabanes, D., and Sousa, S. (2015) Src-dependent tyrosine phosphorylation of non-muscle myosin heavy chain-IIA restricts Listeria monocytogenes cellular infection. *J Biol Chem* 290: 8383–95.

This chapter also includes a copy of the **accepted version** of the following publication:

Cruz, R., Castro, I.P., Almeida, M.T., Moreira, A., Cabanes, D., and Sousa, S. (2018) Epithelial keratins modulate cMet expression and signalling and promote InlB-mediated *Listeria monocytogenes* infection of HeLa cells. *Front Cell Infect Microbiol.* doi: 10.3389/fcimb.2018.00146. (Publication accepted and manuscript production ongoing)

THE JOURNAL OF BIOLOGICAL CHEMISTRY VOL. 290, NO. 13, pp. 8383–8395, March 27, 2015
© 2015 by The American Society for Biochemistry and Molecular Biology, Inc. Published in the U.S.A.

Src-dependent Tyrosine Phosphorylation of Non-muscle Myosin Heavy Chain-IIA Restricts *Listeria monocytogenes* Cellular Infection*

Received for publication, July 11, 2014, and in revised form, January 15, 2015 Published, JBC Papers in Press, January 29, 2015, DOI 10.1074/jbc.M114.591313

Maria Teresa Almeida[‡§¶1], Francisco S. Mesquita[‡§‖2], Rui Cruz[‡§¶1], Hugo Osório[‡], Rafael Custódio[‡§], Cláudia Brito[‡§¶], Didier Vingadassalom[‡‡], Mariana Martins[‡§], John M. Leong[‡‡3], David W. Holden[‖], Didier Cabanes[‡§4], and Sandra Sousa[‡§5]**

*From the [‡]Instituto de Investigação e Inovação em Saúde, Universidade do Porto, 4200 Porto, Portugal, the [§]Group of Molecular Microbiology, Instituto de Biologia Molecular e Celular, Universidade do Porto, 4150-180 Porto, Portugal, the [¶]Instituto de Ciências Biomédicas Abel Salazar, Universidade do Porto, 4050-313 Porto, Portugal, the [‖]Medical Research Council, Centre for Molecular Bacteriology and Infection, Imperial College, London, London SW7 2AZ, United Kingdom, the **Institute of Molecular Pathology and Immunology, University of Porto, 4200-465 Porto, Portugal, and the [‡‡]Department of Molecular Genetics and Microbiology, University of Massachusetts Medical School, Worcester, Massachusetts 01655*

Background: Non-muscle myosin IIA is involved in force generation, movement, and membrane reshaping. Its activity is regulated by phosphorylation of the light chain.
Results: NMHC-IIA head domain is tyrosine-phosphorylated by Src and modulates *Listeria* intracellular levels.
Conclusion: Tyrosine phosphorylation of NMHC-IIA affects the outcome of infection.
Significance: This novel post-translational modification of NMHC-IIA possibly affects its functions.

Bacterial pathogens often interfere with host tyrosine phosphorylation cascades to control host responses and cause infection. Given the role of tyrosine phosphorylation events in different human infections and our previous results showing the activation of the tyrosine kinase Src upon incubation of cells with *Listeria monocytogenes*, we searched for novel host proteins undergoing tyrosine phosphorylation upon *L. monocytogenes* infection. We identify the heavy chain of the non-muscle myosin IIA (NMHC-IIA) as being phosphorylated in a specific tyrosine residue in response to *L. monocytogenes* infection. We characterize this novel post-translational modification event and show that, upon *L. monocytogenes* infection, Src phosphorylates NMHC-IIA in a previously uncharacterized tyrosine residue (Tyr-158) located in its motor domain near the ATP-binding site. In addition, we found that other intracellular and extracellular bacterial pathogens trigger NMHC-IIA tyrosine phosphorylation. We demonstrate that NMHC-IIA limits intracellular levels of *L. monocytogenes*, and this is dependent on the phosphorylation of Tyr-158. Our data suggest a novel mechanism of regulation of NMHC-IIA activity relying on the phosphorylation of Tyr-158 by Src.

Listeria monocytogenes is a human intracellular food-borne bacterial pathogen that causes serious disease in immunocompromised individuals. Within the host it finds suitable replication niches in the liver and spleen, disseminates, and then can reach the central nervous system. In pregnant women, *L. monocytogenes* targets the fetus, eliciting fetal infection and abortions (1). The ability of *L. monocytogenes* to cause disease relies on its capacity to invade nonphagocytic cells, replicate therein, and spread to the entire organism overcoming the intestinal, blood-brain, and fetoplacental barriers (2). Through the expression of bacterial factors, *L. monocytogenes* establishes a cross-talk with host cells favoring the progression of the cellular infection (3). In epithelial cells, *L. monocytogenes* invasion is mainly driven by the bacterial surface proteins InlA and InlB that bind E-cadherin and c-Met, respectively, at the surface of host cells (4, 5). This engagement of host cell receptors triggers tyrosine phosphorylation-mediated signaling, resulting in the local activation of the Arp2/3 complex that initiates actin polymerization at the site of *L. monocytogenes* attachment (6, 7), causing membrane invagination that supports bacterial entry. InlB interaction with the receptor tyrosine kinase c-Met stimulates its autophosphorylation and induces the tyrosine phosphorylation and recruitment of adaptor proteins and the activation of phospho-

* This work was supported by the Fundo Europeu de Desenvolvimento Regional (FEDER) through the Operational Competitiveness Programme (COMPETE), by National Funds through Fundação para a Ciência e Tecnologia (FCT) under Project PTDC/BIA-BCM/100088/2008FCOMP-01-0124-FEDER-008860 and ERANet-Pathogenomics LISTRESS ERA-PTG/0003/2010, Project NORTE-07-0124-FEDER-000002-Host-Pathogen Interactions, co-funded by Programa Operacional Regional do Norte (ON.2-O Novo Norte), under the Quadro de Referência Estratégico Nacional, through FEDER, by FCT, and by a Research Grant 2014 by the European Society of Clinical Microbiology and Infectious Diseases (ESCMID) (to S. S.). M. T. A. received a Travel Grant from Boehringer Ingelheim Fonds.
[1] Recipients of Fundação para a Ciência e Tecnologia Doctoral Fellowships BD/43352/2008 and BD/90607/2012.
[2] Recipient of EMBO Long Term Post-doctoral Fellowship EMBO ALTF 864-2012.
[3] Present address: Sackler School of Graduate Biomedical Sciences, Tufts University School of Medicine, Boston, MA 02111.
[4] To whom correspondence may be addressed: Group of Molecular Microbiology, Instituto de Biologia Molecular e Celular, Rua do Campo Alegre 823, 4150-180 Porto, Portugal. Tel.: 351226074907; Fax: 351226099157; E-mail: didier@ibmc.up.pt.
[5] Supported by Ciência 2008 and FCT Investigator Programs COMPETE, POPH, and FCT. To whom correspondence may be addressed: Group of Molecular Microbiology, Instituto de Biologia Molecular e Celular, Rua do Campo Alegre 823, 4150-180 Porto, Portugal. Tel.: 351226074907; Fax: 351226099157; E-mail: srsousa@ibmc.up.pt.

Downloaded from http://www.jbc.org/ at UNIVERSIDADE DO PORTO on October 8, 2015

inositide 3-kinase (PI3K) (5, 8, 9). Phosphatidylinositol 3,4,5-triphosphate generated by PI3K accumulates at the cell membrane during *L. monocytogenes* infection (8) and plays a crucial role in the recruitment of molecules controlling actin polymerization, such as Rac1 and WAVE2 (6, 10–12). In turn, InlA binding to E-cadherin induces the activation of Src tyrosine kinase that subsequently phosphorylates cortactin, E-cadherin, and the clathrin heavy chain (7, 13, 14). Although cortactin and clathrin tyrosine phosphorylations are critical events for actin polymerization and recruitment at the *L. monocytogenes* entry site (7, 13), E-cadherin phosphorylation leads to its ubiquitination, internalization, and further degradation (14). The combined action of these events leads to the internalization the *L. monocytogenes* into epithelial cells.

In this study we aimed to identify new cellular proteins undergoing tyrosine phosphorylation in response to *L. monocytogenes* infection, and we address whether such post-translational modification would regulate cellular infection. The tyrosine-phosphorylated proteins were recovered from *L. monocytogenes*-infected epithelial cells and subjected to mass spectrometry identification. We identified the non-muscle myosin heavy chain IIA (NMHC-IIA)[6] as one of the enriched tyrosine-phosphorylated proteins recovered upon *L. monocytogenes* infection.

NMHC-IIA is an actin-binding protein with motor and contractile properties, involved in cellular processes requiring force generation, cell movement, and membrane reshaping (15). In infection, NMHC-IIA is critical for viral entry (16, 17) and supports invasion (18) and dissemination (19) of various bacteria. Although the serine/threonine phosphorylation of the regulatory light chain is a well known mechanism to regulate non-muscle myosin IIA activity (15), our knowledge on the regulation of the heavy chain is limited, and NMHC-IIA tyrosine phosphorylation has never been characterized. Here, we show that NMHC-IIA undergoes tyrosine phosphorylation in response to several bacterial pathogens. Our data indicate that upon *L. monocytogenes* cellular infection NMHC-IIA was phosphorylated in tyrosine residue 158 by the host Src kinase. In the presence of blebbistatin, a chemical inhibitor of myosin II activity, the percentage of cells showing *L. monocytogenes*-associated actin foci was increased and correlated with higher levels of intracellular *L. monocytogenes*. In addition, increased numbers of intracellular *L. monocytogenes* were also found in cells depleted of NMHC-IIA as well as in conditions where NMHC-IIA tyrosine phosphorylation is prevented. These results show the involvement of NMHC-IIA in *L. monocytogenes* infection and point to the regulatory role of its phosphorylation in tyrosine 158, which could affect NMHC-IIA activity. Our findings describe a novel post-translational modification of NMHC-IIA with important implications in bacterial infection. Taking into account the central role of NMHC-IIA in key cell biology processes, our data also suggest the existence of a new mechanism of NMHC-IIA regulation that could be of critical importance in the canonical functions of non-muscle myosin IIA.

[6] The abbreviations used are: NMHC-IIA, non-muscle myosin heavy chain IIA; NMHC-IIB, non-muscle myosin heavy chain IIB; WCL, whole cell lysate; m.o.i., multiplicity of infection; NI, noninfected; IP, immunoprecipitation; NT, nontreated; Ctr, control; MLCK, myosin light chain kinase; EPEC, enteropathogenic *E. coli*; EHEC, enterohaemorrhagic *E. coli*; KSHV, Kaposi sarcoma-associated herpesvirus.

TABLE 1
List of bacterial strains used in this study and the corresponding growth conditions
BHI is brain-heart infusion.

Bacterial strains	Growth media	*T*
		°C
L. monocytogenes (EGDe)	BHI (Difco)	37
L. innocua (CLIP 11262)	BHI	37
L. innocua-inlB	BHI erythromycin 5 μg/ml	37
E. coli DH5α	LB (Difco)	37
EPEC	LB ampicillin 100 μg/ml (Amp100)	37
EHEC	LB	37
E. coli K12-*inv*	LB Amp100	37
E. coli K12-Δ*inv*	LB Amp100	37
Y. pseudotuberculosis	LB Amp100	26

EXPERIMENTAL PROCEDURES

Bacterial Strains and Cell Lines—*Listeria* and *Escherichia coli* strains were grown aerobically at 37 °C, with shaking, in brain-heart infusion and lysogeny broth (LB) media, respectively. *Yersinia* was grown aerobically at 26 °C, with shaking, in LB media. When required, antibiotics were added to growth media. Details are provided in Table 1. Caco-2 cells (ATCC HTB-37) were cultivated in minimum Eagle's medium with L-glutamine, supplemented with nonessential amino acids, sodium pyruvate, and 20% fetal bovine serum (FBS). HeLa (ATCC CCL-2), HEK293 (ATCC CRL-1573), and COS-7 (ATCC CRL-1651) cells were cultivated in DMEM with glucose (4.5 g/liter) and L-glutamine, supplemented with 10% FBS. Cells were maintained at 37 °C in a 5% CO_2-enriched atmosphere. Cell culture media and supplements were from Lonza.

Plasmids, Antibodies, and Reagents—Plasmids used are listed in Table 2. Plasmids GFP-NMHC-IIA-Y158F and GFP-NMHC-IIA-Y190F were generated using GFP-NMHC-IIA-WT from Addgene (20) and the QuikChange XL site-directed mutagenesis kit (Agilent Technologies). For NMHC-IIA rescue assays, a plasmid encoding siRNA-resistant GFP-NMHC-IIA-WT transcripts was generated. Oligonucleotide sequences are provided in Table 3. Antibodies are listed in Table 4. F-actin was labeled with Alexa Fluor 647- or 555-conjugated phalloidin (Invitrogen). Chemical inhibitors Y-26732 (Sigma), blebbistatin, and PP1 (Calbiochem) were handled as recommended. FluoSpheres carboxylate-modified microspheres were from Invitrogen (F-8814).

Determination of Intracellular Bacteria—The levels of intracellular bacteria were determined as described (21). When indicated, cells were incubated with serum-free medium containing blebbistatin, PP1, or DMSO. Cells were challenged with prewashed *L. monocytogenes* at a multiplicity of infection (m.o.i.) of 50 or with *Yersinia pseudotuberculosis* (m.o.i. 10) for 60 min, treated with 20 μg/ml gentamicin for 90 min, washed in PBS, and lysed with 0.2% Triton X-100, and serial dilutions were plated for CFU counting. For immunofluorescence scoring, cells infected with *L. monocytogenes* (m.o.i. 50) were treated with 100 μg/ml gentamicin for 10 min and washed with 20 μg/ml gentamicin prior fixation.

Immunoprecipitation Assays—HeLa or Caco-2 cells grown until confluence were washed twice with warm phosphate-

Downloaded from http://www.jbc.org/ at UNIVERSIDADE DO PORTO on October 8, 2015

TABLE 2
List of plasmids used in this study

Plasmid	Description	Source
GFP-NMHCIIA-WT	pEGFP-C3:CMV-GFP-NMHC IIA	Addgene (no. 11347)
GFP-NMHCIIA-Y158F	pEGFP-C3:CMV-GFP-NMHC IIA (Y158F)	This study
GFP-NMHCIIA-Y190F	pEGFP-C3:CMV-GFP-NMHC IIA (Y190F)	This study
GFP-NMHCIIA-WT-siRes	pEGFP-C3:CMV-GFP-NMHC IIA siRNA resistant	This study
Src-KD	pcDNA3-Src kinase-dead (A430V)	S. J. Parsons, University of Virginia

TABLE 3
List of antibodies used in this study
WB is Western blot, and IF is immunofluorescence.

Antigen	Species	Applications	Reference	Source
Phosphotyrosine	Mouse	IP (1:300) WB (1:1000)	4G10, 05-321	Millipore
Phosphotyrosine	Mouse	WB (1:1000)	PY20, P4110	Sigma
Actin	Mouse	WB (1:5000)	AC-15, A5441	Sigma
NMHC-IIA	Mouse	IF (1:1000)	ab55456	Abcam
GFP	Mouse	IP (1:100) WB (1:500)	B2, sc-9996	Santa Cruz Biotechnology
NMHC-IIA pY158	Rabbit	WB (1:500)	AP3775a	Abgent
Listeria	Rabbit	IF (1:200)	ab35132	Abcam
NMHC-IIA	Rabbit	IP (1:100) WB (1:5000)	M8064	Sigma
c-Src	Rabbit	WB (1:500)	GD11, 05-184	Millipore
c-Src	Rabbit	WB (1:1000)	ab109381	Abcam
NMHC-IIB	Rabbit	WB (1:1000)	M7939	Sigma-Aldrich
Anti-rabbit or anti-mouse HRP	Goat	WB	BI2413C BI2407	PARIS
Anti-rabbit or anti-mouse Alexa Fluor 488	Goat	IF	A11034 A11001	Invitrogen
Anti-rabbit or anti-mouse Cy3	Goat	IF	111-165-144 115-165-146	Jackson ImmunoResearch
Anti-rabbit or anti-mouse Cy5	Goat	IF	111-175-144 115-175-146	Jackson ImmunoResearch

TABLE 4
Sequences of siRNA duplexes, shRNAs, and primers used in this study

siRNA duplexes			
Name		**Oligo Sequence (5'-3')**	**Source**
NMHCIIA-si#1 (Pool of 3 siRNAs)	A	Sense: CAUCUACUCUGAAGAGAUUtt	Santa Cruz Biotechnology (#sc-61120)
		Antisense: AAUCUCUUCAGAGUAGAUGtt	
	B	Sense: GAAGAUCAAUCCAUCUUGUtt	
		Antisense: ACAAGAUGGAUUGAUCUUCtt	
	C	Sense: CCAAAGAGAACGAGAAGAAtt	
		Antisense: UUCUUCUCGUUCUCUUUGGtt	
NMHCIIA-si#2		Sense: GAAGAUCAAUCCAUCUUGUtt	Santa Cruz Biotechnology (#sc-61120B)
		Antisense: ACAAGAUGGAUUGAUCUUCtt	
NMHCIIB-si		Sense: GCAAUACAGUGGGACAGUUtt	Sigma-Aldrich (#00072460)
		Antisense: AACUGUCCCACUGUAUUGCtt	
shRNAs Sequence (5'-3') and Source			
Src	CCGGGTGGCTTACTACTCCAAACATCTCGAGATGTTTGGAGTAGTAAGCCACTTTTT **Sigma-Aldrich (TRCN0000023597)**		
Control	CCGGGCGCGATAGCGCTAATAATTTCTCGAGAAATTATTAGCGCTATCGCGCTTTTT **Sigma-Aldrich (SHC016)**		
Primers sequences (5'-3')			
NMHC-IIA-Y158F	Fw: CTATGCCATCACAGACACCGCCTTCAGGAGTATGATGCAAGAC		
	Rev: GTCTTGCATCATACTCCTGAAGGCGGTGTCTGTGATGGCATAG		
NMHC-IIA-Y190F	Fw: CACCAAGAAGGTCATCCAGTTTCTGGCGTACGTGGCGTCTCG		
	Rev: CGAGGACGCCACGTACGCCAGAACTGGATGACCTTCTTGGTG		
NMHC-IIA-WT-siRes	Fw: GATGCAAGACCGAGAGGATCAATCCATACTGTGCACTGGTGAATC		
	Rev: GATTCACCAGTGCACAGTATGGATTGATCCTCTCGGTCTTGCATC		
c-Src	Fw: CTGTTCGGAGGCTTCAACTC		
	Rev: CCACCAGTCTCCCTCTGTGT		
HPRT1	Fw: GGCGTCGTGATTAGTGATG		
	Rev: CACCCTTTCCAAATCCTCAG		

buffered saline (PBS), serum-starved (5 h), and left noninfected (NI) or incubated with pre-washed *L. monocytogenes* (21) at m.o.i. 200 for different periods of time or with *E. coli* (EPEC, EHEC, or K12-*inv* strains) at m.o.i. 200 for 4 h as described (22). When indicated, cells were treated with 10 μM PP1 or 50 μM Y-27632 30 min before infection. After washing twice with ice-

Downloaded from http://www.jbc.org/ at UNIVERSIDADE DO PORTO on October 8, 2015

cold PBS, cells were lysed in 1 ml of lysis buffer (1% IgePal CA-630 (Sigma), 50 mM Tris, pH 7.5, 150 mM NaCl, 2 mM EDTA, 1 mM 4-(2-aminoethyl)benzenesulfonyl fluoride (Interchim), PhosSTOP, and cOmplete Protease Inhibitor Mixture (Roche Applied Science)), and lysates were recovered after centrifugation (15,000 × *g*, 15 min, 4 °C). Cell lysates (500 μg) were incubated overnight (4 °C) with 1 μg of anti-phosphotyrosine 4G10 or 5 μg of anti-NMHC-IIA antibodies. Immune complexes were captured with 50 μl of Pure Proteome protein A or G magnetic beads (Millipore). Immunoprecipitated fractions were resolved by SDS-PAGE, and gels were silver-stained using the ProteoSilver™ plus silver staining kit (Sigma) or processed for immunoblotting. For kinase assay, HEK293 cells were harvested and lysed 24 h post-transfection, GFP fusion proteins were immunoprecipitated with anti-GFP-conjugated agarose beads (sc-9996 AC, Santa Cruz Biotechnology) and eluted in 0.2 M glycine, pH 2.5.

Protein Identification by Mass Spectrometry (MS)—Protein identification was performed by MALDI TOF/TOF mass spectrometry as described (23). Protein bands were excised from SDS-polyacrylamide gels, reduced with dithiothreitol, alkylated with iodoacetamide, and in-gel digested with trypsin. Peptides were extracted, desalted, concentrated using Ziptips (Millipore), crystallized onto a MALDI sample plate, and analyzed using a 4700 Proteomics Analyzer MALDI-TOF/TOF (Applied Biosystems). Peptidic mass spectra were acquired in reflector positive mode at a 700–4000 *m*/*z* mass window, and proteins were identified by peptide mass fingerprint using Mascot software (Matrix Science, UK) integrated in the GPS Explorer software (ABSCIEX) and searched against the SwissProt/UniProt *Homo sapiens* protein sequence database. The maximum error tolerance was 35 ppm, and up to two missed cleavages were allowed.

Phosphopeptide Analysis by MS—Bands corresponding to NMHC-IIA, from anti-NMHC-IIA IPs of NI and *L. monocytogenes*-infected HeLa cells, were processed as described above. Phosphopeptides were selectively enriched by titanium dioxide chromatography (TiO2 Mag-Sepharose, GE Healthcare). MALDI matrix used was 9 mg/ml 2′,4′,6′-trihydroxyacetophenone monohydrate, 5 mg/ml diammonium citrate, in 50:50, v/v, water/acetonitrile. Mass spectra were acquired in a 4800 Plus MALDI TOF/TOF analyzer mass spectrometer (AB SCIEX) both in reflector negative and MS/MS modes.

Immunoblotting—Proteins were resolved in SDS-polyacrylamide gels and transferred onto Nitrocellulose membranes (Hybond ECL, GE Healthcare). Membranes were blocked with 5% skimmed milk in buffer A (150 mM NaCl, 20 mM Tris-HCl, pH 7.4, and 0.1% Triton X-100) for 1 h at room temperature or overnight at 4 °C. Primary and secondary antibodies were diluted in 2.5% skimmed milk in buffer A. Membranes used for anti-phosphotyrosine detection were blocked with Western Blocker solution (Sigma), also used to dilute primary and secondary antibodies.

Immunofluorescence Analysis—Cells were fixed in 3% paraformaldehyde (15 min), quenched with 20 mM NH_4Cl (1 h), permeabilized with 0.1% Triton X-100 (5 min), and blocked with 1% BSA in PBS (30 min). Antibodies were diluted in PBS containing 1% BSA. Coverslips were incubated for 1 h with primary antibodies washed three times in PBS and incubated 45 min with secondary antibodies and phalloidin Alexa 555 or 647. DNA was counterstained with DAPI (Sigma). Coverslips were mounted onto microscope slides with Aqua-Poly/Mount (18606, Polysciences). Images were collected with a confocal laser-scanning microscope (Zeiss Axiovert LSM 510 or Leica SP2 AOBS S.E.) and processed using Adobe Photoshop software.

Transfection and Lentiviral Transduction—The lentiviral shRNA expression plasmids Mission pLKO.1-puro (control) and Mission shRNA-c-Src (Sigma) were used in combination with the envelope plasmid pMD.G and packaging plasmid pCMVR8.91. Packaging, envelope, and shRNA vector plasmids were co-transfected into HEK293 cells. Viral supernatants were harvested after 72 h, filtered, and incubated with target HeLa cells for 48 h at 37 °C. Puromycin was used to select for individual clones. The knockdown was verified by immunoblot and/or real time RT-PCR.

Transfection of siRNA Duplexes and Plasmid DNA—HeLa cells seeded in 24- or 6-well plates were transfected with 60 nM control siRNA-D (sc-44232 Santa Cruz Biotechnology) or specific siRNAs for NMHC-IIA or NMHC-IIB depletion, using Lipofectamine RNAiMax (Invitrogen) following the manufacturer's instructions. Assays were performed 48 h later. Sequences of siRNAs are provided in Table 4. For transient protein expression, HeLa cells were seeded in 24-well plates (1×10^5 cells/well), 6-well plates (4×10^5 cells/well), or 10-cm dishes (3×10^6 cells/dish) and transfected at 90% confluency with 500 ng, 2.5 μ, or 15 μg of plasmid DNA, respectively, using Lipofectamine 2000 (Invitrogen). Assays were performed 24 h later. For rescue assays, HeLa cells were transfected with NMHC-IIA-si#2 and 24 h later transiently transfected with plasmids encoding siRNA-resistant GFP-NMHC-IIA-WT.

Kinase Assay—Kinase assays were performed using the Src assay kit (17-131, Millipore), following the manufacturer's instructions. Anti-GFP-immunoprecipitated fractions from HEK293 cells expressing GFP-NMHC-IIA variants were incubated (10 min, 30 °C) with 10 units of recombinant Src (14–117, Millipore), in 30 μl of kinase reaction buffer supplemented with 9 μl of manganese/ATP mixture and 10 μCi of [γ-^{32}P]ATP (PerkinElmer Life Sciences). Reactions, including an Src-specific substrate or lacking Src, were used as controls. Reactions were precipitated with 40% TCA and spotted onto P81 phosphocellulose paper squares, washed three times with 0.75% phosphoric acid, once with acetone, and transferred to microtubes containing UniverSol liquid scintillation mixture (MP Biomedicals). Incorporation of ^{32}P was determined in a Wallac 1450 MicroBeta TriLux liquid scintillation counter (PerkinElmer Life Sciences), as counts/min. Radioactivity measurements were performed in duplicate in two independent assays.

Statistical Analyses—Statistical analyses were performed with Prism 6 software (GraphPad Software, Inc.). One-way analysis of variance with post hoc testing analyses were used for pairwise comparison of means from at least three unmatched groups. Two-tailed Student's *t* test was used to compare means of two samples and one-sample *t* test to compare with samples

Downloaded from http://www.jbc.org/ at UNIVERSIDADE DO PORTO on October 8, 2015

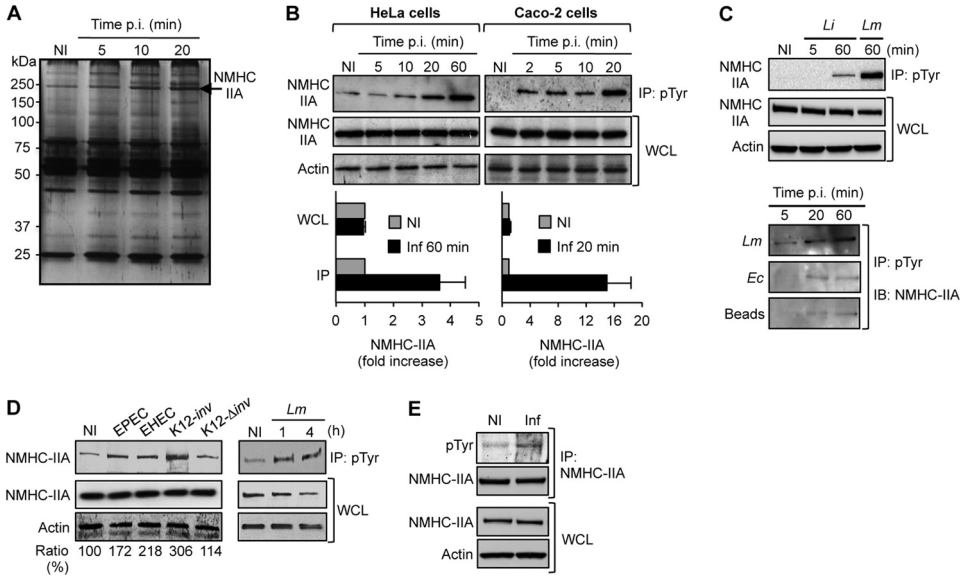

FIGURE 1. **NMHC-IIA is tyrosine-phosphorylated in response to human bacterial pathogens.** *A,* silver-stained acrylamide gel showing the tyrosine phosphorylation profiles of NI and *L. monocytogenes*-infected HeLa cells for the indicated periods of time. Total tyrosine-phosphorylated proteins were immunoprecipitated with an anti-Tyr(P) antibody. Molecular mass standards are indicated. *Arrow* shows a protein band with increased intensity over the time of infection and identified by mass spectrometry analysis as NMHC-IIA. *B,* HeLa and Caco-2 cells were left NI or incubated with *L. monocytogenes* and harvested at indicated time points post-infection (*p.i.*). Tyrosine-phosphorylated proteins were immunoprecipitated (*IP: pTyr*) from WCL, and NMHC-IIA was detected by immunoblot (*NMHC-IIA*) in IP fractions and WCL. Detection of actin protein levels served as loading control. *Bottom panels* show quantifications of NMHC-IIA signals from at least three independent experiments in WCL and IP fractions of NI and *L. monocytogenes*-infected HeLa (60 min p.i.) and Caco-2 (20 min p.i.) cells. *C,* HeLa cells were left NI or incubated with either *L. monocytogenes* (*Lm*), *L. innocua* (*Li*) (*top panels*), *E. coli* DH5α (*Ec*), or latex beads (*bottom panels*). Tyrosine-phosphorylated proteins were immunoprecipitated from WCL recovered at different time points and NMHC-IIA was analyzed by immunoblot (*IB*) in IP fractions and WCL. *D,* HeLa cells were left NI or incubated, for 4 h, with pathogenic *E. coli* (EPEC and EHEC) and *E. coli* K12 expressing a functional (*inv*) or mutated variant (Δ*inv*) of *Y. pseudotuberculosis* invasin. Cells were also incubated with *L. monocytogenes* for 1 and 4 h (*right panel*). Tyrosine-phosphorylated proteins were immunoprecipitated and NMHC-IIA detected by immunoblot in IP fractions and WCL. Quantifications of NMHC-IIA signals for each IP fraction related to WCL are indicated (ratio). Values represent the mean of three independent experiments. *E,* NMHC-IIA was immunoprecipitated (*IP: NMHC-IIA*) from WCL of NI and *L. monocytogenes*-infected (*Inf*, 60 min) HeLa cells. Tyrosine-phosphorylated proteins (*pTyr*) and NMHC-IIA were detected in immunoprecipitates. As control, NMHC-IIA and actin were also detected in WCL.

arbitrarily fixed to 100. Differences were not considered statistically significant for p value ≥ 0.05.

RESULTS

NMHC-IIA Is Tyrosine-phosphorylated in Response to Bacterial Infection—To identify new host proteins undergoing tyrosine phosphorylation (Tyr(P)) in response to *L. monocytogenes* and that could affect *L. monocytogenes* cellular infection, we compared the Tyr(P) protein profiles of *L. monocytogenes*-infected and noninfected (NI) HeLa cells. Cell extracts were collected at different time points post-inoculation and subjected to IP using anti-phosphotyrosine antibodies (anti-Tyr(P)). IP fractions were resolved by SDS-PAGE followed by silver staining. Bands showing variable intensities in *L. monocytogenes*-infected *versus* NI cells were excised and processed for mass spectrometry identification. A band corresponding to an ≈250-kDa protein and displaying increased intensity throughout the infection (Fig. 1*A*) was identified as the human NMHC-IIA (data not shown).

To validate this result, HeLa and Caco-2 cells were incubated with *L. monocytogenes* for different time periods, and the presence of NMHC-IIA in anti-Tyr(P) IP fractions was assessed by immunoblot using NMHC-IIA-specific antibodies. We detected a time-dependent increase of NMHC-IIA in IP fractions from *L. monocytogenes*-infected cells (Fig. 1*B*). Levels of NMHC-IIA in Tyr(P) fraction increased 3.5-fold after 60 min of *L. monocytogenes* incubation with HeLa cells and 15-fold in Caco-2 cells upon 20 min of *L. monocytogenes* infection (Fig. 1*B*). Levels of NMHC-IIA in whole cell lysates (WCL) were not affected by infection (Fig. 1*B*), showing that increased levels of NMHC-IIA in IP samples are not related to an augmentation of NMHC-IIA expression. Incubation of HeLa cells with the nonpathogenic species *Listeria innocua* for 60 min only induced a small enrichment of NMHC-IIA in the anti-Tyr(P) IP fractions as compared with *L. monocytogenes* (Fig. 1*C*). In addition, NMHC-IIA was barely detected in IP fractions from HeLa cells stimulated by *E. coli* DH5α or latex beads (Fig. 1*C*). Altogether, these results indicate that the enrichment of NMHC-IIA in the pool of Tyr(P) proteins is associated with the pathogenic features of *L. monocytogenes* and is not a broad cellular response to any extracellular stimuli.

To investigate whether the same response could be induced upon infection with other human bacterial pathogens, HeLa cells were incubated for 4 h with the extracellular pathogenic *E. coli* EPEC and EHEC or the invasive *E. coli* K12 expressing the *Y. pseudotuberculosis* invasin (K12-*inv*) (24), an infection model allowing the study of signaling pathways triggered downstream from the invasin-integrin interaction. As compared with NI conditions, NMHC-IIA appeared slightly increased in anti-Tyr(P) IP fractions from EPEC- and EHEC-infected cells. Strikingly, K12-*inv* induced a robust enrichment of NMHC-IIA in IP samples that is abolished in cells incubated with bacteria harboring a disrupted invasin-encoding gene

Downloaded from http://www.jbc.org/ at UNIVERSIDADE DO PORTO on October 8, 2015

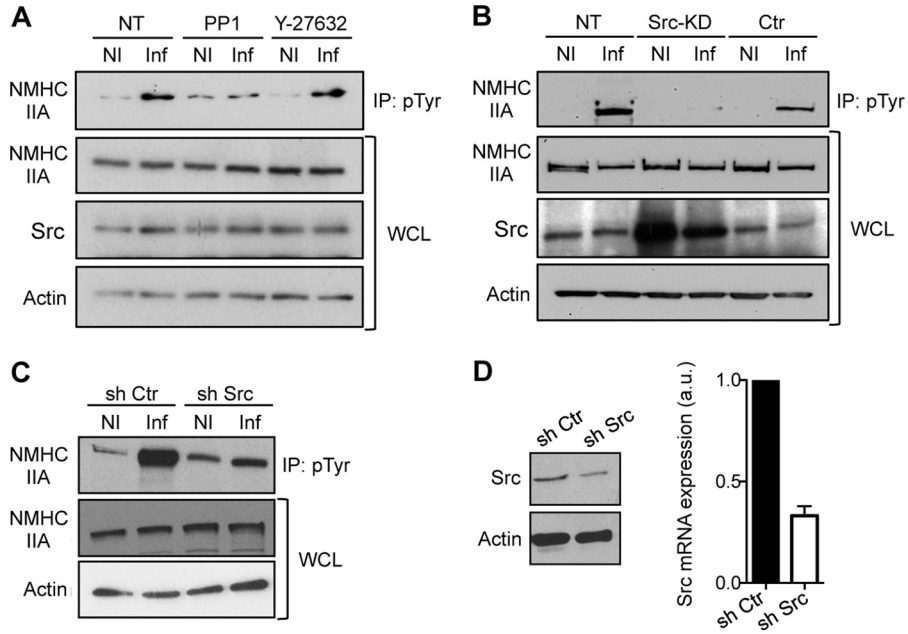

FIGURE 2. **Activity of Src kinase is required for NMHC-IIA tyrosine phosphorylation upon *L. monocytogenes* cellular infection.** *A,* HeLa cells pretreated with PP1 (10 μM) or Y-27632 (50 μM) during 30 min were left NI or incubated with *L. monocytogenes* for 1 h (*Inf*) in the presence of the same concentrations of drugs. Nontreated (*NT*) HeLa cells were used as control. *B,* HeLa cells NT, transfected with a control empty plasmid (*Ctr*), or with an Src kinase-dead (*Src-KD*)-encoding plasmid. *C,* HeLa cells stably expressing an shRNA control (*sh Ctr*) or a specific shRNA targeting Src expression (*sh Src*). Cells in *B* and *C* were left NI or incubated with *L. monocytogenes* for 1 h (*Inf*). *A–C,* total tyrosine-phosphorylated proteins were immunoprecipitated, and NMHC-IIA was detected by immunoblot in IP fractions and WCL. Detection of actin levels served as loading control. Src protein levels were also confirmed by immunoblot. *D,* efficiency of Src depletion in sh Src HeLa cells was assessed by immunoblot using actin protein detection as loading control (*left panel*) and by quantitative RT-PCR (*right panel*). Src mRNA expression is represented relative to the expression of control HPRT1. In sh Ctr cells, the relative expression was arbitrarily fixed to 1.

(K12-Δ*inv*, Fig. 1*D*). For comparison, cells were also incubated with *L. monocytogenes* for 1 and 4 h (Fig. 1*D*). These results indicate that the enrichment of NMHC-IIA in the pool of Tyr(P) proteins is an event triggered by several human bacterial pathogens.

Our data suggest that bacterial infection either induces the direct NMHC-IIA Tyr(P) or stimulates its interaction with a protein that itself undergoes Tyr(P). To address this issue, endogenous NMHC-IIA was immunoprecipitated from NI and *L. monocytogenes*-infected HeLa cells, and Tyr(P) proteins were detected by immunoblot. A band showing a consistent 1.5-fold increase in intensity in infected samples was detected at the molecular weight of NMHC-IIA (Fig. 1*E*). Immunoprecipitated levels of NMHC-IIA were similar in NI and *L. monocytogenes*-infected cells. These results support a direct Tyr(P) of NMHC-IIA triggered by *L. monocytogenes* infection.

NMHC-IIA-Tyr(P) Induced by L. monocytogenes Cellular Infection Requires the Activity of Src Tyrosine Kinase—Considering our previous findings revealing the key role of the tyrosine kinase Src during *L. monocytogenes* invasion (7), we addressed the role of this kinase in NMHC-IIA-Tyr(P) in the context of *L. monocytogenes* infection. Prior to *L. monocytogenes* incubation, HeLa cells were treated with PP1, an inhibitor of Src family kinases, or with Y-27632, an inhibitor of the serine/threonine kinase ROCK that regulates NMHC-IIA activity through the phosphorylation of the regulatory light chain of myosin II and limits *L. monocytogenes* internalization (25). Given that NMHC-IIA-Tyr(P) is hardly detected by using anti-Tyr(P) antibodies in immunoblot, cell lysates were subjected to anti-Tyr(P) IP assay and NMHC-IIA was detected in IP fractions. The increase in NMHC-IIA-Tyr(P) induced by *L. monocytogenes* infection of nontreated cells (NT) was abolished in PP1-treated cells while being not affected by Y-27632 treatment (Fig. 2*A*), suggesting that NMHC-IIA-Tyr(P) requires Src kinase activity and occurs independently from ROCK activity. In addition, we interfered with Src activity by overexpressing an Src kinase-dead variant (Src-KD) (26). Levels of NMHC-IIA-Tyr(P) induced by *L. monocytogenes* infection were assessed in HeLa cells nontransfected (NT), transfected, with an empty plasmid (Ctr) or overexpressing Src-KD. In contrast to NT and Ctr cells showing increased levels of NMHC-IIA-Tyr(P) upon *L. monocytogenes* infection, in cells overexpressing Src-KD the NMHC-IIA-Tyr(P) was almost undetectable (Fig. 2*B*). To further confirm these data, we targeted the expression of endogenous Src by using specific shRNAs. We observed that *L. monocytogenes*-induced NMHC-IIA-Tyr(P) occurred in shRNA control (sh Ctr) and was clearly diminished in shRNA Src-expressing (sh Src) HeLa cells, in which Src expression is reduced by 60% (Fig. 2, *C* and *D*). Altogether, these data demonstrate that Src activity is required for NMHC-IIA-Tyr(P) triggered by bacterial infection.

Host Src Kinase Phosphorylates NMHC-IIA in Tyrosine Residue 158—The NMHC-IIA amino acid sequence includes 34 tyrosine residues, most of which are located in the myosin motor domain (Fig. 3*A*). To identify the NMHC-IIA tyrosine residues phosphorylated by Src upon *L. monocytogenes* infection, we used combined *in silico* approaches (NetPhos 2.0 and NetPhosK). Nine tyrosine residues were predicted as potentially phosphorylated, among which only the tyrosine in position 158 (Tyr-158) was a putative substrate for Src kinase (Fig.

Downloaded from http://www.jbc.org/ at UNIVERSIDADE DO PORTO on October 8, 2015

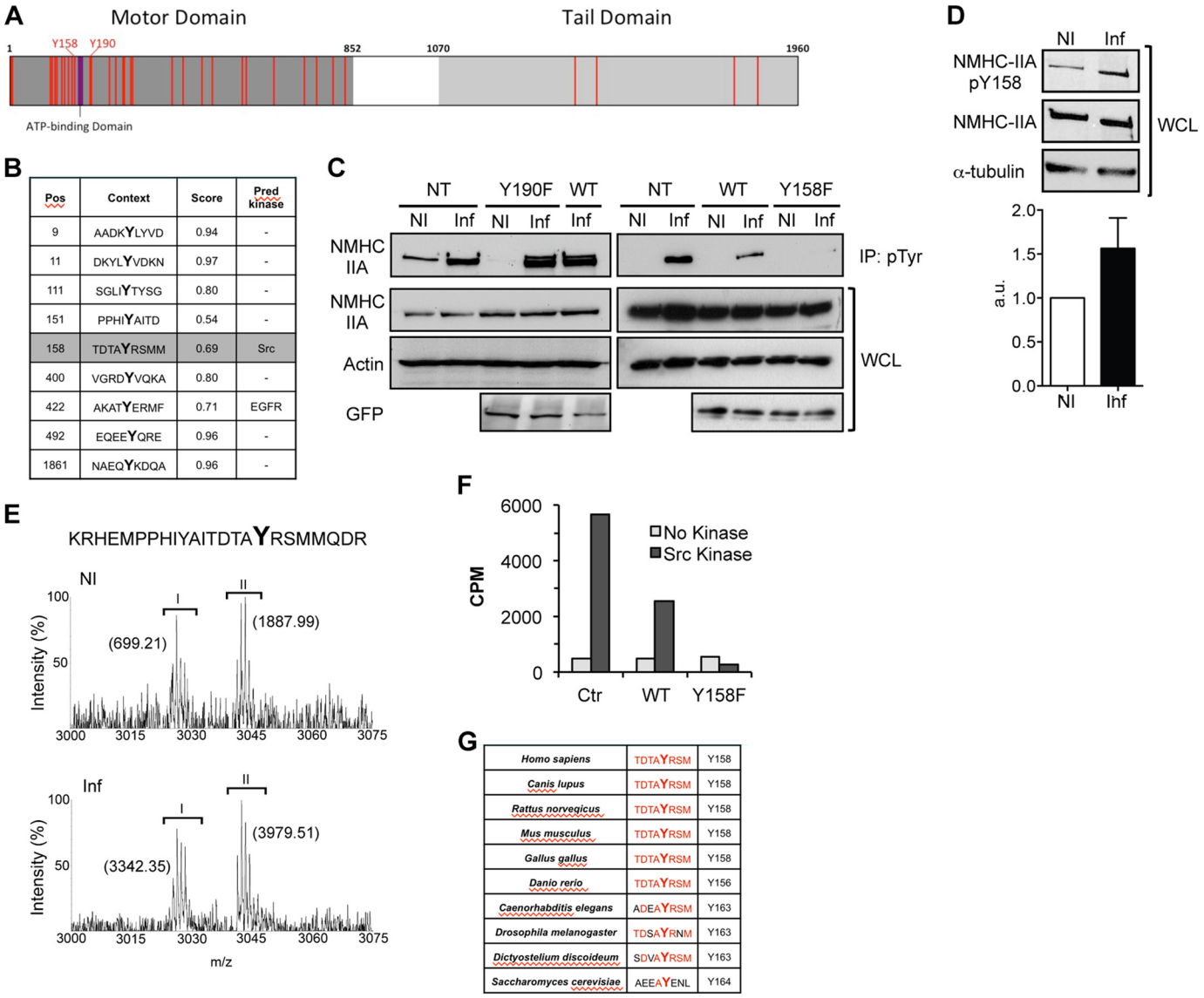

Pos	Context	Score	Pred kinase
9	AADK**Y**LYVD	0.94	-
11	DKYL**Y**VDKN	0.97	-
111	SGLI**Y**TYSG	0.80	-
151	PPHI**Y**AITD	0.54	-
158	TDTA**Y**RSMM	0.69	Src
400	VGRD**Y**VQKA	0.80	-
422	AKAT**Y**ERMF	0.71	EGFR
492	EQEE**Y**QRE	0.96	-
1861	NAEQ**Y**KDQA	0.96	-

Homo sapiens	TDTA**Y**RSM	Y158
Canis lupus	TDTA**Y**RSM	Y158
Rattus norvegicus	TDTA**Y**RSM	Y158
Mus musculus	TDTA**Y**RSM	Y158
Gallus gallus	TDTA**Y**RSM	Y158
Danio rerio	TDTA**Y**RSM	Y156
Caenorhabditis elegans	ADEA**Y**RSM	Y163
Drosophila melanogaster	TDSA**Y**RNM	Y163
Dictyostelium discoideum	SDVA**Y**RSM	Y163
Saccharomyces cerevisiae	AEEA**Y**ENL	Y164

FIGURE 3. **NMHC-IIA tyrosine residue in position 158 is phosphorylated in response to *L. monocytogenes* infection.** *A,* schematic representation of NMHC-IIA showing the distribution of tyrosine residues (*red bars*). Tyrosine residues in position 158 (*Y158*) and 190 (*Y190*) are highlighted. ATP-binding site, motor, and tail domains are indicated. *B, in silico* predictions obtained from NetPhos 2.0 and NetPhosK servers, for tyrosine phosphorylation potential (score) and putative kinase involved. The position and amino acid environment of tyrosine residues showing a phosphorylation potential above the threshold (score >0.5) are indicated. *C,* HeLa cells expressing the wild type GFP-NMHC-IIA (*WT*) and the mutants GFP-NMHC-IIA-Y158F (*Y158F*) or GFP-NMHC-IIA-Y190F (*Y190F*) were left NI or incubated with *L. monocytogenes* for 1 h (*Inf*). NMHC-IIA was detected by immunoblot in anti-Tyr(P) immunoprecipitates and WCL. Detection of GFP indicates similar expression levels of NMHC-IIA constructs and actin levels served as loading control. *D,* HeLa cells were left NI or incubated with *L. monocytogenes* for 1 h (*Inf*). Total cell extracts were used in immunoblot using an antibody raised against NMHC-IIA-Tyr(P)-158. Total levels of NMHC-IIA were detected using an anti-NMHC-IIA antibody, and α-tubulin levels were used as loading control. *Bottom panel* shows quantification of NMHC-IIA-Tyr(P)-158 signals from three independent experiments in NI and *L. monocytogenes*-infected HeLa cells. *E,* mass spectra from NMHC-IIA acquired after phosphopeptide enrichment from NI and infected HeLa cells. Two peak clusters marked as *I* (monoisotopic peak at *m/z* 3025.37 $[M - H]^-$) and *II* (monoisotopic peak at *m/z* 3041.36 $[M - H]^-$ with oxidized methionine) were detected. The corresponding NMHC-IIA peptide (amino acid 142–165) is indicated, and Tyr-158 is highlighted. The area of the clusters in NI and infected conditions is indicated in *parentheses*. *F,* anti-GFP IP fractions obtained from WCL of HEK293 cells expressing either GFP-NMHC-IIA-WT (*WT*) or GFP-NMHC-IIA-Y158F (*Y158F*) were used in *in vitro* Src kinase assays. A synthetic peptide was used as positive control (*Ctr*). Incorporation of radiolabeled [γ-^{32}P]ATP was measured in counts/min for each condition. Results are representative of two independent experiments. *G,* comparative analysis of the NMHC-IIA amino acid sequence from different species, focused in the region encompassing the tyrosine on position 158.

3*B*). To assess these *in silico* predictions and taking into account that *L. monocytogenes*-induced NMHC-IIA-Tyr(P) requires Src kinase activity (Fig. 2), we determined whether NMHC-IIA-Tyr(P) occurs upon *L. monocytogenes* infection of cells ectopically expressing either GFP-tagged NMHC-IIA-Y158F (in which Tyr-158 residue was replaced by a phenylalanine), NMHC-IIA-Y190F (harboring the same amino acid substitution in position 190, randomly selected, and unrelated to *in silico* predictions), or NMHC-IIA-WT (wild type NMHC-IIA). *L. monocytogenes* infection of nontransfected (NT), NMHC-IIA-WT-, and NMHC-IIA-Y190F-overexpressing cells generated increased levels of NMHC-IIA-Tyr(P) as compared with NI cells, although the overexpression of NMHC-IIA-Y158F largely limited *L. monocytogenes*-induced NMHC-IIA-Tyr(P) (Fig. 3*C*). Exogenous NMHC-IIA-WT and NMHC-IIA-Y190F were occasionally detected in anti-Tyr(P) IP fractions of *L.*

Downloaded from http://www.jbc.org/ at UNIVERSIDADE DO PORTO on October 8, 2015

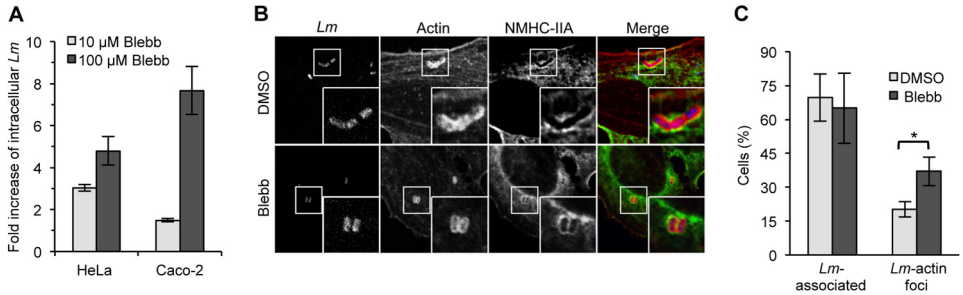

FIGURE 4. ***L. monocytogenes* intracellular levels increased upon inhibition of NMHC-IIA activity.** *A,* levels of intracellular *L. monocytogenes* (*Lm*) were assessed by gentamicin protection assay and CFU counting in HeLa and Caco-2 cells treated with 10 or 100 μM blebbistatin (*Blebb*). *Graph* shows the fold increase of intracellular *L. monocytogenes* determined as the ratio of intracellular bacteria in cells treated with the active *versus* the inactive enantiomer of blebbistatin. *B,* single confocal sections of HeLa cells infected with *L. monocytogenes* in the presence of DMSO (control) or 50 μM active blebbistatin. Infected cells were immunolabeled for NMHC-IIA (*green*) and *L. monocytogenes* (*blue*) and stained for actin (*red*). *C,* immunofluorescence scoring of DMSO- and active blebbistatin-treated HeLa cells associated with *L. monocytogenes* and showing *L. monocytogenes*-associated actin foci. Results are means ± S.D. from three independent experiments, each done in duplicate. Statistically significant differences are indicated: *, $p < 0.05$.

monocytogenes-infected cells (data not shown). Levels of endogenous NMHC-IIA were comparable in the different conditions, and GFP fusion proteins were expressed similarly in NI and infected cells (Fig. 3*C*). These results corroborate *in silico* predictions and suggest the central role of Tyr-158 in NMHC-IIA-Tyr(P) triggered upon infection. To validate our results, total lysates from NI and *L. monocytogenes*-infected cells were probed with an antibody raised against a peptide comprising the phosphorylated Tyr-158 residue of NMHC-IIA (Tyr(P)-158). In agreement with our data, levels of NMHC-IIA-Tyr(P)-158 were increased 1.5-fold in *L. monocytogenes*-infected cells (Fig. 3*D*). In addition, samples enriched in NMHC-IIA phosphopeptides from NI and *L. monocytogenes*-infected cells were analyzed by mass spectrometry. A phosphopeptide spanning Tyr-158 (amino acids 142–165, KRHEMPPHIYAITD-TA**Y**RSMMQDR) was detected at *m/z* 3025.37 $[M - H]^-$ (Fig. 3*E*, *cluster I*) and at 3041.36 $[M - H]^-$ with an oxidized methionine (Fig. 3*E*, *cluster II*). In infected samples, the area of cluster I that is correlated with the abundance of the corresponding phosphopeptide was increased 4.8-fold. Cluster II appeared 2.1-fold more abundant in *L. monocytogenes*-infected samples as compared with NI. Cluster I was further characterized and validated by MS/MS sequencing. Altogether, our data show that phosphorylation occurs at Tyr-158.

We further evaluated whether NMHC-IIA-Tyr(P) occurs specifically on Tyr-158 through Src activity, performing an *in vitro* kinase assay. GFP-NMHC-IIA-WT or Y158F ectopically expressed in HEK293 cells was highly enriched through immunoprecipitation using an anti-GFP antibody and incubated with purified Src kinase and [γ-^{32}P]ATP. A synthetic peptide substrate for Src was used as positive control. In the absence of kinase, the control peptide (Ctr) and IP fractions of NMHC-IIA-WT and Y158F showed residual levels of [γ-^{32}P]ATP incorporation. In the presence of Src kinase, the NMHC-IIA-WT-enriched IP fraction and the control peptide became radiolabeled, whereas the radioactivity incorporation in the NMHC-IIA-Y158F enriched sample remained at a basal level (Fig. 3*F*).

Altogether these results strongly suggest that Tyr-158 of NMHC-IIA is a substrate for Src kinase, becoming phosphorylated in response to *L. monocytogenes* infection, and put forward the putative role of this event in cellular infection. In addition, Tyr-158 appears extremely conserved among species ranging from *Saccharomyces cerevisiae* to *H. sapiens* (Fig. 3*G*), pointing to the broad importance for Tyr-158 in the regulation of highly conserved canonical functions of NMHC-IIA.

Inhibition of NMHC-IIA Activity Affects Intracellular Levels of L. monocytogenes—To assess the role of NMHC-IIA activity in cellular infection, we measured intracellular levels of *L. monocytogenes* following chemical inhibition of NMHC-IIA. Blebbistatin, a specific inhibitor of myosin II activity (27), was added (10 or 100 μM) to HeLa and Caco-2 cells, and *L. monocytogenes* infection efficiency was quantified by gentamicin protection assays. As control, we used an inactive form of blebbistatin. *L. monocytogenes* intracellular levels were increased by 2–8-fold, in a dose-dependent manner in both cell lines, following treatment with the active as compared with the inactive enantiomer of blebbistatin (Fig. 4*A*). Untreated and inactive blebbistatin-treated cells showed similar levels of intracellular *L. monocytogenes* (data not shown). Our data are in agreement with a previous report showing that blebbistatin treatment of L2 cells increases *L. monocytogenes* adhesion and invasion (25). Recruitment of NMHC-IIA and formation of actin foci at *L. monocytogenes* entry sites were both detected in control (DMSO) and active blebbistatin-treated HeLa cells (Fig. 4*B*). Although the percentage of *L. monocytogenes*-associated cells remained similar in both conditions, the percentage of cells showing *L. monocytogenes*-actin foci increased in the presence of active blebbistatin (Fig. 4*C*). Together, our results indicate that the ATPase activity of NMHC-IIA is not required for its localization to the sites of *L. monocytogenes* uptake and does not influence the interaction of *L. monocytogenes* with host cells. However, inhibition of NMHC-IIA ATPase activity fosters the formation of *L. monocytogenes*-actin foci, which correlates with increased rates of intracellular bacteria.

Reduced Expression of NMHC-IIA Increases the Level of Intracellular L. monocytogenes—To further address the role of NMHC-IIA in *L. monocytogenes* cellular infection, levels of adherent and intracellular *L. monocytogenes* were quantified by gentamicin protection assays in NMHC-IIA-depleted HeLa cells, using two siRNAs (si#1 and si#2). In accordance with the data described above, levels of intracellular *L. monocytogenes* increased 2-fold in NMHC-IIA-depleted (IIA-si#1 and IIA-si#2) as compared with control siRNA-transfected cells (Ctr)

Downloaded from http://www.jbc.org/ at UNIVERSIDADE DO PORTO on October 8, 2015

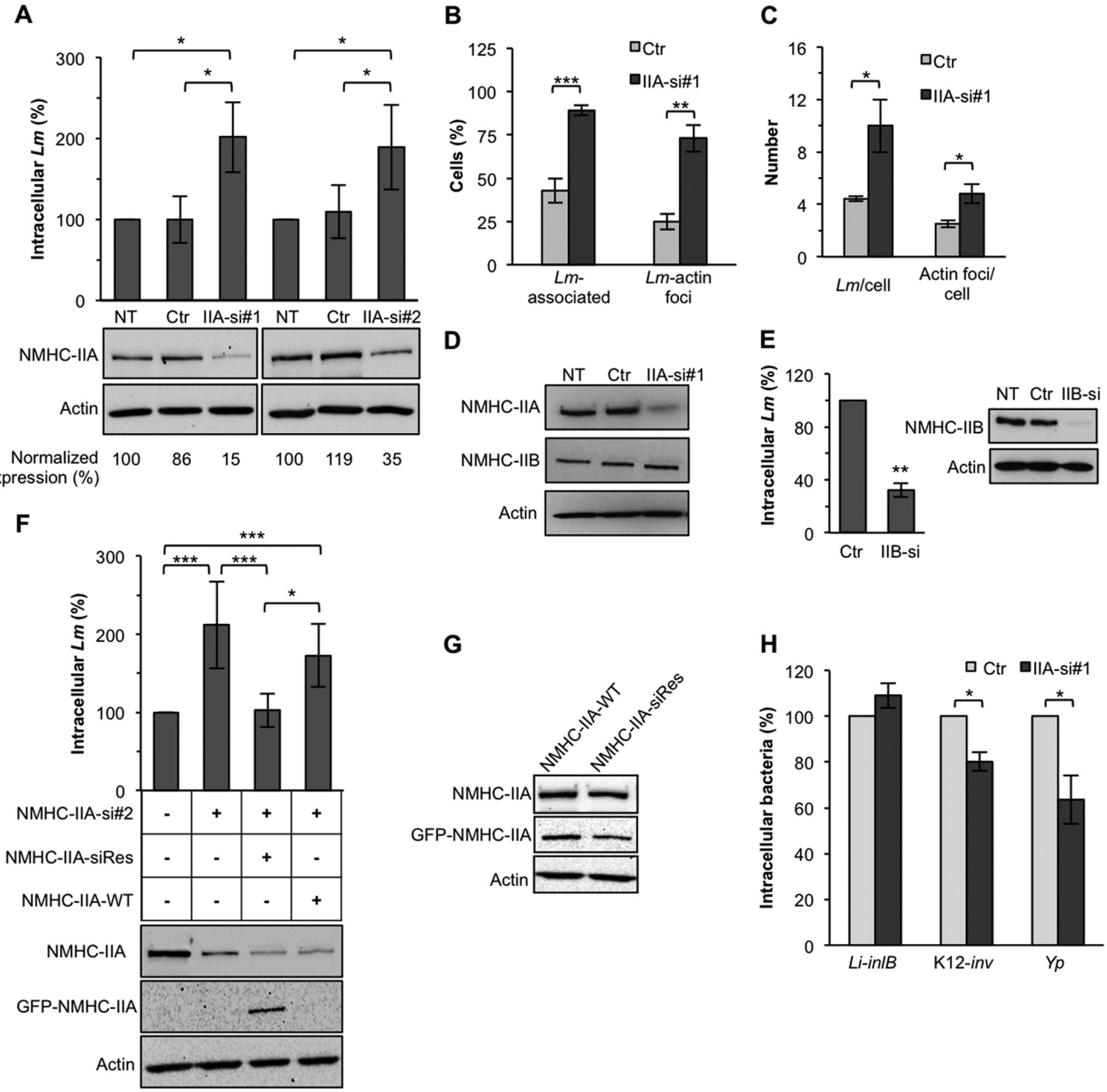

FIGURE 5. **Depletion of NMHC-IIA facilitated *L. monocytogenes* cellular infection.** *A,* intracellular levels of *L. monocytogenes* (*Lm*) assessed by gentamicin protection assay in HeLa cells NT or transfected with either control siRNA (*Ctr*) or NMHC-IIA-specific siRNAs (*si#1* and *si#2*). Efficiency of NMHC-IIA knockdown was assessed by immunoblot and quantified. Indicated values (normalized expression) are relative to actin and NMHC-IIA expression levels in NT cells. *B,* percentage of control (*Ctr*) or NMHC-IIA-depleted cells (*IIA-si#1*) associated with *L. monocytogenes* and showing *L. monocytogenes*-associated actin foci, evaluated by immunofluorescence scoring. *C,* number of bacteria and actin foci per cell in control and NMHC-IIA-depleted conditions. *D,* depletion of NMHC-IIA does not affect the expression of NMHC-IIB. NMHC-IIB expression levels were evaluated by immunoblot in NMHC-IIA-depleted (*IIA-si#1*) as compared with control (*NT* and *Ctr*) cells. Actin was used as loading control. *E,* intracellular levels of *L. monocytogenes* were assessed by gentamicin protection assay in HeLa cells transfected with either control siRNA (*Ctr*) or NMHC-IIB-specific siRNA (*IIB-si*). Efficiency of NMHC-IIB knockdown was assessed by immunoblot using actin protein detection as loading control. *F,* expression of NMHC-IIA was restored in si#2-depleted cells through the expression of a siRNA-resistant GFP-NMHC-IIA (*NMHC-IIA-siRes*). Intracellular levels of *L. monocytogenes* assessed by gentamicin protection assay in HeLa cells expressing different levels of NMHC-IIA are shown. Nontreated and NHMC-IIA-depleted cells expressing a wild type GFP-NMHC-IIA (*NMHC-IIA-WT*) were used as controls. Endogenous NMHC-IIA silencing and GFP-NMHC-IIA expression was evaluated by immunoblot. Detection of actin levels served as loading control. *G,* Western blot showing expression levels of endogenous (anti-NMHC-IIA, M8064, Sigma) and ectopically expressed NMHC-IIA (anti-GFP, B2, Santa Cruz Biotechnology) in HeLa cells transfected either with GFP-NMHC-IIA-WT or GFP-NMHC-IIA-siRes expression vectors. *H,* intracellular levels of *L. innocua* expressing *inlB* (*L. innocua* (*Li*)-*inlB*), *E. coli* K12 expressing the invasin (*K12-inv*), and *Y. pseudotuberculosis* (*Yp*) were assessed by gentamicin protection assay in HeLa cells transfected with either control siRNA (*Ctr*) or NMHC-IIA-specific siRNA (*IIA-si#1*). *A* and *F,* number of intracellular *L. monocytogenes* in NT cells was normalized to 100%, and those in siRNA-transfected cells were expressed as relative values to NT cells. *E* and *H,* numbers of intracellular bacteria were normalized to 100% in Ctr cells and expressed as relative values in the other conditions. Results shown in *A–C, E, F,* and *H* are means ± S.E. of at least three independent experiments, each done in triplicate. Statistically significant differences are indicated: *, $p < 0.05$; **, $p < 0.01$ and ***, $p < 0.001$.

(Fig. 5*A*). NMHC-IIA depletion assessed by immunoblot reached 85% in si#1-transfected cells and 65% when using si#2 (Fig. 5*A*). Levels of adhered *L. monocytogenes* were also augmented in NMHC-IIA-depleted cells (data not shown). Immunofluorescence analysis of *L. monocytogenes*-infected NMHC-IIA-depleted cells revealed a 2-fold increase in the percentage

Downloaded from http://www.jbc.org/ at UNIVERSIDADE DO PORTO on October 8, 2015

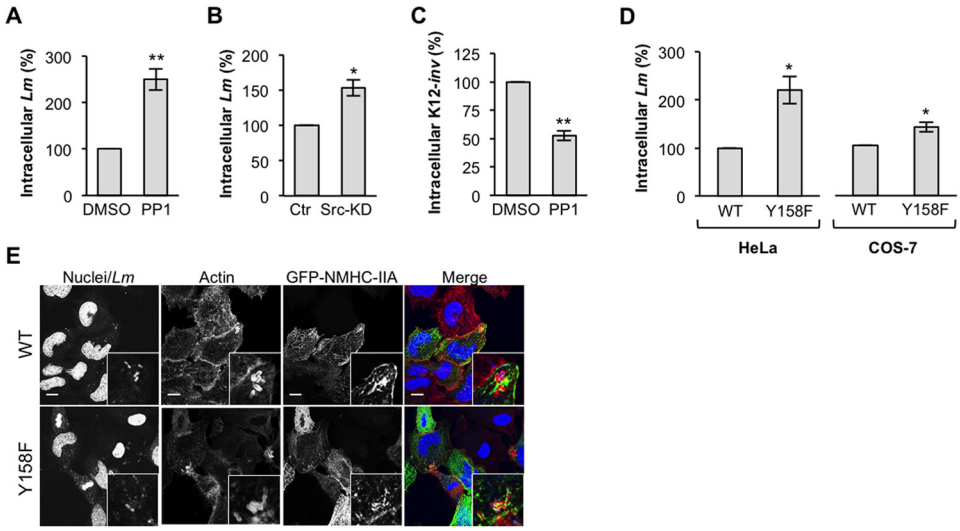

FIGURE 6. **NMHC-IIA phosphorylation in tyrosine 158 is required to limit *L. monocytogenes* cellular infection.** Intracellular levels of *L. monocytogenes* were assessed by gentamicin protection assays in the presence of 10 μM PP1 (*A*) or in HeLa cells expressing Src-KD (*B*). *C,* levels of intracellular K12-*inv* were assessed by gentamicin protection assay in HeLa cells treated with 10 μM of PP1. *D,* intracellular levels of *L. monocytogenes* were assessed by gentamicin protection assays in HeLa and COS-7 cells expressing either GFP-NMHC-IIA-WT (*WT*) or GFP-NMHC-IIA-Y158F (*Y158F*). Results shown in *A–D* are means ± S.E. of three independent experiments, each done in triplicate Numbers of intracellular bacteria were normalized to 100% in control cells and expressed as relative values in the other experimental conditions. Statistically significant differences are indicated: *, $p < 0.05$; **, $p < 0.01$. *E,* single confocal section of COS-7 cells ectopically expressing either GFP-NMHC-IIA-WT or Y158F variants incubated with *L. monocytogenes* for 1 h and stained for actin (phalloidin, *red*) and DNA (DAPI, *blue*) (*scale bar,* 10 μm).

of cells associated with *L. monocytogenes* and a 3-fold increase in the percentage of cells showing *L. monocytogenes*-associated actin foci (Fig. 5*B*). The number of bacteria and actin foci per cell were also increased in NMHC-IIA-depleted cells (Fig. 5*C*), correlating with increased levels of intracellular bacteria. Our data indicate that, although *L. monocytogenes* association with cells does not require NMHC-II activity, it is modulated by NMHC-IIA itself probably through the interaction with other proteins.

To discard the hypothesis that increased levels of intracellular *L. monocytogenes* detected in NMHC-IIA-depleted cells could result from the overexpression of the isoform B of non-muscle myosin heavy chain (NMHC-IIB), we confirmed that expression levels of NMHC-IIB were similar in NMHC-IIA-depleted cells and control cells (Fig. 5*D*). In addition, we found that *L. monocytogenes* intracellular levels decreased 3-fold in NMHC-IIB-depleted HeLa cells (Fig. 5*E*), suggesting that NMHC-IIA and -IIB play opposite roles in *L. monocytogenes* infection and thus undermining the possibility of their mutual functional replacement. To definitively reinforce our findings and exclude potential uncontrolled off-target effects, we performed gentamicin protection assays following gene rescue experiments. We created an siRNA-resistant GFP-NMHC-IIA construct (NMHC-IIA-siRes) by introducing silent point mutations within the si#2 target sequence. We found that increased levels of intracellular *L. monocytogenes* detected upon NMHC-IIA depletion (IIA-si#2) dropped to control levels in NMHC-IIA-depleted cells expressing NMHC-IIA-siRes (Fig. 5*F*). In contrast, the expression of NMHC-IIA-WT in NMHC-IIA-depleted cells did not restore control levels of intracellular *L. monocytogenes*. Immunoblot analysis confirmed that the expression of endogenous NMHC-IIA was diminished in the presence of si#2 and that ectopically expressed NMHC-IIA was only detected in NMHC-IIA-siRes-transfected cells (Fig. 5*F*). However, in the absence of si#2, both NMHC-IIA-WT and siRes variants are expressed at similar levels (Fig. 5*G*). Together, these results confirm that the increase in *L. monocytogenes* intracellular levels observed in NMHC-IIA-depleted cells is specifically due to NMHC-IIA depletion.

To analyze whether the role of NMHC-IIA on intracellular levels of bacteria was specific for *L. monocytogenes* or could be broadened to other bacterial infectious processes, we performed gentamicin protection assays using *L. innocua* expressing InlB (*L. innocua-inlB*), the major internalin driving *L. monocytogenes* entry in HeLa cells (28), K12-*inv,* and *Y. pseudotuberculosis.* Numbers of intracellular *L. innocua-inlB* were not significantly different in NMHC-IIA-depleted and Ctr cells (Fig. 5*H*). In contrast, levels of intracellular K12-*inv* and *Y. pseudotuberculosis* were significantly lower in NMHC-IIA-depleted cells (Fig. 5*H*). Our data indicate that NMHC-IIA is specifically triggered by pathogenic *L. monocytogenes* and is independent of an InlB-mediated uptake. In contrast, the invasin-mediated uptake requires NMHC-IIA. Interestingly, NMHC-IIA and -IIB were shown to be required for SopB-mediated invasion of *Salmonella* (18). Our findings, together with published reports, reveal that NMHC-IIA plays opposite roles in different infection models; although it is required for an utmost *Y. pseudotuberculosis* and *Salmonella* infection, it has a restrictive role in *L. monocytogenes* cellular infection.

Function of NMHC-IIA in L. monocytogenes Infection Relies on the Phosphorylation of Its Tyrosine 158—We reported above two important observations. 1) NMHC-IIA is tyrosine-phosphorylated by Src kinase upon *L. monocytogenes* incubation with cells. 2) *L. monocytogenes* intracellular levels are increased in conditions of NMHC-IIA depletion or inhibition of its activity, demonstrating that NMHC-IIA activity limits *L. monocytogenes* infection. To investigate whether both findings could be interconnected, we evaluated levels of intracellular bacteria

Downloaded from http://www.jbc.org/ at UNIVERSIDADE DO PORTO on October 8, 2015

under conditions where NMHC-IIA-Tyr(P) does not occur. We used cells with compromised Src activity (PP1 treatment and Src-KD overexpression) and cells expressing an NMHC-IIA nonphosphorylatable variant (NMHC-IIA-Y158F). Levels of intracellular *L. monocytogenes* showed a 2.5-fold increase in PP1-treated HeLa cells as compared with control DMSO-treated cells (Fig. 6*A*). In agreement, we observed an increase in *L. monocytogenes* intracellular levels in cells expressing Src-KD (Fig. 6*B*). Inversely, intracellular levels of K12-*inv* decreased 2-fold in PP1-treated cells (Fig. 6*C*), as reported previously (29). Increased levels of intracellular *L. monocytogenes* detected in conditions of Src inactivation and thus in the absence of NMHC-IIA-Tyr(P) correlate with our data showing that reduced levels or inactivation of NMHC-IIA resulted in increased numbers of intracellular *L. monocytogenes*. Our data also suggest an association between the role of NMHC-IIA in *Y. pseudotuberculosis* invasin-mediated uptake and invasin-triggered NMHC-IIA-Tyr(P).

To further confirm the role of NMHC-IIA-Tyr(P) in the *L. monocytogenes* cellular infection, we evaluated intracellular levels of *L. monocytogenes* in HeLa and COS-7 cells transiently expressing either the GFP-NMHC-IIA-WT (WT) or the non-phosphorylatable variant GFP-NMHC-IIA-Y158F (Y158F). In contrast to HeLa cells, COS-7 cells naturally lack NMHC-IIA expression, thus appearing as a valuable experimental model to address the effect of exogenously expressed NMHC-IIA variants in absence of the endogenous protein. Equivalent expression levels of both constructs were verified by flow cytometry and immunoblot (data not shown). *L. monocytogenes* intracellular rates were determined by gentamicin protection assays in cell populations containing about 50% of transfected cells. As compared with NMHC-IIA-WT, the expression of NMHC-IIA-Y158F led to increased levels of intracellular *L. monocytogenes* in both cell lines (Fig. 6*D*). Thus, NMHC-IIA-Y158F expression recapitulates the increase of intracellular *L. monocytogenes* in NMHC-IIA-depleted or inactivated cells. Furthermore, both GFP-NMHC-IIA-WT and GFP-NMHC-IIA-Y158F showed the same localization and accumulate at the site of *L. monocytogenes* entry in HeLa cells (Fig. 6*E*). These results indicate that although NMHC-IIA subcellular localization and recruitment to the site of bacterial uptake are unrelated to Tyr-158, the phosphorylation of this specific NMHC-IIA tyrosine plays a key role in restraining *L. monocytogenes* infection.

DISCUSSION

Pathogens interfere with host phosphorylation cascades to foster adhesion, invasion, and intracellular survival. Here, we searched for new host proteins undergoing tyrosine phosphorylation upon *L. monocytogenes* infection. We showed that NMHC-IIA is tyrosine-phosphorylated in response to *L. monocytogenes* as well as to other human bacterial pathogens such as EPEC, EHEC, and K12-*inv*. In *L. monocytogenes* infection, this previously unknown tyrosine phosphorylation event is triggered by Src kinase on residue Tyr-158 of NMHC-IIA, and it limits intracellular bacterial levels.

Myosin II activity is regulated by phosphorylation events in serine and threonine residues of the regulatory light chain (15). NMHC-IIA also undergoes serine and threonine phosphorylations, which regulate the assembly of myosin II filaments *in vitro* and are thought to control subcellular localization of NMHC-IIA and contractility that depends on the actin cross-linking activity of NMHC-IIA (15). Although NMHC-IIA was detected in studies aiming to unravel the global phosphotyrosine signaling in cancer tissues (30, 31), its tyrosine phosphorylation has never been characterized. Our data constitute the first report showing and characterizing NMHC-IIA-Tyr(P). Our preliminary *in silico* analysis suggests an important and broad role for NMHC-IIA Tyr(P) in position 158 as follows. 1) Tyr-158 is highly conserved among species ranging from *S. cerevisiae* to *H. sapiens*. 2) An *in silico* study suggested that Tyr-163 of muscle myosin heavy chain (matching Tyr-158 in NMHC-IIA) could be phosphorylated (32). 3) Tyr-158 is located in the motor domain of NMHC-IIA near the ATP-binding pocket. 4) Analysis of the crystal structure of the myosin motor domain (33) showed that Tyr-158 is exposed at the surface of the protein and is thus accessible for phosphorylation. Thus, we hypothesize that the phosphorylation of NMHC-IIA Tyr-158 could modulate NMHC-IIA activity most probably by affecting its ability to bind and/or hydrolyze ATP. However at this point any other mechanism could be envisaged. In addition, it is likely that NMHC-IIA-Tyr(P) in Tyr-158 occurs in specific physiological conditions engaging NMHC-IIA activity and thus plays a role in the regulation of the highly conserved canonical functions of NMHC-IIA. The functional and structural outcomes of such modification are now critical to elucidate.

Our data suggest that, upon infection, only a small pool of NMHC-IIA becomes phosphorylated in Tyr-158, probably concentrated in a restricted subcellular localization and/or interacting with specific partners, which would impact infection. Yet, we observed that both NMHC-IIA-WT and Y158F concentrated around bacteria at the entry site. We also found that phosphorylation of Tyr-158 does not affect the phosphorylation of the myosin regulatory light chain,[7] which is achieved by MLCK and is required for activation of myosin II motor activity (15). Interestingly, Src was previously shown recruited to membrane blebs where it associates with MLCK and myosin II (34, 35). In response to cell swelling, Src and MLCK form a complex in which Src activates MLCK, and both regulate a compensatory membrane retrieval that requires myosin II (35). It is thus conceivable that Src and MLCK could work together to fine-tune the activity of myosin II in the context of infection.

Myosin II isoforms were recently involved in viral and bacterial infections either promoting or limiting pathogen progression. However, their role in such processes is still mainly descriptive. NMHC-IIA is required for Kaposi sarcoma-associated herpesvirus and HSV1 entry into cells (16, 17, 36), facilitates *Salmonella* invasion, and regulates its intracellular growth (18, 37) and promotes *Chlamydia* dissemination (19). Conversely, myosin II limits bacterial cell-to-cell spread by restraining *L. monocytogenes* protrusion formation (38) and participating in the formation of *Shigella*-associated septin cages (39). NMHC-IIB is involved in the formation of actin-rich structures that accumulate near the *Salmonella*-containing vacuole and

[7] M. T. Almeida, D. Cabanes, and S. Sousa, unpublished data.

Downloaded from http://www.jbc.org/ at UNIVERSIDADE DO PORTO on October 8, 2015

restrain bacterial intracellular multiplication (40). Altogether, these data suggest that the different outcomes associated with myosin II function during infection are probably related to the cellular machinery engaged in the various infectious processes. Our results indicate that NMHC-IIA activity limits *L. monocytogenes* infection most probably hindering cellular invasion by interfering with the formation of *L. monocytogenes*-induced actin foci. NMHC-IIA-depleted or inactivated cells were reported to lose cytoplasm cohesion and show increased membrane activity and plasticity (41, 42). These phenotypes could thus suggest that the increased numbers of intracellular *L. monocytogenes* observed in such cells would be greatly due to the disruption membrane rigidity. However, if this was the case, cells displaying low NMHC-IIA activity should be more permissive to any extracellular pathogen, which was not observed in KSHV (17), HSV1 (16), and *Salmonella* (18) infections. In addition, we show here that NMHC-IIA sustains invasin-mediated *Y. pseudotuberculosis* infection, and the invasion rate of *L. innocua* expressing InlB was not significantly increased by NMHC-IIA depletion, thus excluding a nonspecific cell invasion mechanism.

NMHC-IIA participates in cellular processes associated with phosphotyrosine signaling, which are largely usurped by bacteria, namely *L. monocytogenes* and *Y. pseudotuberculosis* (43), during infection. NMHC-IIA regulates protrusion formation and cell migration through the generation of actin retrograde flow (44, 45); it is required for integrin-mediated adhesion maturation (46); it controls cell-cell adhesion promoting E-cadherin clustering and stabilizing cellular junctions (47); and it governs the polarization of epithelial cells generating forces to maintain the epithelia (48). Whether NMHC-IIA is Tyr(P) in these processes is unknown.

In intercellular junctions, NMHC-IIA is critical for the E-cadherin localization (47), and Src activation is required for actin polymerization at cell-cell contacts (49) as it is during E-cadherin-mediated *L. monocytogenes* invasion (7). Interestingly, Src activation and recruitment of c-Cbl are key events to control c-Met signaling (50). Our data show that Src activity restricts intracellular levels of *L. monocytogenes* in HeLa cells in which *L. monocytogenes* uptake is mainly mediated by c-Met and present the hypothesis that Src is acting through the tyrosine phosphorylation of NMHC-IIA to inhibit entry. Remarkably, in KSHV infection, which depends on integrin and Src activation (51), NMHC-IIA interacts with the ubiquitin ligase c-Cbl (17). The complex c-Cbl·NMHC-IIA associates with the receptor tyrosine kinase EphA2 that amplifies Src signaling to promote viral macropinocytosis (36). It is thus possible that c-Cbl, which is required for *L. monocytogenes* infection (52), associates with NMHC-IIA and c-Met to modulate *L. monocytogenes* infection through tyrosine phosphorylation events. To invade cells, *Y. pseudotuberculosis* binds β1-integrin (53), which interacts with NMHC-IIA via its cytoplasmic tail to regulate cell migration (54). As in adhesion and cell migration processes (55), during *Y. pseudotuberculosis* infection the engagement of β1-integrin leads to the activation of Src kinase (56), which could also act on NMHC-IIA triggering its tyrosine phosphorylation at the site of bacterial attachment thereby promoting *Y. pseudotuberculosis* infection.

Our data open new perspectives in the regulatory mechanisms governing NMHC-IIA functions in infection and physiological cellular processes. Further work should reveal whether NMHC-IIA-Tyr(P) affects its motor activity, binding partners, and/or the formation of actomyosin filaments.

Acknowledgments—pcDNA3-Src-KD was kindly provided by S. J. Parsons (University of Virginia). We are grateful to C. Portugal, R. Socodato, and J. B. Relvas (Glial Cell Biology, Instituto de Biologia Molecular e Celular, Porto, Portugal) for their help with Src depletion experiments. We thank F. Carvalho for the critical reading of the manuscript and members of Cabanes group for helpful discussions. We are grateful to Rui Appelberg for Ph.D. co-supervision of M. T. A. and R. C.

REFERENCES

1. Allerberger, F., and Wagner, M. (2010) Listeriosis: a resurgent foodborne infection. *Clin. Microbiol. Infect.* **16,** 16–23
2. Lecuit, M. (2005) Understanding how *Listeria monocytogenes* targets and crosses host barriers. *Clin. Microbiol. Infect.* **11,** 430–436
3. Camejo, A., Carvalho, F., Reis, O., Leitão, E., Sousa, S., and Cabanes, D. (2011) The arsenal of virulence factors deployed by *Listeria monocytogenes* to promote its cell infection cycle. *Virulence* **2,** 379–394
4. Mengaud, J., Ohayon, H., Gounon, P., Mege R-M., and Cossart, P. (1996) E-cadherin is the receptor for internalin, a surface protein required for entry of *L. monocytogenes* into epithelial cells. *Cell* **84,** 923–932
5. Shen, Y., Naujokas, M., Park, M., and Ireton, K. (2000) InIB-dependent internalization of *Listeria* is mediated by the Met receptor tyrosine kinase. *Cell* **103,** 501–510
6. Bierne, H., Gouin, E., Roux, P., Caroni, P., Yin, H. L., and Cossart, P. (2001) A role for cofilin and LIM kinase in *Listeria*-induced phagocytosis. *J. Cell Biol.* **155,** 101–112
7. Sousa, S., Cabanes, D., Bougnères, L., Lecuit, M., Sansonetti, P., Tran-Van-Nhieu, G., and Cossart, P. (2007) Src, cortactin and Arp2/3 complex are required for E-cadherin-mediated internalization of *Listeria* into cells. *Cell. Microbiol.* **9,** 2629–2643
8. Ireton, K., Payrastre, B., Chap, H., Ogawa, W., Sakaue, H., Kasuga, M., and Cossart, P. (1996) A role for phosphoinositide 3-kinase in bacterial invasion. *Science* **274,** 780–782
9. Ireton, K., Payrastre, B., and Cossart, P. (1999) The *Listeria monocytogenes* protein InlB is an agonist of mammalian phosphoinositide 3-kinase. *J. Biol. Chem.* **274,** 17025–17032
10. Kühbacher, A., Dambournet, D., Echard, A., Cossart, P., and Pizarro-Cerdá, J. (2012) Phosphatidylinositol 5-phosphatase oculocerebrorenal syndrome of Lowe protein (OCRL) controls actin dynamics during early steps of *Listeria monocytogenes* infection. *J. Biol. Chem.* **287,** 13128–13136
11. Bierne, H., Miki, H., Innocenti, M., Scita, G., Gertler, F. B., Takenawa, T., and Cossart, P. (2005) WASP-related proteins, Abi1 and Ena/VASP are required for *Listeria* invasion induced by the Met receptor. *J. Cell Sci.* **118,** 1537–1547
12. Seveau, S., Bierne, H., Giroux, S., Prévost, M. C., and Cossart, P. (2004) Role of lipid rafts in E-cadherin- and HGF-R/Met-mediated entry of *Listeria monocytogenes* into host cells. *J. Cell Biol.* **166,** 743–753
13. Bonazzi, M., Vasudevan, L., Mallet, A., Sachse, M., Sartori, A., Prevost, M. C., Roberts, A., Taner, S. B., Wilbur, J. D., Brodsky, F. M., and Cossart, P. (2011) Clathrin phosphorylation is required for actin recruitment at sites of bacterial adhesion and internalization. *J. Cell Biol.* **195,** 525–536
14. Bonazzi, M., Veiga, E., Pizarro-Cerdá, J., and Cossart, P. (2008) Successive post-translational modifications of E-cadherin are required for InlA-mediated internalization of *Listeria monocytogenes*. *Cell. Microbiol.* **10,** 2208–2222
15. Vicente-Manzanares, M., Ma, X., Adelstein, R. S., and Horwitz, A. R. (2009) Non-muscle myosin II takes centre stage in cell adhesion and migration. *Nat. Rev. Mol. Cell Biol.* **10,** 778–790
16. Arii, J., Goto, H., Suenaga, T., Oyama, M., Kozuka-Hata, H., Imai, T., Minowa, A., Akashi, H., Arase, H., Kawaoka, Y., and Kawaguchi, Y. (2010) Non-muscle myosin IIA is a functional entry receptor for herpes simplex

Downloaded from http://www.jbc.org/ at UNIVERSIDADE DO PORTO on October 8, 2015

virus-1. *Nature* **467,** 859–862
17. Valiya Veettil, M., Sadagopan, S., Kerur, N., Chakraborty, S., and Chandran, B. (2010) Interaction of c-Cbl with myosin IIA regulates Bleb associated macropinocytosis of Kaposi's sarcoma-associated herpesvirus. *PLoS Pathog.* **6,** e1001238
18. Hänisch, J., Kölm, R., Wozniczka, M., Bumann, D., Rottner, K., and Stradal, T. E. (2011) Activation of a RhoA/myosin II-dependent but Arp2/3 complex-independent pathway facilitates *Salmonella* invasion. *Cell Host Microbe* **9,** 273–285
19. Hybiske, K., and Stephens, R. S. (2007) Mechanisms of host cell exit by the intracellular bacterium *Chlamydia*. *Proc. Natl. Acad. Sci. U.S.A.* **104,** 11430–11435
20. Wei, Q., and Adelstein, R. S. (2000) Conditional expression of a truncated fragment of nonmuscle myosin II-A alters cell shape but not cytokinesis in HeLa cells. *Mol. Biol. Cell* **11,** 3617–3627
21. Reis, O., Sousa, S., Camejo, A., Villiers, V., Gouin, E., Cossart, P., and Cabanes, D. (2010) LapB, a novel *Listeria monocytogenes* LPXTG surface adhesin, required for entry into eukaryotic cells and virulence. *J. Infect. Dis.* **202,** 551–562
22. Campellone, K. G., Roe, A. J., Løbner-Olesen, A., Murphy, K. C., Magoun, L., Brady, M. J., Donohue-Rolfe, A., Tzipori, S., Gally, D. L., Leong, J. M., and Marinus, M. G. (2007) Increased adherence and actin pedestal formation by dam-deficient enterohaemorrhagic *Escherichia coli* O157:H7. *Mol. Microbiol.* **63,** 1468–1481
23. Osório, H., and Reis, C. A. (2013) Mass spectrometry methods for studying glycosylation in cancer. *Methods Mol. Biol.* **1007,** 301–316
24. Isberg, R. R., and Falkow, S. (1985) A single genetic locus encoded by *Yersinia pseudotuberculosis* permits invasion of cultured animal cells by *Escherichia coli* K-12. *Nature* **317,** 262–264
25. Kirchner, M., and Higgins, D. E. (2008) Inhibition of ROCK activity allows InlF-mediated invasion and increased virulence of *Listeria monocytogenes*. *Mol. Microbiol.* **68,** 749–767
26. Wilson, L. K., Luttrell, D. K., Parsons, J. T., and Parsons, S. J. (1989) pp60c-src tyrosine kinase, myristylation, and modulatory domains are required for enhanced mitogenic responsiveness to epidermal growth factor seen in cells overexpressing c-src. *Mol. Cell. Biol.* **9,** 1536–1544
27. Straight, A. F., Cheung, A., Limouze, J., Chen, I., Westwood, N. J., Sellers, J. R., and Mitchison, T. J. (2003) Dissecting temporal and spatial control of cytokinesis with a myosin II Inhibitor. *Science* **299,** 1743–1747
28. Pizarro-Cerdá, J., Kühbacher, A., and Cossart, P. (2012) Entry of *Listeria monocytogenes* in mammalian epithelial cells: an updated view. *Cold Spring Harb. Perspect. Med.* **2,** a010009
29. Alrutz, M. A., and Isberg, R. R. (1998) Involvement of focal adhesion kinase in invasin-mediated uptake. *Proc. Natl. Acad. Sci. U.S.A.* **95,** 13658–13663
30. Guo, A., Villén, J., Kornhauser, J., Lee, K. A., Stokes, M. P., Rikova, K., Possemato, A., Nardone, J., Innocenti, G., Wetzel, R., Wang, Y., MacNeill, J., Mitchell, J., Gygi, S. P., Rush, J., *et al.* (2008) Signaling networks assembled by oncogenic EGFR and c-Met. *Proc. Natl. Acad. Sci. U.S.A.* **105,** 692–697
31. Rikova, K., Guo, A., Zeng, Q., Possemato, A., Yu, J., Haack, H., Nardone, J., Lee, K., Reeves, C., Li, Y., Hu, Y., Tan, Z., Stokes, M., Sullivan, L., Mitchell, J., *et al.* (2007) Global survey of phosphotyrosine signaling identifies oncogenic kinases in lung cancer. *Cell* **131,** 1190–1203
32. Harney, D. F., Butler, R. K., and Edwards, R. J. (2005) Tyrosine phosphorylation of myosin heavy chain during skeletal muscle differentiation: an integrated bioinformatics approach. *Theor. Biol. Med. Model.* **2,** 12
33. Dominguez, R., Freyzon, Y., Trybus, K. M., and Cohen, C. (1998) Crystal structure of a vertebrate smooth muscle myosin motor domain and its complex with the essential light chain: visualization of the pre-power stroke state. *Cell* **94,** 559–571
34. Barfod, E. T., Moore, A. L., Melnick, R. F., and Lidofsky, S. D. (2005) Src regulates distinct pathways for cell volume control through Vav and phospholipase Cγ. *J. Biol. Chem.* **280,** 25548–25557
35. Barfod, E. T., Moore, A. L., Van de Graaf, B. G., and Lidofsky, S. D. (2011) Myosin light chain kinase and Src control membrane dynamics in volume recovery from cell swelling. *Mol. Biol. Cell* **22,** 634–650
36. Chakraborty, S., Veettil, M. V., Bottero, V., and Chandran, B. (2012) Kaposi's sarcoma-associated herpesvirus interacts with EphrinA2 receptor to amplify signaling essential for productive infection. *Proc. Natl. Acad. Sci. U.S.A.* **109,** E1163–E1172
37. Wasylnka, J. A., Bakowski, M. A., Szeto, J., Ohlson, M. B., Trimble, W. S., Miller, S. I., and Brumell, J. H. (2008) Role for myosin II in regulating positioning of *Salmonella*-containing vacuoles and intracellular replication. *Infect. Immun.* **76,** 2722–2735
38. Rajabian, T., Gavicherla, B., Heisig, M., Müller-Altrock, S., Goebel, W., Gray-Owen, S. D., and Ireton, K. (2009) The bacterial virulence factor InlC perturbs apical cell junctions and promotes cell-to-cell spread of *Listeria*. *Nat. Cell Biol.* **11,** 1212–1218
39. Mostowy, S., Bonazzi, M., Hamon, M. A., Tham, T. N., Mallet, A., Lelek, M., Gouin, E., Demangel, C., Brosch, R., Zimmer, C., Sartori, A., Kinoshita, M., Lecuit, M., and Cossart, P. (2010) Entrapment of intracytosolic bacteria by septin cage-like structures. *Cell Host Microbe* **8,** 433–444
40. Odendall, C., Rolhion, N., Förster, A., Poh, J., Lamont, D. J., Liu, M., Freemont, P. S., Catling, A. D., and Holden, D. W. (2012) The *Salmonella* kinase SteC targets the MAP kinase MEK to regulate the host actin cytoskeleton. *Cell Host Microbe* **12,** 657–668
41. Cai, Y., Rossier, O., Gauthier, N. C., Biais, N., Fardin, M. A., Zhang, X., Miller, L. W., Ladoux, B., Cornish, V. W., and Sheetz, M. P. (2010) Cytoskeletal coherence requires myosin-IIA contractility. *J. Cell Sci.* **123,** 413–423
42. Cai, Y., and Sheetz, M. P. (2009) Force propagation across cells: mechanical coherence of dynamic cytoskeletons. *Curr. Opin. Cell Biol.* **21,** 47–50
43. Veiga, E., and Cossart, P. (2006) The role of clathrin-dependent endocytosis in bacterial internalization. *Trends Cell Biol.* **16,** 499–504
44. Giannone, G., Dubin-Thaler, B. J., Rossier, O., Cai, Y., Chaga, O., Jiang, G., Beaver, W., Döbereiner, H. G., Freund, Y., Borisy, G., and Sheetz, M. P. (2007) Lamellipodial actin mechanically links myosin activity with adhesion-site formation. *Cell* **128,** 561–575
45. Cai, Y., Biais, N., Giannone, G., Tanase, M., Jiang, G., Hofman, J. M., Wiggins, C. H., Silberzan, P., Buguin, A., Ladoux, B., and Sheetz, M. P. (2006) Nonmuscle myosin IIA-dependent force inhibits cell spreading and drives F-actin flow. *Biophys. J.* **91,** 3907–3920
46. Choi, C. K., Vicente-Manzanares, M., Zareno, J., Whitmore, L. A., Mogilner, A., and Horwitz, A. R. (2008) Actin and α-actinin orchestrate the assembly and maturation of nascent adhesions in a myosin II motor-independent manner. *Nat. Cell Biol.* **10,** 1039–1050
47. Smutny, M., Cox, H. L., Leerberg, J. M., Kovacs, E. M., Conti, M. A., Ferguson, C., Hamilton, N. A., Parton, R. G., Adelstein, R. S., and Yap, A. S. (2010) Myosin II isoforms identify distinct functional modules that support integrity of the epithelial zonula adherens. *Nat. Cell Biol.* **12,** 696–702
48. Bertet, C., Sulak, L., and Lecuit, T. (2004) Myosin-dependent junction remodelling controls planar cell intercalation and axis elongation. *Nature* **429,** 667–671
49. McLachlan, R. W., Kraemer, A., Helwani, F. M., Kovacs, E. M., and Yap, A. S. (2007) E-cadherin adhesion activates c-Src signaling at cell-cell contacts. *Mol. Biol. Cell* **18,** 3214–3223
50. Organ, S. L., and Tsao, M. S. (2011) An overview of the c-MET signaling pathway. *Ther. Adv. Med. Oncol.* **3,** S7-S19
51. Chandran, B. (2010) Early events in Kaposi's sarcoma-associated herpesvirus infection of target cells. *J. Virol.* **84,** 2188–2199
52. Veiga, E., and Cossart, P. (2005) Listeria hijacks the clathrin-dependent endocytic machinery to invade mammalian cells. *Nat. Cell Biol.* **7,** 894–900
53. Isberg, R. R., and Leong, J. M. (1990) Multiple β1 chain integrins are receptors for invasin, a protein that promotes bacterial penetration into mammalian cells. *Cell* **60,** 861–871
54. Rivera Rosado, L. A., Horn, T. A., McGrath, S. C., Cotter, R. J., and Yang, J. T. (2011) Association between α4 integrin cytoplasmic tail and nonmuscle myosin IIA regulates cell migration. *J. Cell Sci.* **124,** 483–492
55. Destaing, O., Block, M. R., Planus, E., and Albiges-Rizo, C. (2011) Invadosome regulation by adhesion signaling. *Curr. Opin. Cell Biol.* **23,** 597–606
56. Bruce-Staskal, P. J., Weidow, C. L., Gibson, J. J., and Bouton, A. H. (2002) Cas, Fak and Pyk2 function in diverse signaling cascades to promote *Yersinia* uptake. *J. Cell Sci.* **115,** 2689–2700

Downloaded from http://www.jbc.org/ at UNIVERSIDADE DO PORTO on October 8, 2015

jbc The Journal of Biological Chemistry
AFFINITY SITES
ASBMB American Society for Biochemistry and Molecular Biology

Microbiology:

Src-dependent Tyrosine Phosphorylation of Non-muscle Myosin Heavy Chain-IIA Restricts *Listeria monocytogenes* Cellular Infection

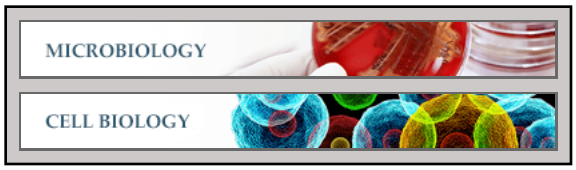

Maria Teresa Almeida, Francisco S. Mesquita, Rui Cruz, Hugo Osório, Rafael Custódio, Cláudia Brito, Didier Vingadassalom, Mariana Martins, John M. Leong, David W. Holden, Didier Cabanes and Sandra Sousa

J. Biol. Chem. 2015, 290:8383-8395.
doi: 10.1074/jbc.M114.591313 originally published online January 29, 2015

Access the most updated version of this article at doi: 10.1074/jbc.M114.591313

Find articles, minireviews, Reflections and Classics on similar topics on the JBC Affinity Sites.

Alerts:
- When this article is cited
- When a correction for this article is posted

Click here to choose from all of JBC's e-mail alerts

This article cites 56 references, 25 of which can be accessed free at
http://www.jbc.org/content/290/13/8383.full.html#ref-list-1

Downloaded from http://www.jbc.org/ at UNIVERSIDADE DO PORTO on October 8, 2015

Epithelial keratins modulate cMet expression and signaling and promote InlB-mediated Listeria monocytogenes infection of HeLa cells

Rui Cruz[1, 2], Isabel Pereira-Castro[3], Maria Teresa Almeida[1], Alexandra Moreira[2, 3], Didier Cabanes[1], Sandra Sousa[1*]

[1]i3S, Instituto de Investigação e Inovação em Saúde, Portugal, [2]Instituto de Ciências Biomédicas Abel Salazar (ICBAS), Universidade do Porto, Portugal, [3]i3S, Instituto de Investigação e Inovação em Saúde, Portugal

Submitted to Journal:
Frontiers in Cellular and Infection Microbiology

Article type:
Original Research Article

Manuscript ID:
336236

Received on:
04 Jan 2018

Revised on:
27 Mar 2018

Frontiers website link:
www.frontiersin.org

In review

Conflict of interest statement

The authors declare that the research was conducted in the absence of any commercial or financial relationships that could be construed as a potential conflict of interest

Author contribution statement

RC, DC and SS conceived and designed the experiments. RC and MTA performed the experiments. RC, IPC, AM, DC and SS analysed the data. RC, DC and SS wrote the manuscript.

Keywords

Intermediate Filaments, Keratins, CMET signaling, Listeria monocytogenes, cellular infection, mRNA stability, Gene Expression

Abstract

Word count: 221

The host cytoskeleton is a major target for bacterial pathogens during infection. In particular, pathogens usurp the actin cytoskeleton function to strongly adhere to the host cell surface, to induce plasma membrane remodelling allowing invasion and to spread from cell to cell and disseminate to the whole organism. Keratins are cytoskeletal proteins that are the major components of intermediate filaments in epithelial cells however, their role in bacterial infection has been disregarded. Here we investigate the role of the major epithelial keratins, keratins 8 and 18 (K8 and K18), in the cellular infection by Listeria monocytogenes. We found that K8 and K18 are required for successful InlB/cMet-dependent L. monocytogenes infection, but are dispensable for InlA/E-cadherin-mediated invasion. Both K8 and K18 accumulate at InlB-mediated internalization sites following actin recruitment and modulate actin dynamics at those sites. We also reveal the key role of K8 and K18 in HGF-induced signaling which occurs downstream the activation of cMet. Strikingly, we show here that K18, and at a less extent K8, controls the expression of cMet and other surface receptors such TfR and integrin β1, by promoting the stability of their corresponding transcripts. Together, our results reveal novel functions for major epithelial keratins in the modulation of actin dynamics at the bacterial entry sites and in the control of surface receptors mRNA stability and expression.

Funding statement

This work receives funding from Norte-01-0145-FEDER-000012 - Structured program on bioengineered therapies for infectious diseases and tissue regeneration, supported by Norte Portugal Regional Operational Programme (NORTE 2020), under the PORTUGAL 2020 Partnership Agreement, through the European Regional Development Fund (FEDER). RC received an FCT Doctoral Fellowship (SFRH/BD/90607/2012) and IP-C a FCT Post-Doctoral Fellowship (SFRH/BPD/107901/2015) through FCT/MEC co-funded by QREN and POPH (Programa Operacional Potencial Humano). SS was supported by FCT Investigator program (COMPETE, POPH, and FCT). We thank IBMC facilities for technical assistance.

Ethics statements

(Authors are required to state the ethical considerations of their study in the manuscript, including for cases where the study was exempt from ethical approval procedures)

Does the study presented in the manuscript involve human or animal subjects: No

Introduction

Intracellular pathogens exploit the host machinery to promote and establish infection. The host cytoskeleton is one of the preferential targets of pathogens and plays essential roles in cellular infection (Haglund and Welch, 2011; Carabeo, 2011; de Souza Santos and Orth, 2015). The role of host actin cytoskeleton in bacterial pathogenesis is by far the most documented (Colonne *et al.*, 2016). Actin filaments and their polymerization machinery are hijacked by several human pathogens at different stages of the infection process. In particular subversion of actin is critical for: 1) stable adhesion of pathogenic *Escherichia coli* (EPEC and EHEC) to the host cell surface, through the formation of actin-rich pedestals (Goosney *et al.*, 2000; Gruenheid *et al.*, 2001; Stradal and Costa, 2017); 2) invasion of epithelial cells by a variety of intracellular bacteria such as *Salmonella typhimurium*, *Shigella flexneri* and *Listeria monocytogenes* which induce actin cytoskeleton rearrangements and host membrane remodeling (Bierne *et al.*, 2005; Sousa *et al.*, 2007; de Souza Santos and Orth, 2015; Valencia-Gallardo *et al.*, 2015; Rolhion and Cossart, 2017); and 3) intracellular movement of cytosolic pathogens such as *S. flexneri*, *Rickettsia conorii* and *L. monocytogenes* which are able to elicit the formation of actin comet tails to promote cell-to-cell spread (Bernardini *et al.*, 1989; Mounier *et al.*, 1990; Welch *et al.*, 1997; Heinzen *et al.*, 1999; Egile *et al.*, 1999; Czuczman *et al.*, 2014; Kuehl *et al.*, 2015).

In contrast to actin, the role of intermediate filaments (IFs), in particular keratins, during bacterial infection is poorly characterized. IFs are also part of the host cytoskeleton and include a large group of proteins that share structural features and form apolar 10 nM wide fibrous filaments (Goldman *et al.*, 2012). Keratins are the largest subfamily of IFs, mainly expressed in the cytoplasm of epithelial cells and their expression profile is regulated in a tissue and differentiation dependent manner (Loschke *et al.*, 2015). Type I and type II keratins form heterodimers and organize into filaments that ensure structural integrity of epithelia and confers mechanical resilience to stress (Haines and Lane, 2012). In epithelial cells, Keratin 8 (K8) and Keratin 18 (K18) are the most common keratin pair (Moll *et al.*, 2008). Besides their biomechanical functions, several studies point keratins as important players in regulatory mechanisms defining health and disease (Pan *et al.*, 2012). K8 and K18 participate in cell cycle regulation by associating with and modulating the distribution of 14-3-3 adaptor proteins (Eriksson *et al.*, 2009). K17 was also reported to interact with 14-3-3 proteins modulating protein synthesis by interfering with mTOR signaling (Kim *et al.*, 2006). Additionally, mice lacking type II keratins display mislocalization of glucose transporters and downregulation of the protein synthesis machinery (Kellner and Coulombe, 2009; Vijayaraj *et al.*, 2009). Keratin defects exacerbate cell death through increased surface expression of cell death receptors and enhanced activation of apoptotic signaling cascades (Caulin *et al.*, 2000; He *et al.*, 2002; Gilbert *et al.*, 2012). Keratins are also increasingly regarded as stress proteins protecting cells and tissues from stress and injury (Toivola *et al.*, 2010).

In the context of infection, keratins are targeted for degradation during adenovirus and *Chlamydia* infection (Chen *et al.*, 1993; Savijoki *et al.*, 2008), facilitate adhesion of EPEC to HeLa cells (Batchelor *et al.*, 2004), and promote internalization of *Salmonella* (Carlson *et al.*, 2002) and intracellular replication of *Trypanosoma cruzi* (Claser *et al.*, 2008). Interestingly, a recent study showed that in corneal epithelial cells keratin 6a is processed into antimicrobial fragments by the ubiquitin-proteasome system to protect the host against infection (Chan *et al.*, 2018). Despite these observations, the molecular and functional details behind keratin involvement in bacterial pathogenesis remain elusive

(Geisler and Leube, 2016) and the possible role of keratins in *L. monocytogenes* infection was never addressed.

L. monocytogenes is a facultative intracellular gram-positive pathogen adapted to thrive in diverse environments (Freitag *et al.*, 2009). In humans, it causes listeriosis, a pernicious foodborne disease (Swaminathan and Gerner-Smidt, 2007) that relies on *L. monocytogenes* capacity to enter and survive into epithelial non-phagocytic cells, through the expression of an arsenal of virulence factors (Camejo *et al.*, 2011). *L. monocytogenes* internalization into non-phagocytic cells is mainly driven by the interaction of the bacterial surface proteins InlA and InlB, with their specific host receptors, respectively E-cadherin and cMet (Mengaud *et al.*, 1996; Shen *et al.*, 2000; Pizarro-Cerdá *et al.*, 2012). The engagement of these host receptors by the bacterial ligands triggers the activation of intracellular signaling pathways that lead to actin polymerization, myosin recruitment and further membrane remodeling, ultimately resulting in the internalization of the bacteria (Ireton *et al.*, 1996; Ireton *et al.*, 1999; Bierne *et al.*, 2001; Sousa *et al.*, 2004; Sousa *et al.*, 2007; Pizarro-Cerdá *et al.*, 2012; Almeida *et al.*, 2015).

In this study, we assessed the role of epithelial keratins K8 and K18, during *L. monocytogenes* infection. We found that both K8 and K18 are required for successful InlB/cMet-mediated internalization of *L. monocytogenes* and HGF-induced signaling. We also observed that K8 and K18 modulate actin dynamics during InlB-driven internalization. Interestingly, we also showed here that K18, and to a lesser extent K8, control the expression of cMet and other surface receptors such as Transferrin Receptor (TfR) and Integrin β1. Indeed, K18 confers transcript stability, thus regulating post-transcriptionally the expression of such membrane proteins.

Materials and Methods

Reagents and antibodies

Primary antibodies used are listed in Table 1. Goat anti-mouse HRP or anti-rabbit HRP (P.A.R.I.S.) secondary antibodies were used at 1:2000 for immunoblotting. For immunofluorescence, secondary antibodies goat anti-rabbit or anti-mouse Alexa Fluor 488 (Invitrogen) and goat anti-mouse or anti-rabbit Cy3 (Jackson Immunoresearch) were used at 1:300. Actin was labeled with Alexa Fluor 647 phalloidin (Invitrogen) or Phalloidin-Tetramethylrhodamine B isothiocyanate (TRITC, Sigma Aldrich). DNA was labeled with 2-(4-Amidinophenyl)-6-indolecarbamidine dihydrochloride (DAPI, Sigma Aldrich). Concanamycin A, MG132 and Actinomycin D were obtained from Sigma Aldrich. HGF was purchased from Peprotech.

Bacterial Strains and Cell Lines

L. monocytogenes EGDe strain was grown at 37ºC with shaking in brain heart infusion (BHI; BD-Difco). *L. innocua* InlB was grown in BHI supplemented with 5 µg/ml erythromycin. *E. coli* K12-*inv* was grown at 37ºC with shaking in lysogeny broth (LB) supplemented with 100 µg/ml ampicillin.

HeLa cells (ATCC CCL-2) were cultured in DMEM supplemented with glucose (4.5 g/l), L-glutamine and 10% fetal bovine serum (FBS, Biowest). Caco-2 cells (ATCC HTB-37) were maintained in EMEM supplemented with 20% FBS, L-glutamine, sodium pyruvate and nonessential amino acids. Cells were maintained at 37°C in a 5% CO_2 atmosphere. Cell culture media and supplements were from Lonza.

Bacterial infections

Cell infections were performed as described (Reis *et al.*, 2010). For adhesion experiments, bacteria in exponential phase of growth were washed and inoculated at a multiplicity of infection (MOI) of 50. After 30 min, cells were washed 5 times with phosphate buffered saline (PBS), lysed in 0.2% Triton-X-100 and serial dilutions were plated for quantification of viable bacteria (colony forming units-CFU). For invasion assays, inoculum was prepared as above and cells were infected for 60 min, washed and incubated with medium supplemented with 20 µg/ml gentamicin for 90 min. Cells were washed, lysed with 0.2% Triton-X-100 and serial dilutions plated for CFU counting. For immunofluorescence scoring of adhered and intracellular *L. innocua*-InlB, HeLa cells were inoculated at a MOI of 50 for 30 min, washed and fixed. Before permeabilization, extracellular bacteria were labeled with a rabbit polyclonal antibody raised against *L. innocua* (R6, kindly provided by Prof Pascale Cossart, Institut Pasteur) and an appropriate secondary antibody. Cells were then permeabilized with 0.1% Triton X-100 and total bacteria were labelled with R6 and a secondary antibody coupled to a different fluorochrome. Total and extracellular bacteria were counted under the microscope. For intracellular replication assays, cells were infected with a MOI of 1 for 60 min, washed and incubated with medium complemented with 20 mg/ml gentamicin for 90 min, washed and lysed 2.5, 5, 7, 9 and 12 h after infection. Adhesion and invasion assays were performed in triplicate and repeated at least 3 times. Replication assays were performed twice in duplicate. For immunofluorescence experiments, cells were infected with *L. innocua* InlB (MOI of 50), washed in PBS and fixed in 3% paraformaldehyde.

Transfection of siRNA Duplexes

HeLa cells were seeded in 24 or 6 well plates and transfected with 46 nM control siRNA-D (sc-44232, Santa Cruz Biotechnology) or with specific siRNAs for K8 or K18 depletion

(oligo sequences on Table 2). For partial depletion, we used 13.8 nM of siRNA duplexes. Transfection was performed with HiPerFect (Qiagen) immediately after cell seeding, according to the manufacturer's instructions. Assays were performed 72 h pot-transfection. Transfection of Caco-2 cells was performed with Amaxa Cell line Nucleofector Kit T (Lonza) using program B-024 and following manufacturer's instructions.

Immunoblotting

Protein samples were diluted in Laemmli buffer containing 5% β-mercaptoethanol, resolved on SDS-PAGE gels and transferred to nitrocellulose membranes (Bio-Rad Laboratories). Membranes were blocked in 4% bovine serum albumin (BSA; Sigma Aldrich) or 5% skimmed milk dissolved in TBS-Triton (150 mM NaCl, 20 mM Tris-HCl, pH 7.4, and 0.1% Triton X-100) for 1 h. Primary antibodies were diluted in 2.5% skimmed milk or 4% BSA and incubated overnight at 4ºC, incubation with HRP-conjugated secondary antibodies was performed at room temperature for 1h. ECL (Thermo Scientific) or SuperSignal West Dura Extended Duration Substrate (Pierce) were used for detection of signal on X-ray films (Thermo Scientific) or digitally acquired in a ChemiDoc XRS+ system (Bio-Rad Laboratories).

Immunoprecipitation assays

Per condition, 2 x 10^6 cells were washed twice with phosphate-buffered saline (PBS) and serum-starved for 8 h at 37°C and 5% CO_2. Then, cells were either left untreated or incubated with 150ng/ml HGF for 5 min. Cells were then washed twice with ice-cold PBS and lysed in 300 µl of lysis buffer (1% NP-40, 50 mM Tris pH 7.5, 150 mM NaCl, 2 mM EDTA, 1 mM AEBSF, PhosSTOP (Roche Pharmaceuticals) and Complete Protease Inhibitor Cocktail (Roche Pharmaceuticals)). Lysates were centrifuged at 15 000 g for 10 min at 4°C and immunoprecipitated with 0.7 µg of anti-phosphotyrosine antibody (4G10) overnight at 4°C. Immune complexes were captured with 50 µl of PureProteome Protein A magnetic beads (Millipore) at 4°C and washed three times with wash buffer (0.2% NP-40, 50 mM Tris pH 7.5, 150 mM NaCl, 2 mM EDTA, 1 mM AEBSF, PhosSTOP, Complete Protease Inhibitor Cocktail). Immunoprecipitated proteins were eluted and boiled in Laemmli buffer.

Cell surface biotinylation assay

Cell surface protein biotinlyation was performed using the EZ-Link Sulfo-NHS-Biotinylation kit (Thermo Scientific) as described in (Martins *et al.*, 2012) and accordingly to manufacturer's protocol. In brief, 2 x 10^6 cells were washed with ice cold PBS (pH 8), incubated with 2 mM Sulfo-NHS-biotin (2 h at 4ºC), washed with cold 100mM glycine in PBS (pH 7.2), harvested, and lysed in RIPA (sc-364162, Santa Cruz Biotechnology). Cell extracts (90 µg) were incubated with 50 µl of neutravidin agarose resin (Thermo Scientific) overnight at 4ºC, with rotation. Resin was washed and captured biotinylated proteins were eluted with Laemmli buffer.

Immunofluorescence microscopy

Cells were fixed in 3% paraformaldehyde (10 min), quenched with 20 mM NH_4Cl (1 h), permeabilized with 0.2% Triton X-100 (6 min), washed and blocked with 1% BSA in PBS. Antibodies were diluted in the blocking buffer. Coverslips were incubated with primary antibodies (1 h), washed in PBS, incubated with secondary antibodies, phalloidin TRITC or Alexa 647 and DAPI for 45 min, and mounted onto microscope slides with Aqua-Poly/Mount. Images were analyzed and collected with an epifluorescent Zeiss Axio

Imager Z1 microscope or an Olympus BX63 microscope. When necessary, Z-stacks were deconvoluted with Huygens Professional Software (SVI, Netherlands) and projected with ImageJ software (NIH).

Ruffle formation assays
Cells were serum starved for 7 h, stimulated with 150ng/ml HGF for 5 and 10 min, fixed in 3% paraformaldehyde (PFA) and processed for immunofluorescence. Cells with at least one actin rich membrane ruffle were scored as ruffle-positive, cells with no ruffles were considered ruffle-negative. Data were obtained from four independent experiments, for which at least 180 cells/condition were analyzed.

Rates of total protein synthesis
Cells ($2x10^6$) were labelled with ^{35}S-methionine (22.5 uCi/ml, PerkinElmer) in methionine free DMEM (2 h at 37ºC), washed twice with PBS and lysed in RIPA buffer. Protein samples diluted in Laemmli buffer were loaded into a 10% polyacrylamide gel and resolved by SDS-PAGE, followed by autoradiography.

Quantitative real-time PCR
Total RNAs were isolated using TripleXtractor (GRiSP), following manufacturer's protocol. Purified RNAs (1 µg) were reverse transcribed with iScript cDNA Synthesis Kit (Bio-Rad Laboratories). Quantitative real-time PCR (qRT-PCR) was performed in 10 µl reactions containing 5 µl iTaq Universal SYBR Green Supermix (Bio-Rad Laboratories), 1 µl of cDNA and 0.1 µl of 10 µM forward and reverse primers (Table 2), using the following protocol: 3 min (95ºC), followed by 40 cycles of 10 s (95ºC), 20 s (55.6ºC) and 20 s (72ºC). Each target gene was analyzed in triplicate and blank control was included for each primer pair. The comparative threshold method (ΔΔCt) was used to analyze the amplification data after normalization of the test and control sample expression values to a housekeeping reference gene (GAPDH).

mRNA stability assays
Cells were incubated with Actinomycin D (5 µg/ml) for 1 and 2 h to inhibit *de novo* RNA synthesis. Cells were harvested and RNAs isolated, reverse transcribed and analyzed by qRT-PCR. GAPDH was used as reference gene and fold changes were normalized to the untreated control. At least three independent experiments were performed for each gene of interest.

InlB-coated beads assays
Purified InlB (350 µg) was covalently coupled to 200 µl of a 4% aqueous suspension of 1.0 µm carboxylated modified latex beads (Thermo Scientific), following manufacturer's instructions. To synchronize the uptake, HeLa cells were incubated with InlB-coated beads at 4ºC, centrifuged (5 min at 320g) and incubated at 37ºC. Cells were washed in ice cold PBS and processed for immunofluorescence. At least 20 cells and more than 150 beads were analyzed per condition, in at least three independent experiments. To assess internalization, extracellular beads were stained with anti-InlB B4-6 antibody (Braun *et al.*, 1999) before cell permeabilization. Samples were then analyzed in a high-throughput widefield fluorescence microscope (IN Cell Analyzer 2000, GE Healthcare). Total beads number was quantified in brightfield. Per condition, at least 500 cells and 5000 beads were analyzed.

Statistical Analyses

Statistical analyses were performed with Prism 7 software (GraphPad) using: two-tailed unpaired Student's *t* test for comparison of means between two samples, one-tailed *t* test for comparisons with samples arbitrarily fixed to 100 and one-way ANOVA with Dunnett's *post hoc* analysis to compare different means in relation to a control sample. Differences were not considered statistically significant for p value≥0.05

Results

K8 and K18 favor InlB/cMet-mediated *L. monocytogenes* cellular invasion

We assessed the relevance of keratins during *L. monocytogenes* cellular infection of epithelial cell lines, which mainly express K8 and K18 (Moll *et al.*, 2008). HeLa and Caco-2 cells were depleted for K8 and/or K18 through an siRNA approach and intracellular *L. monocytogenes* numbers were evaluated by gentamicin protection assays (Almeida *et al.*, 2015). Numbers of intracellular bacteria were significantly decreased in K8, K18 and K8/K18-depleted HeLa cells, as compared to control cells (Fig 1a). In turn, in Caco-2 cells, the depletion of K8 and/or K18 had no effect on the number of intracellular bacteria (Supp Fig 1). Furthermore, K8 and/or K18 depletion in HeLa had no impact on the ability of bacteria to adhere to the cells (Fig 1b). The efficiency of K8 and/or K18 depletion in the different cell lines was confirmed by western blot analysis, using GAPDH as loading control (Supp Fig 2). Altogether these data indicate that K8 and K18 are required for internalization of *L. monocytogenes* in HeLa cells, but not in Caco-2 cells.

L. monocytogenes invasion of epithelial cells is mainly driven by the interaction of the bacterial surface proteins InlA and InlB with their host receptors E-cadherin and cMet, respectively (Mengaud et al., 1996; Shen et al., 2000). In HeLa cells *Listeria* internalization largely occurs through the InlB/cMet axis, while in Caco-2 cells invasion relies essentially on the InlA/E-cadherin interplay (Shen *et al.*, 2000; Sousa *et al.*, 2007). The observation that keratins are specifically required for *L. monocytogenes* infection of HeLa, but not Caco-2 cells suggested that K8 and K18 are particularly important for the InlB/cMet-mediated internalization pathway. To confirm this, we evaluated in K8- and/or K18-depleted HeLa cells the internalization of *Listeria innocua* expressing InlB (*L. innocua*-InlB), which invades non-phagocytic cells exclusively through the InlB pathway (Braun *et al.*, 1999). Similarly to what we observed for *L. monocytogenes*, internalization of *L. innocua*-InlB was compromised in K8- and/or K18-depleted cells (Fig 1c and d), thus confirming that K8 and K18 are required for efficient InlB/cMet-mediated entry of *L. monocytogenes* into human epithelial cells. Finally, we found that K8 and K18 are not involved in intracellular replication of *L. monocytogenes* in HeLa cells (Supp Fig 3). Taken together, these results demonstrate that K8 and K18 play a key role in InlB/cMet-mediated internalization of *L. monocytogenes*.

K8 and K18 accumulate at InlB-mediated internalization sites

To further characterize the role of K8 and K18 in InlB-driven invasion of *Listeria*, we investigated their cellular distribution in infected cells. HeLa cells were infected with *L. innocua*-InlB, fixed and processed for immunofluorescence. K8, K18 and cMet were immunolabelled using specific antibodies, DNA was stained using DAPI and actin was detected by phalloidin staining. K8 or K18 accumulated at the vicinity of the bacteria within minutes after infection (Fig 2a), together with F-actin and cMet, two proteins already described to accumulate at sites of entering bacteria (Bierne *et al.*, 2001). Quantifications of actin, K8 and K18 recruitments to the bacterial entry site were performed at different time points and are shown in Fig 2b. Although K8 and K18 recruitments were less frequent than actin recruitments, these observations further support the involvement of K8 and K18 in early steps of *Listeria* cellular invasion.

K8 and K18 modulate actin dynamics at InlB-mediated entry sites

The entry process of *L. monocytogenes* into epithelial cells is a dynamic process that engages actin rearrangements and membrane remodeling (Pizarro-Cerdá *et al.*, 2012). To

gain better understanding of the dynamics of keratin recruitment to the sites of internalization and to further dissect the role of keratins in such process, we used InlB-coated beads whose entry mimics the InlB/cMet-mediated *L. monocytogenes* internalization (Braun *et al.*, 1999; Pizarro-Cerdá *et al.*, 2002). HeLa cells were incubated with InlB-coated beads for different periods of time and processed for immunofluorescence analysis. As we reported for *L. innocua*-InlB (Fig 2), K8 and K18 accumulated around entering InlB-coated beads (Fig 3a). We quantified the percentage of InlB-coated beads associated with actin, and K8 and K18 recruitments at different incubation time points (Fig 3b). As previously reported (Bierne *et al.*, 2001), actin filaments rapidly accumulate at the vicinity of InlB-coated beads. Actin recruitment peaked at 15 minutes, with 60% of the beads associated to actin filaments, and promptly decreased afterwards. In turn, K8 and K18 recruitments to the vicinity of InlB-coated beads appeared later, being maximum at 30 minutes and sustained for longer incubation periods (Fig 3b). These data indicate that actin and keratin recruitments are sequential events during the internalization process of beads. To assess the potential role of K8/K18 on actin dynamics, HeLa cells depleted for K8 or K18 were incubated with InlB-coated beads for different periods of time, processed for immunofluorescence and actin recruitments around beads were quantified. In accordance to our results in Fig 3b, in control cells actin rings surrounding InlB-coated beads peaked at 15 minutes after incubation to then rapidly decrease at later time points (Fig 3c). In K8- and K18-depleted cells, while the percentage of InlB-coated beads associated to actin rings were equivalent to those of control cells at 15 minutes, they remain significantly higher at 30 minutes (Fig 3c). In cells partially depleted for K8 or K18 the levels of InlB-beads associated to actin rings are intermediate between those of control and more robustly depleted cells (Supp Fig 4). Thus, the persistence of polymerized actin around entering InlB-beads depends on the expression levels of K8 and K18. Low K8 and K18 expression increases the time during which polymerized actin associates with InlB-entering beads. These data strongly suggest a role for K8/K18 in the regulation of actin depolymerization necessary for the effective internalization of particles (Bierne *et al.*, 2001).

K8 and K18 control HGF/cMet-mediated signaling

The data obtained in the context of *Listeria* InlB/cMet-mediated internalization suggested a role for K8/K18 in cMet downstream signaling. It was previously demonstrated that InlB triggers cMet similarly to its natural ligand, the hepatocyte growth factor (HGF) (Li *et al.*, 2005). Indeed, both HGF and InlB bind and activate cMet, and share common downstream signaling cascades that trigger MAPK and PI3-kinase pathways to promote either cell migration and proliferation or bacterial internalization (Ireton *et al.*, 1996; Tang *et al.*, 1998; Shen *et al.*, 2000; Copp *et al.*, 2003). To assess the potential role of K8/K18 in the HGF/cMet signaling pathway, we analyzed and quantified the formation of HGF-induced membrane ruffles in control, K8- and K18-depleted cells. Cells were stimulated with HGF for different time periods, fixed and processed for immunofluorescence. Membrane ruffles were detected through actin staining, which locally accumulate at the cortex of the cells undergoing ruffling (Fig 4a). Cells with at least one actin-rich membrane ruffle were scored as positive. While in control cells, HGF stimulation quickly induced the formation of actin rich ruffles that peaked at 5 minutes, in K8-and K18-depleted cells ruffle formation was compromised even at longer time points (Fig 4b). These data indicate that K8 and K18 also play a role in HGF-induced cMet signaling.

To further dissect the role of K8/K18 in cMet downstream signaling, we assessed HGF-dependent activation of PI3-kinase (PI3K) in control, K8 and K18-depleted cells. Serum-starved cells were incubated with HGF for 5 minutes, washed and lysed. Cell lysates were

subjected to anti-phosphotyrosine immunoprecipitation and revealed for the PI3K p85 subunit. Western blots of phosphotyrosine enriched protein fractions showed decreased levels of the PI3K p85 subunit in K8/K18-depleted cells (Fig 4c), indicating an impaired association of PI3K with tyrosine phosphorylated proteins in absence of keratins and suggesting a defect in PI3K activation. In addition, K18-depleted cell lysates were directly subjected to immunoblot analysis to detect phosphorylation of Akt on serine 473 (P-Akt, S473), a direct downstream target of PI3K activity (Basar *et al.*, 2005; Vanhaesebroeck *et al.*, 2012; Gessain *et al.*, 2015). As expected, in control cells HGF stimulation induced robust phosphorylation of Akt, which is extensively compromised in K18-depleted cells (Fig 4d, e). Together, these results demonstrate that K18, and to a lesser extent K8, are important players in the cMet-mediated signaling cascade and suggest that K8/K18 are involved upstream the activation of PI3K.

cMet expression is dependent on K8 and K18

To identify the precise role of K8/K18 in cMet-mediated signaling upstream PI3K activation, we assessed the expression and activation levels of cMet. Indeed, both InlB-mediated *L. monocytogenes* internalization and the formation of HGF-triggered membrane ruffles rely on the surface expression and auto-phosphorylation of cMet on tyrosine residues (Shen *et al.*, 2000). Interestingly, K8 and K18 were reported as modulators of the expression and/or localization of surface proteins such as the apoptotic receptor Fas, the chloride transporter DRA and the cystic fibrosis transmembrane conductance regulator (CFTR) (Gilbert *et al.*, 2001; Duan *et al.*, 2012; Asghar *et al.*, 2016). Thus, this raises the possibility that keratins may also modulate cMet expression and/or activity. We evaluated the levels of total cMet expression and activation upon HGF stimulation in whole cell lysates of control, K8- and K18-depleted cells. Surprisingly, we observed that cells depleted for K8 or K18 displayed reduced levels of total cMet (Fig 5a-c). Nevertheless, upon HGF stimulation cMet activation, as measured by phosphotyrosine immunoprecipitation assays, was detected at variable extents in those cells (Fig 5a). To determine if the low levels of total cMet expression observed in K8- and K18- depleted cells also result in a reduction of cell surface associated cMet, we specifically analyzed and quantified cell surface expression of cMet by performing biotinylation assays. Surface proteins of control, K8- and K18-depleted cells were labelled using a membrane-impermeable biotinylation reagent, recovered with neutravidin-coupled beads and analyzed by immunoblot. In agreement with the observed reduced levels of total cMet expression, K8 or K18 depletion resulted in decreased levels of cMet at the cell surface (Fig 5b, c). Altogether, these data clearly indicate that K8 and K18 control the global and surface expression of cMet, thus impacting cMet-mediated signaling events elicited by ligands such as HGF and *L. monocytogenes* InlB.

K18 controls the expression of other transmembrane receptors

Given that K8 and K18 were already reported as modulators of expression of surface proteins (Duan *et al.*, 2012; Asghar *et al.*, 2016) and taking into account our data, we hypothesized that K8 and K18 may have a broad role in controlling the expression of surface receptors. To investigate this hypothesis, we assessed the impact of K8 and K18 on the expression and surface localization of transferrin receptor (TfR) and integrin β1 in HeLa cells. Immunoblot analysis of whole cell lysates and surface biotinylated fractions revealed that K18 depletion resulted in a striking decrease of total and cell surface associated levels of both TfR and integrin β1 (Fig 6a-c). K8 depletion lead to a mild reduction of total and surface localized TfR and had no significant effect on the expression of integrin β1 (Fig 6a-c). Additionally, we performed similar experiments in

Caco-2 cells and observed that K18 depletion also lead to a reduction of total and surface levels of cMet, TfR and integrin β1 (Supp Fig 5), suggesting that the mechanism through which K18 regulates the expression of these proteins is conserved in different cellular systems. Interestingly, the expression of E-cadherin is not dependent on keratins (Supp Fig 4).
To functionally assess the impact of integrin β1 downregulation induced by K18 depletion, we measured levels of internalization of *E.coli* K12 expressing the *Yersinia* invasin (K12-*inv*), which is strictly dependent on the interaction of the bacterial invasin with the host integrin β1 (Isberg and Leong, 1990). As expected, K18-depleted cells showed reduced levels of intracellular K12-*inv* (Fig 6d). Taken together, these results demonstrate that K18, and to a lesser extend K8, control the expression of some cell surface receptors, in turn modulating signaling events taking place downstream the engagement of these receptors.

Protein synthesis and stability do not depend on K18 expression
The decrease of total levels of cMet, TfR and integrin β1 observed in K18-depleted cells lead us to put forward the possibility that protein synthesis would be impaired in these cells. Indeed, K8/18 depletion was reported to lead to reduced protein synthesis in human H4 neuroglioma cells (Galarneau *et al.*, 2007). In addition, mTOR signaling and, consequently, protein synthesis were shown to be impaired in keratinocytes lacking Keratin 17 (Kim *et al.*, 2006). We thus assessed if mTOR signaling and global protein synthesis were compromised in K18-depleted HeLa cells, which would account for the reduced levels of cMet, TfR and integrin β1. The ribosomal protein S6 is the target of p70S6K, a major mTOR effector (Magnuson *et al.*, 2012), and S6 phosphorylation is thus used as a readout for mTOR activity (Biever *et al.*, 2015; González *et al.*, 2015). To evaluate the involvement of K18 in mTOR signaling activity, we thus analyzed the level of phosphorylated S6 in control and K18-depleted HeLa cells. S6 phosphorylation was detected in both control and K18-depleted cells (Fig 7a), indicating that mTOR activity is not compromised and suggesting that mTOR-dependent protein synthesis is not impaired in absence of K18. To assess the rate of bulk protein synthesis, control or K18-depleted cells were incubated with radiolabeled methionine to be incorporated into newly synthesized proteins. Total protein extracts were resolved by SDS-PAGE and labelled proteins detected by autoradiography. No major defect was detected in K18-depleted as compared to control cells (Fig 7b), indicating that the global initiation rate of translation is not compromised in cells lacking K18. The same samples were used in immunoblot to confirm the down-regulation of cMet, integrin β1 and TfR expression in K18-depleted cells (Fig 7c). These observations demonstrate that K18 does not impact significantly protein translation and *de novo* synthesis and suggest that other mechanisms should govern the K18-dependent expression of cMet, TfR and integrin β1.
Interestingly, K18 was previously reported to enhance the stability of the surface protein CFTR (Duan *et al.*, 2012). We thus hypothesized that K18 could promote the stability of cMet, integrin β1 and TfR by minimizing their degradation. To investigate this hypothesis, control and K18-depleted HeLa cells were treated with the lysosomal inhibitor concanamycin A alone or together with the proteosomal inhibitor MG132 for different time periods. Cell extracts were immunoblotted for cMet and TfR. In both conditions tested, control and K18-depleted cells behaved similarly and no significant accumulation of cMet, integrin β1 and TfR was detected upon blockage of protein degradation (Fig 7d).

Altogether, these results indicate that the downregulation in the expression of cMet, TfR and integrin β1 detected in K18-depleted cells is not due to a defect on protein synthesis or stability.

K18 promotes transcripts stability

Besides translation and protein stability, regulation at the transcriptional level represents another mechanism to control protein expression. We therefore assessed if K18 depletion had an impact on transcript levels of the different receptors by qRT-PCR on mRNAs extracted from control and K18-depleted HeLa cells. *cMet*, *TfR* and *integrin β1* mRNA levels were strongly decreased in K18-depleted cells (Fig 8a), with reductions ranging from 54% for *cMet* to up to 94% for *TfR*. Such reduced mRNA levels should therefore be responsible for the reduced cMet, TfR and integrin β1 protein levels detected in K18-depleted cells.

Decreased steady state mRNA levels may result from a reduction in transcription or from higher instability of the mRNA (Wu and Brewer, 2012). To assess the involvement of K18 in the stability of *cMet*, *TfR* and *integrin β1* transcripts, we measured mRNA decay in cells treated with the transcription inhibitor Actinomycin D. Control and K18-depleted HeLa cells were left untreated (0 h) or incubated with Actinomycin D for 1 and 2 h, total RNAs were extracted and analyzed by qRT-PCR. We observed that *cMet*, *TfR* and *integrin β1* mRNAs consistently displayed a higher rate of decay in K18-depleted cells (Fig 8b), thus, indicating higher instability of these transcripts in cells lacking K18.

Taken together, these results demonstrate that K18 confers stability to specific transmembrane receptor mRNAs thus ensuring steady state protein levels.

Discussion

Manipulation of the host cell cytoskeleton is a hallmark of the cellular infection by several human bacterial pathogens. Intermediate filaments were reported to participate in the infection process of different pathogens (Geisler and Leube, 2016), however the molecular details remain sparse. Here we demonstrate for the first time that epithelial K8 and K18 play a dual role during *L. monocytogenes* cellular infection. We found that K8 and K18 are specifically required for the successful InlB/cMet-mediated *L. monocytogenes* cell invasion by modulating the actin dynamics at the entry site and by controlling the expression of *cMet* itself. Interestingly, K18 also appeared to control the expression of other cell surface receptors, such as TfR and integrin β1, by promoting mRNA stability, thus suggesting a broader role for keratins in the regulation of gene expression.

During infection, K8 and/or K18 were previously shown to assist toxin internalization (Nava-Acosta and Navarro-Garcia, 2013), to favour intracellular pathogen replication (Claser *et al.*, 2008) and to allow stable pathogen docking to the host cell surface (Carlson *et al.*, 2002; Batchelor *et al.*, 2004; Russo *et al.*, 2016). Moreover, K8 and K18 were shown to be targeted for degradation during viral and bacterial infections (Chen *et al.*, 1993; Seipelt *et al.*, 2000; Savijoki *et al.*, 2008), however the functional details of these roles remain elusive.

Keratins, as other IFs, are dynamic filament networks that interact with a multitude of proteins serving as scaffolds to organize signaling platforms and regulate different processes (Pallari and Eriksson, 2006). How K8 and K18 modulate the actin dynamics during InlB-mediated cellular invasion is still unknown. Indeed, despite several reports pointing to an interplay between actin and keratin cytoskeletons, the molecular details of such a crosstalk remain largely unidentified (Jiu *et al.*, 2015). The link between keratins and actin is thought to be mediated by their association with linker proteins such as plectin and dystrophin (Stone *et al.*, 2005; Karashima *et al.*, 2012). However, other IFs such as vimentin interact directly with actin or indirectly through motors protein like myosin IIB (Esue *et al.*, 2006; Menko *et al.*, 2014). Actin filaments were suggested to promote the assemble of keratin network (Windoffer *et al.*, 2006; Kölsch *et al.*, 2009) by favouring the retrograde transports of keratin subunits. Interestingly, the formation of EGF-induced actin-rich lamellipodia was shown to be followed by the extension of the keratin network and *de novo* nucleation at the lamellipodia itself (Felkl *et al.*, 2012). K8 and 18 were reported to interact with Grb2 and Cbl (Robertson *et al.*, 1997; Blagoev *et al.*, 2003; Duan *et al.*, 2012), proteins involved in cMet signaling and InlB-dependent entry of *L. monocytogenes* (Ireton *et al.*, 1999). In addition, keratins were found to regulate the size and organization of lipid rafts (Gilbert *et al.*, 2012; Gilbert *et al.*, 2016), which serve as surface membrane platforms promoting clustering of signaling molecules (Pizarro-Cerdá and Cossart, 2009), and whose integrity is required for successful InlB-mediated *L. monocytogenes* infection (Seveau *et al.*, 2004). It is thus possible that, through interaction with adaptor proteins downstream the activation of cMet at specific places at the host plasma membrane, K8 and K18 may modulate actin dynamics at InlB entry sites. The identification of host proteins interacting with K8 and K18 specifically upon *L. monocytogenes* infection or canonical HGF-induced cMet activation should uncover the molecular details of keratin-mediated actin dynamics modulation.

Strikingly, our data highlight the role of K18 in the control of the expression of several cell surface receptors such as cMet, TfR and integrin β1. These findings are in agreement with a growing body of evidence that suggests that keratins regulate gene expression and translation (Asghar *et al.*, 2016). Indeed, mice that lack type I or type II keratins display perturbed transcription (Kumar *et al.*, 2015; Kumar *et al.*, 2016) and impaired protein

expression (Vijayaraj *et al.*, 2009). Keratin 17 was recently reported to be present in the nucleus where it interacts with the promoter regions of cytokine genes and the transcriptional regulator AIRE (Hobbs *et al.*, 2015) thus regulating inflammatory response. Additionally, K17 regulates the shuttling between the nucleus and the cytoplasm of proteins such as hnRNP K (Chung *et al.*, 2015), 14-3-3σ (Kim *et al.*, 2006) and $p27^{KIP1}$ (Escobar-Hoyos *et al.*, 2015). Nuclear accumulation of non-filamentous K18 was detected when exportin1-mediated nuclear export is inhibited (Kumeta *et al.*, 2013), suggesting that K18, among others, may assist the nucleocytoplasmic shutting of proteins. These observations, together with our data showing that K18 ensures the stability of certain mRNAs and thus promotes the expression of proper protein levels, tempt us to speculate that K18 may affect the shuttling of RNA-binding proteins (RBPs) from the nucleus to the cytoplasmic compartment, or the binding of specific RBPs involved in mRNA stabilization, and thus impact mRNA stability. In support to this hypothesis, K18 was shown to interact with hnRNP R (Havugimana *et al.*, 2012), an RBP that binds and stabilizes the mRNA of MHC class I genes, thus enhancing their translation (Reches *et al.*, 2016). In addition, while searching for K18 interactors (our unpublished data), we identified by mass spectrometry the heat-shock cognate protein 70 (Hsc70), a chaperone that is able to bind and stabilize the mRNA of the proapoptotic protein Bim (Matsui *et al.*, 2007). We also identified the PTB-associated splicing factor (PSF), an RNA and DNA binding protein that regulates transcription, alternative splicing and mRNA stability (Yarosh *et al.*, 2015). Finally, K18 was reported to interact with the mRNA degradation machinery protein Pan2 (Bett *et al.*, 2013), involved in the initial trimming of polyadenylated tails of mRNA, a process that favors further mRNA deadenylation and subsequent degradation (Wu and Brewer, 2012). Together with K18, knockout of K8 results in perturbed mRNA levels of multiple genes (Habtezion *et al.*, 2011; Asghar *et al.*, 2016; Lähdeniemi *et al.*, 2017).

Grounded in these previous studies and our data, we propose here that K18 might modulate the stability of particular transcripts probably by interacting with specific RBPs in the cytoplasm, thus modulating the fate of the associated transcripts and ultimately controlling gene expression. The molecular understanding of the role of K18 in mRNA stability and protein expression requires further studies to identify putative RBPs interacting with K18.

Acknowledgements
This work received funding from Norte-01-0145-FEDER-000012 - Structured program on bioengineered therapies for infectious diseases and tissue regeneration, supported by Norte Portugal Regional Operational Programme (NORTE 2020), under the PORTUGAL 2020 Partnership Agreement, through the European Regional Development Fund (FEDER). RC received an FCT Doctoral Fellowship (SFRH/BD/90607/2012) and IP-C a FCT Post-Doctoral Fellowship (SFRH/BPD/107901/2015) through FCT/MEC co-funded by QREN and POPH (Programa Operacional Potencial Humano). SS was supported by FCT Investigator program (COMPETE, POPH, and FCT). We thank IBMC facilities for technical assistance.

Author contributions
RC, DC and SS conceived and designed the experiments. RC and MTA performed the experiments. RC, IPC, AM, DC and SS analyzed the data. RC, DC and SS wrote the manuscript.

Conflict of Interest Statement
The authors confirm that there are no known conflicts of interest associated with this publication and there has been no financial support for this work that could have influenced its outcome.

References

Almeida, M.T., Mesquita, F.S., Cruz, R., Osório, H., Custódio, R., Brito, C., *et al.* (2015) Src-dependent Tyrosine Phosphorylation of Non-muscle Myosin Heavy Chain-IIA Restricts Listeria monocytogenes Cellular Infection. *J Biol Chem* **290**: 8383–8395.
Asghar, M.N., Priyamvada, S., Nyström, J.H., Anbazhagan, A.N., Dudeja, P.K., and Toivola, D.M. (2016) Keratin 8 knockdown leads to loss of the chloride transporter DRA in the colon. *Am J Physiol - Gastrointest Liver Physiol* **310**: G1147–G1154.
Basar, T., Shen, Y., and Ireton, K. (2005) Redundant roles for Met docking site tyrosines and the Gab1 pleckstrin homology domain in InlB-mediated entry of Listeria monocytogenes. *Infect Immun* **73**: 2061–74.
Batchelor, M., Guignot, J., Patel, A., Cummings, N., Cleary, J., Knutton, S., *et al.* (2004) Involvement of the intermediate filament protein cytokeratin-18 in actin pedestal formation during EPEC infection. *EMBO Rep* **5**: 104–10.
Bernardini, M.L., Mounier, J., D'Hauteville, H., Coquis-Rondon, M., and Sansonetti, P.J. (1989) Identification of icsA, a plasmid locus of Shigella flexneri that governs bacterial intra- and intercellular spread through interaction with F-actin. *Proc Natl Acad Sci U S A* **86**: 3867–71.
Bett, J.S., Ibrahim, A.F.M., Garg, A.K., Kelly, V., Pedrioli, P., Rocha, S., and Hay, R.T. (2013) The P-body component USP52/PAN2 is a novel regulator of HIF1A mRNA stability. *Biochem J* **451**: 185–94.
Bierne, H., Gouin, E., Roux, P., Caroni, P., Yin, H.L., and Cossart, P. (2001) A role for cofilin and LIM kinase in Listeria-induced phagocytosis. *J Cell Biol* **155**: 101–12.
Bierne, H., Miki, H., Innocenti, M., Scita, G., Gertler, F.B., Takenawa, T., and Cossart, P. (2005) WASP-related proteins, Abi1 and Ena/VASP are required for Listeria invasion induced by the Met receptor. *J Cell Sci* **118**: 1537–47.
Biever, A., Valjent, E., and Puighermanal, E. (2015) Ribosomal Protein S6 Phosphorylation in the Nervous System: From Regulation to Function. *Front Mol Neurosci* **8**: 75.
Blagoev, B., Kratchmarova, I., Ong, S.-E., Nielsen, M., Foster, L.J., and Mann, M. (2003) A proteomics strategy to elucidate functional protein-protein interactions applied to EGF signaling. *Nat Biotechnol* **21**: 315–8.
Braun, L., Nato, F., Payrastre, B., Mazié, J.C., and Cossart, P. (1999) The 213-amino-acid leucine-rich repeat region of the listeria monocytogenes InlB protein is sufficient for entry into mammalian cells, stimulation of PI 3-kinase and membrane ruffling. *Mol Microbiol* **34**: 10–23.
Camejo, A., Carvalho, F., Reis, O., Leitão, E., Sousa, S., and Cabanes, D. (2011) The arsenal of virulence factors deployed by Listeria monocytogenes to promote its cell infection cycle. *Virulence* **2**: 379–94.
Carabeo, R. (2011) Bacterial subversion of host actin dynamics at the plasma membrane. *Cell Microbiol* **13**: 1460–9.
Carlson, S. a., Omary, M.B., and Jones, B.D. (2002) Identification of cytokeratins as accessory mediators of Salmonella entry into eukaryotic cells. *Life Sci* **70**: 1415–1426.
Caulin, C., Ware, C.F., Magin, T.M., and Oshima, R.G. (2000) Keratin-dependent, epithelial resistance to tumor necrosis factor-induced apoptosis. *J Cell Biol* **149**: 17–22.
Chan, J.K.L., Yuen, D., Too, P.H.M., Sun, Y., Willard, B., Man, D., and Tam, C. (2018) Keratin 6a reorganization for ubiquitin-proteasomal processing is a direct antimicrobial response. *J Cell Biol* **217**: 731–744.
Chen, P.H., Ornelles, D.A., and Shenk, T. (1993) The adenovirus L3 23-kilodalton proteinase cleaves the amino-terminal head domain from cytokeratin 18 and disrupts the

cytokeratin network of HeLa cells. *J Virol* **67**: 3507–14.
Chung, B.M., Arutyunov, A., Ilagan, E., Yao, N., Wills-Karp, M., and Coulombe, P.A. (2015) Regulation of C-X-C chemokine gene expression by keratin 17 and hnRNP K in skin tumor keratinocytes. *J Cell Biol* **208**: 613–627.
Claser, C., Curcio, M., Mello, S.M. de, Silveira, E. V, Monteiro, H.P., and Rodrigues, M.M. (2008) Silencing cytokeratin 18 gene inhibits intracellular replication of Trypanosoma cruzi in HeLa cells but not binding and invasion of trypanosomes. *BMC Cell Biol* **9**: 68.
Colonne, P.M., Winchell, C.G., and Voth, D.E. (2016) Hijacking Host Cell Highways: Manipulation of the Host Actin Cytoskeleton by Obligate Intracellular Bacterial Pathogens. *Front Cell Infect Microbiol* **6**: 1–8.
Copp, J., Marino, M., Banerjee, M., Ghosh, P., and Geer, P. van der (2003) Multiple regions of internalin B contribute to its ability to turn on the Ras-mitogen-activated protein kinase pathway. *J Biol Chem* **278**: 7783–9.
Czuczman, M. a., Fattouh, R., Rijn, J.M. van, Canadien, V., Osborne, S., Muise, A.M., *et al.* (2014) Listeria monocytogenes exploits efferocytosis to promote cell-to-cell spread. *Nature* **509**: 230–4.
Duan, Y., Sun, Y., Zhang, F., Zhang, W.K., Wang, D., Wang, Y., *et al.* (2012) Keratin K18 increases cystic fibrosis transmembrane conductance regulator (CFTR) surface expression by binding to its C-terminal hydrophobic patch. *J Biol Chem* **287**: 40547–59.
Egile, C., Loisel, T.P., Laurent, V., Li, R., Pantaloni, D., Sansonetti, P.J., and Carlier, M.F. (1999) Activation of the CDC42 effector N-WASP by the Shigella flexneri IcsA protein promotes actin nucleation by Arp2/3 complex and bacterial actin-based motility. *J Cell Biol* **146**: 1319–32.
Eriksson, J.E., Dechat, T., Grin, B., Helfand, B., Mendez, M., Pallari, H., and Goldman, R.D. (2009) Introducing intermediate filaments: from discovery to disease. *J Clin Invest* **119**: 1763–71.
Escobar-Hoyos, L.F., Shah, R., Roa-Pena, L., Vanner, E. a., Najafian, N., Banach, A., *et al.* (2015) Keratin-17 Promotes p27KIP1 Nuclear Export and Degradation and Offers Potential Prognostic Utility. *Cancer Res* **75**: 3650–3662.
Esue, O., Carson, A.A., Tseng, Y., and Wirtz, D. (2006) A direct interaction between actin and vimentin filaments mediated by the tail domain of vimentin. *J Biol Chem* **281**: 30393–9.
Felkl, M., Tomas, K., Smid, M., Mattes, J., Windoffer, R., and Leube, R.E. (2012) Monitoring the cytoskeletal EGF response in live gastric carcinoma cells. *PLoS One* **7**: e45280.
Freitag, N., Port, G., and Miner, M. (2009) Listeria monocytogenes—from saprophyte to intracellular pathogen. *Nat Rev Microbiol* **7**: 623–8.
Galarneau, L., Loranger, A., Gilbert, S., and Marceau, N. (2007) Keratins modulate hepatic cell adhesion, size and G1/S transition. *Exp Cell Res* **313**: 179–94.
Geisler, F., and Leube, R.E. (2016) Epithelial Intermediate Filaments: Guardians against Microbial Infection? *Cells* **5**: 1–18.
Gessain, G., Tsai, Y.-H., Travier, L., Bonazzi, M., Grayo, S., Cossart, P., *et al.* (2015) PI3-kinase activation is critical for host barrier permissiveness to Listeria monocytogenes. *J Exp Med* **212**: 165–183.
Gilbert, S., Loranger, A., Daigle, N., and Marceau, N. (2001) Simple epithelium keratins 8 and 18 provide resistance to Fas-mediated apoptosis. The protection occurs through a receptor-targeting modulation. *J Cell Biol* **154**: 763–73.
Gilbert, S., Loranger, A., Lavoie, J.N., and Marceau, N. (2012) Cytoskeleton keratin regulation of FasR signaling through modulation of actin/ezrin interplay at lipid rafts in

hepatocytes. *Apoptosis* **17**: 880–94.
Gilbert, S., Loranger, A., Omary, M.B., and Marceau, N. (2016) Keratin impact on PKCδ- and ASMase-mediated regulation of hepatocyte lipid raft size - implication for FasR-associated apoptosis. *J Cell Sci* **129**: 3262–73.
Goldman, R.D., Cleland, M.M., Murthy, S.N.P., Mahammad, S., and Kuczmarski, E.R. (2012) Inroads into the structure and function of intermediate filament networks. *J Struct Biol* **177**: 14–23.
González, A., Shimobayashi, M., Eisenberg, T., Merle, D.A., Pendl, T., Hall, M.N., and Moustafa, T. (2015) TORC1 promotes phosphorylation of ribosomal protein S6 via the AGC kinase Ypk3 in Saccharomyces cerevisiae. *PLoS One* **10**: e0120250.
Goosney, D.L., Gruenheid, S., and Finlay, B.B. (2000) Gut feelings: enteropathogenic E. coli (EPEC) interactions with the host. *Annu Rev Cell Dev Biol* **16**: 173–89.
Gruenheid, S., DeVinney, R., Bladt, F., Goosney, D., Gelkop, S., Gish, G.D., *et al.* (2001) Enteropathogenic E. coli Tir binds Nck to initiate actin pedestal formation in host cells. *Nat Cell Biol* **3**: 856–9.
Habtezion, A., Toivola, D.M., Asghar, M.N., Kronmal, G.S., Brooks, J.D., Butcher, E.C., and Omary, M.B. (2011) Absence of keratin 8 confers a paradoxical microflora-dependent resistance to apoptosis in the colon. *Proc Natl Acad Sci U S A* **108**: 1445–50.
Haglund, C.M., and Welch, M.D. (2011) Pathogens and polymers: microbe-host interactions illuminate the cytoskeleton. *J Cell Biol* **195**: 7–17.
Haines, R.L., and Lane, E.B. (2012) Keratins and disease at a glance. *J Cell Sci* **125**: 3923–8.
Havugimana, P.C., Hart, G.T., Nepusz, T., Yang, H., Turinsky, A.L., Li, Z., *et al.* (2012) A census of human soluble protein complexes. *Cell* **150**: 1068–81.
He, T., Stepulak, A., Holmström, T.H., Omary, M.B., and Eriksson, J.E. (2002) The intermediate filament protein keratin 8 is a novel cytoplasmic substrate for c-Jun N-terminal kinase. *J Biol Chem* **277**: 10767–74.
Heinzen, R.A., Grieshaber, S.S., Kirk, L.S. Van, and Devin, C.J. (1999) Dynamics of actin-based movement by Rickettsia rickettsii in vero cells. *Infect Immun* **67**: 4201–7.
Hobbs, R.P., DePianto, D.J., Jacob, J.T., Han, M.C., Chung, B.-M., Batazzi, A.S., *et al.* (2015) Keratin-dependent regulation of Aire and gene expression in skin tumor keratinocytes. *Nat Genet* **47**: 933–8.
Ireton, K., Payrastre, B., Chap, H., Ogawa, W., Sakaue, H., Kasuga, M., and Cossart, P. (1996) A role for phosphoinositide 3-kinase in bacterial invasion. *Science* **274**: 780–782.
Ireton, K., Payrastre, B., and Cossart, P. (1999) The Listeria monocytogenes protein InlB is an agonist of mammalian phosphoinositide 3-kinase. *J Biol Chem* **274**: 17025–32.
Isberg, R.R., and Leong, J.M. (1990) Multiple beta 1 chain integrins are receptors for invasin, a protein that promotes bacterial penetration into mammalian cells. *Cell* **60**: 861–71.
Karashima, T., Tsuruta, D., Hamada, T., Ishii, N., Ono, F., Hashikawa, K., *et al.* (2012) Interaction of plectin and intermediate filaments. *J Dermatol Sci* **66**: 44–50.
Kellner, J.C., and Coulombe, P.A. (2009) Keratins and protein synthesis: the plot thickens. *J Cell Biol* **187**: 157–9.
Kim, S., Wong, P., and Coulombe, P. a (2006) A keratin cytoskeletal protein regulates protein synthesis and epithelial cell growth. *Nature* **441**: 362–5.
Kölsch, A., Windoffer, R., and Leube, R.E. (2009) Actin-dependent dynamics of keratin filament precursors. *Cell Motil Cytoskeleton* **66**: 976–85.
Kuehl, C.J., Dragoi, A.-M., Talman, A., and Agaisse, H. (2015) Bacterial spread from

cell to cell: beyond actin-based motility. *Trends Microbiol* **23**: 558–66.
Kumar, V., Behr, M., Kiritsi, D., Scheffschick, A., Grahnert, A., Homberg, M., *et al.* (2016) Keratin-dependent thymic stromal lymphopoietin expression suggests a link between skin blistering and atopic disease. *J Allergy Clin Immunol* **138**: 1461–1464.e6.
Kumar, V., Bouameur, J.-E., Bär, J., Rice, R.H., Hornig-Do, H.-T., Roop, D.R., *et al.* (2015) A keratin scaffold regulates epidermal barrier formation, mitochondrial lipid composition, and activity. *J Cell Biol* **211**: 1057–75.
Kumeta, M., Hirai, Y., Yoshimura, S.H., Horigome, T., and Takeyasu, K. (2013) Antibody-based analysis reveals "filamentous vs. non-filamentous" and "cytoplasmic vs. nuclear" crosstalk of cytoskeletal proteins. *Exp Cell Res* **319**: 3226–37.
Lähdeniemi, I.A.K., Misiorek, J.O., Antila, C.J.M., Landor, S.K.-J., Stenvall, C.-G.A., Fortelius, L.E., *et al.* (2017) Keratins regulate colonic epithelial cell differentiation through the Notch1 signalling pathway. *Cell Death Differ* **24**: 984–996.
Li, N., Xiang, G.-S.S., Dokainish, H., Ireton, K., and Elferink, L. a. (2005) The Listeria protein internalin B mimics hepatocyte growth factor-induced receptor trafficking. *Traffic* **6**: 459–73.
Loschke, F., Seltmann, K., Bouameur, J., and Magin, T.M. (2015) Regulation of keratin network organization. *Curr Opin Cell Biol* **32**: 56–64.
Magnuson, B., Ekim, B., and Fingar, D.C. (2012) Regulation and function of ribosomal protein S6 kinase (S6K) within mTOR signalling networks. *Biochem J* **441**: 1–21.
Martins, M., Custodio, R., Camejo, A., Almeida, M.T., Cabanes, D., and Sousa, S. (2012) Listeria monocytogenes triggers the cell surface expression of Gp96 protein and interacts with its N terminus to support cellular infection. *J Biol Chem* **287**: 43083–43093.
Matsui, H., Asou, H., and Inaba, T. (2007) Cytokines direct the regulation of Bim mRNA stability by heat-shock cognate protein 70. *Mol Cell* **25**: 99–112.
Mengaud, J., Ohayon, H., Gounon, P., Mege R-M, and Cossart, P. (1996) E-cadherin is the receptor for internalin, a surface protein required for entry of L. monocytogenes into epithelial cells. *Cell* **84**: 923–32.
Menko, A.S., Bleaken, B.M., Libowitz, A.A., Zhang, L., Stepp, M.A., and Walker, J.L. (2014) A central role for vimentin in regulating repair function during healing of the lens epithelium. *Mol Biol Cell* **25**: 776–90.
Moll, R., Divo, M., and Langbein, L. (2008) The human keratins: biology and pathology. *Histochem Cell Biol* **129**: 705–33.
Mounier, J., Ryter, A., Coquis-Rondon, M., and Sansonetti, P.J. (1990) Intracellular and cell-to-cell spread of Listeria monocytogenes involves interaction with F-actin in the enterocytelike cell line Caco-2. *Infect Immun* **58**: 1048–58.
Nava-Acosta, R., and Navarro-Garcia, F. (2013) Cytokeratin 8 is an epithelial cell receptor for Pet, a cytotoxic serine protease autotransporter of Enterobacteriaceae. *MBio* **4**: e00838-13.
Pallari, H.-M., and Eriksson, J.E. (2006) Intermediate filaments as signaling platforms. *Sci STKE* **2006**: pe53.
Pan, X., Hobbs, R.P., and Coulombe, P. a (2012) The expanding significance of keratin intermediate filaments in normal and diseased epithelia. *Curr Opin Cell Biol* **25**: 47–56.
Pizarro-Cerdá, J., and Cossart, P. (2009) Listeria monocytogenes membrane trafficking and lifestyle: the exception or the rule? *Annu Rev Cell Dev Biol* **25**: 649–70.
Pizarro-Cerdá, J., Jonquières, R., Gouin, E., Vandekerckhove, J., Garin, J., and Cossart, P. (2002) Distinct protein patterns associated with Listeria monocytogenes InlA- or InlB-phagosomes. *Cell Microbiol* **4**: 101–15.
Pizarro-Cerdá, J., Kühbacher, A., and Cossart, P. (2012) Entry of Listeria

monocytogenes in mammalian epithelial cells: an updated view. *Cold Spring Harb Perspect Med* **2**.
Reches, A., Nachmani, D., Berhani, O., Duev-Cohen, A., Shreibman, D., Ophir, Y., *et al.* (2016) HNRNPR Regulates the Expression of Classical and Nonclassical MHC Class I Proteins. *J Immunol* **196**: 4967–4976.
Reis, O., Sousa, S., Camejo, A., Villiers, V., Gouin, E., Cossart, P., and Cabanes, D. (2010) LapB, a novel Listeria monocytogenes LPXTG surface adhesin, required for entry into eukaryotic cells and virulence. *J Infect Dis* **202**: 551–62.
Robertson, H., Langdon, W.Y., Thien, C.B., and Bowtell, D.D. (1997) A c-Cbl yeast two hybrid screen reveals interactions with 14-3-3 isoforms and cytoskeletal components. *Biochem Biophys Res Commun* **240**: 46–50.
Rolhion, N., and Cossart, P. (2017) How the study of Listeria monocytogenes has led to new concepts in biology. *Future Microbiol* **12**: 621–638.
Russo, B.C., Stamm, L.M., Raaben, M., Kim, C.M., Kahoud, E., Robinson, L.R., *et al.* (2016) Intermediate filaments enable pathogen docking to trigger type 3 effector translocation. *Nat Microbiol* **1**: 16025.
Savijoki, K., Alvesalo, J., Vuorela, P., Leinonen, M., and Kalkkinen, N. (2008) Proteomic analysis of Chlamydia pneumoniae-infected HL cells reveals extensive degradation of cytoskeletal proteins. *FEMS Immunol Med Microbiol* **54**: 375–84.
Seipelt, J., Liebig, H.D., Sommergruber, W., Gerner, C., and Kuechler, E. (2000) 2A proteinase of human rhinovirus cleaves cytokeratin 8 in infected HeLa cells. *J Biol Chem* **275**: 20084–9.
Seveau, S., Bierne, H., Giroux, S., Prévost, M.-C., Cossart, P., Préost, M.C., and Cossart, P. (2004) Role of lipid rafts in E-cadherin-- and HGF-R/Met--mediated entry of Listeria monocytogenes into host cells. *J Cell Biol* **166**: 743–53.
Shen, Y., Naujokas, M., Park, M., and Ireton, K. (2000) InIB-dependent internalization of Listeria is mediated by the Met receptor tyrosine kinase. *Cell* **103**: 501–10.
Sousa, S., Cabanes, D., Bougnères, L., Lecuit, M., Sansonetti, P., Tran-Van-Nhieu, G., and Cossart, P. (2007) Src, cortactin and Arp2/3 complex are required for E-cadherin-mediated internalization of Listeria into cells. *Cell Microbiol* **9**: 2629–43.
Sousa, S., Cabanes, D., El-Amraoui, A., Petit, C., Lecuit, M., and Cossart, P. (2004) Unconventional myosin VIIa and vezatin, two proteins crucial for Listeria entry into epithelial cells. *J Cell Sci* **117**: 2121–30.
Souza Santos, M. de, and Orth, K. (2015) Subversion of the cytoskeleton by intracellular bacteria: lessons from Listeria, Salmonella and Vibrio. *Cell Microbiol* **17**: 164–173.
Stone, M.R., O'Neill, A., Catino, D., and Bloch, R.J. (2005) Specific interaction of the actin-binding domain of dystrophin with intermediate filaments containing keratin 19. *Mol Biol Cell* **16**: 4280–93.
Stradal, T.E.B., and Costa, S.C.P. (2017) Type III Secreted Virulence Factors Manipulating Signaling to Actin Dynamics. *Curr Top Microbiol Immunol* **399**: 175–199.
Swaminathan, B., and Gerner-Smidt, P. (2007) The epidemiology of human listeriosis. *Microbes Infect* **9**: 1236–43.
Tang, P., Sutherland, C.L., Gold, M.R., and Finlay, B.B. (1998) Listeria monocytogenes invasion of epithelial cells requires the MEK-1/ERK-2 mitogen-activated protein kinase pathway. *Infect Immun* **66**: 1106–12.
Toivola, D.M., Strnad, P., Habtezion, A., and Omary, M.B. (2010) Intermediate filaments take the heat as stress proteins. *Trends Cell Biol* **20**: 79–91.
Valencia-Gallardo, C.M., Carayol, N., and Tran Van Nhieu, G. (2015) Cytoskeletal

mechanics during Shigella invasion and dissemination in epithelial cells. *Cell Microbiol* **17**: 174–82.
Vanhaesebroeck, B., Stephens, L., and Hawkins, P. (2012) PI3K signalling: the path to discovery and understanding. *Nat Rev Mol Cell Biol* **13**: 195–203.
Vijayaraj, P., Kröger, C., Reuter, U., Windoffer, R., Leube, R.E., and Magin, T.M. (2009) Keratins regulate protein biosynthesis through localization of GLUT1 and -3 upstream of AMP kinase and Raptor. *J Cell Biol* **187**: 175–84.
Welch, M.D., Iwamatsu, A., and Mitchison, T.J. (1997) Actin polymerization is induced by Arp2/3 protein complex at the surface of Listeria monocytogenes. *Nature* **385**: 265–9.
Windoffer, R., Kölsch, A., Wöll, S., and Leube, R.E. (2006) Focal adhesions are hotspots for keratin filament precursor formation. *J Cell Biol* **173**: 341–8.
Wu, X., and Brewer, G. (2012) The regulation of mRNA stability in mammalian cells: 2.0. *Gene* **500**: 10–21.
Yarosh, C.A., Iacona, J.R., Lutz, C.S., and Lynch, K.W. (2015) PSF: Nuclear busy-body or nuclear facilitator? *Wiley Interdiscip Rev RNA* **6**: 351–367.

Figure Legends

Figure 1. K8 and K18 promote *Listeria* infection of HeLa cells. (a) Intracellular levels of *L. monocytogenes* were determined by gentamicin protection assay and CFU counting in HeLa cells left untransfected (NT) or transfected with either control (Ctr) or siRNA specifically targeting K8 (K8-si, left panel), K18 (K18-si, middle panel) and both (K8/K18-si, right panel). (b) Adhesion of *L. monocytogenes* was assessed in HeLa cells left unstransfected (NT) or transfected with Ctr, K8 or K18 siRNA. (c and d) Intracellular levels of *L. innocua* expressing InlB (*L. innocua* InlB) were determined (c) by gentamicin protection assays and CFU counting in HeLa cells left unstransfected (NT) or transfected with Ctr or specific siRNA targeting K8 (K8-si left panel), K18 (K18-si, left panel) and both (K8/K18-si, right panel) or by (d) immunofluorescence scoring of extracellular and total bacteria. Values of intracellular or adherent bacteria in NT cells were normalized to 100% and the levels of infection in the remaining conditions are expressed as relative values. Values represent the mean ±S.E. of at least three independent experiments, each done in triplicate. Statistically significant differences are indicated: *, $p<0.05$; **, $p<0.01$, ***, $p<0.001$ and ****, $p<0.0001$

Figure 2. K8 and K18 are recruited at the bacterial entry site during InlB-mediated cellular invasion**. (a)** Representative widefield microscopy stack projections of HeLa cells incubated with *L. innocua* InlB for 5 minutes, fixed and immunostained for cMet (green) and for K8 (upper panels, green) or K18 (lower panels, green). F-actin was stained with phalloidin (red), DNA with DAPI (blue). Scale bar, 5 µm. Arrows indicate bacteria that display accumulation of K8, K18, cMet and F-actin at their vicinity. Insets show high-magnification images. Scale bar, 2 µm. (b) Quantification of K8, K18 and actin recruitments to the entry site of *L. innocua* InlB. Results are expressed as the percentage of total number of bacteria associated to cells. Values are the mean ±S.E. of at least three independent experiments.

Figure 3. K8 and K18 assist actin depolymerization during later stages of internalization. (a and b) Kinetic analysis of actin, K8 and K18 recruitments during internalization of InlB-coated latex beads. (a) Stack projections of widefield microscopy images of HeLa cells incubated with InlB-coated latex beads for different periods of time, fixed, immunostained for K8 or K18 (green) and labelled for F-actin with TRITC-phalloidin (red). Scale bar, 3 µm. Insets show high-magnification images. Scale bar, 1 µm. (b) Quantification of beads positive for K8, K18 or actin recruitment. Results are expressed as the percentage of particles associated with either protein in relation to the total number of particles associated to cells. The total number of beads was determined in brightfield. Values are the mean ±S.E. of at least three independent experiments. For determination of beads internalization, extracellular beads were stained with anti-InlB before cell permeabilization and total beads number quantified in brightfield. Values are shown in percentage and are representative of two independent experiments. (c) Quantification of InlB-coated latex beads associated to polymerized actin in HeLa cells transfected with control (Ctr) or specific siRNA targeting K8 (K8-si) or K18 (K18-si). Cells were incubated with InlB-coated latex beads for 15, 30 and 60 minutes, fixed and stained for F-actin. Beads displaying actin recruitment were considered recruitment-positive. The total number of beads associated to cells was determined in brightfield. Values represent the mean ±S.E. of at least three independent experiments. Statistically significant differences are indicated: ***, $p<0.001$.

Figure 4. K8 and K18 mediate cMet downstream signaling. (a) Immunofluorescence microscopy images of control (Ctr), K8 (K8-si) or K18 (K18-si) depleted HeLa cells left untreated or incubated with HGF (150 ng/ml) for 5 and 10 min (HGF-5' and HGF-10'). Cells were fixed and stained for actin with TRITC-phalloidin. Images show the actin-rich membrane ruffles (arrows) induced by the HGF stimulation of cMet. Scale bar, 20 μm. (b) Quantification of actin-rich membrane ruffles in Ctr, K8- and K18-depleted cells. Cells without ruffles were considered ruffle-negative, whereas cells with at least one actin-rich membrane ruffle were scored as ruffle-positive. Values result from four independent experiments and are expressed as fold change with respect to untreated control cells. (c) Ctr, K8 and K18-depleted HeLa cells were incubated with 150 ng/ml HGF for 5 minutes, washed and lysed. Tyrosine phosphorylated proteins were immunoprecipitated (IP: pTyr) from whole cell lysates (WCL) and p85 was detected by immunoblot (p85) in IP fractions and WCL. Detection of actin was used as loading control. (d) Immunoblot to detect P-Akt (S473), total Akt and actin on total extracts of Ctr and K18-depleted HeLa cells left untreated (NT) or incubated with 150 ng/ml HGF for 5 minutes. (e) Densitometry analysis of the ratio of P-Akt (S473) over total Akt, in conditions of HGF stimulation. For control cells the value was arbitrarily fixed to 1. Values represent the mean ±S.E. of three independent experiments. Statistically significant differences are indicated: *, $p<0.05$ and **, $p<0.01$.

Figure 5. Total expression, surface localization and activation of cMet are perturbed in cells expressing low levels of K8 and K18. (a) HeLa cells transfected with Ctr, K8 and K18-targeting siRNAs were left untreated (NT) or incubated with 150 ng/ml HGF for 5 minutes, washed and lysed. Tyrosine phosphorylated proteins were immunoprecipitated (IP: pTyr) from whole cell lysates (WCL) and cMet was analyzed by immunoblot (cMet) in IP fractions and WCL. GAPDH detection was used as loading control. (b) Surface exposed proteins of control (Ctr), K8- (K8-si) and K18-depleted (K18-si) HeLa cells were biotinylated and recovered from total cell extracts following neutravidin pull down assays. Biotinylated samples, corresponding to surface exposed proteins, and whole cell lysates (WCL) were immunoblotted to detect cMet, K8, K18 and actin. (c) Quantifications of cMet in WCL (left panel) and in biotinylated samples (right panel) from at least three independent experiments. Statistically significant differences are indicated: *, $p<0.05$, ***, $p<0.001$ and ****, $p<0.0001$. (a.u., arbitrary units).

Figure 6. K8 and K18 depletion perturbs expression and surface localization of transmembrane receptors. (a) Surface proteins of control (Ctr), K8- (K8-si) and K18-depleted (K18-si) HeLa cells were biotinylated, recovered from total cell extracts and pulled down using neutravidin beads. Biotinylated samples, which corresponds to surface exposed proteins, and whole cell lysates (WCL) were immunoblotted to detect cMet, TfR and integrin β1, together with Actin, K8 and K18. (b) Quantifications of TfR in WCL (left panel) and in biotinylated samples (right panel) from at least three independent experiments. (c) Quantifications of integrin β1 in WCL (left panel) and in biotinylated samples (right panel) from at least three independent experiments. Statistically significant differences are indicated: *, $p<0.05$, ***, $p<0.001$ and ****, $p<0.0001$. (a.u., arbitrary units). (d) Functional impact of K18 in the expression of ITGB1 was assessed by gentamicin survival assay and CFU counting in K18-depleted HeLa cells (K18-si) incubated with invasive *E. coli* K12 expressing the *Y. pseudotuberculosis* invasin (K12-inv). Values of intracellular bacteria in Ctr cells were normalized to 100% and the entry levels in K18-si cells are expressed as relative values. Values are the mean ±S.E. of three

independent experiments, each done in triplicate. Statistically significant differences are indicated: **, p<0.01, ***, p<0.001 and ****, p<0.0001.

Figure 7. K18 depletion does not dampen mTOR/S6K signaling, global protein translation and receptor degradation. (a) Activation of mTOR/S6K signaling pathway in K18 (K18-si) depleted HeLa cells was assessed by immunoblotting whole cell extracts against phosphorylated S6 (S6(P)), total S6, cMet, K18 and Actin as loading control. Immunoblot representative of three different experiments. (b) Rate of total protein synthesis was assessed by ^{35}S-methionine incorporation of HeLa cells transfected with control (Ctr) or K18 targeting (K18-si) siRNA. Autoradiography representative of two independent experiments. (c) Depletion efficiency of the samples that were used for the ^{35}S-methionine incorporation assay. (d) After transfection with control (Ctr) or siRNA targeting K18 (K18-si), HeLa cells were incubated with 100 nM of the lysosomal inhibitor Concanamycin A alone (*upper* panel) or together with the proteasomal inhibitor 10 μM MG132 (*lower* panel) for different periods of time. Lysates were collected and immunoblotted for cMet, TfR, integrin β1, K18 and Actin as a loading control. Immunoblots are representative of at least two independent experiments.

Figure 8. K18 favors expression of cMet, TFRC and integrin β1, by promoting transcript stability. (a) mRNAs were extracted from control (Ctr) and K18-depleted (K18-si) HeLa cells and qRT-PCR was performed using *GAPDH* as a housekeeping gene. Data are represented as mean ±S.E. from at least three independent experiments (b) Control and K18 depleted cells were left untreated or were treated with 5 μg/ml of the transcriptional inhibitor Actinomycin D for different periods of time. Transcript levels for cMet, TfR and integrin β1 were determined by qRT-PCR. Fold changes are relative to *GAPDH* and were normalized to untreated control. Results are from at least three independent experiments. Statistically significant differences are indicated: *, p<0.05; **, p<0.01, ***, p<0.001 and ****, p<0.0001.

Supplemental Figure Legends

Supplemental Figure 1. Keratin 8 (K8) and Keratin 18 (K18) are dispensable for *Listeria* infection of Caco-2 cells. Intracellular levels of *L. monocytogenes* were assessed by gentamicin protection assay and CFU counting in intestinal epithelial cell line Caco-2 cells that were left untransfected (NT) or transfected with control siRNA (Ctr) or with siRNAs specifically targeting K8 (K8-si, left panel), K18 (K18-si, middle panel) or both (K8/K18-si, right panel). The number of intracellular *L. monocytogenes* in NT cells was normalized to 100%, and those in siRNA-transfected cells were expressed as relative values to NT cells. Values are the mean ±S.E. of at least three independent experiments, each done in triplicate.

Supplemental Figure 2. K8 and K18 depletion efficiency in HeLa and Caco-2 cells. Efficiency of protein knockdown in (a) HeLa and (b) Caco-2 cells was assessed by western immunoblot using GAPDH as loading control. (c) Immunofluorescence images of Ctr and K8- (K8-si) or K18- (K18-si) depleted HeLa cells labelled for K8 and K18. Signal intensity was quantified. The values in Ctr cells were normalized to 1, and those in K8- and K18-depleted cells were expressed as relative values. Values are the mean ±S.E. of three independent experiments.

Supplemental Figure 3. K8 and K18 are not important for *Listeria* intracellular replication in HeLa cells. (a) Intracellular replication of *L. monocytogenes* in HeLa cells left untransfected (NT) or transfected with control (Ctr) or both K8 and K18 siRNA (K8/K18-si). Values represent the mean of duplicate samples from one representative experiment out of two independent experiments. (b) Efficiency of protein knockdown was assessed by western blot using GAPDH as loading control.

Supplemental Figure 4. K8 and K18 assist actin depolymerization during InlB-mediated internalization. Quantification of InlB-coated latex beads associated to polymerized actin in HeLa cells transfected with control (Ctr) or different concentrations of specific siRNA targeting K8 (K8-si) or K18 (K18-si). The use of 46 nM siRNA allows the maximum keratin depletion while 13.8 nM allows partial depletion. Cells were incubated with InlB-coated latex beads for 15, 30 and 60 minutes, fixed and stained for F-actin. Beads displaying actin recruitment were considered recruitment-positive. The total number of beads associated to cells was determined in brightfield. Values represent the mean ±S.E. of two independent experiments.

Supplemental Figure 5. K18 depletion perturbs expression and surface localization of transmembrane receptors in Caco-2 cells. Biotinylated surface proteins of control (Ctr) and K18-depleted (K18-si) Caco-2 cells were recovered from total cell extracts and pulled down using neutravidin beads. Biotinylated samples and whole cell lysates (WCL) were immunoblotted to detect cMet, TfR and integrin β1. (a) Immunoblot representative of two independent experiments. (b) Quantifications of E-cadherin, cMet, TfR and integrin β1 in WCL and in biotinylated samples from two independent experiments.

Table 1: List of antibodies used in this study. WB: Western blot, IF: immunofluorescence.

Antigen	Species	Applications	Reference	Source
Phosphotyrosine	Mouse	IP (1:360)	4G10, 05-321	Millipore
Actin	Mouse	WB (1:5000)	A5441	Sigma Aldrich
GAPDH	Mouse	WB (1:15000)	sc-32233	Santa Cruz Biotechnologies
K8	Mouse	WB (1:450), IF (1:200)	sc-8020	Santa Cruz Biotechnologies
K8	Rabbit	WB (1:10000), IF (1:400)	ab53280	Abcam
K18	Mouse	WB (1:2000), IF (1:200)	sc-6259	Santa Cruz Biotechnologies
K18	Rabbit	WB (1:10000), IF (1:400)	ab52948	Abcam
cMet	Rabbit	WB (1:175), IF (1:150)	Sc-10	Santa Cruz Biotechnologies
TfR	Mouse	WB (1:1500)	13-6800	Thermo
Integrin-β1	Rabbit	WB (1:1000)	ab52971	Abcam
PI3Kp85	Rabbit	WB (1:1500)	06-195	Millipore
e-cadherin	Rabbit	WB (1:300)	sc-7870	Santa Cruz Biotechnologies
S6	Mouse	WB (1:1600)	2317	Cell Signalling
Phospho-S6	Rabbit	WB (1:1000)	4856	Cell Signalling
Akt	Rabbit	WB (1:1000)	4685	Cell Signalling
P-Akt (S473)	Rabbit	WB (1:1500)	4060	Cell Signalling

Table 2: Sequences of siRNA duplexes used in this study.

siRNA duplexes		
Name	Oligo Sequence (5'-3')	Source
K8	Sense: CUGGGAAGGAGGCCGCUAU Antisense: AUAGCGGCCUCCUUCCCAG	SIGMA (Sasi_Hs01_00166576)
K18	Sense: GAGAGGAGCUAGACAAGUA Antisense: UACUUGUCUAGCUCCUCUCUC	SIGMA (SASI_Hs01_00145009)

Table 3: Sequences of primers used in this study.

Primer sequences (5'-3')	
cMet	Fw: CCCTATCAAATATGTCAACG Rev: TCAGAAGTGTCCTATTAAAGC
TFRC	Fw: GGAATATGGAAGGAGACT Rev: ATAGTGATCTGGTTCTACA
ITGB1	Fw: GCCATTATTATGATTATCCTTCT Rev: GTTCCTACTGCTGACTTAG
GAPDH	Fw: CCTCAAGATCATCAGCAATG Rev: CACGATACCAAAGTTGTCAT

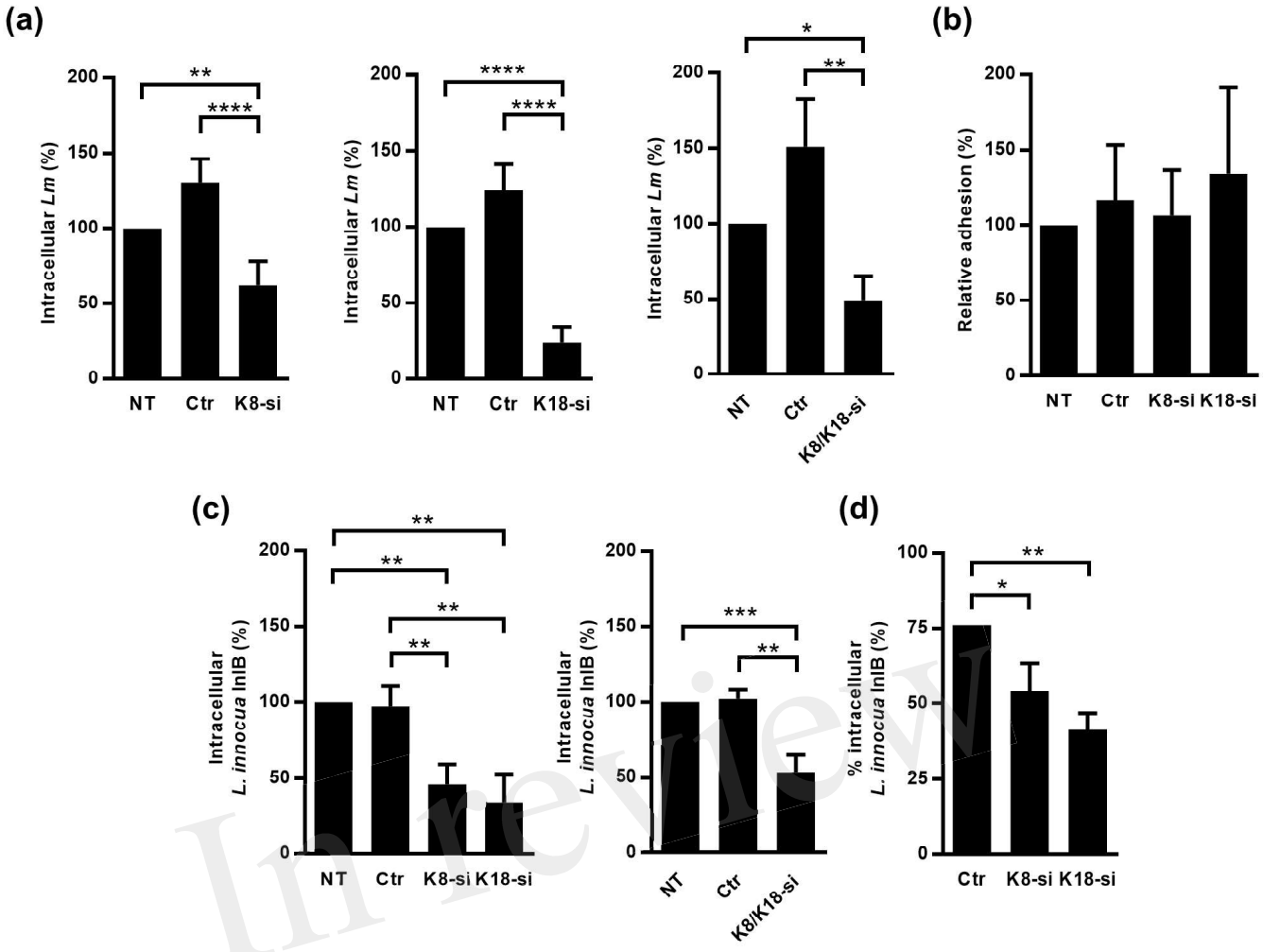

In review

Figure 1. K8 and K18 promote *Listeria* infection of HeLa cells.

Figure 2.TIF

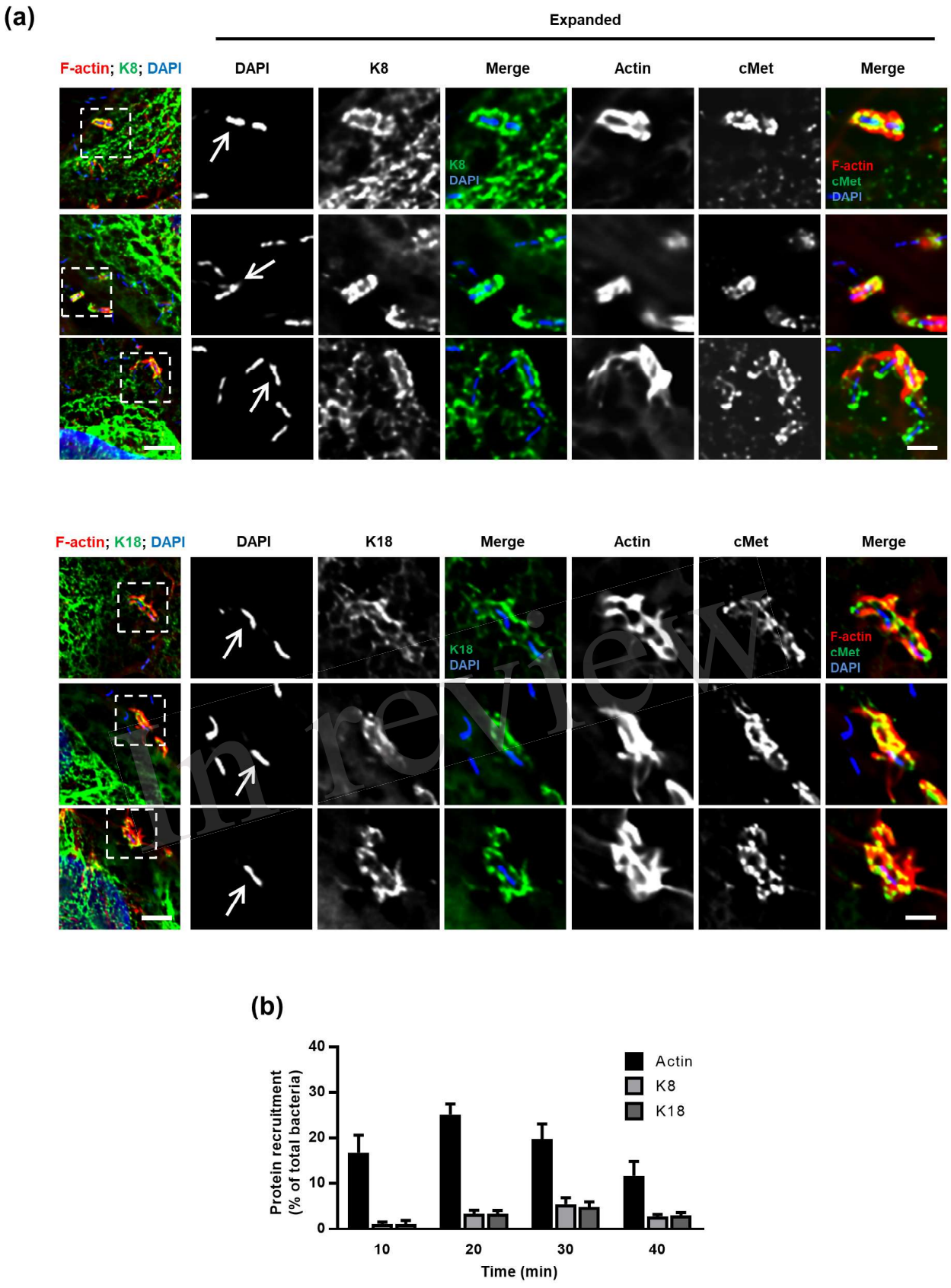

Figure 2. K8 and K18 are recruited at bacterial entry site during InlB-mediated cellular invasion.

In review

Figure 3.TIF

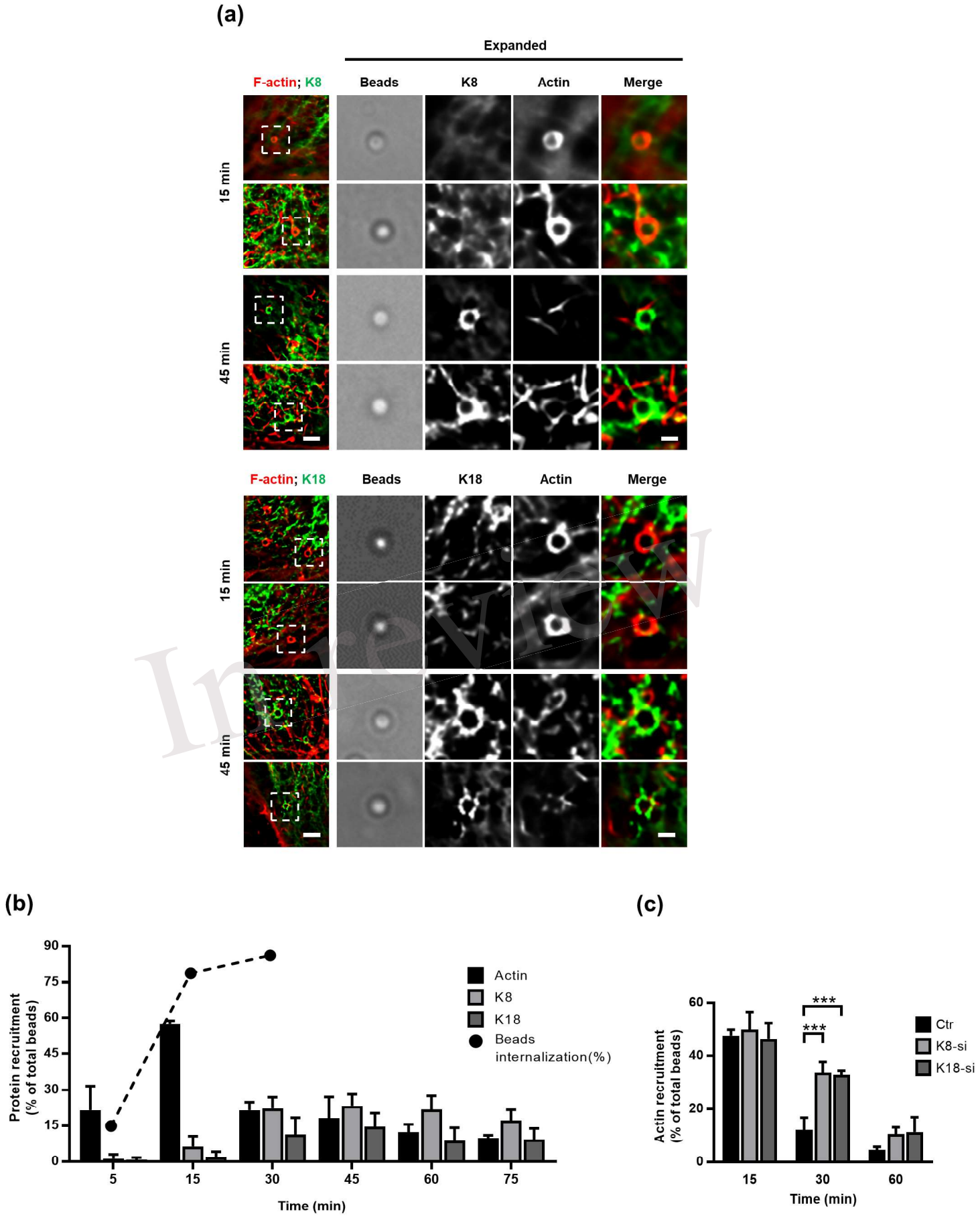

Figure 3. K8 and K18 assist actin depolymerization during later stages of internalization.

In review

Figure 4.TIF

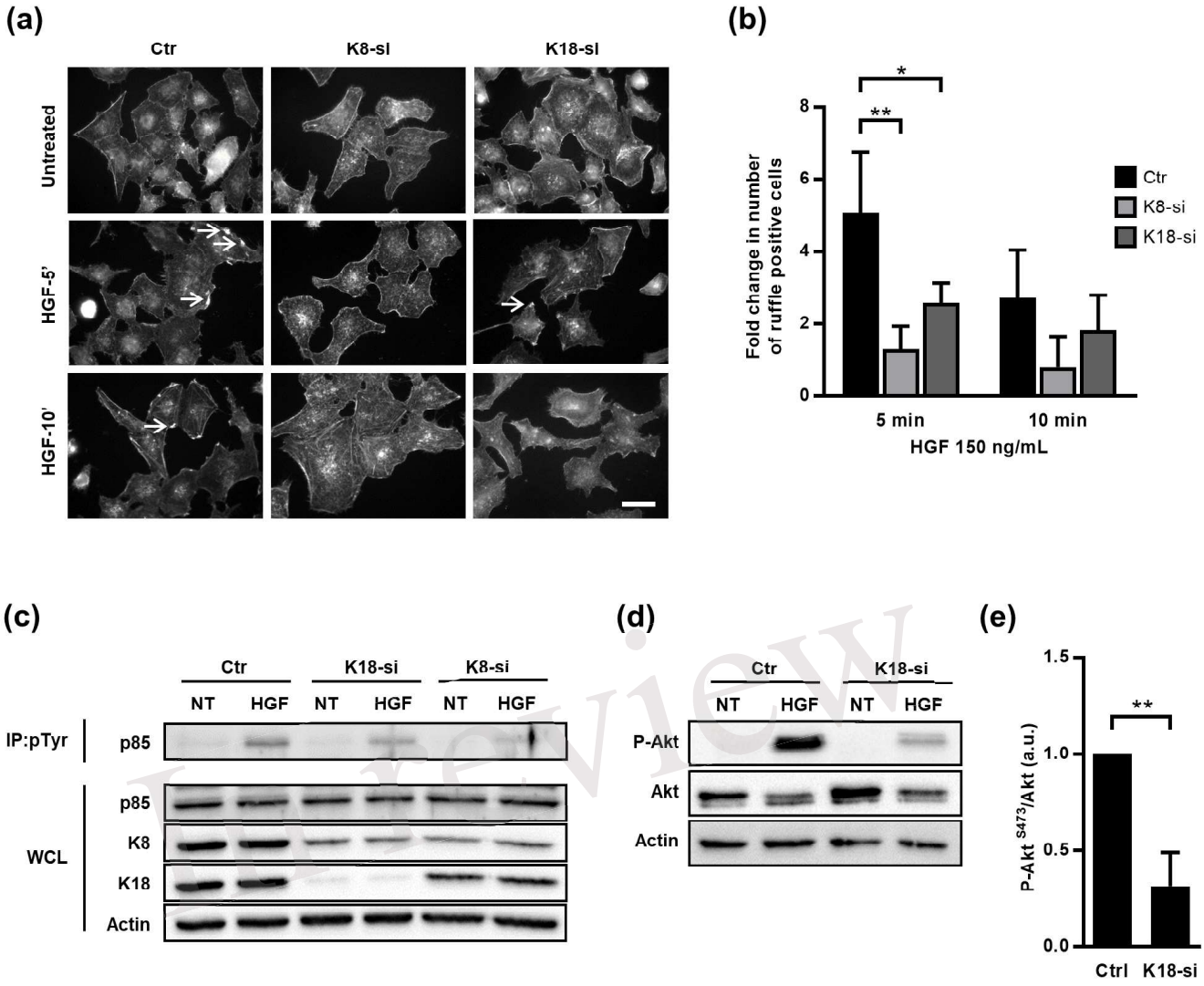

In review

Figure 4. K8 and K18 mediate cMet downstream signaling.

Figure 5.TIF

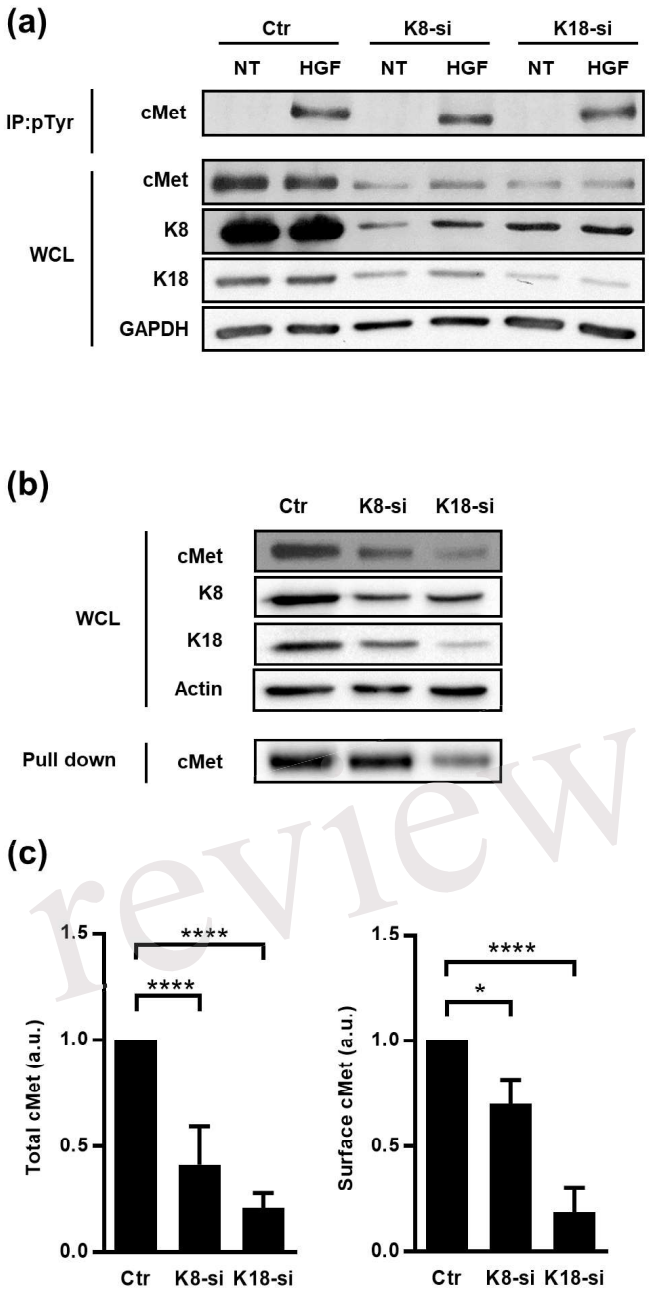

In review

Figure 5. Total expression, surface location and activation of cMet are perturbed in cells expressing low levels of K8 and K18.

Figure 6.TIF

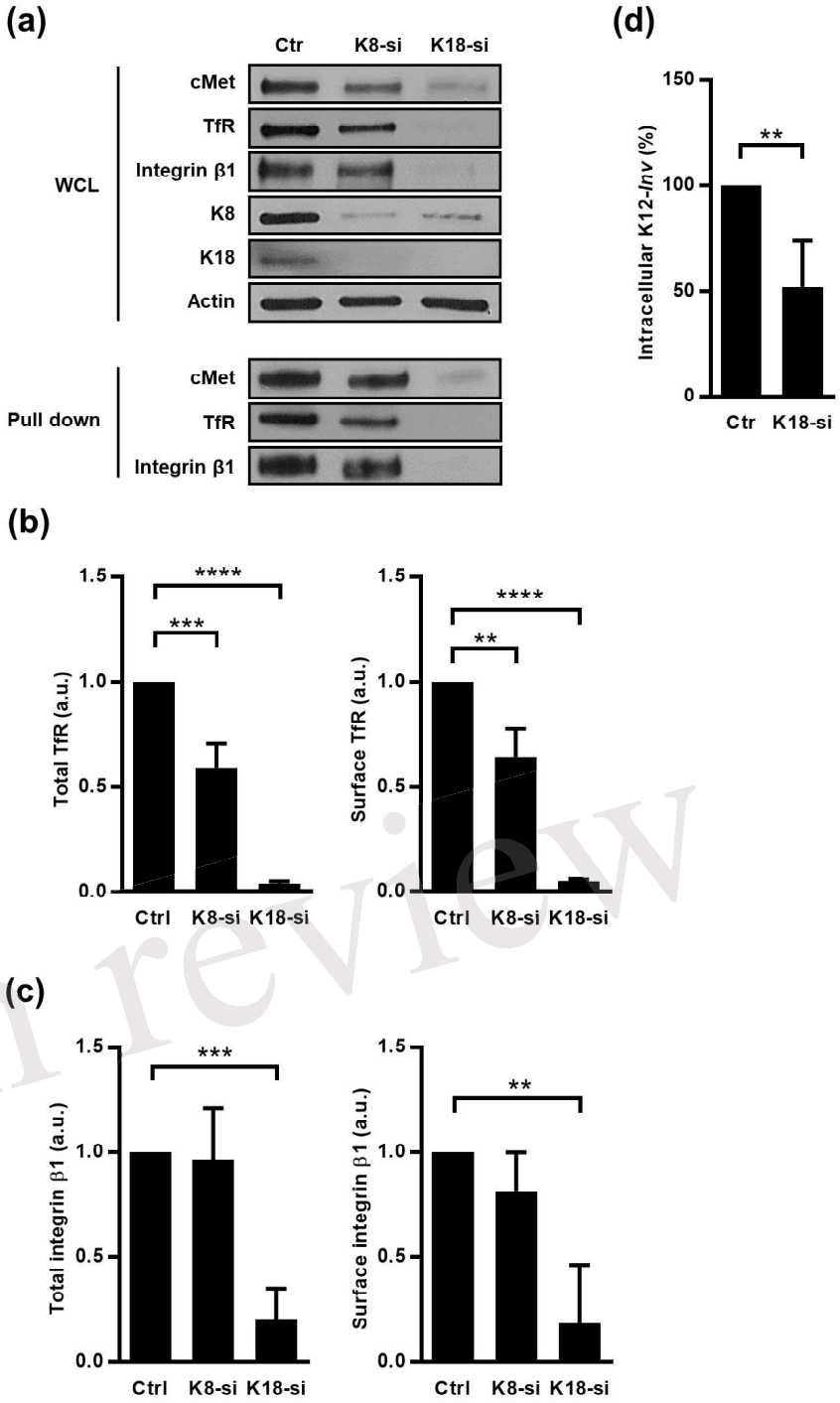

In review

Figure 6. K8 and K18 depletion perturbs expression and surface location of transmembrane receptors.

Figure 7.TIF

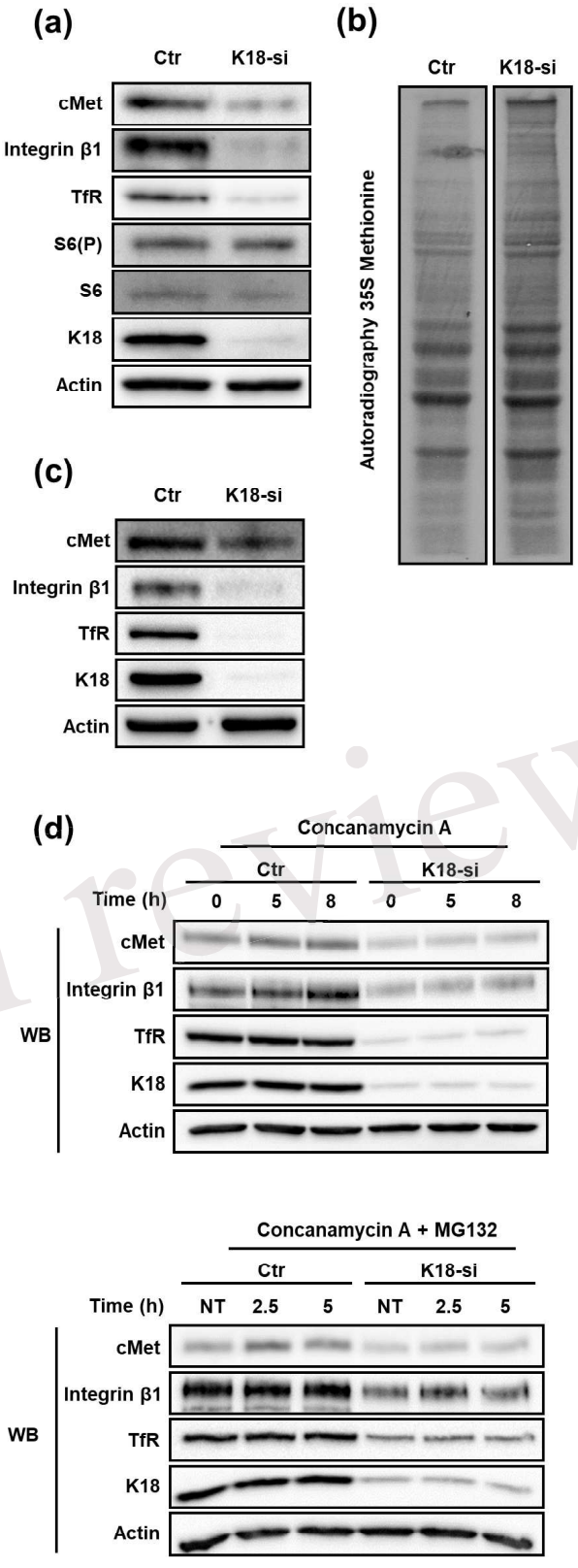

In review

Figure 7. K18 depletion does not dampen mTOR/S6K signaling, global protein translation and receptor degradation.

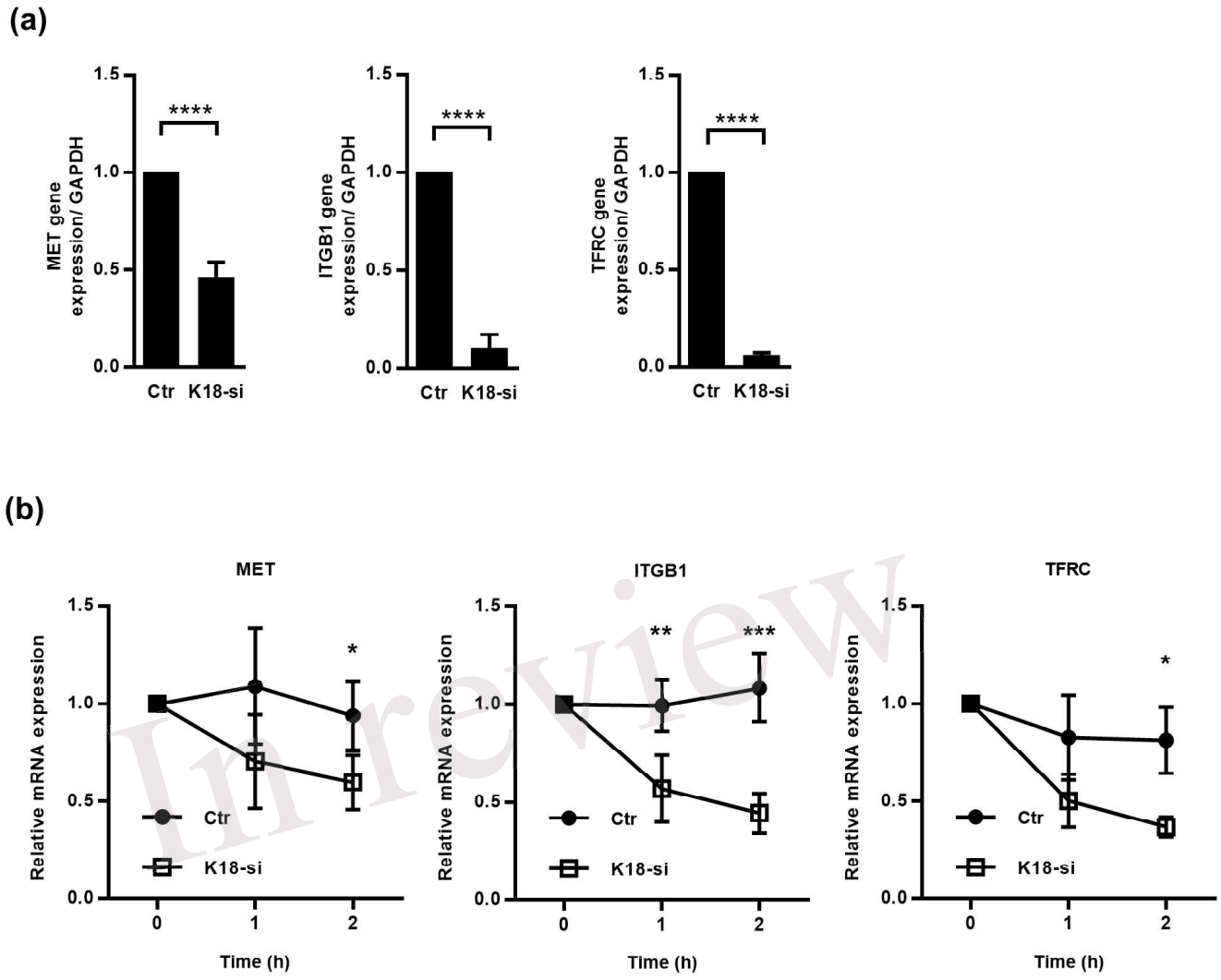

In review

Figure 8. K18 favors expression of cMet, TFRC and integrin β1, by promoting transcript stability.

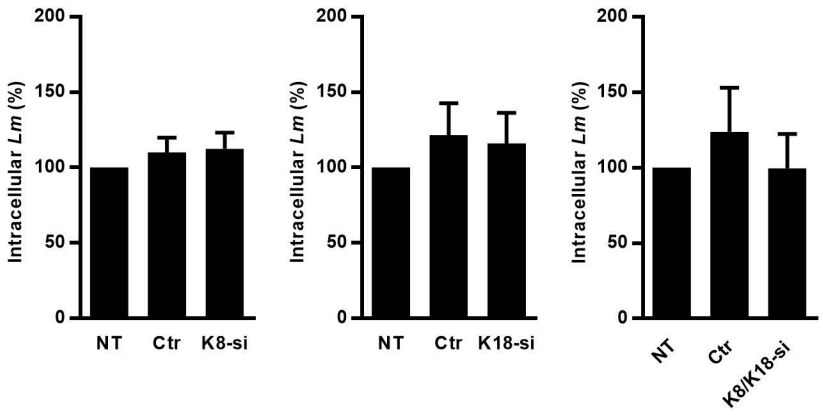

Supplemental Figure 1. Keratin 8 (K8) and Keratin 18 (K18) are dispensable for *Listeria* infection of Caco-2 cells.

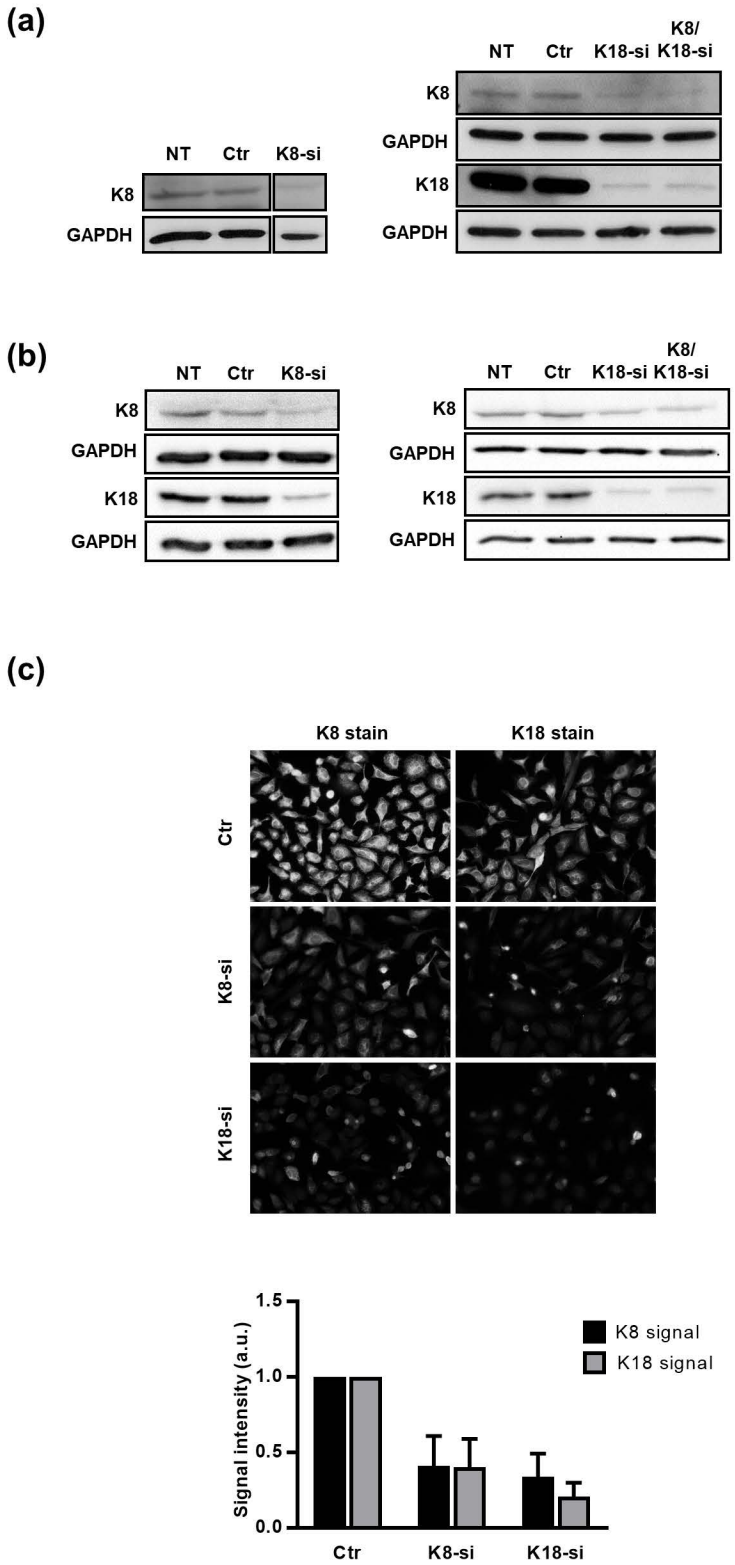

Supplemental Figure 2. K8 and K18 depletion efficiency in HeLa and Caco-2 cells

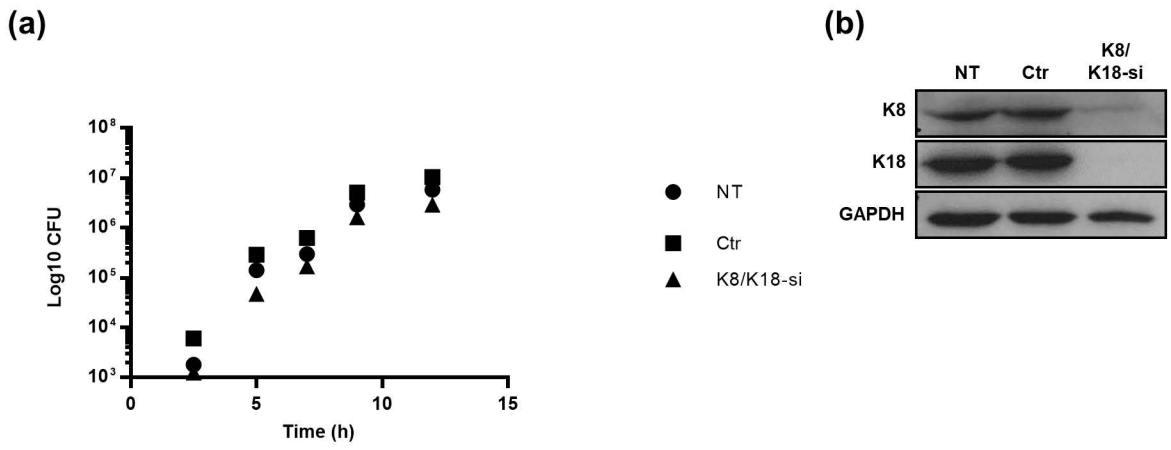

Supplemental Figure 3. K8 and K18 are not important for *Listeria* intracellular replication in HeLa cells.

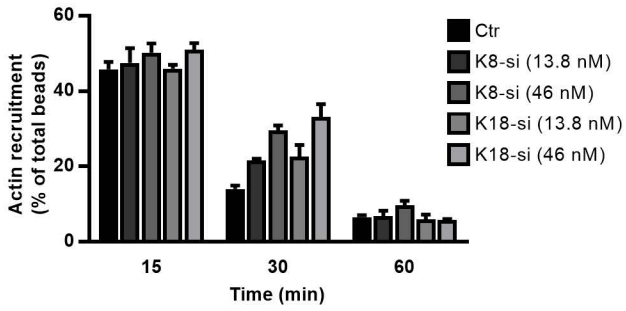

Supplemental Figure 4. K8 and K18 assist actin depolymerization during InlB-mediated internalization.

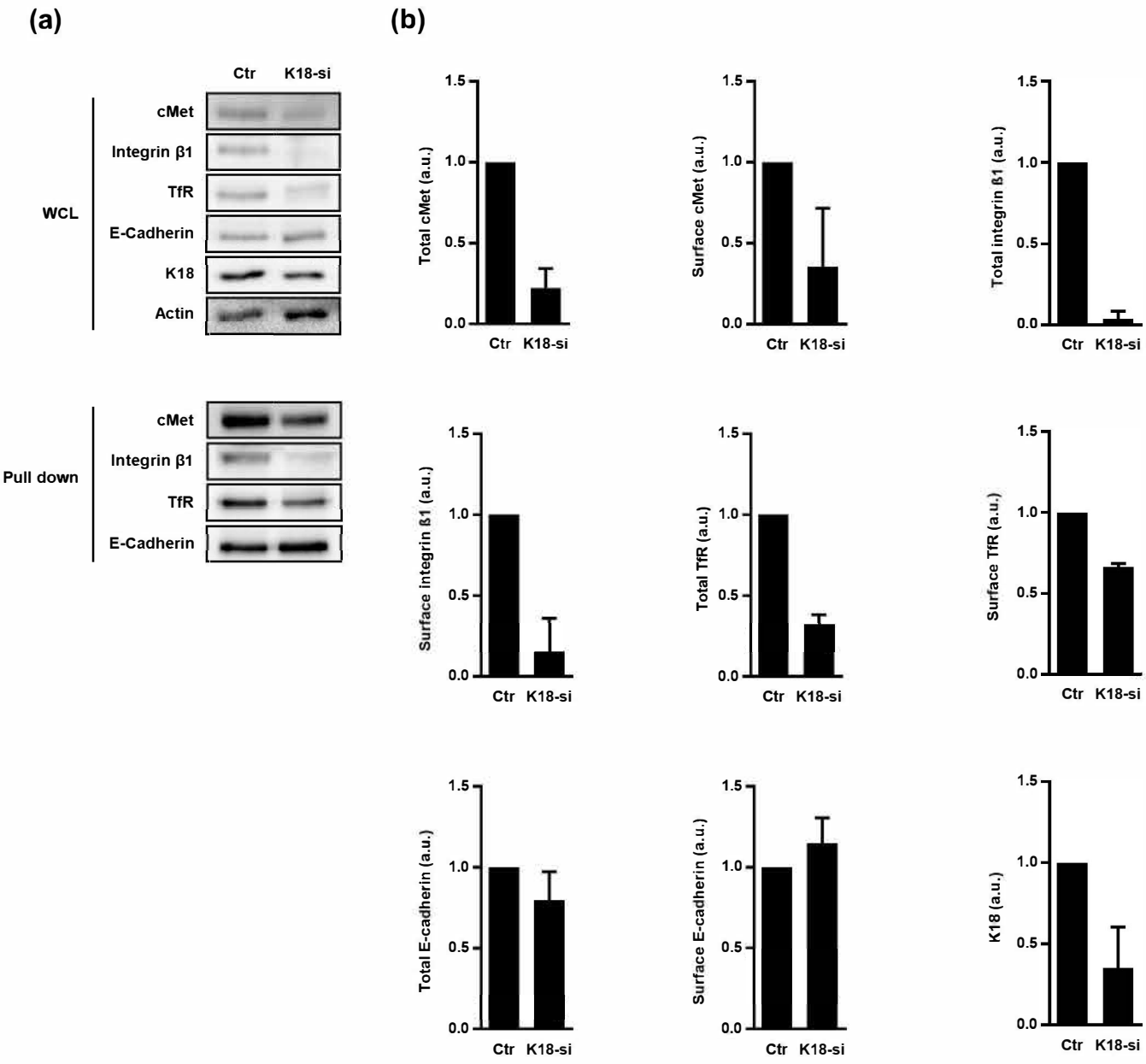

Supplemental Figure 5. K18 depletion perturbs expression and surface location of transmembrane receptors in Caco-2 cells.